Intrinsic reflection asymmetry in atomic nuclei

P. A. Butler

Department of Physics, Oliver Lodge Laboratory, University of Liverpool, P. O. Box 147, Liverpool L69 3BX, United Kingdom

W. Nazarewicz

Department of Physics and Astronomy, University of Tennessee, Knoxville, Tennessee 37996;
Physics Division, Oak Ridge National Laboratory, P.O. Box 2008, Oak Ridge, Tennessee 37831;
and Institute of Theoretical Physics, Warsaw University, ul. Hoża 69, PL-00-681 Warsaw, Poland

The experimental and theoretical evidence for intrinsic reflection-asymmetric shapes in nuclei is reviewed. The theoretical methods discussed cover a wide spectrum, from mean-field theory and its extensions to algebraic and cluster approaches. The experimental data for nuclear ground states and at low and high spin, cited as evidence for reflection asymmetry, are collected and categorized. The extensive data on electric dipole transition moments and their theoretical interpretation are surveyed, along with available data on electric octupole moments. The evidence for reflection-asymmetric molecular states in light nuclei is summarized. The application of reflection-asymmetric theories to descriptions of the fission barrier, bimodal fission, superdeformation, and hyperdeformations is reviewed, and some other perspectives in the wider context of nuclear physics are also given.
[S0034-6861(96)00102-X]

CONTENTS

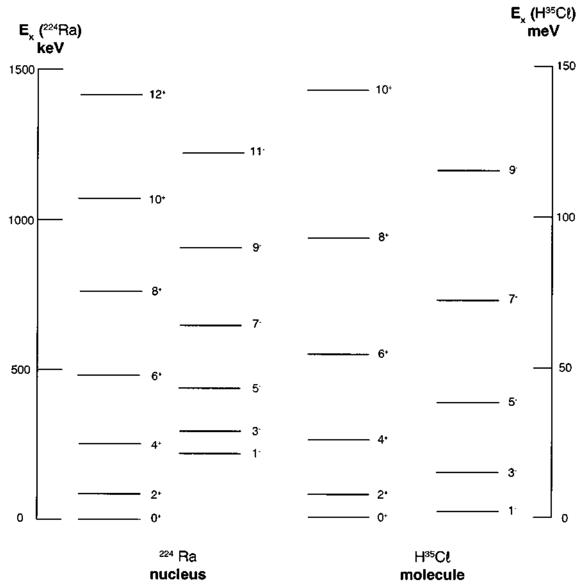

FIG. 1. The low-lying rotational spectra of ^{224}Ra, compared with that of the H^{35}Cl molecule. The spectrum of ^{224}Ra is taken from Poynter *et al.* (1989a). The rotational constants for the H^{35}Cl molecule are taken from Landolt-Börnstein (1974).

I. INTRODUCTION

The existence of nuclei with stable deformed shapes was realized early in the history of nuclear physics. The observation of large quadrupole moments led to the suggestion that some nuclei might have spheroidal shapes, which was confirmed by the observation of rotational band structures and measurements of their properties. For most deformed nuclei, a description as an axial- and reflection-symmetric spheroid is adequate to reproduce the band's spectroscopy. Because such a shape is symmetric under space inversion, all members of the rotational band will have the same parity; however, with the first observation of negative-parity states near the ground state by the Berkeley group in the 1950s (Asaro *et al.*, 1953; Stephens *et al.*, 1955), the possibility arose that some nuclei might have a shape asymmetric under reflection, such as a pear shape (Strutinsky, 1956; Lee and Inglis, 1957).

Extensive investigations into the structure of nuclei with low-lying negative-parity states has led to the conclusion that, while reflection-asymmetric shapes can play a role in the band structure, they are not as stable as the familiar quadrupole deformations. The situation is illustrated by the low-lying spectrum of a representative case, ^{224}Ra. Its spectrum is compared to that of the linear molecule HCl in Fig. 1. The molecule's reflection asymmetry permits both parities in its rotational spectrum, perfectly interleaved according to the energy formula $E_J \sim J(J+1)$. The spectrum of ^{224}Ra has both parities as well, but in two bands that are displaced from each other. Nevertheless, there are good reasons for describing such a system as a common band. Experimentally, not only the proximity of energies, but also the dipole transitions between the subbands are characteristic of an intrinsic shape having an electric dipole moment. The displacement of the two parities means that fluctuations of shape back to symmetry must also be significant. In light nuclei, the resonances observed in collisions and other reactions may also be interpreted in terms of "molecular states" of alpha particles and other light clusters, which lack reflection symmetry. Analogies have also been drawn between molecular and baryonic spectra, describing baryons as symmetric or asymmetric tops (Iachello, 1989).

This review addresses both experimental and theoretical progress in this area. On the experimental side, spectroscopy has been extended to very high spins, and indicative transitions, including dipole and octupole, can now be measured. On the theoretical side, following an early phase of phenomenological theory, we have moved to an era where stable shapes can be predicted and understood from self-consistent mean-field theory, and furthermore the softness of the reflection-asymmetric deformation that was apparent in Fig. 1 is described by a more sophisticated theory going beyond the mean field.

The organization of this review is as follows. Section II contains the definitions of parameters used to define the nuclear shape in terms of both mass and charge distribution. Section III summarizes in detail various theoretical approaches, some of which have been reviewed earlier (Leander, 1985a; Nazarewicz, 1985; Rohoziński, 1988; Åberg *et al.*, 1990). Sections IV and V collect experimental data pertaining to energy levels and transitions, and ground-state properties, respectively; for previous reviews of experimental systematics, see Leander and Sheline (1984), Leander and Chen (1988), Jain *et al.* (1990), Ahmad and Butler (1993), and Sheline (1993a). Section VI explores the properties of the rotating nuclear reflection-asymmetric shape and discusses them in terms of experimental observations. Section VII examines theoretical models of the electric dipole transition moment, an important observable in this context; for an earlier review see Butler and Nazarewicz (1991). Section VIII presents a survey of molecular structures in nuclei in the sd and fp shell, and of theoretical methods used to describe these light systems. Section IX discusses how the concept of octupole mass deformation has been applied to the description of fission and (more recently) to super- and hyperdeformed nuclear states. Finally, Sec. X offers a broader perspective on the consequences of nuclear reflection asymmetry and on future avenues of investigation.

II. DEFINITIONS

The anisotropy of nuclear shape is described in terms of intrinsic moments and deformation parameters. Shape parametrizations and intrinsic moments specific to reflection-asymmetric nuclei (e.g., octupole deformed) are discussed below in Sec. II.A (isoscalar moments) and Sec. II.B (isovector electric dipole moment).

A. Reflection-asymmetric shapes

In many applications, the nuclear shape is parametrized in terms of a spherical harmonic (multipole) expansion. The spheroidal nuclear surface is defined by means of standard deformation parameters $\alpha_{\lambda\mu}$ describing the length of the radius vector pointing from the origin to the surface (Bohr, 1952; Hill and Wheeler, 1953):

$$R(\Omega)=c(\alpha)R_0\left[1+\sum_{\lambda=2}^{\lambda_{\max}}\sum_{\mu=-\lambda}^{+\lambda}\alpha_{\lambda\mu}Y^*_{\lambda\mu}(\Omega)\right], \tag{1}$$

with $c(\alpha)$ being determined from the volume-conservation condition and $R_0=r_0A^{1/3}$. The requirement that the radius be real imposes the condition

$$(\alpha_{\lambda\mu})^*=(-)^\mu\alpha_{\lambda-\mu}. \tag{2}$$

The three dipole deformations, $\alpha_{1\pm1}$ and α_{10}, are given by the constraint that fixes the center of mass (c.m.) at the origin of the body-fixed frame:

$$\int_V \mathbf{r}d^3\mathbf{r}=0, \tag{3}$$

where V is the total volume enclosed by the surface defined in Eq. (1). For shapes axially symmetric with respect to the z axis, all deformation parameters with $\mu \neq 0$ vanish. The remaining deformation parameters $\alpha_{\lambda0}$ are usually called β_λ:

$$\beta_\lambda\equiv\alpha_{\lambda0}. \tag{4}$$

For a well-defined axial octupole minimum in the total energy, the intrinsic charge octupole moment is

$$\mathcal{Q}_{30,c}\equiv\int 2r^3P_{30}\rho_c(\boldsymbol{r})d^3\boldsymbol{r}, \tag{5}$$

where $\rho_c(\boldsymbol{r})$ is the charge density. Assuming ρ_c=const inside the sharp surface of Eq. (1), $\mathcal{Q}_{30,c}$ can be related to the deformations β_λ by (Leander and Chen, 1988)

$$\mathcal{Q}_{30,c}=\frac{3}{\sqrt{7\pi}}ZR_0^3\bar{\beta}_3, \tag{6}$$

where

$$\bar{\beta}_3=\beta_3+\frac{5}{\sqrt{4\pi}}\left(\frac{4\sqrt{5}}{15}\beta_2\beta_3+\frac{6}{11}\beta_3\beta_4+\frac{60\sqrt{7}}{91\sqrt{11}}\beta_4\beta_5+\cdots\right). \tag{7}$$

The mass octupole moment and corresponding deformations are defined in a similar way.

There exist several parametrizations of reflection-asymmetric shapes other than the α and β parametrizations discussed above. A compilation of other parametrizations is contained in the Appendix.

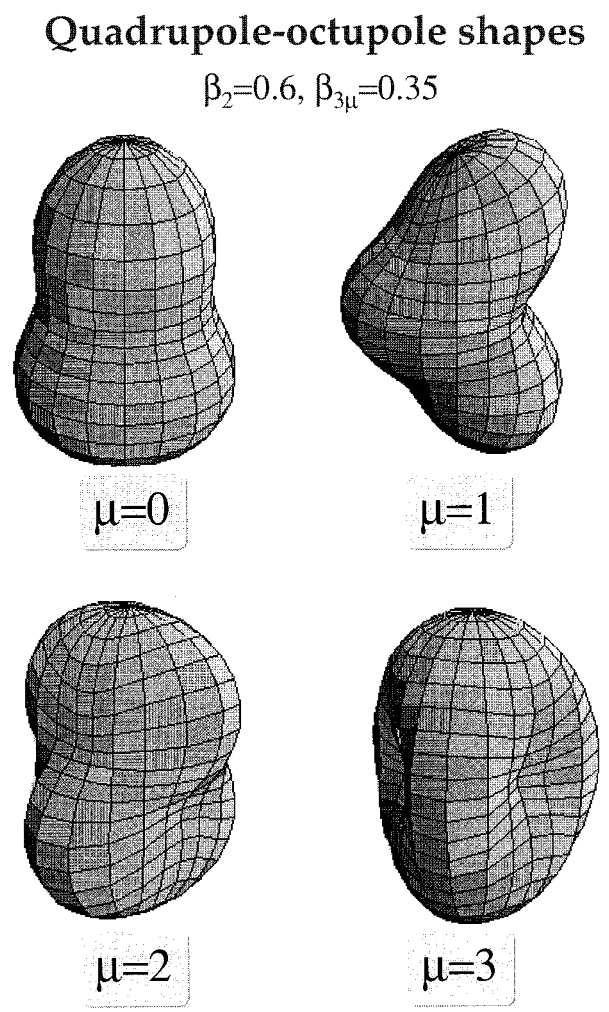

FIG. 2. Quadrupole-octupole shapes represented by multipole expansion, Eq. (1). In all cases, the same axial quadrupole deformation $\alpha_{20}=\beta_2=0.6$ is assumed. The four shapes correspond to octupole deformations with $\mu=0, 1, 2,$ and 3 [$\alpha_{30}=\beta_{30}$; $\alpha_{3-\mu}=(-1)^\mu\alpha_{3\mu}=\beta_{3\mu}/2$; $\beta_{3\mu}=0.35$]. (Courtesy of T. Misu.)

The number of deformation parameters that appear in the multipole expansion Eq. (1) grows rapidly with λ. For instance, the general quadrupole-plus-octupole shape is described by two quadrupole deformations (α_{20} and α_{22}, or β_2 and γ) and seven independent deformations $\alpha_{3\mu}$. Figure 2 displays four shapes resulting from the superposition of axial quadrupole and octupole deformations with $\mu=0, 1, 2,$ and 3.

A general parametrization of the combined quadrupole-octupole field, covering all possible shapes without double counting, was proposed by Rohoziński (1990). The basic requirements are that the parametrization obeys simple transformation rules under O_h (a group of 48 transformations changing the names and arrows of the axes), and have simple ranges for the parameters. After introducing the seven real Cartesian components $a_{3\mu}$ and $b_{3\mu}$ (Rohoziński *et al.*, 1982; Rohoziński, 1988),

$$\alpha_{30}=a_{30},\quad \alpha_{3\pm\mu}=\frac{(\pm1)^\mu}{\sqrt{2}}(a_{3\mu}\pm ib_{3\mu})\quad(\mu=1,2,3), \tag{8}$$

the latter can be expressed in terms of one "radial" coordinate β_3 ($\beta_3 \geqslant 0$) and six "angular" biharmonic coordinates ($\delta_0,\delta_1,\delta_2,\gamma_0,\gamma_1,\gamma_2$) describing both the octupole distortion and its orientation with respect to the intrinsic frame defined by the quadrupole tensor. The coordinates given by Eq. (8) can be expressed as

$$\begin{aligned}
a_{30}&=\beta_3\cos\delta_0\cos\delta_1\cos\gamma_1,\\
a_{31}&=\beta_3\cos\delta_0\sin\delta_1\cos\delta_2\cos\gamma_2,\\
a_{32}&=\beta_3\cos\delta_0\cos\delta_1\sin\gamma_1,\\
b_{31}&=\beta_3\cos\delta_0\sin\delta_1\sin\delta_2\cos\gamma_3,\\
b_{32}&=\beta_3\sin\delta_0,\\
b_{33}&=\beta_3\cos\delta_0\sin\delta_1\sin\delta_2\sin\gamma_3,
\end{aligned}\tag{9}$$

where $-\pi/2\leqslant\delta_0\leqslant\pi/2$, $0\leqslant\delta_i\leqslant\pi/2$ $(i=1,2)$, $-\pi/2\leqslant\gamma_1\leqslant\pi/2$, $-c-\pi/2\leqslant\gamma_2\leqslant\pi/2-c$, $c-\pi/2\leqslant\gamma_3\leqslant\pi/2+c$, and $\sin c=\sqrt{5/8}$, $\cos c=\sqrt{3/8}$ (Rohoziński, 1990).

Attempts to find a unique parametrization of the pure-octupole field defining an intrinsic frame (i.e., without involving the quadrupole field) turned out to be less successful (Hamamoto, Zhang, and Xie, *et al.*, 1991).

B. The electric dipole moment

The nuclear electric dipole moment is a measure of the shift between the center of charge and the center of mass of the nucleus. Assuming that nucleons are pointlike particles, the $E1$ moment is

$$\boldsymbol{D}=\sum_{i=1}^{Z} e_i(\boldsymbol{r}_{p,i}-\boldsymbol{R}_{\mathrm{c.m.}})=e(\boldsymbol{r}_p-Z\boldsymbol{R}_{\mathrm{c.m.}}).\tag{10}$$

Neglecting the proton-neutron mass difference ($A\boldsymbol{R}_{\mathrm{c.m.}}=\boldsymbol{r}_p+\boldsymbol{r}_n$), $\boldsymbol{D}$ is equal to

$$\boldsymbol{D}=e\frac{N}{A}\boldsymbol{r}_p-e\frac{Z}{A}\boldsymbol{r}_n.\tag{11}$$

Equation (11) can be written alternatively as

$$\boldsymbol{D}=e\frac{ZN}{A}(\boldsymbol{r}_{p,\mathrm{c.m.}}-\boldsymbol{r}_{n,\mathrm{c.m.}}),\tag{12}$$

where $\boldsymbol{r}_{p,\mathrm{c.m.}}=\boldsymbol{r}_p/Z$ and $\boldsymbol{r}_{n,\mathrm{c.m.}}=\boldsymbol{r}_n/N$ are the center-of-mass coordinates for protons and neutrons, respectively.

For reflection-symmetric systems, the nucleonic (proton and neutron) densities have three symmetry planes, so that $\langle\boldsymbol{r}_n\rangle=\langle\boldsymbol{r}_p\rangle=0$, and hence $\langle\boldsymbol{D}\rangle=0$ (the notaton $\langle\cdots\rangle$ denotes the expectation value in the intrinsic state). However, if density distributions are reflection asymmetric, then in general $\boldsymbol{r}_{p,\mathrm{c.m.}}\neq\boldsymbol{r}_{n,\mathrm{c.m.}}$, and a large static $E1$ moment may arise in the intrinsic frame. For an axially deformed system, having $\langle x\rangle=\langle y\rangle=0$, the intrinsic dipole moment is aligned along the symmetry axis (z axis), and its value D_0 can be calculated directly from Eq. (11). In the most general case of triaxial and reflection-asymmetric density distributions, the intrinsic dipole moment is characterized by three spherical components, $D_{\pm1}$ and D_0.

III. THEORETICAL DESCRIPTIONS

In this section, we review the many theoretical approaches to reflection-asymmetric nuclear shapes. We begin in Sec. III.A with general arguments, before moving on to the reflection-asymmetric mean-field approach (Sec. III.B) and its extensions (Sec. III.C), algebraic approaches (Sec. III.D), cluster models (Sec.III.E), and, for completeness, vibrational models (Sec. III.F).

A. Microscopic origin of static octupole deformations

The mechanism responsible for the appearance of static deformations in nuclei arises from the degeneracy of eigenvalues of a single-particle Hamiltonian around the Fermi level, leading to instability with respect to shape vibrations (spontaneous symmetry breaking). This is the Jahn-Teller effect (Jahn and Teller, 1937; Reinhard and Otten, 1984). Stable reflection-asymmetric deformations in the body-fixed frame can be attributed to a parity-breaking odd-multipolarity interaction which couples intrinsic states of opposite parity.

To illustrate the transition from symmetric to reflection-asymmetric shapes, we use arguments based on the random-phase approximation (RPA) with a separable multipole interaction. A simple nuclear Hamiltonian representing nuclear vibrations, the pairing-plus-multipole Hamiltonian, can be written as (Lane, 1964; Soloviev, 1976):

$$H=\sum_j e_j c_j^{+}c_{j'}-\frac{1}{2}\sum_{\lambda}\kappa_{\lambda}\sum_{\mu=-\lambda}^{+\lambda}Q_{\lambda\mu}^{+}\cdot Q_{\lambda\mu}+H_{\mathrm{pair}},\tag{13}$$

where the first term on the right-hand side is the spherical shell-model potential, the second term represents a long-range separable multipole-multipole force generating the collective motion, H_{pair} is the pairing Hamiltonian, and j stands for the set of quantum numbers (n,ℓ,j). In Eq. (13), $Q_{\lambda\mu}$ is the multipole operator

$$Q_{\lambda\mu}^{+}=\sum_{jj'}\langle j|f_{\lambda}(r)Y_{\lambda\mu}(\Omega)|j'\rangle c_j^{+}c_{j'},\tag{14}$$

where $f_{\lambda}(r)$ is the radial form factor [given, e.g., by the derivative of the average potential (Bohr and Mottelson, 1975)]. A coupling between single-particle states of opposite parity is produced by the octupole-octupole ($\lambda=3$) residual interaction. For the Hamiltonian [Eq. (13)] representing simple octupole vibrations, the excitations E_{oct} of the system can be computed by means of the RPA; they are solutions to the dispersion equation (Lane and Pendlebury, 1960; Veje, 1966; Soloviev, 1976; Ring and Schuck, 1980)

$$\sum_{j,j'}\frac{|\langle j\|Q_3\|j'\rangle|^2(u_jv_{j'}+u_{j'}v_j)^2(E_j+E_{j'})}{(E_j+E_{j'})^2-E_{\mathrm{oct}}^2}=\frac{7}{\kappa_3},\tag{15}$$

where $E_j=\sqrt{(e_j-\lambda)^2+\Delta^2}$ are the quasiparticle energies, and u_j and v_j are the usual BCS occupation coefficients.

The lowest root of Eq. (15) represents the low-frequency collective octupole vibration. If the coupling

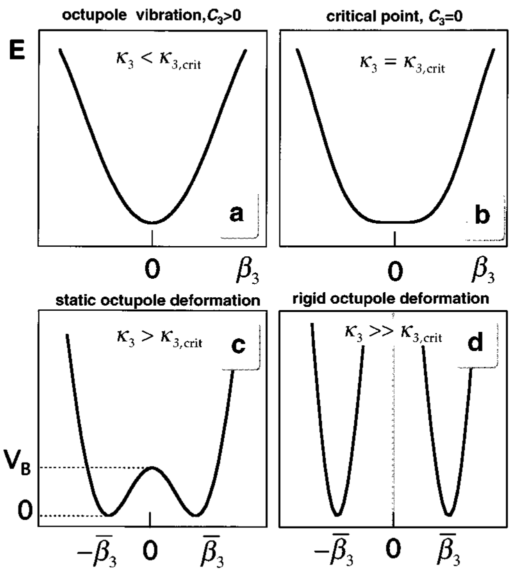

FIG. 3. Total nuclear energy as a function of octupole deformation β_3, for different values of octupole coupling κ_3. The vibrational limit (a) corresponds to small values of κ_3. Here the octupole stiffness $C_3=(d^2E/d\beta_3^2)_{\beta_3=0}$, is positive. At the point of instability (b) $\kappa_3=\kappa_{3,\rm crit}$ [Eq. (16)], $C_3=0$ and the system becomes unstable to octupole vibrations. For $\kappa_3>\kappa_{3,\rm crit}$ (c) the system is permanently deformed ($C_3<0$); the parity splitting results from tunneling between two degenerate minima at $\beta_3=\pm\bar\beta_3$, separated by a barrier V_B. In the limit of rigid octupole deformation (d), i.e, an infinite barrier separating the minima, the parity splitting vanishes.

constant κ_3 is relatively small, the system behaves like a vibrator [Fig. 3(a)]. If the value of κ_3 is increased, vibrations become more and more collective and the vibrational frequency decreases. At the critical point, defined by

$$\kappa_{3,\rm crit}=7\left\{\sum_{j,j'}\frac{|\langle j\|Q_3\|j'\rangle|^2(u_jv_{j'}+u_{j'}v_j)^2}{E_j+E_{j'}}\right\}^{-1},\qquad(16)$$

the lowest solution of Eq. (15) has zero energy, i.e., the collective vibrational state becomes degenerate with the ground state [Fig. 3(b)]. At this point the RPA breaks down, the system becomes unstable against vibration induced by the octupole-octupole force (Thouless, 1961), and further increase of the coupling constant leads to permanent intrinsic octupole deformation [see Fig. 3(c)]. Pairing correlations, through the change in the energy denominator in Eq. (15) and the reduction of the numerator through the uv factor, tend to increase the critical value of κ_3. One can thus say that pairing has a tendency to make the system less octupole deformed.

It is important to remember that actual nuclei are relatively small systems, and that finite-size effects, which manifest themselves through dynamical correlations (fluctuations), are crucial. The fluctuations wash out transitions from the "spherical" to the "deformed" phase and result in a smooth and continuous pattern of $E_{\rm oct}$ and octupole deformation β_3, proportional to $\langle 0^+\|Q_3\|3^-\rangle$ (see the discussion in Sec. III.C). Even for the best cases of nuclear stable octupole deformations, the octupole barriers separating the two degenerate minima are relatively small, i.e., the extreme limit of the rigid static octupole deformation shown in Fig. 3(d) is never approached.

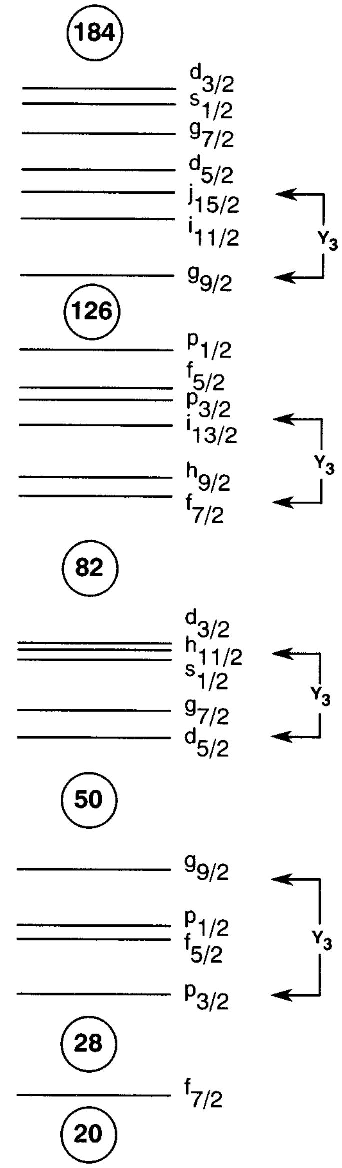

FIG. 4. Nuclear spherical single-particle levels. The most important octupole couplings are indicated.

As can be seen in Eq. (16), the necessary condition for the presence of low-energy octupole collectivity is the existence, near the Fermi level, of pairs of orbitals strongly coupled by the octupole interaction. As shown in Fig. 4, for normally deformed systems the condition for strong octupole coupling is satisfied for particle numbers associated with the maximum ΔN=1 interaction between the intruder subshell (ℓ,j) and the normal-parity subshell ($\ell-3$,$j-3$). The regions of nuclei with strong octupole correlations correspond to particle numbers near 34 ($g_{9/2}\leftrightarrow p_{3/2}$ coupling), 56 ($h_{11/2}\leftrightarrow d_{5/2}$ coupling), 88 ($i_{13/2}\leftrightarrow f_{7/2}$ coupling), and 134 ($j_{15/2}\leftrightarrow g_{9/2}$ coupling).

That is, the tendency towards octupole deformation occurs just above closed shells.

B. Reflection-asymmetric mean-field approach

The concept of stable octupole deformation appears naturally in the unconstrained mean-field approach, in which the average potential, and consequently the total energy, is a functional of the nucleonic density (Ring and Schuck, 1980).

The average nuclear mean field, in which nucleons move as independent particles, can be obtained from the Hartree-Fock (HF) theory. The starting point is the general two-body Hamiltonian

$$H=\sum_{ij} t_{ij}c_i^+c_j+\frac{1}{4}\sum_{ijkl} \bar{v}_{ijkl}c_i^+c_j^+c_lc_k, \tag{17}$$

where $\bar{v}_{ijkl}$ is the antisymmetrized matrix element of a two-body effective (usually density-dependent) force. The A-body wave function is approximated by a Slater determinant whose orbitals are determined by minimization of the total energy. This variation leads to an eigenvalue problem which defines both the single-particle orbitals $\{\Phi_i,\ i=1,\ldots,A\}$ and the single-particle energies e_i:

$$(t+\Gamma)\Phi_i=e_i\Phi_i. \tag{18}$$

The resulting self-consistent HF potential,

$$\Gamma_{ij}[\rho]=\sum_{kl} \bar{v}_{ikjl}\rho_{lk}, \tag{19}$$

depends on the orbitals through the density matrix ρ.

The pairing (particle-particle) components of the effective force can be approximated in the framework of the BCS theory, or they can be treated on the same footing as the particle-hole interactions through the Hartree-Fock-Bogolyubov (HFB) theory. The solution of the HF+BCS or HFB equations gives the binding energy of the nucleus, either at the local minimum or as a function of collective parameters q_i such as shape deformations (constrained HFB theory).

As early as 1957, Bleuler and Terreaux proposed that the single-particle wave functions of the nuclear shell model or the HF method should have no definite parity. Extension of the HF formulation to the mixed-parity Slater determinants was accomplished by Amiet and Huguenin (1963, 1966) and Müller-Schwartz (1967).

If the intrinsic parity is broken, the intrinsic state χ is not an eigenstate of the parity operator $\mathcal{P}$. The states with good parity p can be constructed by means of projection:

$$\Psi_p=\mathcal{N}_p(1+p\mathcal{P})\chi,\ \ \mathcal{N}_p^{-2}=2(1+p\langle\chi|\mathcal{P}|\chi\rangle). \tag{20}$$

The energy of the projected state E_p=$\langle\Psi_p|H|\Psi_p\rangle$ is given by

$$E_p=E-p\,\frac{\langle\mathcal{P}\rangle E-\langle H\mathcal{P}\rangle}{1+p\langle\mathcal{P}\rangle}, \tag{21}$$

where E=$\langle\chi|H|\chi\rangle$ is the HF energy. As can be seen in Eq. (21) (Amiet and Huguenin, 1966),

$$E_+\leqslant E\leqslant E_- \quad \text{if } E<\langle H\mathcal{P}\rangle/\langle\mathcal{P}\rangle. \tag{22}$$

The mean value of the parity in the intrinsic state is usually very small. The wave function of the single-particle orbital ψ_i can be decomposed into two components with good parity

$$\psi_i=a_i^{(+)}\psi_i^{(+)}+a_i^{(-)}\psi_i^{(-)},\ \ |a_i^{(+)}|^2+|a_i^{(-)}|^2=1. \tag{23}$$

The parity content of the single-particle state is given by

$$\langle\psi_i|\mathcal{P}|\psi_i\rangle=|a_i^{(+)}|^2-|a_i^{(-)}|^2, \tag{24}$$

which yields

$$\langle\chi|\mathcal{P}|\chi\rangle=\prod_{i=1,A}(|a_i^{(+)}|^2-|a_i^{(-)}|^2). \tag{25}$$

It is instructive to analyze expressions (21), (22), and (25) using the simple two-level model proposed by Lipkin, Meshkov, and Glick (1965). The model Hamiltonian,

$$H=\epsilon K_0-\frac{1}{2}V(K_+K_++K_-K_-), \tag{26}$$

describes a system of N fermions distributed among two levels of different parity, each having an N-fold degeneracy, and separated by an energy ϵ. The particles interact via a monopole-type residual interaction with strength V that scatters particles between upper and lower levels. In Eq. (26), K_0 and $K_\pm$ are quasispin operators. The most general Slater determinant in this case is (Agassi *et al.*, 1966; Ring and Schuck, 1980) $\chi=|\phi\rangle=\exp[\tan(\phi/2)K_+]|0\rangle$. After introducing the effective coupling strength κ_3=$(N-1)V/\epsilon$, we can write the HF energy and the energy of the projected states in closed form (Agassi *et al.*, 1966).

The critical value of the coupling strength in the Lipkin-Meshkov-Glick model is κ_3=1. For $\kappa_3<1$ the potential-energy curve $E(\phi)$ has only one minimum, at ϕ=0 (vibrational limit). For $\kappa_3>1$ a stable deformation develops, $\bar{\phi}=\pm\arccos(1/\kappa_3)$. The overlap (25) in the Lipkin-Meshkov-Glick model is given by

$$\langle\phi|\mathcal{P}|\phi\rangle=\cos^N\phi, \tag{27}$$

i.e., the parity content of the HF ground state is close to zero for large values of κ_3. The behavior of E and E_p as a function of ϕ is displayed in Fig. 5 for κ_3=0.25, 1, and 2. We see that for large values of κ_3 the minima of E and $E_\pm$ correspond to very similar values of ϕ. This is not true for smaller values of κ_3, for which the deformation of the $p=-1$ state ($\bar{\phi}_-$) is larger than that of the p=1 state ($\bar{\phi}_+$). (For realistic calculations, see Fig. 8 below.)

1. Mean-field symmetries

Any mean-field solution, when deformed, breaks one of the basic symmetries of the nuclear Hamiltonian. However, not all symmetries of the wave functions are destroyed in the self-consistent calculations (Ring and

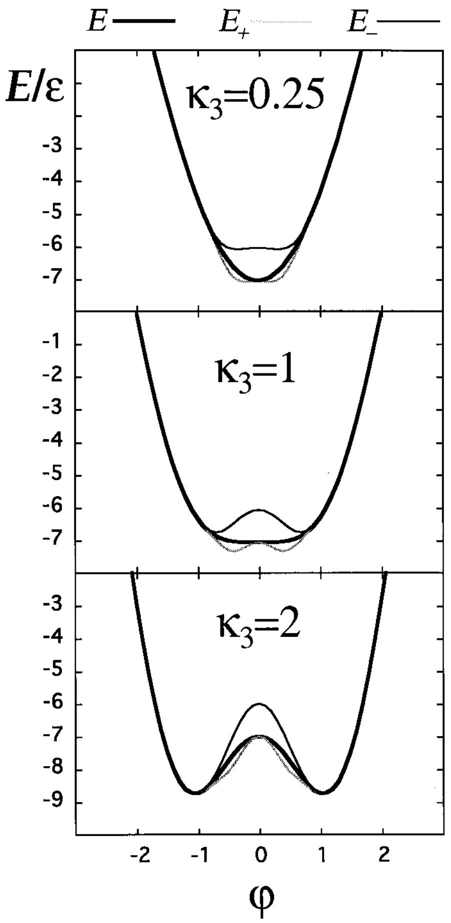

FIG. 5. HF energy (thick solid line) and projected energy curves (grey line, positive parity; thin line, negative parity) for the Lipkin-Mechkov-Glick model as a function of deformation ϕ for κ_3=0.25, 1, and 2, and for N=14.

Schuck, 1980). The remaining *self-consistent symmetries* provide a simplification of the calculation as well as a convenient labeling of the individual orbitals. Among the possible remaining symmetries, the most usual are those associated with the following operators (Goodman, 1974; Bohr and Mottelson, 1975; Bohr, 1976):

(i) time reversal (T);
(ii) space inversion (parity) ($\mathscr{P}$);
(iii) rotation around the symmetry axis (giving rise to the good quantum number K);
(iv) Rotations $R_\kappa=\exp(-i\pi I_\kappa)$, κ=1, 2, 3, through the angle π around the three principal axes of the mean field (the finite symmetry group defined by these three rotations is called D_2);
(v) reflections $S_\kappa=\mathscr{P}\cdot R_\kappa^{-1}$ through planes containing the two principal axes of the mean field.

Depending on the underlying mean-field theory and the constraints, the mean-field solution will possess none or several of these symmetries.

If the rotation is approximated by means of the cranking approach, one has to analyze the Routhian

$$H^\omega=H-\omega I_1, \tag{28}$$

rather than the Hamiltonian H. Due to the cranking term ωI_1, the only self-consistent symmetries that can possibly remain in the rotating nucleus are P, R_1, and S_1.

To discuss the possible nuclear shapes that remain invariant with respect to different self-consistent symmetries, it is convenient to perform the multipole decomposition of the density matrix ρ:

$$\rho=\sum_{\lambda\mu}\rho_{\lambda\mu} \tag{29}$$

(Dobaczewski and Skalski, 1989). Using Eq. (29), we can express the average field [Eq. (19)] as (Ring and Schuck, 1980; Dobaczewski and Skalski, 1989)

$$\Gamma[\rho]=\sum_{\lambda\mu}\beta_{\lambda\mu}Q_{\lambda\mu}, \tag{30}$$

where $\beta_{\lambda-\mu}=(-1)^\mu\beta^*_{\lambda\mu}$ and $Q_{\lambda\mu}$ transforms as a rank-λ spherical tensor. The transformation properties of spherical tensors $Q_{\lambda\mu}$ are

$$\mathscr{P}Q_{\lambda\mu}\mathscr{P}^{-1}=(-1)^\lambda Q_{\lambda\mu}, \tag{31}$$

$$R_1Q_{\lambda\mu}R_1^{-1}=(-1)^\lambda Q_{\lambda-\mu}, \tag{32}$$

$$S_1Q_{\lambda\mu}S_1^{-1}=Q_{\lambda-\mu}. \tag{33}$$

If the mean field commutes both with $\mathscr{P}$ and R_1, the eigenstates of H^ω can be characterized by the intrinsic parity π and the signature quantum number r, which is the eigenvalue of R_1. In this case the λ-odd components vanish and $\beta_{\lambda\mu}=(-1)^\mu\beta_{\lambda-\mu}$, i.e., the spherical tensors $Q_{\lambda\mu}$ ($\mu\neq 0$), appear in the combinations

$$Q'_{\lambda\mu}\equiv Q_{\lambda\mu}+(-1)^\mu Q_{\lambda-\mu},\quad \mu>0. \tag{34}$$

Relation (34) also holds for the most general field that commutes with S_1. However, in this case both even and odd values of λ appear in the multipole expansion given by Eq. (30). (For instance, the octupole shapes shown in Fig. 2 are S_1 invariant.)

The eigenstates of H^ω can be characterized by the simplex quantum number s, which is the eigenvalue of S_1 (Nazarewicz *et al.*, 1984a; Frauendorf and Pashkevich, 1984; Nazarewicz and Olanders, 1985a, 1985b). For the application of simplex symmetry to rotational spectra, see Sec. VI.

To take advantage of the S_1 symmetry, a new single-particle basis must be constructed. The Goodman transformation (Goodman, 1974) from the strong-coupling basis $|k,\Omega_k\rangle$ to basis states of good simplex reads (Nazarewicz and Olanders, 1985a, 1985b)

$$|k,s=+i\rangle=\frac{1}{\sqrt{2}}[-|k,\Omega_k\rangle+(-1)^{\Omega_k-1/2}|\overline{k,\Omega_k}\rangle], \tag{35}$$

$$|k,s=-i\rangle=\frac{1}{\sqrt{2}}[|\overline{k,\Omega_k}\rangle+(-1)^{\Omega_k-1/2}|k,\Omega_k\rangle], \tag{36}$$

where Ω_k is the single-particle angular momentum projection on the axis of quantization, and $|\overline{k,\Omega_k}\rangle=T|k,\Omega_k\rangle$, where $T|\pi jm\rangle=\pi(-1)^{j+m}|\pi j-m\rangle$.

Symmetry properties of spherical tensors in the basis given by Eq. (35) were discussed by Leander *et al.* (1986). In particular, they demonstrated that the transition matrix element between parity partners $|k,s\rangle$ and $|k,-s\rangle$ vanishes, i.e., $\langle k,s|Q_{\lambda\mu}|k,-s\rangle=0$.

In several works, the nonaxial octupole fields have been treated in selected combinations that guarantee the presence of some self-consistent symmetries and thus facilitate calculations. Li *et al.* (1991) discussed symmetry properties of the general one-body Hamiltonian and applied them to triaxial octupole deformations (assuming one symmetry plane). Skalski (1991) assumed the presence of two mirror reflections, S_1 and S_2; this leaves only even-μ components in Eq. (34). In his following study, Skalski (1992) considered rather general mean fields containing axially symmetric components with $\lambda=2, 3, 4$, and triaxial octupole deformations given by Eq. (34), the latter treated separately (i.e., one triaxial deformation at a time).

As discussed by Hamamoto, Mottelson, *et al.* (1991), the symmetry groups of the pure-octupole fields [Eq. (34)] with $\mu=1$, 2, and 3, are respectively C_{2v}, T_d, and D_{3h}. This leads to the classification of single-particle levels in terms of corresponding irreducible representations (irreps). In the presence of axial reflection-symmetric shapes the symmetries C_{2v} and D_{3h} are preserved, but T_d reduces to the lower symmetry D_{2d} (Skalski, 1992). Consequently, in the presence of an axial quadrupole field (i) all the single-particle levels of the same simplex interact in the Q'_{31} field (C_{2v} has one 2D spinor irrep), (ii) there are two groups of noninteracting states in the Q'_{32} field (D_{2d} has two nonequivalent 2D spinor irreps), and (iii) there are two groups of noninteracting states in the Q'_{33} field (D_{3h} has three nonequivalent 2D spinor irreps). The combination of $\mu=0$ and 2, and $\mu=1$ and 3 fields reduces the symmetry group to C_{2v}.

Examples of single-particle diagrams in the Q'_{32} field can be found in Li and Dudek (1994). Eichler and Faessler (1970) in their study of the trigonal symmetry in light nuclei considered systems invariant with respect to the trigonal C_3 symmetry, i.e., with respect to rotations of 120° about the z axis. (For the α-like nuclei the interesting symmetry point groups are $D_{\infty h}$, T_d, and D_{3h}. The group C_3 is a common lower-symmetry subgroup). The self-consistent symmetry in question, C_3, conserves the quantum number $q=\Omega \bmod 3$. A tetrahedral perturbation of the spherical harmonic-oscillator potential was considered by Elliott *et al.* (1985); they classified the single-particle levels using the irreps of T_d.

2. Shell-correction method

Mean fields, in which nucleons move as independent particles, can be obtained from a knowledge of the forces acting between nucleons using self-consistent HF theory. For a particular choice of nucleon-nucleon force and proton and neutron number, the variational principle determines whether this field is spherical or deformed.

The deformed-shell model developed in the 1950s (Rainwater, 1950; Moszkowski, 1955; Nilsson, 1955) is an approximation to the HF approach. Here, the field Γ is not determined self-consistently from Eq. (19), but is assumed to be a phenomenological average potential which contains a central part, a spin-orbit term, and a Coulomb potential for protons. All of these terms depend explicitly on a set of external deformation parameters defining the nuclear surface.

The earliest calculations employing the reflection-asymmetric deformed-shell approach (Lee and Inglis, 1957; see also Johansson, 1961) investigated the effect of spin-orbit coupling on the stability of pear-shaped deformations using wave functions of a spheroidal harmonic-oscillator potential. Vogel (1968) studied the dependence of the nuclear potential energy on β_3 in the $218 \leq A \leq 232$ region using a modified harmonic-oscillator potential with pairing, and found no cases with nonzero octupole deformation.

The deformed-shell model alone cannot be used to predict binding energies. This is because the deformed-shell model energy differs from the full HF energy by the two-body interaction term. On the other hand, it is well known that binding energies are accounted for with good accuracy by the classical model of the liquid drop (Myers and Swiatecki, 1969). The two approaches are merged into the shell-correction (SC) method (also known as the macroscopic-microscopic, or Nilsson-Strutinsky method) (Strutinsky, 1967; Brack *et al.*, 1972). The main assumption of the SC method is that the total energy of a nucleus can be separated into two parts,

$$E=E_{\mathrm{macr}}+E_{\mathrm{shell}}, \tag{37}$$

where E_{macr} is the macroscopic energy (depending smoothly on the number of nucleons), and E_{shell} is the shell-correction term, which fluctuates with particle number (reflecting the nonuniformities of the single-particle level distribution, i.e., shell effects). The macroscopic part is usually replaced by the corresponding liquid-drop (or droplet) model value, while the shell-correction term is calculated using the deformed independent-particle model.

Before discussing the results of the SC method, it should be emphasized that it is not a self-consistent theory. Thus it should be viewed as a practical recipe, deficient in a number of respects. Its formal justification in terms of the HF approach is given by the so-called Strutinsky energy theorem (Strutinsky, 1974; Brack and Quentin, 1981). This theorem states that the difference between the HF energy and the SC energy is of second order in the density fluctuations, provided that the deformed-shell potential gives a similar spectrum to the averaged HF potential.

Möller and Nilsson (1970) calculated the effect on the potential-energy surface in the lead and actinide region of simultaneous P_3 and P_5 degrees of freedom using the SC method with a modified harmonic-oscillator potential, and found instability with respect to octupole deformation (see also Möller, 1972, for a comprehensive description of the method as applied to an investigation into the fission process; a different approach was employed by Mustafa *et al.* (1973), who used a two-center model including asymmetric deformation). Möller *et al.* (1972) carried out similar calculations, which suggested that ^{224}Ra has the largest equilibrium octupole deformation.

In light nuclei, the spin-orbit interaction is relatively weak and, in addition, the diffuseness of the nuclear surface is comparable to the nuclear radius. Consequently, the harmonic-oscillator model gives a fairly good approximation to the nuclear average potential. The first study of static octupole shapes in light nuclei with $N=Z$ from ^{12}C to ^{44}Ti, based on the SC method, was carried out by Leander and Larsson (1975). They employed the modified harmonic-oscillator potential parametrized through quadrupole (K=0,2), octupole (K=0,3), and higher-order deformations, finding minima in ε_3 for mid-shell nuclei at very large quadrupole deformation. Hellström (1977) explicitly included triaxial octupole deformations with K=2.

In the presence of the small perturbing octupole potential $V=\beta_{3\mu}Q_{3\mu}$, the shell driving force (i.e., the dependence of the shell correction on deformation) is determined by the second-order correction $\delta E^{(2)}_{\rm shell}$, which is proportional to the square of the corresponding deformation $\beta_{3\mu}$:

$$\delta E^{(2)}_{\rm shell}=C_{3\mu}\beta^2_{3\mu}. \tag{38}$$

(The first-order term vanishes, since the expectation value of the octupole moment is zero in the parity-conserving wave function. The exact expression for $\delta E^{(2)}_{\rm shell}$ can be found in Nazarewicz *et al.*, 1995.) The shell-energy octupole-stiffness coefficient $C_{3\mu}$ determines the octupole susceptibility of the shell energy. If $C_{3\mu}$ is negative, there exists a shell force favoring stable deformations. On the other hand, if $C_{3\mu}$ is positive, the shell correction tends to restore reflection symmetry. Since for nuclei with $Z\lesssim 104$ the liquid-drop model favors spherical ground-state shapes, one can say that stable octupole deformations can only arise from shell-effects, i.e., from the shell driving force.

The behavior of $E_{\rm shell}$ obtained in the Woods-Saxon (WS) potential, as a function of β_3 and particle number (at typical ground-state deformations β_2 and β_4), is shown in Fig. 6 (for a similar plot based on the modified harmonic-oscillator model, see Leander *et al.*, 1982). We see that the shell correction favors octupole deformation ($C_{30}<0$) near particle numbers N=134 and Z=90. Other octupole-driving particle numbers expected from the SC method are 34 and 56, in nice agreement with the schematic diagram of Fig. 4. From different combinations of those particle numbers, several regions of candidates for reflection-asymmetric shapes emerge.

Möller and Nix (1981) showed that there is a substantial ground-state octupole instability in their calculations based on the folded Yukawa deformed potential and Yukawa-plus-exponential macroscopic energy, much softer to high-multipole deformations than the standard liquid drop model with sharp surfaces used previously. This was extended by Leander *et al.* (1982), who made a systematic study of the Po-U region. Nazarewicz *et al.* (1984b) employed a similar model using the WS potential to analyze octupole instability in both medium- and heavy-mass nuclei. The octupole-deformation energy curves for even-even isotopes of Rn, Ra, Th, and U obtained from the SC+WS model of Nazarewicz *et al.* (1984b) are shown in Fig. 7. In the same work, it was shown that nuclei around ^{146}Ba and ^{114}Xe should also exhibit octupole instability, although the deformation is much softer than for the Ra-Th region.

Nazarewicz and co-workers applied the cranked shell-correction method to investigate the behavior of nuclear shape as a function of spin for both the Ra-Th region (Nazarewicz *et al.*, 1984a, 1987) and the region around Z=58, N=88 (Nazarewicz and Tabor, 1992).

Chasman (1986) investigated the effect of allowing the hexacontatetrapole deformation (λ=6) parameter to vary freely, instead of being fixed as in earlier studies. He found that the binding energy increased by approximately 1 MeV for many nuclei in the mass region $220<A<230$. Chasman and Ahmad (1986) also investigated the γ degree of freedom using the SC method with a WS potential. They found a region of γ softness for Ra and Rn isotopes with $220<A<226$ and for several nuclei with N=130.

Sobiczewski *et al.* (1988), Rozmej *et al.* (1988), and Ćwiok and Nazarewicz (1989a, 1989b) demonstrated that by treating higher-order multipole deformations ($\beta_5,\beta_6,\dots$) in a self-consistent manner it is possible to further lower the octupole minima in a WS model. For instance, inclusion of higher-order deformations lowers the octupole minima in ^{144,146,148}Ba by 200–300 keV. One-quasiparticle bandheads in odd-A actinide nuclei were calculated in a deformed self-consistent WS model by Ćwiok and Nazarewicz (1989a, 1991), who pointed out the importance of specialization energy (i.e., extra energy required to find a transition state at the octupole barrier with quantum numbers matching those of the reflection-asymmetric ground state) for the barrier heights. In other mass regions, deformed SC-WS calculations have also been made for ^{64}Ge (Ennis *et al.*, 1991; Skalski, 1991) and for even-even nuclei near ^{112}Ba (Skalski, 1990).

As discussed in Secs. II.A and III.B.1, the consistent treatment of triaxial octupole deformations with $\mu\neq 0$ is difficult. In an early work, Gavron *et al.* (1977) demonstrated in SC calculations that the simultaneous inclusion of triaxiality and reflection asymmetry is important around the third saddle point in actinides (see also Åberg *et al.*, 1980). Banana-type octupole deformations (μ=1) at superdeformed shapes were investigated by Chasman (1991) and Skalski (1992) using the SC method with a WS potential (see Sec. IX.B.2 for more discussion). Li and Dudek (1994) considered $\alpha_{\lambda\mu}$ deformations with λ=2, 3, 4, and 5, and predicted static α_{32} deformation (with all other deformations vanishing) in ^{222}Rn.

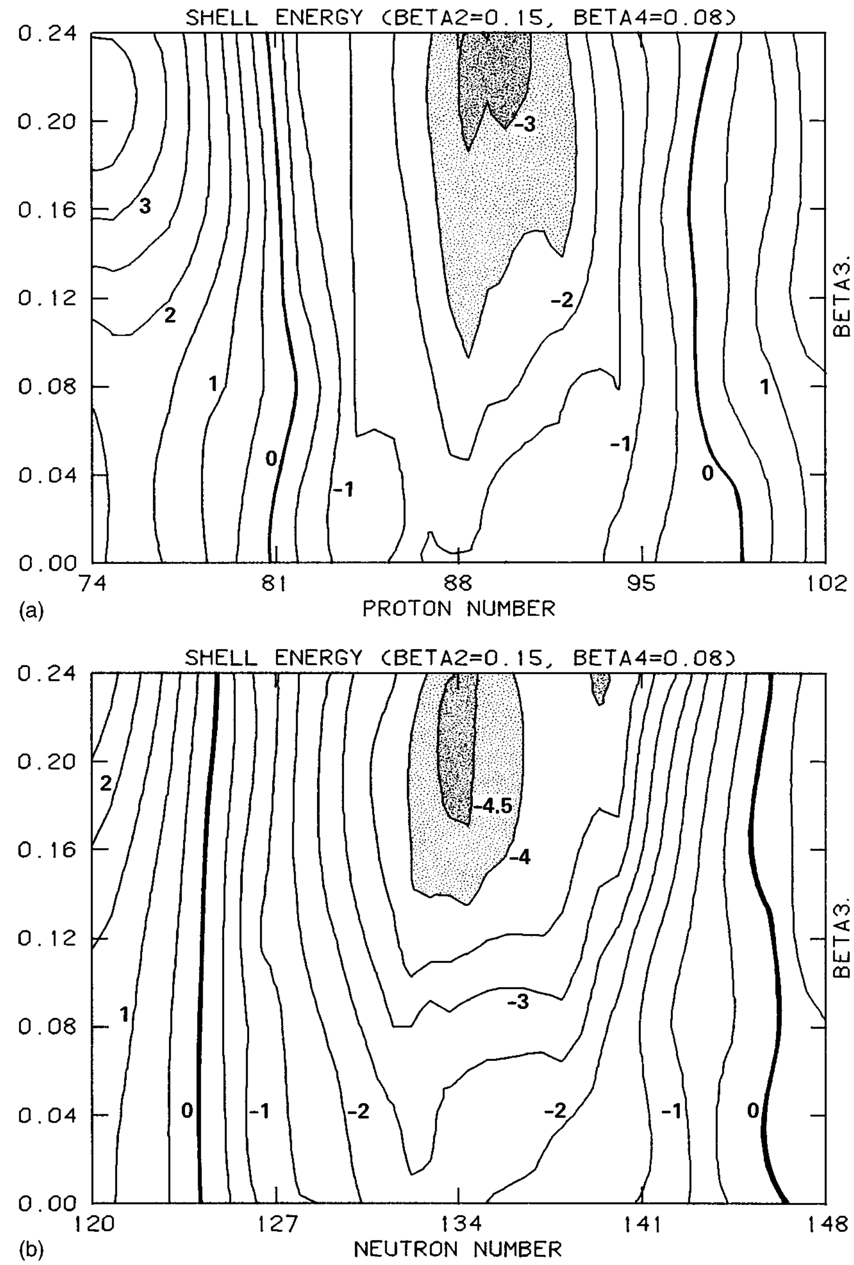

FIG. 6. WS proton (top) and neutron (bottom) shell correction plotted versus particle number and octupole deformation β_3. Other deformations are β_2=0.15, β_4=0.08 (Nazarewicz *et al.*, 1984b). The contours are labeled by their values in MeV.

In the context of metallic clusters, octupole instability with respect to nonaxial octupole modes $Y_{3\mu}$, $\mu \neq 0$, has been investigated by simulating the one-particle spectrum of the infinite-well potential using that of a modified oscillator potential (Hamamoto, Mottelson, *et al.* 1991; Frisk *et al.* 1994). It is found that the μ=3 and μ=2 octupole deformations, when treated one at a time, give rise to a strong shell structure.

3. Self-consistent methods

Early HF studies for light nuclei involving parity mixing of intrinsic wave functions were carried out by several authors. Kelson (1965) was able to reproduce approximately the negative-parity collective band in ^{16}O by projecting out a Slater determinant containing $s_{1/2}p_{1/2}d_{3/2}$ states using the HF method with a Rosenfeld two-body interaction. The mechanism of parity mixing in single-particle orbitals in the HF framework was also investigated by several other workers, including Amiet and Huguenin (1966), Ebenhöh (1966), Röhl (1966), Parikh and Ullah (1967), and Bassichis and Svenne (1967), to improve the agreement with the observed spin-orbit splittings and magnetic moments. Müller-Schwartz (1968) pointed out that the low-lying 0^- state predicted by Amiet and Huguenin (1966) is unrealistic and that the ground state in ^{16}O has no parity mixing, although excited states might have such mixing. This has been supported by Blomquist and Molinari (1968) and Burr *et al.* (1969), who demonstrated that the parity-breaking deformations are excluded in practically all cases for light nuclei if realistic interactions (in particular the tensor force) are included. Krappe and Wahsweiler (1967) calculated the energy surfaces of ^{16}O,

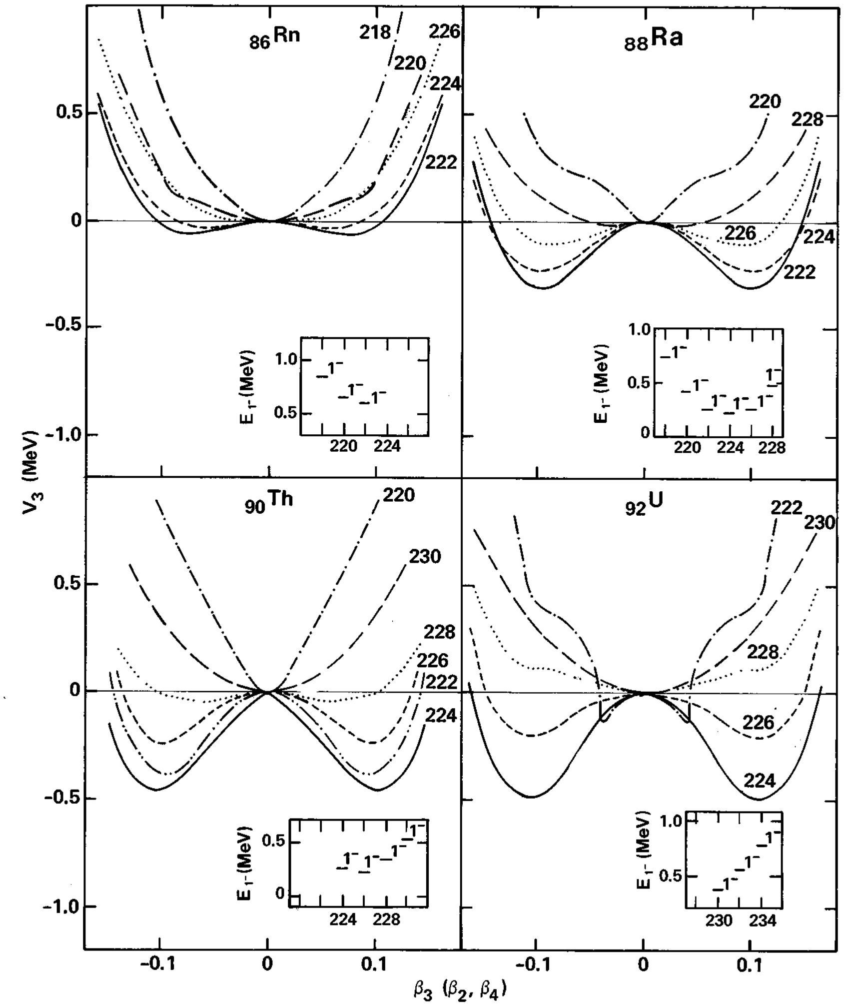

FIG. 7. Octupole-deformation energy curves for even-even isotopes of Rn, Ra, Th, and U obtained in the SC+WS model of Nazarewicz *et al.* (1984b). Insets show experimental energies of the lowest negative-parity states in these isotopes.

^{20}Ne, and ^{24}Mg using the single-particle parity-mixed wave functions and a Hamiltonian with a simple two-body local potential of Serber-exchange type. They obtained a pronounced octupole softness. Castel and Svenne (1969) performed HF calculations with the Yale-Shakin potential for a number of sd nuclei. They calculated large values of $B(E3,3^-\rightarrow0^+)$, 10–18 s.p.u. (single-particle units), but in each case found that the octupole deformation was zero. The most octupole-soft nuclei were predicted to be ^{30}Si and ^{38}Ar. Giraud and Sauer (1970) found parity-mixed HF solutions for ^{16}O, ^{19}F, ^{20}Ne, ^{24}Mg, and ^{28}Si using a Gaussian or Yukawa force with a Rosenfeld-exchange mixture. In particular, they obtained states of mixed parity and having a triaxial shape. Eichler and Faessler (1970) investigated the static octupole shapes with K=0 and 3 in ^{12}C, ^{16}O, and ^{20}Ne by means of a constrained HF method with the Yale-Shakin and Volkov potentials. They obtained small static trigonal octupole moments Q_{33}. For other parity-mixed calculations for ^{16}O, see also Do Dang *et al.* (1976) and Elliott *et al.* (1985).

Bonche *et al.* (1986) performed HF+BCS calculations, using the Skyrme III effective interaction, of the energy as a function of deformations q_2 and q_3 (defined as expectation values of the quadrupole moment and r^3Y_{30}, respectively) of ^{222}Ra. Significantly, they find a minimum for a nonzero value of the octupole moment. Strong quadrupole-octupole coupling was also predicted by the HF+BCS calculations of Bonche (1988) for ^{144}Ba. The potential-energy curves versus q_3, corresponding to q_2=400, 600, and 800 fm^2, are displayed in Fig. 8. The HF results are compared to the parity-projected energies given by Eq. (21).

Praharaj (1986) performed parity-mixed deformed HF calculations for $^{142-148}$Ba and $^{146-148}$Ce, and showed that ^{142,144}Ba and ^{148}Ba are unstable to octupole deformation (see, however, the comment in Nazarewicz, 1987).

Robledo *et al.* (1987) and Egido and Robledo (1990) employed the HF+BCS method with the Gogny interaction to calculate reflection-asymmetric minima in ^{222,224}Ra, ^{222}Rn, and $^{142-148}$Ba. They obtained reflection-asymmetric minima in all cases. By constraining the position of the c.m. coordinate at the origin, they were able to calculate intrinsic dipole moments in these nuclei (see Sec. VII.C).

4. Particle-plus-rotor model

There have been several attempts to explain spectroscopic properties of reflection-asymmetric nuclei using concepts based on the particle-plus-rotor model. This is

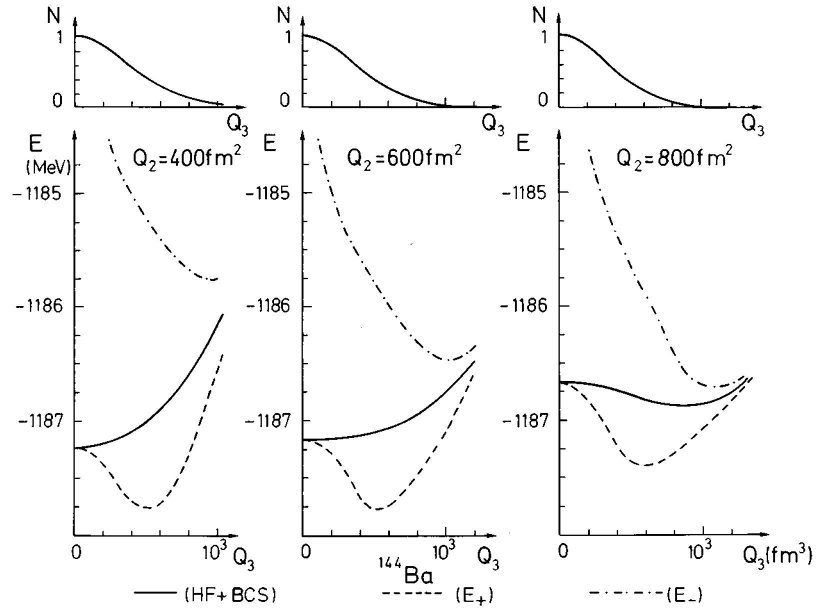

FIG. 8. Potential-energy curves for ^{144}Ba obtained in HF+BCS+Skyrme calculations of Bonche (1988). The HF results (solid line) are compared with the parity-projected curves, E_+ (dashed line) and E_- (dashed-dotted line). The upper portion shows the overlaps, Eq. (25).

a highly phenomenological model that aims at reproduction and interpretation of low-lying experimental spectra. The microscopic input to this model, namely equilibrium deformations, pairing gaps, and the intrinsic single-particle Hamiltonian, is taken from self-consistent HF calculations or from the SC method.

Assuming a large deformation and the strong-coupling scheme, the particle-plus-rotor Hamiltonian can be written as (Bohr and Mottelson, 1975)

$$H = H_{\mathrm{intr}} + H_{\mathrm{rot}}, \tag{39}$$

where the rotor part is given by

$$H_{\mathrm{rot}} = \frac{\hbar^2}{2\mathscr{J}}(\boldsymbol{I}-\boldsymbol{j})^2 \tag{40}$$

and the intrinsic part is

$$H_{\mathrm{intr}} = H_{\mathrm{core}} + H_{\mathrm{s.p.}}. \tag{41}$$

The single-particle Hamiltonian can be approximated by the deformed (reflection-asymmetric) field and the BCS pairing. The space of the reflection-asymmetric particle-plus-rotor model Hamiltonian is spanned by the symmetrized wave functions (Bohr and Mottelson, 1975)

$$\Psi^{\nu}_{IMKp} = \mathscr{N}(1+R_1)D^{I}_{MK}(1+p\mathscr{P}_c\mathscr{P}_{\mathrm{s.p.}})\Phi_a\chi^{\nu}_K, \tag{42}$$

where $\mathscr{N}$ is a normalization constant, $\mathscr{P}_c$ is the core parity operator, $\mathscr{P}_{\mathrm{s.p.}}$ is the valence (single-particle) parity operator, $p=\pm 1$ is the total parity, Φ_a describes the core with the same orientation in space as the single-particle potential, and χ^{ν}_K is the wave function of the valence n-quasiparticle configuration $(K=\Omega_1+\Omega_2+\cdots+\Omega_n)$.

One of the earliest applications of this model to odd-A nuclei was that of Zaikin (1966), who calculated $B(E3)$ rates in ^{19}F. Leander and Sheline (1984) introduced the phenomenological core Hamiltonian that accounts for the parity splitting in the doubly even core, $E(0^-)$:

$$H_{\mathrm{core}} = \frac{1}{2}E(0^-)(1-\mathscr{P}_c) = \frac{1}{2}E(0^-)(1-p\mathscr{P}_{\mathrm{s.p.}}). \tag{43}$$

They applied the model to make extensive investigations of the spectroscopy of odd-A nuclei, and accounted for the ground-state properties of odd-A Ra isotopes and decoupling parameters for K=1/2 bands in Ra and Ac isotopes, using a folded Yukawa average potential to calculate single-particle levels. This model was subsequently developed by Leander and Chen (1987, 1988) using a WS deformed potential. The properties of the low-lying spectra in nuclei with A=219–229 were calculated and found to be in reasonable agreement with experiment. Finally, Sheline, Chen, and Leander (1988) applied the model to ^{223}Ra.

Brink *et al.* (1987) have derived results similar to those of Leander and Sheline (1984) by taking a model in which the valence nucleons are coupled to the observed energy spectrum of the even-even core, instead of a model assuming some particular symmetry for the intrinsic system. The extension of these techniques to odd-odd nuclei has been accomplished by Afanasjev *et al.* (1991).

C. Beyond the mean field

As already discussed in Sec. III.A, correlations due to the final size are important in describing properties of transitional systems. Since even in the best cases the predicted gain in the ground-state energy due to reflection-asymmetric deformations (deformation energy) is around 1–2 MeV, i.e., rather modest, dynamical corrections beyond the mean field play an important role.

The fluctuations smooth out the transition from the reflection-symmetric (vibrational) to the reflection-asymmetric (deformed) regime. This is illustrated in Fig. 9, which shows the parity-splitting energy ΔE between the first excited state (p=–1) and the ground state

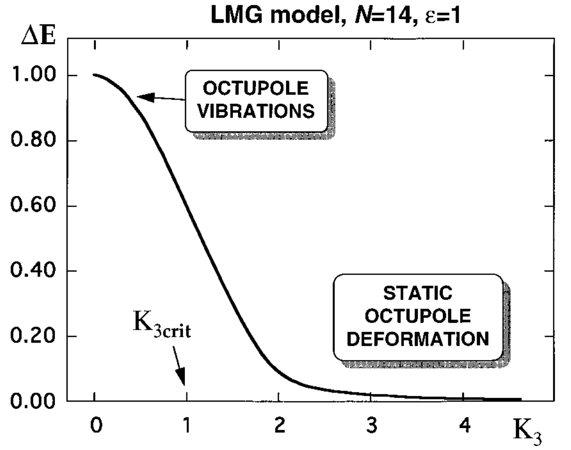

FIG. 9. The parity-splitting energy ΔE (in units of ϵ), between the first excited state (p=–1) and the ground state (p=1) of the Lipkin-Meshkov-Glick model, solved exactly as a function of κ_3 for N=14.

(p=1) for the exact solution of the Lipkin-Meshkov-Glick model (see Fig. 5). In contrast to the static HF theory, which exhibits a rapid phase transition at $\kappa_{3,\mathrm{crit}}$, here the transition from vibrational to deformed regime is smooth.

Some correlations can be accommodated by means of parity projection, performed either after or (better) before variation. However, as discussed by Agassi *et al.* (1966) and Robledo (1992), parity projection does not eliminate the discrepancy around the transition point. The missing correlations have to be incorporated by other methods (see below).

1. Generator-coordinate method

A useful tool for describing the dynamical correlations is the generator-coordinate (GC) method (Ring and Schuck, 1980). The GC wave function is usually taken as a combination of many (projected) product states,

$$\Psi_i^{(\mathrm{GC})}=\int d\mathbf{q}\sum_i f_i(\mathbf{q})\Psi_i(\mathbf{q}), \tag{44}$$

where the $\mathbf{q}$'s are generator coordinates and the generating functions Ψ_i are (projected) eigenstates of the intrinsic Hamiltonian (i=0 denotes the vacuum, i=1 the first excited state, and so on). The wave function in Eq. (44) is rich enough to accommodate correlations absent in the mean-field description. In the simplest applications of this method, the generating functions can be identified with the collective coordinates. The weight functions $f_i(\mathbf{q}$ are determined by means of the variational principle from the Hill-Wheeler equation.

Marcos *et al.* (1983) studied the collective path leading from ^{20}Ne to the separated nuclei ^{16}O + α using both the constrained HF and GC methods, and found that ^{20}Ne has softness to octupole deformation. A GC approach to molecular states was developed by, e.g., Langanke *et al.* (Langanke, 1982; Langanke *et al.*, 1984) and Baye and Descouvemont (1983, 1984) who applied it to $E1$, $E3$ transitions and to reduced α-widths in light nuclei (for other works, see Sec. VIII).

Bonche *et al.* (1991) and Meyer *et al.* (1995) based their calculations on the axial HF+BCS theory with the SkM* effective interaction, and used parity projection and the GC method to investigate the octupole softness and octupole-quadrupole coupling in the superdeformed and hyperdeformed minimum of ^{194}Pb. They found an octupole excitation at about 2 MeV in both methods. A similar method, but with the SIII Skyrme parametrization, was used by Heenen *et al.* (1994) to study octupole excitations in light Xe and Ba nuclei around ^{114}Ba. They found strong octupole correlations in this region in both GC and projected HF+BCS calculations. In the context of the parity-projected HF+BCS method and its relation to the GC method, Egido and Robledo (1991a, 1991b) investigated the importance of parity projection in the description of the negative-parity states in the light actinides. They concluded that, although it is an important effect, it is also necessary to take into account the collective correlations coming from the q_3 collective degree of freedom—and this is particularly important for the calculation of $B(E3)$'s. Robledo (1992) investigated the properties of the Lipkin-Meshkov-Glick model of Eq. (26). Here, the GC technique reproduces the exact solution (Ring and Schuck, 1980). To cure discrepancies in the intermediate region which appear in the projected HF theory, an alternative approach based on a two-configuration mixing has been proposed. As shown by Robledo (1992), this method gives very good agreement with the exact results for all deformation regimes.

Skalski *et al.* (1993a) have studied the coupling between axial quadrupole and octupole modes in $^{94-100}$Zr using the GC+HF method with various Skyrme parametrizations.

The importance of nonaxial octupole components with μ=1 and μ=2 at superdeformed shapes in ^{192,194}Hg and ^{194}Pb was discussed by Skalski *et al.* (1993b). The authors concluded that the μ=0 and μ=2 octupole modes are to a large extent decoupled. The results of two-dimensional GC calculations for the coupled μ=0 and μ=2 modes are shown in Fig. 10. It is seen that the first excited state [Fig. 10(c)] can be understood in terms of the pure μ=0 vibration, while the second excited state [Fig. 10(d)] shows the collective probability density characteristic of the octupole vibration with μ=2.

The coupling between the axial (μ=0) quadrupole and octupole modes at normal and large deformations was addressed by two-dimensional GC+HFB+BCS calculations for ^{194}Pb (Bonche *et al.*, 1994; Meyer *et al.*, 1995). The resulting probability densities suggest that the picture of independent quadrupole and octupole excitations breaks down quickly with increasing excitation energy.

2. Time-dependent Hartree-Fock

The time-dependent Hartree-Fock (TDHF) method is a microscopic quantum-mechanical method that pro-

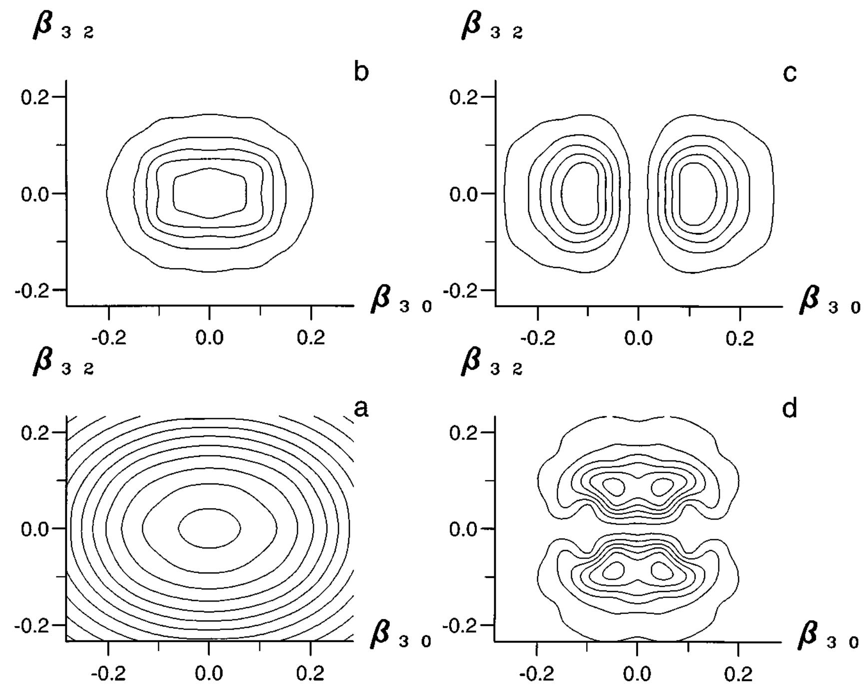

FIG. 10. Potential energy and probability densities of the three lowest GC-method states obtained for superdeformed ^{192}Hg in a two-dimensional (β_{30},β_{32}) calculation (Skalski *et al.*, 1993b): (a) energy (contour-line spacing 1 MeV); (b) ground state density; (c) first excited state density; (d) second excited state density.

vides a consistent description of all collective and single-particle aspects of nuclear motion. The time evolution of the system is given by

$$i\dot{\rho}(t)=[h(t),\rho(t)], \tag{45}$$

where ρ is the density matrix, and h is the TDHF Hamiltonian, which is the sum of the kinetic energy and the time-dependent average field $\Gamma[\rho(t)]$ [Eq. (19)]. In this approach, the system itself determines the path in the multidimensional energy surface; no self-consistent symmetries, restricting the available phase space, are imposed. The wave function is a single product state, which allows for a transparent geometrical interpretation.

Strayer *et al.* (1984) used this method to study the time evolution of the $\alpha+{}^{14}\mathrm{C}\leftrightarrow{}^{18}\mathrm{O}$ system at energies near the Coulomb barrier, and determined the frequencies of isovector dipole and isoscalar quadrupole and octupole giant resonances in ^{18}O. Umar *et al.* (1985) extended these calculations to the $^{12}\mathrm{C}+{}^{12}\mathrm{C}(0^+)$ and $\alpha+{}^{20}\mathrm{Ne}$ systems, calculating molecular resonances in ^{24}Mg.

Negele (1989) and Wolff *et al.* (1992) carried out a model calculation of fission of ^{32}S in three dimensions, also involving reflection-asymmetric deformations. They found a dramatic difference between the results of the static constrained HF (or adiabatic TDHF) and TDHF methods (see Sec. X.F).

3. Collective Schrödinger equation

By making the Gaussian-overlap approximation (GOA), the Hill-Wheeler equation of the GC method is reduced to the collective Schrödinger equation for the collective wave function:

$$\mathcal{H}_{\mathrm{coll}}\Psi_i(\mathbf{q})=E_i\Psi_i(\mathbf{q}), \tag{46}$$

where the collective Bohr Hamiltonian $\mathcal{H}_{\mathrm{coll}}$ depends on the collective mass parameters, the collective matrix, the potential energy, and the zero-point energy correction (Bohr, 1952; Ring and Schuck, 1980). If only one collective variable is considered, e.g., the octupole moment q_3, $\mathcal{H}_{\mathrm{coll}}$ can be written as

$$\mathcal{H}_{\mathrm{coll}}=-\frac{1}{\sqrt{G(q_3)}}\frac{\partial}{\partial q_3}\sqrt{G(q_3)}\frac{1}{2B(q_3)}\frac{\partial}{\partial q_3}+V(q_3)-E_{\mathrm{zpe}}(q_3), \tag{47}$$

where $G(q_3)$ is the collective metric, $B(q_3)$ is the collective mass parameter, $V(q_3)$ is the collective potential, and $E_{\mathrm{zpe}}(q_3)$ is the zero-point energy correction. The collective Schrödinger equation can also be obtained from the adiabatic TDHF method (Ring and Schuck, 1980). The resulting collective parameters are slightly different than in the GC+GOA method [for differences between the two approaches to the collective Schrödinger equation for octupole motion, see Egido and Robledo (1989, 1990)].

The collective Hamiltonian for octupole vibrations was studied by Donner and Greiner (1966). Their Hamiltonian contains a quadrupole-vibrational term, a rotational term, an octupole-vibrational term, and a quadrupole-vibrational interaction.

Zaikin (1966) and Krappe and Wille (1969) considered octupole vibrations with K=0 in the schematic collective Hamiltonian [Eq. (47)] with one collective coordinate β_3:

$$\mathcal{H}_{\mathrm{coll}}=-\frac{1}{2B_{30}}\frac{d^2}{d\beta_3^2}+V(\beta_3). \tag{48}$$

The lowest eigenstates of the Hamiltonian [Eq. (48)] with parity p are approximated [Eq. (20)] by a sum of two Gaussians centered at $\beta_3=\pm\bar{\beta}_3$:

$$\chi(\beta_3)=\left(\frac{\lambda}{\pi}\right)^{1/4}\exp\left[-\frac{\lambda}{2}(\beta_3-\bar{\beta}_3)^2\right]. \tag{49}$$

The quantity λ in Eq. (49) is inversely proportional to the deformation spread of χ, and is assumed to be the variational parameter of the model. In order to obtain the variational solution, the projected ground-state energy E_+ has been minimized with respect to λ. The calculated $B(E3)$ value,

$$B(E3)\propto|\langle\Psi_+|\beta_3|\Psi_-\rangle|^2\propto\frac{\bar{\beta}_3^2}{1-\langle\mathscr{P}\rangle^2}, \tag{50}$$

depends mainly on the value of equilibrium deformation $\bar{\beta}_3$, and is rather insensitive to the height of the octupole barrier V_0. On the other hand, the parity splitting shows significant dependence on V_0 (Nazarewicz and Tabor, 1992). Equation (50) demonstrates that if the nuclear potential becomes very soft with respect to the octupole deformation, the equilibrium deformation becomes a measure not of the deformation parameter but of the frequency, mass and inertia parameters describing the shape vibrations (Zaikin, 1966; Krappe and Wille, 1969; Bohr and Mottelson, 1975).

Leander and Sheline (1984) applied an intermediate-coupling scheme to the light actinides. The Hamiltonian of Eqs. (39)–(41), with $H_{\rm core}$ as in Eq. (48), and a particle-core coupling term approximated by $\kappa\mathscr{Q}_{30}r^3P_3(\theta)$, was diagonalized in the reflection-symmetric basis

$$\Psi^{\nu}_{IMK}=\mathscr{N}(1+R_1)D^I_{MK}\Phi_{n_3}\chi^{\nu}_K, \tag{51}$$

where Φ_{n_3} is an eigenstate of $H_{\rm core}$. In particular, they obtained a very good description of the transitional nucleus ^{229}Th. They concluded that, when applied to nuclei around ^{224}Th, strong coupling generally works better than weak coupling.

Rohoziński and co-workers (Rohoziński, 1978; Rohoziński and Greiner, 1980; Rohoziński *et al.*, 1982; Rohoziński, 1988) extended the collective model of Donner and Greiner (1966) to take into account anharmonicities and couplings between modes in a quadrupole-octupole system. Their collective Hamiltonian can be written as

$$\mathscr{H}_{\rm coll}=\mathscr{H}_{\rm vib}+\mathscr{H}_{\rm rot}+\mathscr{H}_{\text{vib-rot}}. \tag{52}$$

The vibrational Hamiltonian $\mathscr{H}_{\rm vib}$ describes the coupled intrinsic quadrupole-octupole vibrations, $\mathscr{H}_{\rm rot}$ is the rotational Hamiltonian, and $\mathscr{H}_{\rm vib-rot}$ is the rotation-vibration Hamiltonian. After introducing the intrinsic collective variables $\alpha_{\lambda\mu}$ of Eq. (8), and the associated collective momenta and angular momenta, the Hamiltonian [Eq. (52)] acquires a simple geometric interpretation. The total collective angular momentum $\boldsymbol{L}$ is divided into the quadrupole angular momentum $\boldsymbol{L}^{(2)}$ and the contribution $\boldsymbol{L}^{(3)}$ coming from octupole vibrations (Donner and Greiner, 1966). The rotational Hamiltonian can be further decomposed into a rotor part, a Coriolis term (involving the coupling between $\boldsymbol{L}$ and $\boldsymbol{L}^{(3)}$), and a centrifugal term. The collective Hamiltonian, Eq. (52), is diagonalized in the basis of D_{2h}-invariant wave functions of definite angular momentum L and parity.

The collective quadrupole-octupole model was applied to the limiting cases of spherical nuclei and well-deformed axially symmetric nuclei. Rohoziński and Greiner (1983) looked at the effects of Coriolis and centrifugal terms for nuclei with stable octupole deformation. They found dramatic effects on the moments of inertia and $B(E3)$ rates. A simple collective quadrupole-octupole Hamiltonian for nuclei with static quadrupole and octupole deformations was studied by Dzyublik and Denisov (1993) and Denisov and Dzyublik (1993). They obtained simple analytic expressions for the energies of collective states in nuclei with static octupole deformations. Denisov and Dzyublik (1995) investigated the collective Hamiltonian with $\beta_2,\beta_3,\ldots,\beta_N$ deformations, considering also the case of static equilibrium deformations.

Barts *et al.* (1984) also took into account the interaction of octupole and quadrupole degrees of freedom. In their calculations the vibrational variables were separated using the Hartree method, and the wave functions determined using a variational principle. They noted that the inclusion of both degrees of freedom leads to strong breaking of the axial symmetry.

Böning *et al.* (1985) solved Eq. (46) for ^{226}Th assuming the decoupling of odd- and even-multipole deformations (taken as collective coordinates), and taking constant mass parameters. The rotational degree of freedom was ignored in these calculations. See also Sobiczewski and Böning (1987) and Böning *et al.* (1985) for similar calculations for ^{224}Ra. A similar approach, but with the mass parameter determined from the hopping model, was applied by Barranco *et al.* (1988) to the parity splitting in ^{222}Ra.

Provoost *et al.* (1984) applied the adiabatic TDHF method to the $\alpha+^{16}{\rm O}\leftrightarrow^{20}{\rm Ne}$ system, and were able to reproduce the energy difference between the ground state and the lowest state of the negative-parity band.

More microscopic calculations based on the GC+GOE and adiabatic TDHF methods with the Gogny force D1 were performed in order to describe octupole correlations in the light lanthanides (Egido and Robledo, 1990, 1991a, 1991b, 1992; Martín and Robledo, 1994) and light actinides (Egido and Robledo, 1989, 1991a, 1991b; Robledo *et al.*, 1987, 1988).

Robledo *et al.* (1988) performed adiabatic TDHF calculations with q_2 and q_3 as collective variables to calculate the $(0^+)-(0^-)$ energy difference and $E1$,$E3$ transition rates for ^{222}Ra. Egido and Robledo (1989) further applied adiabatic TDHF and GC+GOA techniques to a series of Ra and Th isotopes. They also applied similar methods to the $^{142-148}$Ba isotopes, and found that the octupole barriers are not high enough for the nuclei to be classified as octupole deformed, at least at zero spin (Egido and Robledo, 1990).

An extensive series of calculations using q_3-constrained HF+BCS and adiabatic TDHF methods have also been reported (Egido and Robledo, 1992) for ^{140}Ba, $^{142-150}$Ce, $^{144-152}$Nd, and $^{146-154}$Sm.

4. Other methods

Microscopic many-body calculations were performed by Chasman (1979, 1980), who predicted parity doublets in several odd-A Th, Ac and Pa nuclei. These calculations employed a schematic Hamiltonian as in Eq. (13), with separable multipole-multipole forces, pairing, and projected many-body wave functions. Chasman (1989) has also investigated the role of a $\lambda=5$ particle-hole interaction, and found that the octupole correlation energy in the 1^- state is also independent of the nuclide, even though the corresponding changes in the correlation energy associated with the interaction of multipolarity $\lambda=5$ may be large.

In the multiphonon method, the octupole-plus-pairing Hamiltonian (13) is diagonalized in the truncated basis of multiphonon states

$$|n\rangle=\mathcal{N}_n(Q^+)^n|0\rangle. \tag{53}$$

The collective phonons Q^+ are calculated microscopically, in the Tamm-Dancoff approximation. Piepenbring (1983, 1984, 1985) and Leandri and Piepenbring (1989) applied this method to the Ra-Th isotopes, ^{146}Ba and ^{152}Sm. The multiphonon method gives a microscopic explanation of the low-lying $K^\pi=0^-$ bandhead, for which the RPA fails, and explains why the corresponding two-phonon state appears at much higher energies than $2E(0^-)$. Jammari *et al.* (1983) have studied the quadrupole-octupole multiphonon method using a simple model involving two degenerate j=3/2 multiplets with different parities.

Kammuri and Kishimoto (1978) employed the Hamiltonian of Eq. (13) with quadrupole-quadrupole and octupole-octupole interactions and (monopole and quadrupole) pairing. Using the microscopic boson expansion technique, they studied properties of negative-parity bands in ^{100}Ru, ^{112}Cd, ^{150}Sm, and ^{152}Gd.

Properties of negative-parity bands in ^{72}As have been studied by Petrovici *et al.* (1994) using a many-dimensional variational approach based on the configuration mixing of symmetry-projected complex HFB mean fields. For the Hamiltonian, Petrovici *et al.* employed the (slightly modified) G matrix. So far, however, no systematic calculations of octupole states have been carried out using this method.

D. Algebraic models

Algebraic approaches to negative-parity states are usually based on the assumption that the nucleus can be well described as a system of fermion pairs with angular momentum 0, 1, 2, and 3 (s, p, d, and f pairs), often treated as phenomenological bosons. The predictive power of these models is limited; in most cases they concentrate on the reproduction of existing data.

The prescription of describing negative-parity states by the addition of an f boson to the usual s and d bosons of the interacting-boson model was first mentioned by Iachello and Arima (1974), given in more detail by Arima and Iachello (1975, 1976), and applied to the nucleus ^{150}Sm by De Voigt *et al.* (1975). The interacting-boson Hamiltonian of s, d, and f bosons has the form

$$H_{\mathrm{IBM}}=H_{sd}+H_f+H_{\mathrm{int}}, \tag{54}$$

where H_{sd} is the usual interacting-boson Hamiltonian describing the interacting s and d bosons,

$$H_f=\epsilon_f\sum_\mu f_\mu^+ f_\mu+\frac{1}{2}\sum_{L=0,2,4,6} v_{ffff}^L\sum_M [f^+\times f^+]_{LM}[f\times f]_{LM} \tag{55}$$

is the general (two-body) f-boson Hamiltonian, and H_{int} is the general (two-body) interaction between the positive- and negative-parity bosons. For the inclusion of the g boson, see Dukelsky *et al.* (1983).

Because of the large number of parameters involved, in practical applications various simplifications have been made, such as assuming conservation of the f-boson number, or truncating terms in H_{int}. Sujkowski *et al.* (1977) and Scholten *et al.* (1978) described the excitation energies of the 1_1^-, 3_1^-, 5_1^-, and 1_2^-, 3_2^- levels in the Sm isotopes (using the sdf interacting-boson model) as transitional between the vibrational SU$_5$ limit and the rotational SU$_3$ limit. A systematic study of the octupole bands in rare-earth nuclei was performed by Barfield *et al.* (1986); see also Barfield *et al.* (1988).

Engel and Iachello (1985, 1987) suggested that octupole-deformed nuclei should be described by a system consisting of both p and f bosons, in addition to s and d bosons, whereas the description of octupole vibrations requires only additional f bosons. They have characterized the rotational spectra in the SU$_3$ and O$_4$ symmetry limits, and concluded that neither can be used to describe the experimental data, which are transitional between the octupole vibrational and octupole-deformed limits. Instead, they diagonalized the U$_{16}$ Hamiltonian with a dipole-dipole interaction added. Good fits were obtained for the energy spectra of ^{218}Ra and $^{140-148}$Ba (Kusnezov and Iachello, 1988; Liu *et al.* 1994). Figure 11 displays the $spdf$ interacting-boson model fit to the spectrum and the $B(E1)/B(E2)$ branching ratios of ^{218}Ra (Engel and Iachello, 1987).

Han *et al.* (1985) carried out a systematic study of the negative-parity bands in even-even N=88 nuclei, using a unified set of parameters. They also found that the description of $E1$ transition rates and the position of 1^- states could be improved by including a p boson. Otsuka (1986) investigated the structure of nuclear wave functions in deformed actinide nuclei for an intrinsic Hamiltonian containing an octupole and quadrupole (Nilsson) mean field. He found a significant number of collective dipole (1^-) nucleon pairs in the wave functions of low-lying states, so that p bosons should be added to the description of these nuclei. Otsuka and Sugita (1988) described the $K^\pi=0^+$, $K^\pi=0^-$ bands and transition moments in $^{220-232}$Th (and ^{220}Ra) in terms of an $spdf$-boson model. In their calculations they employed the intrinsic-state formulation (Otsuka, 1986); the intrinsic wave function was assumed to be

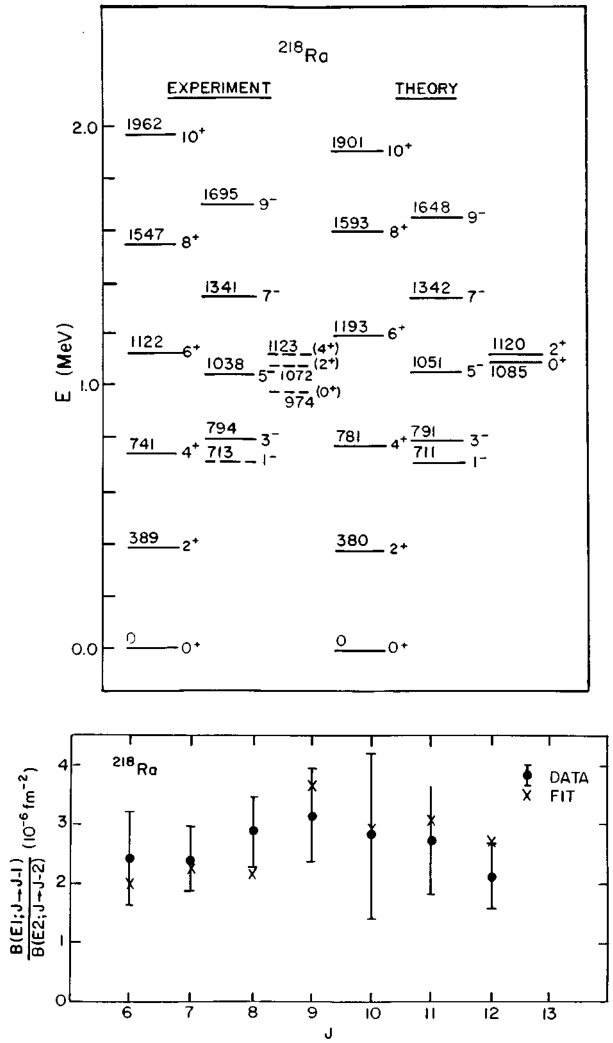

FIG. 11. Theoretical fit to the spectrum (top) and $B(E1)/B(E2)$ branching ratios (bottom) of ^{218}Ra using the *spdf* interacting-boson model (Engel and Iachello, 1987).

$$\Phi \propto (x_0 s^+ + x_1 p^+ + x_2 d^+ + x_3 f^+)^N |0\rangle, \tag{56}$$

with the amplitudes x_i determined from the variational principle (after angular momentum and parity projection). The coherent-state method was applied by Alonso *et al.* (1995) to the *spdf* SU_3 Hamiltonian with quadrupole and octupole interaction. The authors analyzed the transition to stable octupole deformations as a function of the octupole coupling constant κ_3. Another example of the application of the coherent-state formulation based on the projected states of Eq. (56) is the $1/N$ expansion of Lac and Morrison (1995). Using the *spdf* Hamiltonian, they obtained a good fit to the low-spin ($I \leq 10$) spectra of ^{226,228}Th, and to the $E1$, $E2$, and $E3$ transition rates.

Yoshinaga *et al.* (1993) applied the *sdg* proton-neutron interacting-boson model with one *f* boson to a description of the negative-parity states in the Ra isotopes, assuming that there is no octupole deformation in these nuclei, at least at low spin. They were able to reproduce approximately the measured $B(E1)/B(E2)$ branching ratios in these nuclei by adding the additional *g* boson.

Quasimolecular states have also been discussed in the framework of the algebraic vibron model (Iachello, 1981; 1984). The vibron model is a model of interacting monopole σ ($\ell^\pi = 0^+$) and dipole π ($\ell^\pi = 1^-$) bosons. Its group structure is given by the compact group U_4. There are two dynamical symmetry limits of the vibron model, O_4 and U_3. The former describes a system with a permanent dipole deformation, the rigid-molecule limit. The latter, the soft molecular limit, describes the rotational-vibrational spectrum around a spherical equilibrium shape. For extensions of the vibron model, see Daley and Iachello (1986), Cseh (1992). For the relation between the vibron model and the microscopic cluster model, see Cseh *et al.* (1991).

Iachello and Jackson (1982) suggested that α clustering may play an important role in the structure of heavy nuclei, and proposed a model in which the cluster states are built from s, d, and p proton and neutron pairs. This model is able to reproduce the typical low-lying negative-parity state bands seen in heavy nuclei, and small α-decay hindrance factors to members of these bands. Daley and Iachello (1983) developed this model further. The algebraic α-cluster model was used to describe the energy levels of ^{224}Ra, and, with a different selection of parameter values, the $B(E1)/B(E2)$ ratios in ^{218}Ra and ^{222}Th (Daley and Gai, 1984). Extensive calculations of the values of many observables for a large range of Ra, Th, and U isotopes were presented by Daly and Barrett (1986). Daly and Nagarajan (1986) also applied the model to describe the excited collective-parity bands in ^{156}Gd in terms of α clusters.

Alhassid *et al.* (1982) proposed that the underlying structure of an alternating-parity sequence arises from the existence of a molecular band, suggesting in particular an $\alpha + ^{14}$C molecular band in ^{18}O, and $\alpha + ^{214}$Rn in ^{218}Ra. They gave general expressions for sum rules for $E1$ and $E2$ transitions. Yang and Hwang (1987) obtained good agreement between predictions assuming molecular structure in a U_5 model and the observed levels in ^{18}O and ^{20}Ne. Energy staggering in octupole bands in deformed nuclei was studied by Chou *et al.* (1992) and Casten *et al.* (1993) in the simplified *sdf* interacting-boson model. They noted that the staggered pattern of the negative-parity bands, as well as their ordering, results from underlying dynamical symmetry.

For odd-A systems, where the couplings with the odd fermion have to be taken into account, Engel *et al.* (1987) showed that the decoupling-inversion effect in ^{225}Ra (Sec. V.D.3) is reproduced by the interacting boson-fermion model in the SU_3 limit involving a U_{16} boson core (as described above) and $4s$, $3d$, $2g$, and $1i_{13/2}$ single-particle orbitals (see also Alonso *et al.*, 1995). For even-even systems Chuu *et al.* (1993) coupled the *sdf* space of the interacting-boson model to a space spanned by a product of fermion pairs (occupying $f_{5/2}$ and $g_{9/2}$ orbitals) coupled to an *sd* space, to describe negative-parity energy levels in $^{64-76}$Ge.

Ceauşescu and Raduta (1976) employed the boson expansion technique to derive microscopically the quadrupole-octupole Hamiltonian written in terms of the quadrupole and octupole boson operators. This Hamiltonian was applied by Badea *et al.* (1978) to ^{150}Sm, ^{152}Gd, and ^{232}U using the projected coherent-state basis.

Catara *et al.* (1986) have investigated the general nature of negative-parity states in shell-model calculations truncated to generate S, P, D, and F fermion pairs, using a schematic quadrupole-quadrupole and octupole-octupole interaction and space of two degenerate orbitals with opposite parities. This collective pair approximation was extended by Yi *et al.* (1991) to describe energy levels in ^{18}O by including particle-hole states arising from excitation of the core.

Mikhailov *et al.* (1989) applied an interacting multiboson model ($spdf$ bosons) to describe the structure of ^{218}Ra. Dukelski *et al.* (1985) presented a description of low-lying octupole collective modes based upon a self-consistent Hartree-Bose description involving many interacting bosons (ℓ=0, 2, and 3).

E. Cluster models

The natural model for describing cluster configurations in light nuclei is the alpha-cluster model (Dennison, 1940, 1954; Morinaga, 1956; Brink, 1957, 1966; Buck *et al.*, 1975; Rae, 1988). Wildermuth and Kanellopoulos (1958a, 1958b) considered systems composed of clusters heavier than an alpha particle, and suggested a description of ^{20}Ne in terms of an $\alpha+^{16}$O bimolecule [see also Sheline and Wildermuth (1960) and Cseh and Scheid (1992) for a discussion of various cluster configurations in light nuclei].

In the alpha-cluster model (Brink, 1966), the A-body state is constructed from $N=A/4$ orbitals (alpha clusters), each representing two protons and two neutrons in $1s_{1/2}$ states centered around point $\boldsymbol{R}_j$ (j=1,...,N). The single-particle wave function can thus be represented by

$$\phi_i(\boldsymbol{r})=(2\nu/\pi)^{3/4}\exp[-\nu(\boldsymbol{r}-\boldsymbol{R}_j)^2]\chi_i(\xi), \qquad (57)$$

where ν is the oscillator constant and $\chi(\xi)$ is the spin-isospin function. The total wave function Φ is given by the parity- and angular-momentum-projected Slater determinant of the (nonorthogonal) single-particle states given by Eq. (57). In practical applications, the alpha coordinates $\boldsymbol{R}_j$ are treated either as variational parameters or as collective coordinates in GC calculations.

The formation of clusters in nuclei can be treated more microscopically by antisymmetrized molecular dynamics (Horiuchi, 1991). The antisymmetrized-molecular-dynamics wave function of the A-nucleon system is a parity- and angular-momentum-projected Slater determinant with the single-particle wave functions [cf. Eq. (57)]

$$\phi_j(\boldsymbol{r})=(2\nu/\pi)^{3/4}\exp\left[-\nu\left(\boldsymbol{r}-\frac{\boldsymbol{Z}_j}{\sqrt{\nu}}\right)^2+\frac{1}{2}\boldsymbol{Z}_j^2\right]\chi_j(\xi), \qquad (58)$$

where $\boldsymbol{Z}_j$ (j=1,...,A) are the coordinate parameters of *all* nucleons, which are determined from the variational principle. A sample of antisymmetrized-molecular-dynamics calculation for ^{20}Ne is shown in Fig. 44 (see Sec. VIII).

F. Vibrational approaches

In this review we concentrate mainly on static reflection-asymmetric deformations. Consequently, vibrational approaches to octupole modes are discussed only briefly. For a comprehensive review see Rohoziński (1988) and references therein.

Historically, the observation of low-lying negative-parity excitations was explained early on as arising from octupole vibrations of the nuclear surface (Lane and Pendlebury, 1960). Early attempts were also made to reproduce energy levels and transition moments in the $K^\pi=0^-$ and $K^\pi=2^-$ bands observed in many nuclei by assuming octupole Y_{30} vibrations with additional $Y_{3\pm2}$ asymmetric deformation (e.g., Lipas and Davidson, 1961; Davidson, 1962; Lipas, 1963; Leper, 1964). Davidson (1965) proposed a collective octupole Hamiltonian involving seven octupole degrees of freedom. For a critical discussion of those early models, see Rohoziński *et al.* (1982).

The collective model of octupole vibrations was developed by Donner and Greiner (1966), who described octupole states as arising from strong coupling of the octupole phonon to quadrupole rotational-vibrational states. They classified the resulting spectrum of energy levels, and were able to show that the anisotropy of the vibrations arises from the quadrupole-octupole interaction. The collective octupole coupling between states of opposite parity was considered by Zaikin (1966), who studied a collective Bohr Hamiltonian for octupole deformations with K=0 and ±1, and also considered the limit of a static octupole deformation.

As mentioned already in Sec. III.A, there have been many RPA calculations for negative-parity states in spherical nuclei. Yoshida (1962), Tamura and Udagawa (1962), Veje (1966), Raduta *et al.* (1970), and Vdovin and Soloviev (1983) employed separable octupole-octupole interactions. Abbas and Zamick (1980) performed RPA calculations with the contact interaction, and Abbas *et al.* (1981) investigated the 3^- systematics in even-even nuclei with a continuum RPA+Skyrme approach [see also Bal'butsev *et al.* (1991)]. Quasiparticle RPA calculations of octupole states based on a realistic density-dependent interaction were carried out for ^{96}Zr by Rosso *et al.* (1993) and Fayans *et al.* (1994).

A microscopic approach based on the RPA to the nature of octupole vibrational states in deformed nuclei was developed by the Dubna group (Soloviev and Vogel, 1963; Soloviev, 1965, 1976; Ivanova *et al.*, 1976). The Hamiltonian used in their quasiparticle-phonon nuclear model is that of Eq. (13), with the single-particle Hamiltonian represented by the deformed WS potential. In this model, the microscopic phonons are built from two-quasiparticle excitations by means of the RPA, and the quasiparticle-phonon interaction is treated explicitly.

Nosek *et al.* (1993a, 1993b) applied the model to parity doublets in nuclei around ^{153}Eu [see also Alikov *et al.* (1988) for inclusion of the Coriolis mixing]. For other calculations, see Bés (1963), Błocki and Kurcewicz (1969), Faessler *et al.* (1967), and Faessler and Plastino (1967).

Neergård and Vogel (1970a, 1970b) and Vogel (1976) generalized this approach to account for the Coriolis coupling between states of the intrinsic octupole quadruplet ($K^\pi=0^-,1^-,2^-,3^-$). The Hamiltonian of a deformed nucleus was taken as

$$H=H_{\rm intr}+H_{\rm rot}+H_{\rm Coriolis}, \tag{59}$$

where

$$H_{\rm rot}=\frac{\hbar^2}{2\mathscr{J}}(\boldsymbol{I}^2-I_3^2) \tag{60}$$

and

$$H_{\rm Coriolis}=-\frac{\hbar^2}{2\mathscr{J}}(I_+J_-+I_-J_+), \tag{61}$$

where $\boldsymbol{I}$ is the total angular momentum and $\boldsymbol{J}$ is the angular momentum of the octupole phonon. The intrinsic Hamiltonian of Eq. (13) was approximated using the deformed single-particle field (modified harmonic oscillator), stretched octupole-octupole interaction, and seniority-pairing force. The octupole phonons obtained in the RPA are mixed by the Coriolis term Eq. (61), giving rise to the low-lying negative-parity excitations. The inclusion of the Coriolis coupling is crucial for the explanation of experimental $B(E3)$ values, excitation energies of octupole states in deformed nuclei, and large moments of inertia of octupole bands. In particular, Neergård and Vogel (1970a, 1970b) demonstrated that the intrinsic J_+ matrix element in the RPA is very close to the spherical value:

$$\langle K+1|J_+|K\rangle=\sqrt{(3-K)(3+K+1)}. \tag{62}$$

Vogel (1976) extended the RPA calculations to the higher-spin members of octupole bands. At high spin values, transition to the two-quasiparticle regime was predicted. After the two-quasiparticle component involving high-j particles becomes aligned with the rotational axis, the octupole band becomes fragmented. Leandri and Piepenbring (1993) diagonalized the Hamiltonian of Eq. (59) in the strong-coupling two-quasiparticle basis. They obtained a satisfactory description of low-spin states of negative parity in deformed nuclei.

If the rotation is treated by means of the cranking approximation, one has to consider the Routhian given by Eq. (28). Robledo *et al.* (1986) applied the cranked RPA theory based on the Hamiltonian containing the multipole-multipole interaction with $\lambda=2$, 3, and 4, with the multipole operators symmetrized with respect to signature (Sec. III.B.1), and including the monopole-pairing interaction. Their calculations reproduce octupole bands in the actinides, and in particular the transition from the collective octupole regime to the quasiparticle regime discussed by Vogel (1976).

Since the RPA Hamiltonian of Eq. (13) describes particles moving in an average potential well, and interacting by schematic velocity-dependent forces, the wave functions of states with $K^\pi=0^-$ and 1^- contain some admixture of the c.m. motion. In order to project out this spurious component, one can add to the Hamiltonian an additional interaction guaranteeing that the translational and Galilean invariances

$$[H,\boldsymbol{P}_{\rm c.m.}]=0 \quad \text{and} \quad [H,\boldsymbol{R}_{\rm c.m.}]=-i\frac{\hbar}{M_N}\boldsymbol{P}_{\rm c.m.} \tag{63}$$

are satisfied. In Eq. (63) the quantity $\boldsymbol{P}_{\rm c.m.}$ is the momentum vector of the c.m. In practical applications, the conditions given by Eq. (63) are satisfied on the RPA level (Pyatov and Salamov, 1977; Kvasil *et al.*, 1981, 1985; Ćwiok *et al.*, 1984). Neergård and Vogel (1970a, 1970b) and Robledo *et al.* (1986) applied this procedure and found that the c.m. correction is unimportant for the excitation energies and $B(E3)$ rates of heavy nuclei.

In the context of the c.m. problem, of particular interest is the doubly stretched multipole-multipole separable interaction of Sakamoto and Kishimoto (1989), defined in terms of effective octupole operators

$$Q''_{\lambda\mu}=r''^3Y_{\lambda\mu}(\Omega''), \quad x''_i\equiv\frac{\omega_i}{\omega_0}x_i, \ (i=1,2,3). \tag{64}$$

This interaction can be viewed as an improved conventional multipole-multipole force, especially when applied together with the harmonic-oscillator potential with frequencies ω_i. First, it satisfies nuclear self-consistency rigorously, even if the system is deformed. Second, it yields the zero-energy RPA spurious modes, i.e., it automatically separates the translational and reorientation modes. Last, but not least, for this interaction the coupling between octupole and dipole modes disappears. The doubly stretched octupole interaction has been used by Mizutori *et al.* (1990, 1991a, 1991b), Nakatsukasa *et al.* (1992, 1993, 1995), and Crowell *et al.* (1995) to describe octupole correlations at high spins in superdeformed bands (see Sec. IX.B.2), and by Nakatsukasa *et al.* (1992, 1994), Nakatsukasa (1996), and Nazmitdinov and Åberg (1992) to analyze the influence of deformed-shell structures on octupole vibrations (see Sec. IX.B.1). Figure 12 (Nakatsukasa, 1996) illustrates the fragmentation of collective octupole phonons in ^{238}U. In this figure, negative-parity Routhians obtained in the Nilsson cranked RPA method with the doubly stretched octupole interaction are shown as a function of rotational frequency. The lowest-lying rotationally aligned band built upon an octupole phonon is crossed at $\hbar\omega\approx0.25$ MeV by a two-quasiparticle neutron band and quickly loses its collectivity. For higher-lying vibrational bands, this crossing and the following fragmentation appears at lower frequencies.

IV. EXPERIMENTAL SYSTEMATICS

The experimental evidence for reflection asymmetry in nuclei, if examined for an isolated nucleus or a par-

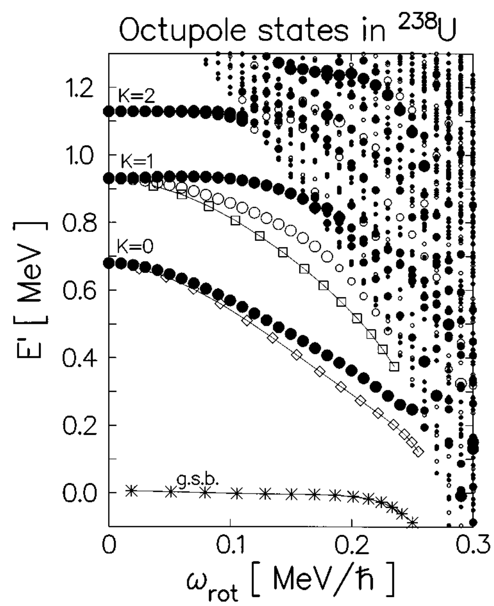

FIG. 12. Fragmentation of collective octupole vibrations in ^{238}U. Negative-parity Routhians obtained in the cranked RPA are shown as a function of rotational frequency. Large, medium, and small circles indicate RPA solutions with $E3$ transition amplitudes larger than 200 e fm^3, between 100 e fm^3 and 200 e fm^3, and lower than 100 e fm^3, respectively. Filled (open) circles indicate odd-I (even-I) band members. Experimental bands (Ward *et al.*, 1995) are denoted by stars, diamonds, and squares (Nakatsukasa, 1996).

ticular nuclear property, is not compelling. A much stronger case is evident, however, when a large body of data containing measurements of many nuclear properties in many nuclei is examined. A review of such data is presented in this and subsequent sections.

A. Low-lying 1^- and 3^- states in even-even nuclei

An obvious manifestation of reflection asymmetry in nuclei is the occurrence of low-lying negative-parity states which are collective in nature. States having such properties were first identified in Ra and Th isotopes with $N \approx 136$ by the Berkeley group (Asaro *et al.*, 1953; Stephens *et al.*, 1954, 1955) using alpha spectroscopy. In this mass region the 1^- and 3^- states remain energetically higher than the 2^+ and 4^+ states, respectively, which rules out a simple interpretation in terms of octupole deformation. Only at higher spin do the negative-parity states become interspersed regularly with the positive-parity states (see Sec. IV.B). Figure 13 shows the variation of the energy of the 1^-, 3^- states as compared to the 2^+, 4^+ states for selected lanthanide nuclei; Fig. 14 shows the corresponding behavior for Ra and Th isotopes. For actinide nuclei the minimum of the energy of negative-parity states is very localized in N, while there are insufficient data to determine the corresponding localization in Z. For the lanthanide region, this minimum value is attained outside the transitional region where octupole effects are strongest ($N \geqslant 90$). The systematic behavior of excited negative-parity states has been discussed by several authors. Neergård and Vogel (1970a) described the properties of negative-parity states in Ra and light Th isotopes in terms of the RPA (see Sec. III.F). Peker *et al.* (1981) also concluded that a vibrational interpretation is appropriate, and that the behavior of the negative-parity states can be explained in terms of Coriolis coupling between the $K^\pi = 0^-$, 1^-, 2^-, and 3^- bandheads. Sheline (1980) compared the behavior of these states in actinide nuclei with excited 0^+ states, and concluded that the $K^\pi = 0^-$ bands and the excited $K^\pi = 0^+$ bands are structurely more related to each other than to the ground-state band. However, the nature of the excited 0^+ states has not been explained satisfactorily. Żylicz (1986) excluded the interpretation of these states in terms of harmonic octupole vibrations, on the grounds that the ratio of energies of the excited 0^+ and 0^- bandheads, which should be 2 for vibrational structure, is in the range 3–4 for the light Ra nuclei.

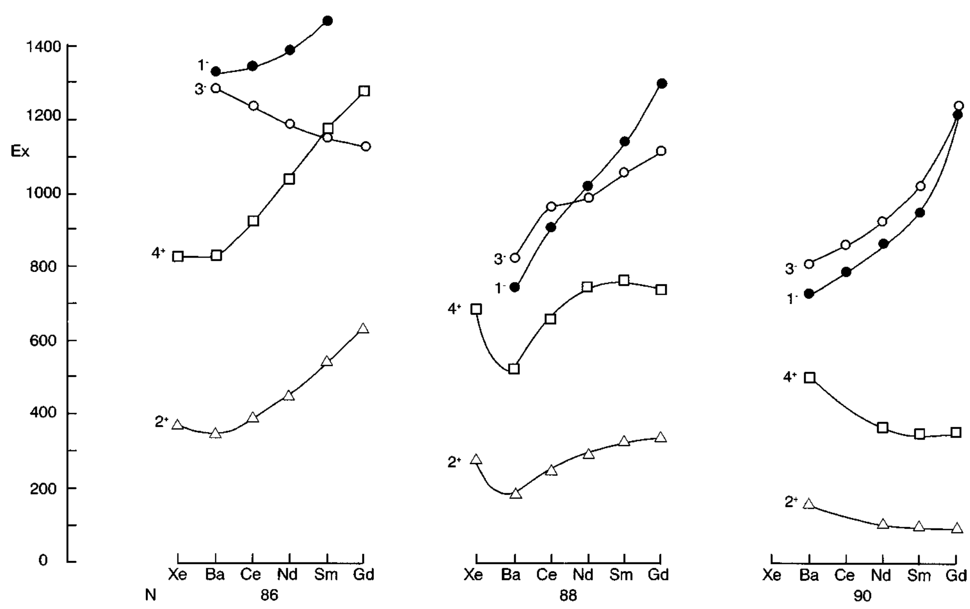

FIG. 13. Excitation energies (keV) of the yrast 2^+, 4^+, 1^-, and 3^- states in the N=86–90 region.

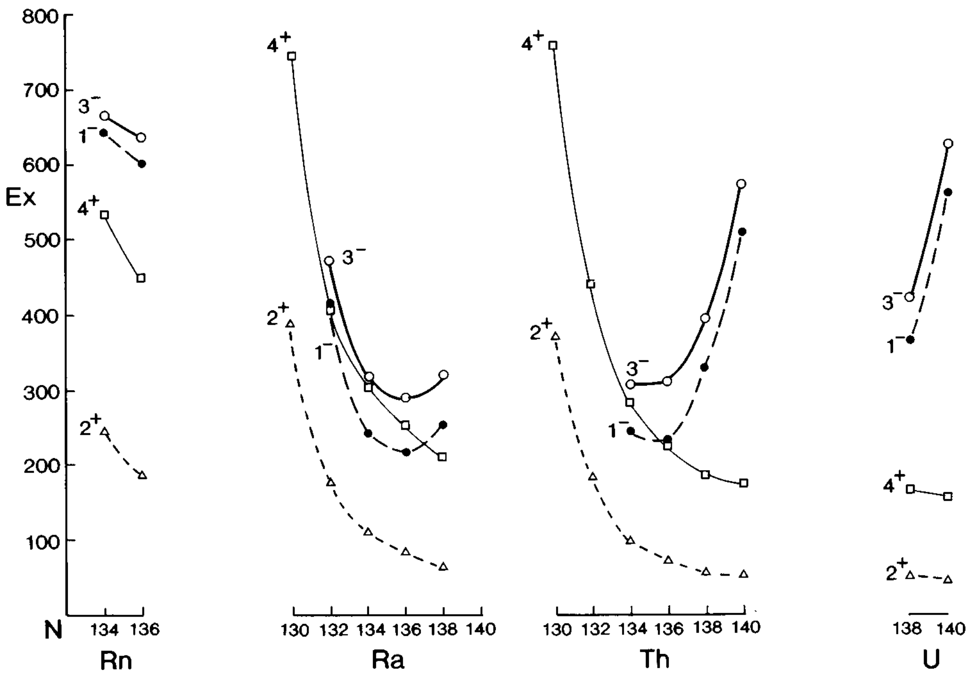

FIG. 14. Excitation energies (keV) of the yrast 2^+, 4^+, 1^-, and 3^- states in the Z=86–92 region.

Kurcewicz *et al.* (1976, 1977) looked for lower-lying 0^+ states populated by alpha decay, without success.

A more extensive analysis of 1^- and 3^- states in actinide and lanthanide nuclei has been carried out by Cottle and Bromley (1986), who characterized the variation of excitation energy of 3^- states in terms of the onset of quadrupole deformation and the filling of the lower-energy member of a $\Delta\ell=3$ pair. They also drew attention to the relation between the relative energies of the 3^- and the 1^- states and the ratio of energies between the 4^+ and the 2^+ states (see Fig. 15). Particularly for the lanthanides, the amount of quadrupole deformation plays a dominant role in determining the relative spacing of the 1^- and 3^- members of the $K^\pi=0^-$ band. This investigation has also been extended (Cottle *et al.*, 1988; Cottle, 1990a) to other regions.

Zamfir *et al.* (1989) have established a simple parametrization for the energies of 3^- states in all nuclei with $A\geqslant 30$ (Fig. 16):

$$E(3_1^-)=19A^{-1/3}-0.5N_t, \tag{65}$$

where N_t is the sum of the valence-nucleon numbers. Deviations from normal behavior characterize nuclei having the strongest octupole correlations (they are in the transitional lanthanide and actinide regions).

B. Alternating-parity rotational bands

The striking experimental feature of even-even nuclei with $Z\approx 88$, $N\approx 134$ and $Z\approx 60$, $N\approx 88$ is the interspacing of negative- and positive-parity states with the sequence $I^+,(I+1)^-,(I+2)^+,\ldots$, for states with $I>5$. The first observations of such band structure in heavy nuclei were in ^{218}Ra (Fernández-Niello *et al.*, 1982) and ^{222}Th (Ward *et al.*, 1983; Bonin *et al.*, 1983). In medium-mass nuclei, sequences of nuclear states with similar features were observed much earlier, for example, in ^{152}Gd (Zolnowski *et al.*, 1975), in ^{150}Sm (Sujkowski *et al.*, 1977), and in ^{150}Gd (Haenni and Sugihara, 1977), but the first connection with static octupole deformation in this mass region was made by Phillips *et al.* (1986), who studied ^{142,144,146}Ba using fission spectroscopy.

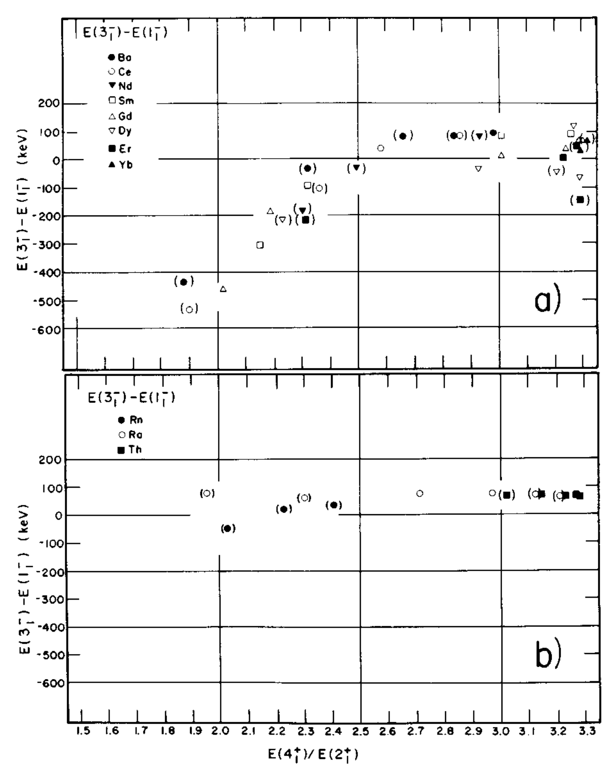

FIG. 15. The systematic behavior of $E(3_1^-)-E(1_1^-)$ in the regions (a) Z=56–70 and (b) Z=82–90. Parentheses denote tentative assignments (Cottle and Bromley, 1986).

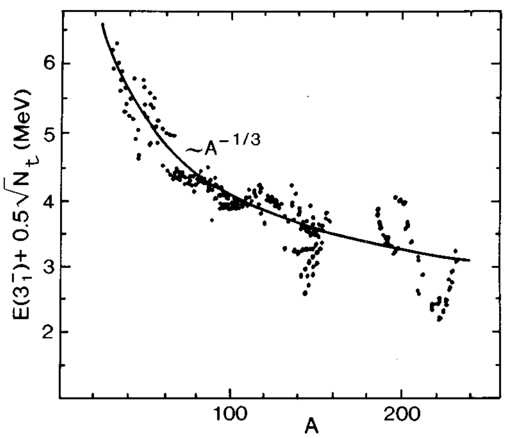

FIG. 16. Mass-number dependence of experimental 3_1^- energies, corrected for a $-0.5\sqrt{N_t}$ dependence, where N_t is the sum of the valence-nucleon numbers, $N_t=N_p+N_n$. All non-doubly-closed shell nuclei with $A\geqslant30$ and $N_t<26$ are included. The curve is an $A^{-1/3}$ function (Zamfir *et al.*, 1989).

Tables I and II list the nuclei in which such bands have been established, together with the reactions and experimental methods employed. Figure 17 shows a typical example, ^{226}Th, in which the sequence has been observed up to spin 20 (Schüler *et al.*, 1986, Ackermann *et al.*, 1993). Available data for even-even nuclei with $Z=88$ and 90, and N=86, 88, and 90 are shown in Figs. 18 and 19. In these figures, the data are plotted as $\mathscr{J}/\hbar^2$ versus $\hbar\omega$ for each parity band; here $\mathscr{J}=\hbar I_x/\omega$ is the kinematic moment of inertia, $I_x=\sqrt{(I+1/2)^2-K^2}$ (I, K in units of $\hbar$) is the angular momentum perpendicular to the symmetry axis, and $\hbar\omega=dE/dI_x$ is the rotational frequency. The division between nuclei exhibiting characteristics of reflection asymmetry and reflection symmetry is apparent for $N>136$ for Th nuclei, for which data are most widely available. The nature of the symmetry becomes apparent in the plots of $\omega(\pi=-1)/\omega(\pi=+1)$ versus I. This ratio should equal 1 for perfectly reflection-asymmetric nuclei, but equals $[4(I-3)-2)]/(4I-2)$ for rotation of an aligned-octupole phonon (Nazarewicz and Olanders, 1985a) (see Fig. 20).

In nuclei with $Z\approx60$, the degeneracy of the positive and negative bands is only apparent between I=7 and I=13, and for N=86 and N=88, in the few cases where extensive data are available. In ^{150}Sm for example, the positive-parity band appears to cross a reflection-symmetric band at $I\approx15$ (Urban *et al.*, 1987) see Sec. VI. For N=90 nuclei the increase in quadrupole deformation pushes the positive-parity states to much lower energies than the octupole states, and the latter states are usually interpreted as being vibrational in origin (see also the discussion in Sheline and Sood, 1986).

Similar structures to that of even-even octupole nuclei are observed in transitional odd-mass and odd-odd nuclei in which the odd particles are weakly coupled to the core. Figure 21 shows the yrast sequence of ^{219}Ra (Cottle *et al.*, 1986) compared to its neighbors ^{218,220}Ra. (The term "yrast" denotes the lowest-energy state having a given angular momentum.) The ground-state band of ^{219}Ra shows an alternating-parity structure, and is consistent with an interpretation in terms of an odd neutron weakly coupled to an average ^{218}Ra–^{220}Ra core. Similar examples have been found in other nuclei with Z=87–90 and $N<132$: ^{217}Fr (Aïche *et al.*, 1988), ^{217}Ra (Roy *et al.*, 1984) ^{219}Ac (Drigert and Cizewski, 1985; Khazrouni *et al.*, 1985; Cristancho *et al.*, 1994), ^{221}Ac (Aïche *et al.*, 1994), ^{221}Th (Dahlinger *et al.*, 1988), and in the odd-odd nuclei ^{216}Fr (Debray *et al.*, 1990), ^{218}Ac (Debray *et al.*, 1994), and ^{220}Ac (Schulz *et al.*, 1991). In the light-lanthanide region the level structure of transitional odd-A nuclei has been interpreted variously in terms of a $h_{11/2}$ proton coupled to an octupole phonon, as in the case of ^{151}Eu (Vermeer *et al.*, 1993, see also Jongman *et al.*, 1994), and a neutron coupled to a reflection-symmetric triaxial core in the case of ^{151}Sm (Khan *et al.*, 1994; see also Basu *et al.*, 1994). Alternating-parity structures have also been observed in ^{143}Ba (Zhu *et al.*, 1995) and in ^{149}Sm (Basu *et al.*, 1994). For nuclei farther away from the closed shell, better examples of parity doubling are seen, as discussed in Sec. V.D.1.

C. Enhanced $E1$ transitions

A common property of nuclei exhibiting the features of reflection asymmetry is the occurrence of relatively large $E1$ transition probabilities between the yrast positive- and negative-parity bands. The $B(E1)$ values in these mass regions range from 10^{-4} to 10^{-2} s.p.u. [typical $B(E1)$ values are less than 10^{-5} s.p.u.] Assuming the strong-coupling limit and axial shape, there is a simple relation between the $E1$ transition probability and the intrinsic (transition) electric dipole moment D_0 (see Sec. II.B):

$$B(E1;IK\rightarrow I'K)=\frac{3}{4\pi}D_0^2\langle IK10|I'K\rangle^2. \tag{66}$$

In the presence of Coriolis coupling and/or triaxiality, relation (66) has to be modified. For K=1/2, for instance, there appears in lowest order a signature-dependent term proportional to (Bohr and Mottelson, 1975)

$$B(E1;I\rightarrow I')=\frac{3}{4\pi}|(I\,\tfrac{1}{2}10|I'\,\tfrac{1}{2})D_0 \\ +(-1)^{I+\frac{1}{2}}(I-\tfrac{1}{2}11|I'\,\tfrac{1}{2})D_1|^2, \tag{67}$$

where $D_{\mu=1}$ is the spherical component of $\boldsymbol{D}$ (see Sec. II.B). [A similar term appears in nuclei with low-lying octupole vibrational states, through the Coriolis coupling between K=0 and K=1 bands (see Sec. VII.E)].

In most cases, absolute values of $B(E1)$ are not available, and D_0 has to be extracted from the known $B(E1)/B(E2)$ branching ratios $T(E1)_{I\rightarrow I-1}/T(E2)_{I\rightarrow I-2}$, in which case the $B(E2)$ rates are assumed to follow the rotational relationship

$$B(E2)=\frac{5}{16\pi}Q_0^2\langle IK20|I'K\rangle^2, \tag{68}$$

TABLE I. Observed alternating-parity rotational bands in nuclei from the Ra-Th region, and reactions used.

Nucleus	Reaction	Reference
^{216}Fr (Z=87)	^{208}Pb(^{11}B,3n)	Debrey *et al.* (1990)
^{217}Fr	^{210}Pb(^{11}B,4n)	Aïche *et al.* (1988)
^{217}Ra (Z=88)	^{208}Pb(^{12}C,3n), ^{208}Pb(^{13}C,4n)	Roy *et al.* (1984)
^{218}Ra	^{208}Pb(^{13}C,3n)	Fernández-Niello *et al.* (1982)
		Gono *et al.* (1986)
	^{13}C(^{208}Pb,3n)	Gai *et al.* (1988)
	^{208}Pb(^{14}C,4n)	Schulz *et al.* (1989)
	^{208}Pb(^{13}C,3n)	Wieland *et al.* (1992b)
^{219}Ra	^{208}Pb(^{14}C,3n)	Cottle *et al.* (1986)
		Wieland *et al.* (1992a)
^{220}Ra	^{208}Pb(^{18}O,α2n)	Burrows *et al.* (1984)
	^{208}Pb(^{14}C,2n)	Cottle *et al.* (1984)
		Celler *et al.* (1985)
		Shriner *et al.* (1985)
	^{208}Pb(^{18}O,α2n)	Smith *et al.* (1995)
^{221}Ra	^{210}Pb(^{14}C,3n)	Fernández-Niello *et al.* (1991)
^{224}Ra	^{226}Ra(^{58}Ni,^{60}Ni)	Poynter *et al.* (1989a)
	^{226}Ra(α,α'2n)	Marten-Tölle *et al.* (1990)
^{226}Ra	^{226}Ra Coulomb excitation	Wollersheim *et al.* (1993)
	^{226}Ra(d,pn)	Ackermann *et al.* (1993)
^{218}Ac (Z=89)	^{209}Bi(^{12}C,3n)	Debray *et al.* (1994)
	^{209}Bi(^{13}C,4n)	Debray *et al.* (1994)
^{219}Ac	^{209}Bi(^{13}C,3n)	Drigert and Cizewski (1985, 1986)
		Khazrouni *et al.* (1985)
		Cristancho *et al.* (1994)
^{220}Ac	^{209}Bi(^{14}C,3n)	Schulz *et al.* (1990, 1991)
^{221}Ac	^{209}Bi(^{14}C,2n)	Aïche *et al.* (1994)
^{220}Th (Z=90)	^{208}Pb(^{16}O,4n)	Bonin *et al.* (1985)
^{221}Th	^{208}Pb(^{16}O,3n)	Dahlinger *et al.* (1985, 1988)
^{222}Th	^{208}Pb(^{18}O,4n)	Ward *et al.* (1983)
		Bonin *et al.* (1985)
		Schwartz *et al.* (1987)
		Smith *et al.* (1995)
^{223}Th	^{208}Pb(^{18}O,3n)	Dahlinger *et al.* (1988)
^{224}Th	^{208}Pb(^{18}O,2n)	Schwartz *et al.* (1986)
	^{226}Ra(α,6n)	Schüler *et al.* (1986), Ackermann *et al.* (1993)
^{225}Th	^{226}Ra(α,5n)	Hughes *et al.* (1990)
^{226}Th	^{226}Ra(α,4n)	Schüler *et al.* (1986), Ackermann *et al.* (1993)
^{228}Th	^{226}Ra(α,2n)	Schüler *et al.* (1986), Ackermann *et al.* (1993)
^{230}U (Z=92)	^{230}Th(α,4n)	Ackermann *et al.* (1993)

where Q_0 is the transition quadrupole moment. Since many nuclei in the mass regions of interest are not good rotors, the use of the strong-coupling formulas, Eqs. (66) and (68), is questionable. Nevertheless, they provide a consistent way to extract D_0 from the data. In particular, for K=0 bands the intrinsic dipole moment is

$$D_0 \approx \left\{ \frac{5(I-1)}{8(2I-1)} \frac{B(E1;I\to I-1)}{B(E2;I\to I-2)} \right\} Q_0. \qquad (69)$$

Tables III and IV give examples of $B(E1)$ values measured for even-even nuclei in the light-lanthanide and actinide regions.

The experimental values of D_0 are shown in Fig 22, where they are compared with the theoretical values of Butler and Nazarewicz (1991) (Sec. VII.B) and of Egido and Robledo (1991b, 1992) (Sec. VII.C). The trends shown in Fig. 22 demonstrate that large fluctuations with

TABLE II. Observed alternating-parity rotational bands in nuclei from the Ba-Sm region, and reactions used.

Nucleus	Reaction	Reference
^{142}Ba (Z=56)	^{252}Cf fission	Phillips *et al.* (1986)
	^{252}Cf, ^{242}Pu fission	Zhu *et al.* (1995)
^{143}Ba	^{252}Cf, ^{242}Pu fission	Zhu *et al.* (1995)
^{144}Ba	^{252}Cf fission	Phillips *et al.* (1986)
	^{252}Cf, ^{242}Pu fission	Zhu *et al.* (1995)
^{146}Ba	^{252}Cf fission	Phillips *et al.* (1986)
	^{252}Cf, ^{242}Pu fission	Zhu *et al.* (1995)
^{144}Ce (Z=58)	^{252}Cf, ^{242}Pu fission	Zhu *et al.* (1995)
^{146}Ce	^{252}Cf fission	Phillips *et al.* (1988)
^{148}Ce	^{252}Cf fission	Phillips *et al.* (1988)
^{146}Nd (Z=60)	^{150}Nd$(\alpha,\alpha'4n)$	Urban *et al.* (1988)
	^{136}Xe(^{13}C,3n)	Urban *et al.* (1991)
^{148}Nd	^{150}Nd$(\alpha,\alpha'2n)$	Urban *et al.* (1988)
	^{252}Cf fission	Durell *et al.* (1988)
	^{148}Nd Coulomb excitation	Ibbotson *et al.* (1991, 1993)
^{151}Pm (Z=61)	^{150}Nd$(\alpha,p2n)$	Vermeer *et al.* (1990)
		Urban *et al.* (1990)
^{148}Sm (Z=62)	^{130}Te(^{22}Ne,4n)	Urban *et al.* (1991)
^{149}Sm	^{148}Nd$(\alpha,3n)$	Basu *et al.* (1994)
^{150}Sm	^{150}Nd$(\alpha,4n)$	Sujkowski *et al.* (1977)
		Urban *et al.* (1987)
^{151}Sm	^{150}Nd$(\alpha,3n)$	Basu *et al.* (1994)
		Khan *et al.* (1994)
^{149}Eu (Z=63)	^{139}La(^{13}C,3n)	Jongman *et al.* (1994)
^{150}Eu	^{136}Xe(^{19}F,5n)	
	^{148}Nd(^{7}Li,5n)	Jongman *et al.* (1994)
^{151}Eu	^{136}Xe(^{19}F,4n)	
	^{148}Nd(^{7}Li,4n)	Jongman *et al.* (1994)
	^{150}Nd(^{6}Li,5n)	Vermeer *et al.* (1993)
^{153}Eu	^{150}Nd(^{7}Li,4n)	Pearson *et al.* (1994)
^{150}Gd (Z=64)	^{150}Sm$(\alpha,4n)$, ^{152}Sm$(\alpha,6n)$	Haenni and Sugihara (1977)
^{152}Gd	^{150}Sm$(\alpha,2n)$, ^{152}Sm$(\alpha,4n)$	Zolnowski *et al.* (1975)

Z and N in the values of D_0 can occur due to shell effects. These fluctuations are discussed in more detail in Sec. VII.

There is less information on the systematic behavior of D_0 as a function of angular momentum. For the transitional nucleus ^{218}Ra, a decrease in $B(E1;I\rightarrow I-1)$ is observed in the spin range 6–8, although it is not clear whether this is associated with the large drop in $B(E2)$ observed below spin 4 (Gai *et al.*, 1988). Gai (1988) has pointed out that the fraction of the $E2$ energy-weighted sum rule exhausted by the lowest 2^+ state is unusually large for the light Ra and Th nuclei. Figure 23 displays the available data for the Ra-Th region for heavier nuclei, whose quadrupole deformation is rather stable; the rotation-induced variation in the quadrupole moment should not influence the value of D_0. For most of these cases the value of D_0/Q_0 stays rather constant with spin, at least above I=6. One exception is ^{226}Ra, where a dip in the value of this quantity is seen at $I\approx 4$. This feature cannot be reproduced by macroscopic-microscopic theories of D_0 (Leander *et al.*, 1986; Butler and Nazarewicz, 1991) for nuclei whose shape remains constant with spin. For ^{226}Ra this seems to be the case, as indicated by the behavior of its quadrupole and octupole moment (see Sec. IV.D). However, fluctuations in the value of D_0 might be expected because of the cancellation effects in its macroscopic and microscopic components that are responsible for small $E1$ moments in ^{224}Ra. In the lanthanides, a similar effect is seen in ^{146}Ba, which shows fluctuations with spin;

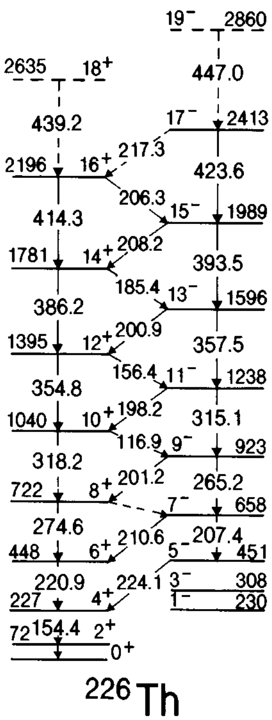

FIG. 17. Level scheme of ^{226}Th, taken from Schüler *et al.* (1986; see also Ackermann *et al.*, 1993). The level and transition energies are in keV.

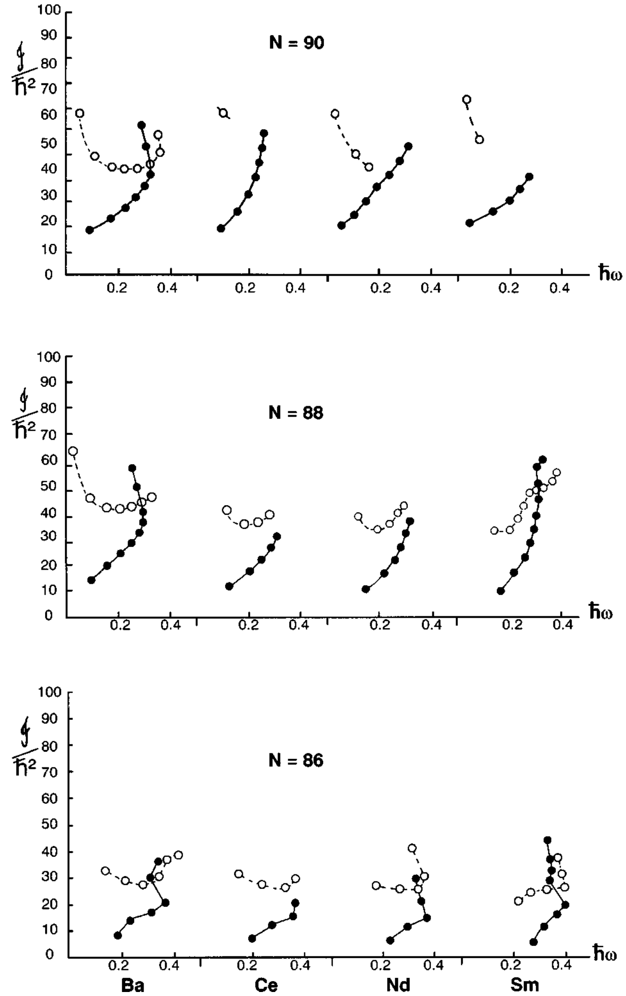

FIG. 18. Kinematic moment of inertia $\mathscr{J}/\hbar^2$ (in MeV^{-1}) as a function of rotational frequency $\hbar\omega$ (in MeV) for rotational bands in even-even nuclei with N=86,88,90.

for this nucleus the overall value of D_0 is rather small, and is probably sensitive to shell effects (see Sec. VII.B). In ^{150}Sm the values of D_0 are seen to decrease markedly for transitions deexciting higher-spin members of the positive-parity ground-state band. This behavior is associated with the restoration of reflection symmetry in this nucleus above spin 10 (see Sec. VI). Similar changes in D_0 are not apparent in ^{142}Ba (Phillips *et al.*, 1986; Mach, Nazarewicz *et al.*, 1990; Zhu *et al.*, 1995).

The occurrence of large $E1$ transition strengths between low-lying states is not confined to nuclei in the "octupole" mass regions around ^{144}Ba and ^{222}Th. The largest $B(E1)$ so far observed experimentally (Millener *et al.*, 1983) is 0.36 s.p.u., for the decay of the 1/2$^-$ state in ^{11}Be. It is believed that this strong $E1$ transition is related to halo properties of ^{11}Be (see Sec. X.D). Large $E1$ transition strengths are also observed in sd-shell nuclei for which $Z \neq N$, for example in ^{18}O (Gai *et al.*, 1983; see also Sec. VIII.B). In heavy nuclei, studies have revealed that large $E1$ transition strengths are observed between high-spin states in nuclei such as ^{163}Er that are well removed from the well-established octupole regions (Butler, 1990; see also Garrett, 1984; Balodis *et al.*, 1991; Ogaza *et al.*, 1993; Brockstedt *et al.*, 1994; Jongman *et al.*, 1994). Nuclear resonance fluorescence studies have shown that the *summed* isovector $E1$ strength for ground-state transitions to low-lying states remains remarkably constant for the mass region A=150–174 (Zilges *et al.*, 1991; Friedrichs *et al.*, 1992). The strongest $E1$ transition observed in these rare-earth nuclei is usually to the lowest 1$^-$ state, although enhanced $E1$ transitions have also been observed to excitations near 2.5 MeV in rare-earth nuclei (Kneissl *et al.*, 1993) and near 3.5 MeV in ^{116,124}Sn (Govaert *et al.*, 1994) (these have been interpreted as arising from two-phonon octupole-γ vibrational excitations). The experimental (e,e') form factor for the lowest 1$^-$ state in ^{48}Ti, ^{164}Dy, ^{232}Th, and ^{238}U has been described in terms of surface octupole vibrations (see Sec. VII.E). Large $B(E1)$ strengths are also observed for low-lying transitions in nuclei near closed shells.

D. $E3$ transitions

For low-lying states in nuclei, the ground-state $E3$ transitions are predominantly isoscalar, and typically exhaust 4–7 % of the isoscalar energy-weighted sum rule (Kirson, 1982; Pignanelli, 1990). Consequently, low-energy $B(E3)$ values are good measures of octupole collectivity (Rohoziński, 1988). In the limit of strong coupling, the octupole deformation β_3 is related

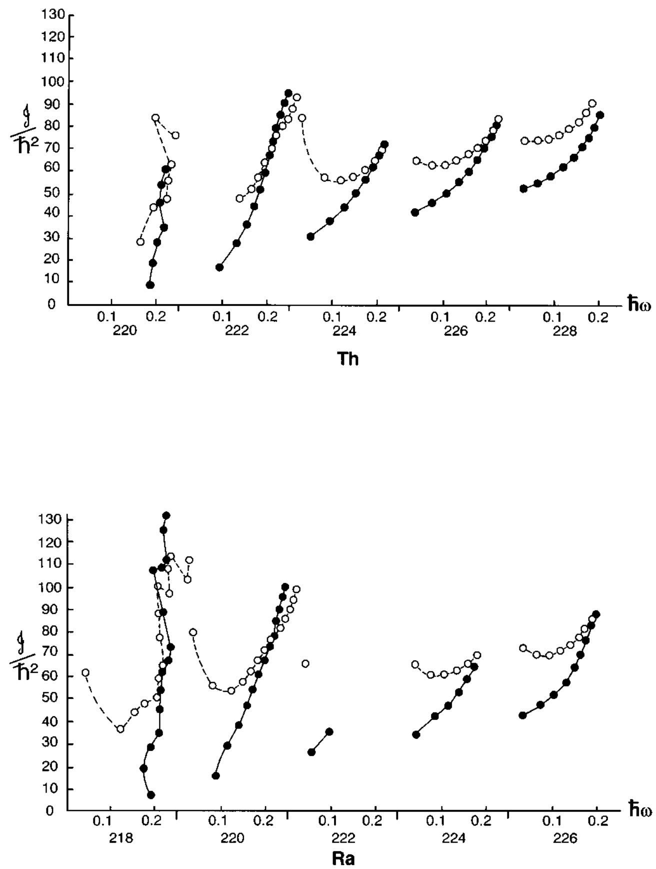

FIG. 19. Kinematic moment of inertia $\mathcal{J}/\hbar^2$ (in MeV^{-1}) as a function of rotational frequency $\hbar\omega$ (in MeV) for rotational bands in even-even nuclei with $Z=88,90$.

to the reduced transition probability $B(E3)\uparrow \equiv B(E3;0^+\rightarrow 3^-)$ from the ground state to the first 3^- state:

$$\beta_3=\frac{4\pi}{ZR^3}\left[\frac{B(E3)\uparrow}{e^2}\right]^{1/2}, \tag{70}$$

where the value of $B(E3)\uparrow$ can be deduced from the partial mean lifetime for $E3$ γ-ray emission to the ground state:

$$\tau_{E3}(s)=(0.0123)E(\mathrm{MeV})_{3_1^-}^{-7}[B(E3)\uparrow/e^2\ \mathrm{fm}^6]^{-1}. \tag{71}$$

The values of the transition probability and experimental octupole deformations deduced from $0^+_{\mathrm{g.s.}}\rightarrow 3^-_1$ transitions have been compiled (Spear, 1989; see also Raman *et al.*, 1991) and are displayed in Fig. 24. Spear and Catford (1990) noted that the maxima in the $B(E3)$ values at N = 34, 56, 88, and 134, and (more ambiguously) at Z=30, 40, 62, and 88 (see Fig. 24) are well correlated with the predicted regions of stable octupole deformation (Sec. III.B). The values of $B(E3)$ are typically 30–50 s.p.u. for lanthanide nuclei in the region of octupole instability; they are plotted as a function of N in Fig. 25. It is evident that this quantity reaches a maximum for N=88–90. This might arise from the change in octupole collectivity between these neutron numbers, as suggested by the corresponding behavior in energy-level spectra (Fig. 18), or from the change in quadrupole deformation, which splits the $E3$ strength over the components $K^\pi=0^-$, 1^-, 2^-, and 3^- (Scholten *et al.*, 1978).

Raman *et al.* (1991) analyzed the anharmonicity of the octupole mode by inspecting the correlation between $B(E3)\uparrow$ and E_{3^-}. Guided by the relation

$$B(E3)\uparrow \propto Z^2A^{1/3}E_{3^-}^{-1} \tag{72}$$

obtained in the limit of the hydrodynamical model (Bohr and Mottelson, 1975), they analyzed the data according to the expression

$$B(E3)\uparrow Z^{-2}A^{-1/3}=KE_{3^-}^{\eta}, \tag{73}$$

where the values of K and η were obtained by means of a least-squares fit to experimental values. They obtained values of η ranging between $\eta\sim -0.7$ in spherical nuclei and $\eta\sim -0.5$ in deformed nuclei, indicating strong anharmonicities.

Although $B(E3;I\rightarrow I')$ has been measured for the transition from ground-state to the lowest 3^--state in many nuclei, there is less information on this quantity for higher-lying members of rotational bands in transitional and deformed nuclei. It has been realized that the yields of high-spin members of octupole bands following multiple Coulomb excitation are quite sensitive to the $E3$ matrix elements connecting them to the ground-state band (Butler, 1988). Figure 26 shows the experimental values for $\lambda=2,3$ of the matrix elements

$$\langle I\|E_\lambda\|I'\rangle=\{(2I+1)B(E\lambda;I\rightarrow I')\}^{1/2} \tag{74}$$

$$=\left\{\frac{(2I+1)(2\lambda+1)}{16\pi}\right\}^{1/2}\langle I0\lambda 0|I'0\rangle\mathcal{Q}_{\lambda 0,c}, \tag{75}$$

obtained for the ground-state $K^\pi=0^+$ band and the lowest $K^\pi=0^-$ band in ^{148}Nd (Ibbotson *et al.*, 1993) and in ^{226}Ra (Wollersheim *et al.*, 1993). In Eq. (75), obtained assuming axial shape and the rotational limit, $\mathcal{Q}_{20,c}$= Q_0, and $\mathcal{Q}_{30,c}$ is the octupole moment. For ^{226}Ra both quadrupole and octupole matrix elements can be fitted with the constant values $\mathcal{Q}_{20,c}$=750 fm^2 and $\mathcal{Q}_{30,c}$=3100 fm^3 (Wollersheim *et al.*, 1993). Application of Eqs. (6) and (7) to the measured matrix elements in ^{226}Ra yields $\beta_3\approx 0.10$ (Wollersheim *et al.*, 1993), in agreement with calculations by Leander *et al.* (1982) and Sobiczewski *et al.* (1988) (see Sec. III.B.2). In ^{148}Nd the corresponding values are $\mathcal{Q}_{20,c}$=400 fm^2 and $\mathcal{Q}_{30,c}$=1500 fm^3 (Ibbotson *et al.*, 1993), with a value of β_3 (≈ 0.12) somewhat higher than that predicted by mean-field calculations (Urban *et al.*, 1988).

Nazarewicz and Tabor (1992) have used the collective model of Krappe and Wille (1969) for octupole deformation (Sec. III.F) to show that $B(E3;0^+\rightarrow 3^-)$ is independent of the curvature of the nuclear potential, whereas the parity splitting is a strong function of this quantity. This implies that if the curvature varies with angular momentum, $\mathcal{Q}_{30,c}$ should remain constant, in contrast to the parity splitting. In addition to this effect, Rohoziński and Greiner (1983) have concluded that the

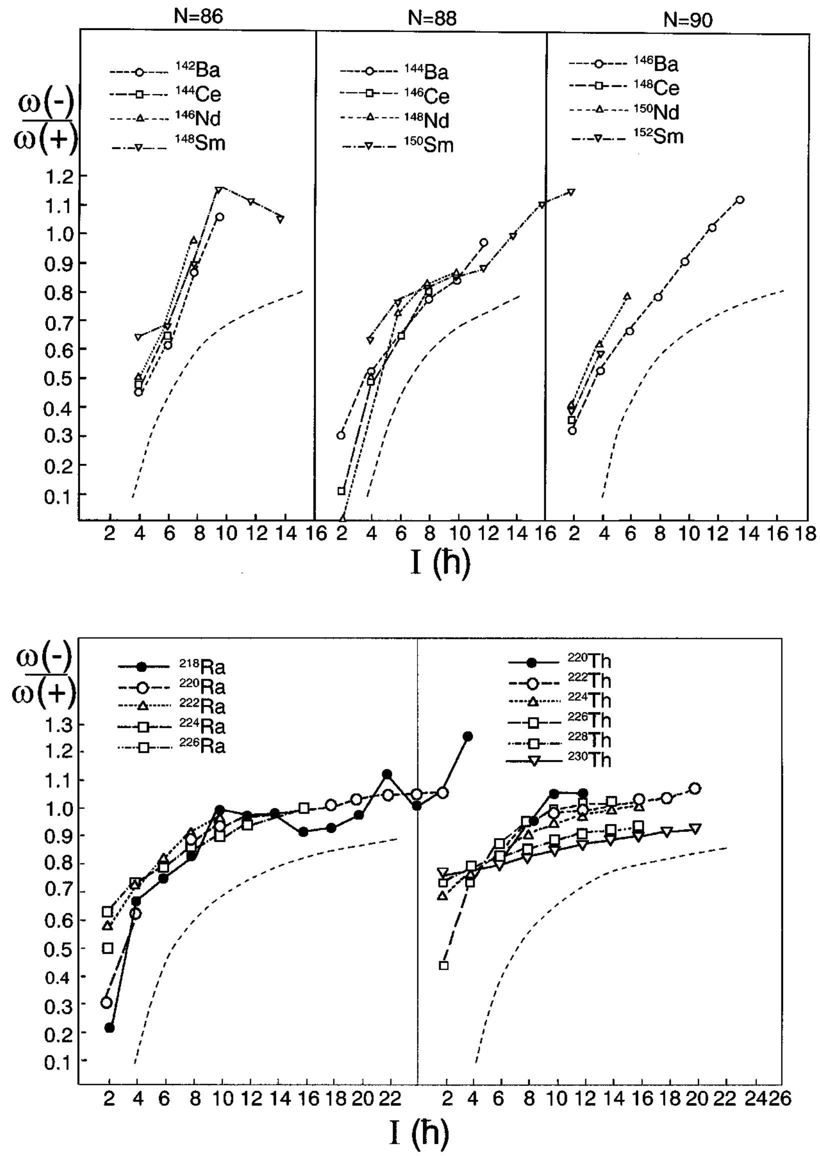

FIG. 20. Plot of $\omega(\pi=-1)/\omega(\pi=+1)$ versus I for nuclei with N=86,88,90 and nuclei with Z=88,90. This ratio should equal unity for rotating rigidly reflection-asymmetric systems. The dashed line shows how it varies in the case of an aligned octupole phonon.

octupole matrix elements should be roughly independent of Coriolis and centrifugal effects, which gives another mechanism for the constancy of $\mathcal{Q}_{30,c}$.

In the *sdf* version of the IBM (cf. Sec. III.D), the $E3$ operator is a one-boson operator obtained by a direct coupling of *sf* and *df* bosons to J=3:

$$Q_{3\mu}=e_3^{(sf)}\{[s^+\times f^*]_{3\mu}+[f^+\times s^*]_{3\mu}\}$$
$$+e_3^{(df)}\{[d^+\times f^*]_{3\mu}+[f^+\times d^*]_{3\mu}\}. \tag{76}$$

Scholten *et al.* (1978) employed Eq. (76) to calculate $B(E3)$ values for the Sm isotopes.

For particular closed-shell or sub-shell nuclei in which there are low-energy particle-hole $E3$ excitations for both protons and neutrons, large $B(E3,0^+\rightarrow 3^-)$ values have been observed (Spear, 1989), for example, in ^{16}O (14 s.p.u.), ^{40}Ca (31 s.p.u.), ^{132}Sn (> 7 s.p.u.; Fogelberg *et al.*, 1994), and ^{208}Pb (34 s.p.u.). The largest values for observed transitions have been measured in ^{96}Zr (Mach, Ćwiok *et al.*, 1990; Ohm *et al.*, 1990; Hofer *et al.*, 1993; Horen *et al.*, 1993), ≈50–60 s.p.u.(see Sec. X.A for calculations), and in ^{148}Gd (77±11 s.p.u.; Piiparinen *et al.*, 1993). Large $E3$ transition strengths have also been reported in the octupole transitional nucleus ^{229}Th between the ground state and the octupole vibrational band built upon the ground state (Bemis *et al.*, 1988). For the $E3$ transitions in the rotational bands of ^{148}Nd and ^{226}Ra, deduced from multiple Coulomb excitation (see above), much larger values have been measured, for example, 142±15 s.p.u. for the $9^-\rightarrow 6^+$ transition in ^{226}Ra (Wollersheim *et al.*, 1993).

V. PROPERTIES OF LOW-LYING STATES

The measured properties of nuclei in their ground state (binding energies, decay properties, and properties of the odd particle) show detailed evidence for strong octupole correlations, which is quite separate from the signature given by a rotational spectrum; a review of these properties is given in this section. For earlier reviews, the reader is referred to the seminal works of

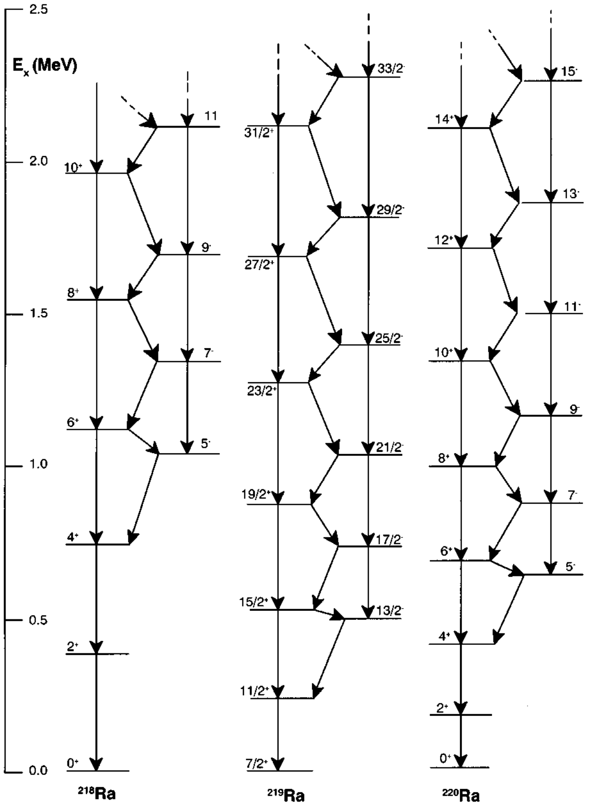

FIG. 21. The yrast sequence of ^{219}Ra, taken from Cottle *et al.* (1986), compared to its neighbors ^{218,220}Ra.

Leander and co-authors (Leander *et al.*, 1982; Leander and Sheline, 1984; Leander and Chen, 1988).

A. Binding energies

An early theoretical indicator of intrinsic reflection asymmetry in nuclei was the necessity of including odd-mass deformation parameters in calculations of ground-state masses. Möller and Nix (1981) were the first to demonstrate that the discrepancies in the calculated and experimental values of the ground-state masses of nuclei with $Z \approx 88$, $A \approx 222$ were reduced substantially by allowing the octupole-deformation parameter to vary in their calculations, which were based on the SC method with the folded Yukawa average potential and the Yukawa-plus-exponential macroscopic energy. These calculations were extended by Leander *et al.* (1982), who made a systematic study of nuclei with $84 \leqslant Z \leqslant 92$ and $130 \leqslant N \leqslant 140$. Leander *et al.* (1982) pointed out that the triangular closed classical orbits with $\Delta \ell = 3,6, \ldots$ in a shell, which give rise to octupole deformation, may only be present with a realistic nuclear potential such as the folded Yukawa potential used by them, or a WS potential, and cannot occur for a modified harmonic-oscillator potential, which can only favor quadrupole and hexadecapole distortions. The results of these calculations are shown in Fig. 27, which shows how the calculated mass-discrepancies evident for nuclei with $Z \approx 88$ and $N \approx 134$ are reduced substantially by octupole deformation. The deviations shown in Fig. 27 occur in precisely the same nuclei for which the calculated potential minimum is lowest for a reflection-asymmetric shape. Möller *et al.* (1995) have recently compiled masses calculated using both the droplet model and the folded Yukawa microscopic model, which can be used to map regions of octupole deformation throughout the periodic table.

Leander *et al.* (1982) found that the octupole-deformed minima are typically 1–2 MeV lower than the energy in the modified oscillator at the same deformation. This difference was further discussed by Nazarewicz *et al.* (1984b), who pointed out that the binding-energy gain $E_{\mathrm{def,asym}}$ associated with reflection-asymmetric deformations is governed primarily by the spacing between the strongly interacting subshells with $\Delta \ell = 3$ [see Sec. III.A and Eq. (15)]. For instance, the energy separation between the spherical $2f_{7/2}$ and $1i_{13/2}$ proton shells in ^{224}Th is 50 keV in the folded Yukawa model of Leander *et al.* (1982), and 600 keV in the WS model of Nazarewicz *et al.* (1984b). This translates into $E_{\mathrm{def,asym}}$=1 MeV (folded Yukawa) and 450 keV (WS). A further increase in $E_{\mathrm{def,asym}}$ can be achieved by allowing for higher-multipolarity deformations in calculations based on the SC method (Chasman, 1986; Sobiczewski *et al.*, 1988; Rozmej *et al.*, 1988; Ćwiok and Nazarewicz, 1989a).

B. Alpha-decay properties

The study of alpha decay and the nature of nuclear states populated by this mechanism was important historically for the identification of low-lying negative-parity states and their subsequent interpretation in terms of octupole modes. There is little evidence that alpha decay in itself is enhanced by the presence of octupole correlations, as there is no observed correlation between alpha reduced widths and N,Z values corresponding to high octupole collectivity; see Fig. 28, taken from Toth *et al.* (1986). The figure shows a plot against neutron number of the reduced widths δ^2 (Rasmussen, 1959) for ground-state to ground-state alpha transitions connecting even-even nuclei with $78 \leqslant Z \leqslant 100$. The discontinuity at N=126 is attributed to a shell-structure effect. Theoretical approaches to alpha decay in which the four nucleons in the parent nucleus that eventually constitute the alpha particle are described by a shell model find that the inclusion of octupole deformation increases the value of δ^2 by 30% (Insolia *et al.*, 1991). Delion *et al.* (1992) used the same technique to make a systematic study of alpha decay in heavy octupole nuclei using a restricted (β_2, β_3) deformation space.

The property of alpha decay which does appear to be important in the determination of octupole collectivity is the relative decay width to different states in the same nucleus. This is usually described by the hindrance factor f, which is a measurement relative to the decay width to the ground state of even-even nuclei. The systematics of this quantity for low-lying negative-parity states in the actinides has been presented by Leander and Sheline (1984), and more recently extended by

TABLE III. Experimental intrinsic $E1$ moments D_0 for even-even nuclei from the Ba-Sm region.

Nucleus	I range	$\|D_0\|$ (expt.) (e fm)	Reference
^{142}Ba	$I=1$	0.115(3)	Mach, Nazarewicz *et al.* (1990)
	$I=9$	0.13(2)	Phillips *et al.* (1986); Mowbray *et al.* (1989) Zhu *et al.* (1995)
^{144}Ba	$I=7$	0.071(10)	Phillips *et al.* (1986); Zhu *et al.* (1995)
	$I=8$–11	0.14(3)	Phillips *et al.* (1986); Zhu *et al.* (1995)
^{146}Ba	$I=1$–3	0.06(4)	Mach, Nazarewicz *et al.* (1990)
	$I=5$–7	0.009(3)	Phillips *et al.* (1986); Zhu *et al.* (1995)
^{144}Ce	$I=7$	0.17(5)	Mowbray *et al.* (1989)
^{146}Ce	$I=7$	0.11(2)	Phillips *et al.* (1988)
	$I=8$–11	0.20(2)	Phillips *et al.* (1988)
^{146}Nd	$I=1$	0.14(5)	Zilges *et al.* (1992)
	$I=7$–11	0.17(2)	Urban *et al.* (1988); Urban *et al.* (1991)
^{148}Nd	$I=1$	0.24(6)	Pitz *et al.* (1990)
	$I=1-4$	0.13(3)	Ibbotson *et al.* (1993)
	$I=5-8$	0.24(3)	Ibbotson *et al.* (1991, 1993)
	$I=6$–8	0.23(3)	Urban *et al.* (1988)
^{150}Nd	$I=1$	0.26(5)	Pitz *et al.* (1990)
^{148}Sm	$I=1$	0.12(2)	Metzger *et al.* (1965, 1976)
	$I=3$	0.18(4)	Jungclaus, Börner *et al.* (1993)
	$I<7$	0.13(1)	Urban *et al.* (1991)
	$I>7$	0.22(2)	Urban *et al.* (1991)
^{150}Sm	$I=1$	0.202(9)	Pitz *et al.* (1990)
	$I=1$	0.118(5)	Jungclaus, Börner *et al.* (1993)
	$I=3$	0.185(5)	Jungclaus, Börner *et al.* (1993)
	$I=7$–15	0.19(3)	Urban *et al.* (1987)
^{152}Sm	$I=1$	0.24(3)	Jungclaus, Börner *et al.* (1993)
	$I=1$	0.37(3)	Jungclaus, Belgya *et al.* (1993)
	$I=1$	0.313(9)	Metzger (1976)
	$I=3$	0.34(3)	Jungclaus, Börner *et al.* (1993)
	$I=3$	0.38(7)	Jungclaus, Belgya *et al.* (1993)
^{150}Gd	$I=4$–6	0.08(2)	Haenni and Sugihara (1977)

Poynter *et al.* (1989b); this is shown in Fig. 29. As can be seen, the values of f for decays to the 1^- level decrease as N becomes smaller, in fact becoming close to unity for Ra and Rn nuclei with $N \leqslant 136$. This has been interpreted (Leander and Sheline, 1984) as resulting from a change of the structure of the low-lying negative-parity states from dynamic vibration to static octupole deformation.

The systematic study of alpha transitions to excited states in odd-A nuclei was also carried out by Leander and Sheline (1984). Their studies showed that, in some cases, states having opposite parity must possess similar structures, since there are small hindrance factors to both states. This is illustrated for the case of the odd-mass Ac isotopes in Fig. 30. These systematics have been extended by Sheline and Bossinga (1991; see also Sheline, 1993b), who pointed out that odd-A and odd-odd nuclei have lower hindrance factors than the corresponding even-even nuclei. The cases where alpha decay has been observed to such parity doublets (see Sec. V.D.1) with values of $f<100$ are presented in Table V. Unfavored transitions typically have values of $f>100$.

C. Exotic decay

The question of the possible existence of cluster structure in ground states of heavy nuclei has attracted much attention, especially because of the observed exotic decay branches via ^{14}C, ^{24}Ne, ^{28}Mg, and others (Rose and Jones, 1984; Price, 1989). Several authors have drawn attention to the similarity in properties between alpha decay and exotic decay (Poenaru *et al.* 1984, 1985; Barwick *et al.*, 1986), although Shi and Swiatecki (1987) have pointed out that exotic decays of heavy nuclei

TABLE IV. Experimental intrinsic $E1$ moments D_0 for even-even nuclei from the Ra-Th region.

Nucleus	I range	$\lvert D_0 \rvert$ (expt.) (e fm)	Reference
^{218}Ra	$I=6$	0.23(5)	Gai *et al.* (1988)
	$I=7$–11	0.339(17)	Gai *et al.* (1988)
^{220}Ra	$I=7$–17	0.27(7)	Burrows *et al.* (1984); Cottle *et al.* (1984)
^{222}Ra	$I=3$	0.38(6)	Ruchowska *et al.* (1992)
^{224}Ra	$I=3$–5	0.028(4)	Poynter *et al.* (1989a); Marten-Tölle (1990)
	$I=7$–9	<0.11	Poynter *et al.* (1989a)
^{226}Ra	$I=1$–5	0.06–0.10	Wollersheim *et al.* (1993)
	$I=7$–12	0.12–0.21	Wollersheim *et al.* (1993)
	$I=7$–11	0.16(1)	Ackermann *et al.* (1993)
^{228}Ra	$I=3$	0.011(1)	Ruchowska *et al.* (1982)
^{220}Th	$I=6-11$	0.25(3)	Bonin *et al.* (1985)
^{222}Th	$I=6$–15	0.38(7)	Ward *et al.* (1983); Bonin *et al.* (1983)
^{224}Th	$I=11$–17	0.52(2)	Ackermann *et al.* (1993)
^{226}Th	$I=9$–19	0.30(1)	Ackermann *et al.* (1993)
^{228}Th	$I=9$–13	0.120(3)	Ackermann *et al.* (1993)
^{230}Th	$I=7$–15	0.04(1)	Lauterbach *et al.* (1984)
^{230}U	$I=11$–13	0.16(5)	Ackermann *et al.* (1993)

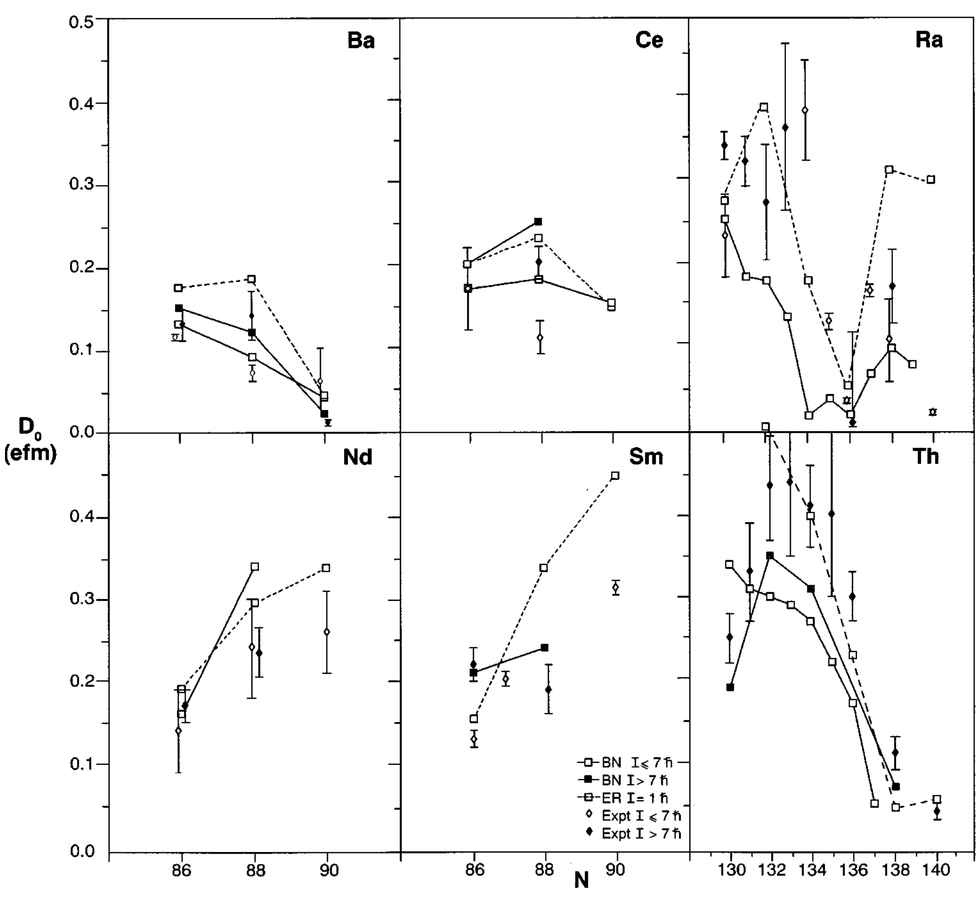

FIG. 22. Experimental (with error bars) and calculated intrinsic $E1$ moments for Ba, Ce, Nd, Sm, Ra, and Th isotopes. Open symbols are measurements or calculations for low-spin states ($I \leqslant 7$); closed symbols are for higher-spin states ($I \geqslant 8$). Calculated values were obtained using the SC method with the WS potential (solid lines; Butler and Nazarewicz, 1991) and in the HF-Gogny model (dotted lines; Egido and Robledo, 1991b, 1992).

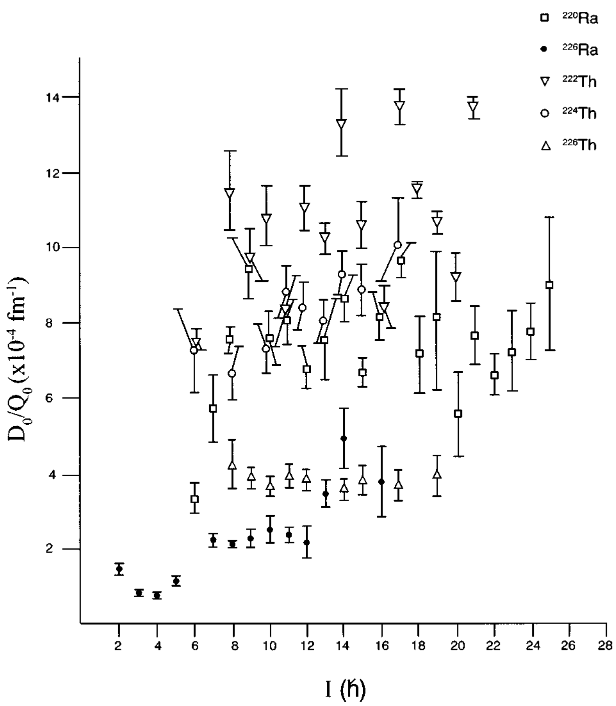

FIG. 23. D_0/Q_0 plotted as a function of spin I for ^{220}Ra (Smith *et al.*, 1995), ^{226}Ra (Wollersheim *et al.*, 1993; Ackermann *et al.*, 1993), ^{222}Th (Smith *et al.*, 1995), ^{224,226}Th (Ackermann *et al.*, 1993).

would occur with about the same frequency whether the parent nucleus were deformed or not.

A connection (Hussonnois *et al.*, 1990a, 1990b, 1991; Sheline and Ragnarsson, 1991a, 1991b; Dumitrescu, 1994) has been made between the ground-state structure of reflection-asymmetric ^{223}Ra and the observed (Brillard *et al.*, 1989; Hourani *et al.*, 1991) hindrance factors of ^{14}C decay to excited states in ^{209}Pb [although recent high-resolution studies by Hourani *et al.* (1995) have failed to confirm the previous observation of large hindrance factors for decay to both negative- and positive-parity states]. This tends to support the suggestion that there is a link between cluster preformation and strong octupole collectivity (Herrmann *et al.*, 1986; Depta *et al.*, 1986; Poenaru *et al.*, 1994), although substantially more data are required to establish this. (For review, see Sandulescu and Greiner, 1992; Hussonnois and Ardisson, 1994.)

Delion *et al.* (1994) have performed microscopic calculations of heavy-cluster spontaneous emission using a *spherical* shell-model technique, applied previously to alpha decay (Delion *et al.*, 1992). They obtained very good agreement with experiment for ^{14}C decay from ^{222,224,226}Ra, and made a prediction for ^{114}Ba$\rightarrow^{12}$C+^{102}Sn decay, assuming spherical shapes. (For identification of ^{114}Ba and its cluster radioactivity, see Guglielmetti *et al.*, 1995.)

Cseh *et al.* (1993) applied the vibron model coupled with the pseudo-SU$_3$ shell model (Sec. III.D) to describe clusterization in heavy nuclei. As an example they considered the clusterization of ^{224}Ra to the ^{210}Pb+^{14}C system.

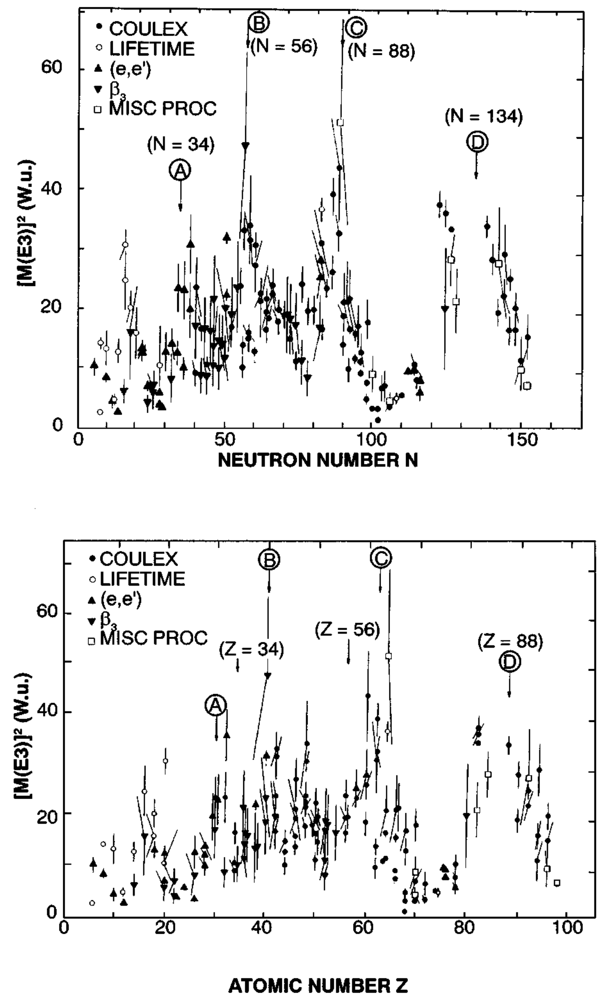

FIG. 24. Plot of $|M(E3)|^2$, the $E3$ transition strength of $0_1^+\rightarrow3_1^-$ transitions for even-even nuclei, as a function of neutron number N (top) and proton number Z (bottom). The various symbols indicate the experimental procedures used to obtain the data (Coulomb excitation, lifetime measurements, inelastic electron scattering, deduction from β_3 values obtained from inelastic scattering of particles, and miscellaneous procedures). The peaks labeled A, B, C, D in the lower plot occur at Z values of the stable nuclei having N values corresponding to peaks A, B, C, D, respectively, in the upper figure (Spear and Catford, 1990).

D. Spectroscopic properties of the odd particle

The presence of intrinsic reflection-asymmetric deformations influences spectroscopic properties (parity splittings, ground-state spins and magnetic moments, Coriolis matrix elements, spectroscopic factors, radii, electromagnetic transitions, alpha-decay rates) of odd-A and odd-odd nuclei.

Leander and Sheline (1984) reviewed the properties of odd-A actinide nuclei, and outlined spectroscopic fingerprints of stable octupole deformation. For the spectroscopy of the odd-A Ra isotopes, see also the reviews by Sheline and Sood (1991) and Sheline (1993a).

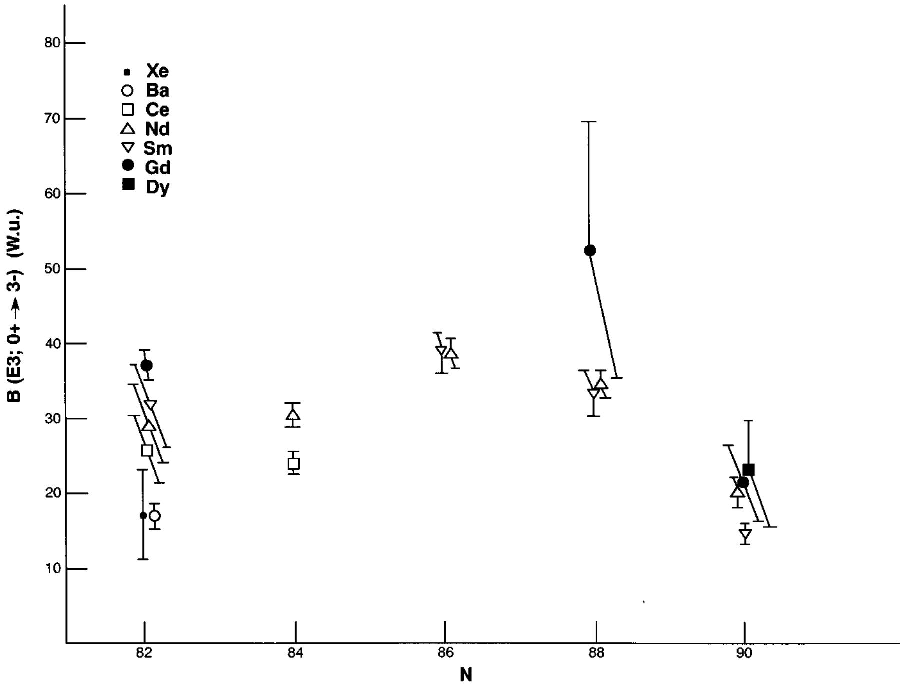

FIG. 25. Values of $B(E3;0_1^+ \rightarrow 3_1^-)$ for nuclei with N=82, 84, 86, 88, and 90. The data are taken from Spear (1989) except for ^{142}Ce, ^{144}Nd (taken from Spear *et al.*, 1989), ^{146}Nd (Sandor *et al.*, 1993b), ^{148}Nd (Ibbotson *et al.*, 1993), and ^{150}Nd (Sandor *et al.*, 1993a).

1. Parity doublets

It was first emphasized by Chasman (1980) that a signature of intrinsic reflection asymmetry in well-deformed odd-A nuclei would be the appearance of parity doubling, i.e., for each bandhead there should be another bandhead close in energy with the same value of K and opposite parity.

In the reflection-asymmetric particle-plus-rotor of Leander and Sheline (1984), the parity splitting between members of a parity doublet in odd-A or odd-odd nuclei is [see Eq. (43)]

$$\Delta E = E(0^-)\langle \mathscr{P}_{\text{s.p.}} \rangle; \tag{77}$$

i.e., it is always reduced compared to the value for the even-even core [see Eqs. (24) and (25); also Brink *et al.* (1987)].

All models of odd-A nuclei predict that the parity splitting of the $K^{\pm}$ bands should be smaller than for the

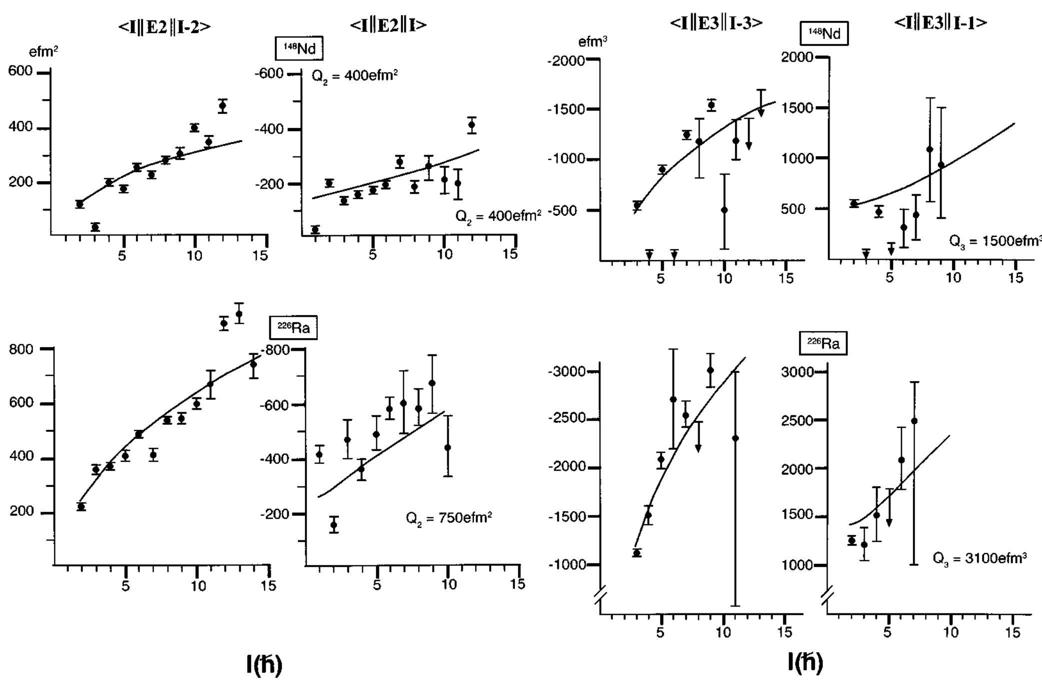

FIG. 26. Plot of $E2$ and $E3$ matrix elements versus spin I deduced from Coulomb-excitation measurements for ^{148}Nd (Ibbotson *et al.*, 1993) and ^{226}Ra (Wollersheim *et al.*, 1993). Solid lines join points calculated assuming a constant electric quadrupole or octupole moment.

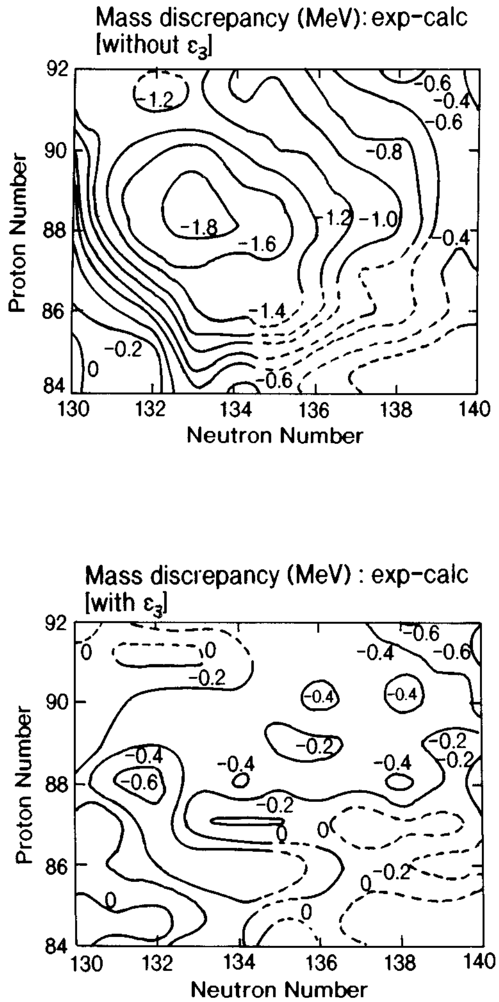

FIG. 27. Top: Experimental mass minus calculated mass, with only the mass-symmetric shape coordinates ε_2 and ε_4 included in the calculations. Dashed contours indicate regions where there are no experimental data. Bottom: Experimental mass minus calculated mass, with both mass-symmetric (ε_2 and ε_4) and mass-asymmetric (ε_3) coordinates included in the calculations (Leander *et al.*, 1982).

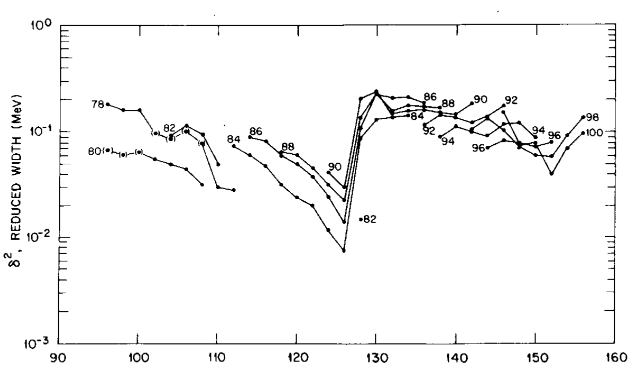

FIG. 28. Reduced widths for s-wave α transitions plotted as a function of neutron number for nuclei with $78 \leqslant Z \leqslant 100$. Values enclosed in parentheses for Z=78 and Z=80 are based on estimated α branches (Toth *et al.*, 1986).

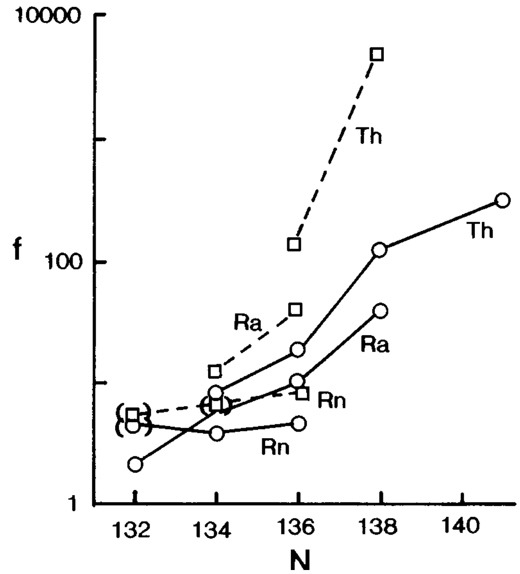

FIG. 29. Systematics of α hindrance factors f to the 1^- (full curve, round symbols), and the 3^- (dotted curves, square symbols), levels in the nuclei shown. N is the neutron number. Points in brackets are α hindrance factors to levels with unconfirmed I^π. The lines through the data points are to guide the eye only (Poynter *et al.*, 1989b).

$K^\pi = 0^+$ and (extrapolated) 0^- bandheads in the adjacent even-even nuclei, so that the experimental observation of parity doublets does not provide a particularly good test for these models. Also, as pointed out by Leander and Sheline (1984), closely spaced parity doublets will occur among the Nilsson orbitals in the deformed-shell model for reflection-symmetric shapes, especially if pairing reduces the quasiparticle energy spacing. Nevertheless, the observation of a multiple band structure in ^{223}Th (Dahlinger *et al.*, 1988) in particular offers evidence for reflection asymmetry in an odd-mass nucleus. In this nucleus (see Fig. 31) strong $E1$ and $M1$ transitions are seen connecting the bands of different parity and signature. The energy degeneracy of these bands is highlighted in Fig. 32, where $\mathscr{J}/\hbar^2$ is plotted versus $\hbar\omega$ for ^{223}Th and compared with adjacent even-even nuclei. Similar band structure has been observed in ^{225}Th (Hughes *et al.*, 1990), which is also compared with adjacent even-even nuclei in Fig. 32, in ^{221}Ra (Ackermann *et al.*, 1989; Fernández-Niello *et al.*, 1991) in ^{151}Pm (Vermeer *et al.*, 1990; Urban *et al.*, 1990), and in ^{153}Eu (Pearson *et al.*, 1994) (but see next subsection).

At low spin, numerous cases of parity doubling have been observed, assigned as such usually on the basis of alpha hindrance factors (see Sec. V.B), although sometimes from the nature of observed electromagnetic transitions or other spectroscopic properties. The observed features of these bands are contained within Tables V and VI, which list the locations of low-lying single-particle states in actinide and lanthanide nuclei, respectively, together with their important experimental properties.

The K=0 parity-doublet band in the odd-odd nucleus

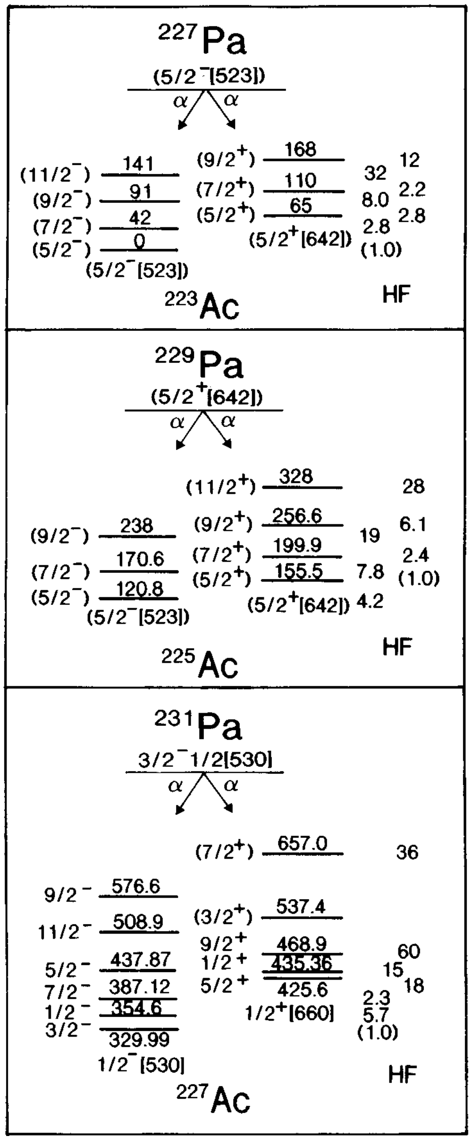

FIG. 30. Experimentally observed favored α decay into closely spaced parity doublets of odd-A Ac isotopes. The observed hindrance factors to the right of the levels are normalized to unity for the "natural" favored transition (Leander and Sheline, 1984). The level energies are in keV.

^{224}Ac has been observed to have extremely small splittings between states of the same spin and opposite parity (Sheline *et al.*, 1991, 1993). In this nucleus the Newby splitting, which displaces the even- and odd-spin members in K=0 bands, in odd-odd nuclei, has been determined for each of the $K=0^+$ and $K=0^-$ bands, and shown to be consistent (see Table V) with the expectation for reflection-asymmetric systems of the same absolute value but opposite sign. Recently the K assignments of this band have been called into question (Ahmad *et al.*, 1994). For the nucleus ^{229}Pa, on the edge of the region of octupole deformation, recent experiments using particle, γ, and e^- spectroscopy (Grafen *et al.*, 1991; Lösch *et al.*, 1994; Levon *et al.*, 1994) have shown that the original assignment of a $5/2^\pm$ parity doublet separated by 220 eV (Ahmad *et al.*, 1982) has probably no experimental basis. Sheline (1993b) has pointed out that the alpha decay of ^{229}Pa suggests that it has octupole deformation in its ground state, and that there must exist a $5/2^\pm$ parity doublet in this nucleus.

2. Ground-state spins and magnetic moments

Indirect evidence for the occurrence of intrinsic reflection asymmetry comes from the spectroscopic properties of the odd particle, e.g., spin, magnetic moment, decoupling parameter, and transfer spectroscopic factor. The single-particle orbitals as a function of β_2 and β_3 are given for protons with $Z>82$ and neutrons with $N>126$ in Fig. 33, taken from Leander and Chen (1988). The energies of orbitals lying close to each other which are mixed by the octupole interaction (e.g., $g_{9/2,\Omega=5/2}$, $j_{15/2,\Omega=5/2}$ for neutrons) are strongly perturbed by octupole deformation, so that the ground-state spin and magnetic moments are expected to be different for β_3=0 and for $\beta_3 \neq 0$.

The strong-coupling expression for the rotational gyromagnetic factor g_K ($K>1/2$),

$$g_K=\frac{1}{K}[Kg_\ell+(g_s-g_\ell)\langle\chi_K^\nu|s_z|\chi_K^\nu\rangle], \tag{78}$$

shows that the octupole coupling involving spin-flipped orbitals may lead to the hybridization of magnetic dipole properties. (For K=1/2 the magnetic decoupling parameter has to be considered.) Sheline and Leander (1983) applied this expression to describe the magnetic moments in the $3/2^\pm$ doublets of ^{227}Ac, and Ragnarsson (1983) has applied it to the magnetic moments in ^{225,227}Ra. Sheline (1986) has pointed out that in the case of ^{223}Ra, the similarity in magnetic moments of the ground state and the $3/2^-$ bandhead at 50.2 keV (see Table V) can be accounted for naturally by assuming both are part of a parity doublet. Figure 34 shows the values of $\langle\chi_K^\nu|s_z|\chi_K^\nu\rangle$ in odd-A isotopes of Ac and Pa, as calculated by Leander and Sheline (1984). The value of this quantity for ^{227}Ac, extracted from the measured g factor by means of Eq. (78), agrees well with the prediction of reflection-asymmetric theory.

As yet, however, the data are rather sparse for g factors measured for the many transitions observed in parity-doublet bands populated at high spin by heavy-ion reactions. In the cases of ^{151}Pm (Vermeer *et al.*, 1990) and ^{153}Eu (Pearson *et al.*, 1994), the intrinsic g factors obtained from the $B(M1)/B(E2)$ branching ratios are systematically quite different for the transitions between the positive-parity members and between the negative-parity members, which suggests that these bands have different intrinsic structure. Indeed, calculations of magnetic moments in these nuclei using the rotor-plus-particle model are able to reproduce the experimental values without invoking static intrinsic reflection asymmetry (Afanasjev and Ragnarsson, 1995; see also Afanasjev, 1993, and Afanasjev and Mizutori, 1995). More recently, it has been observed that the magnetic properties of transitions for each parity of a band

TABLE V. Properties of odd-mass and odd-odd nuclei in the Fr-Th region. The energies and K^π values of bandheads are given, together with values of the decoupling parameter a for K=1/2 bands, α-decay hindrance factor (h.f.) for favored transitions, and intrinsic electric dipole moment D_0 for transitions within parity-doublet bands.

Nucleus	K^π	Energy (keV)	a	h.f.	D_0 (e fm)	Other
^{219}Fr (Liang *et al.*, 1991)						
	$\frac{1}{2}^-$	81	7.03			
	$\frac{1}{2}^+$	$\approx$330	-7.78			
	$\frac{5}{2}^+$	384.3		10		
	$\frac{5}{2}^-$	490.3		2.9		
	$\frac{3}{2}^-$	56.15		9.3 ($\frac{7}{2}^-$)		
	$\frac{3}{2}^+$	369.6		$>$19 ($\frac{7}{2}^+$)		
^{221}Fr (Sheline, 1988b; Liang, Péghaire *et al.*, 1990)						
	$\frac{1}{2}^-$	26.0	4.3	11 ($\frac{7}{2}^-$)	0.102 ± 0.008	
	$\frac{1}{2}^+$	145.8	-2.6	65 ($\frac{7}{2}^+$)		
	$\frac{3}{2}^-$	36.6		17	0.076 ± 0.003	
	$\frac{3}{2}^+$	224.6		28		
^{223}Fr (Kurcewicz *et al.*, 1992; Sheline *et al.*, 1995)						
	$\frac{3}{2}^-$	0		7.6	0.24 ± 0.04	
	$\frac{3}{2}^+$	160.45		42		
	$\frac{1}{2}^-$	55.0	-1.36			
	$\frac{1}{2}^+$	149.3	0.96			
^{221}Ra (Ackermann *et al.*, 1989; Liang, Paris *et al.*, 1990; Fernández-Niello *et al.*, 1991)						
	$\frac{5}{2}^+$	0			0.36 ± 0.10	
	$\frac{5}{2}^-$	103.4				
	$\frac{3}{2}^+$	321.3		1.9		
	$\frac{3}{2}^-$	485.3		$\approx$15		
^{223}Ra (Sheline, 1986; Sheline, Chen, and Leander, 1988; Briançon *et al.*, 1990; Abdul-Hadi *et al.*, 1993)						
	$\frac{3}{2}^+$	0			0.124 ± 0.010	$\mu=0.28\pm0.014$
	$\frac{3}{2}^-$	50.19				$\mu=0.42\pm0.06$
	$\frac{5}{2}^+$	234.92			0.043 ± 0.012	
	$\frac{5}{2}^-$	369.43				
	$\frac{1}{2}^+$	286.16	1.35	5.6 ($\frac{1}{2}^+$)	0.078 ± 0.012	
				16 ($\frac{3}{2}^+$)		
	$\frac{1}{2}^-$	350.50	-2.15	36 ($\frac{1}{2}^-$)		
				14 ($\frac{3}{2}^-$)		
^{225}Ra (Sheline *et al.*, 1983, 1989; Reich *et al.*, 1986; Helmer *et al.*, 1987; Andersen *et al.*, 1989)						
	$\frac{1}{2}^+$	0	1.89		0.14 ± 0.02	
	$\frac{1}{2}^-$	55.2	-2.56			
	$\frac{3}{2}^+$	149.9				
	$\frac{3}{2}^-$	225.1				
	$\frac{5}{2}^+$	236.3		1.57		
	($\frac{5}{2}^-$)	394.2		23		
^{227}Ra (Borge *et al.*, 1987; Sheline, 1989b; Mach *et al.*, 1994)						
	$\frac{3}{2}^+$	0			0.098 ± 0.011	
	$\frac{3}{2}^-$	90.0				
	$\frac{1}{2}^+$	120.7	-1.71			
	$\frac{1}{2}^-$	296.6	0.62			
^{223}Ac (Ahmad *et al.*, 1989; Sheline *et al.*, 1990)						
	$\frac{3}{2}^-$	4.1		5.1 ($\frac{5}{2}^-$)		
	$\frac{3}{2}^+$	88.9		$\approx$14 ($\frac{5}{2}^+$)		
	$\frac{5}{2}^-$	0		2.5	$>$0.18	
	$\frac{5}{2}^+$	64.6		7.0		
^{225}Ac (Ahmad *et al.*, 1984, 1987)						
	$\frac{3}{2}^-$	0			0.171 ± 0.014	
	$\frac{3}{2}^+$	40.1				
	$\frac{5}{2}^-$	120.8		7.5		
	$\frac{5}{2}^+$	155.7		1.8		

TABLE V. (*Continued*).

Nucleus	K^{π}	Energy (keV)	a	h.f.	D_0 (e fm)	Other
^{227}Ac (Sheline and Leander, 1983; Ishii *et al.*, 1985; Martz *et al.*, 1988)						
	$\frac{3}{2}^-$	0			0.0297 ± 0.0001	$g_K=0.92\pm0.06$
	$\frac{3}{2}^+$	27.4				$g_K=0.96\pm0.10$
	$(\frac{5}{2}^-)$	273.1				
	$(\frac{5}{2}^+)$	304.6				
	$\frac{1}{2}^-$	354.6	-2.01	13 $(\frac{1}{2}^-)$		
				5.2 $(\frac{7}{2}^-)$		
	$\frac{1}{2}^+$	435.4	4.56	>35 $(\frac{1}{2}^+)$		
				83 $(\frac{7}{2}^+)$		
^{224}Ac (Sheline *et al.*, 1991, 1993; Ahmad *et al.* 1994)						
	(0^-)	0				$E^N=1.99$ keV
	(0^+)	(22.0)				$E^N=-0.37$ keV
	(1^+)	66.0				
	(1^-)	89.3				
	3^-	353.9		20		
	3^+	360.2		12		
^{223}Th (Dahlinger *et al.*, 1988)						
	$\frac{5}{2}^+$ $\frac{5}{2}^-$	0			0.44 ± 0.09	
^{225}Th (Hughes *et al.*, 1990)						
	$\frac{3}{2}^+$ $\frac{3}{2}^-$	0			0.40 ± 0.10	
^{227}Th (Liang *et al.*, 1994, 1995)						
	$\frac{1}{2}^+$	0	2.97			
	$\frac{1}{2}^-$	67.2	-2.68			
	$\frac{3}{2}^+$	24.3		44 ± 5		
	$\frac{3}{2}^-$	142.0		≈440		
	$\frac{5}{2}^-$	448.0				
	$\frac{5}{2}^+$	547.0				
^{229}Pa (Levon *et al.*, 1994)						
	$\frac{1}{2}^-$	15.1	–1.71		0.09 ± 0.04	
	$\frac{1}{2}^+$		1.51			
	$\frac{1}{2}^-$	1540	–1.75			
	$\frac{1}{2}^+$	1593	1.90			

in ^{147}Pm are similar at intermediate spin values. This has been interpreted as being consistent with this nucleus having stable octupole deformation in this spin region (Urban *et al.*, 1995).

Comparison with theory of the ground-state properties for actinide nuclei has been carried out by Ragnarsson (1983), Leander and Sheline (1984), Leander and Chen (1988), Ćwiok and Nazarewicz (1991), and Jain *et al.* (1990). The assignment of ground-state orbitals to these nuclei is given in Fig. 33. In general, the agreement is very good between the experimental values of $I_{\text{g.s.}}$ and $\mu_{\text{g.s.}}$ and the values calculated assuming $\beta_3\approx0.1$ for Rn, Fr, Ra, Ac, and Pa isotopes with $N\leqslant140$; but if $\beta_3=0$, it is difficult in some cases to find appropriate orbitals so that both $I_{\text{g.s.}}$ and $\mu_{\text{g.s.}}$ can be matched by calculations. Particularly interesting is the nucleus ^{225}Ra, which is expected to exhibit coexistence of reflection-symmetric and reflection-asymmetric configurations (Sheline *et al.*, 1989; Ćwiok and Nazarewicz, 1991). In this case it is difficult to explain the ground-state spin (I=1/2) (Ahmad *et al.*, 1983) without invoking octupole mixing [see, however, Piepenbring (1984)].

In the light-lanthanide nuclei, similar conclusions were reached (Leander *et al.*, 1985; Ćwiok and Nazarewicz, 1989b) in describing the ground-state spins and electromagnetic moments of ^{143,145}Cs (Coc *et al.*, 1987) and ^{145}Ba (Mueller *et al.*, 1983). The structure of parity doublets in ^{151}Pm and ^{153,155}Eu was studied by Nosek *et al.* (1993a) in the quasiparticle-phonon nuclear model (Sec. III.F). They found strong octupole correlations only in the K=1/2 states. Spectroscopic properties of odd-A nuclei around ^{112}Ba have been discussed by Heenen *et al.* (1994).

For the odd-odd nuclei ^{228,230}Pa, Herrmann *et al.* (1989) have noted that the measured ground-state magnetic moments are best fitted by including orbitals which are associated with large driving forces toward octupole shapes. Ekström *et al.* (1986) made a similar analysis of the ground-state moments of ^{223,225,227}Fr, but was unable to draw any firm conclusion on the presence of octupole deformation, as the data were also reproduced by

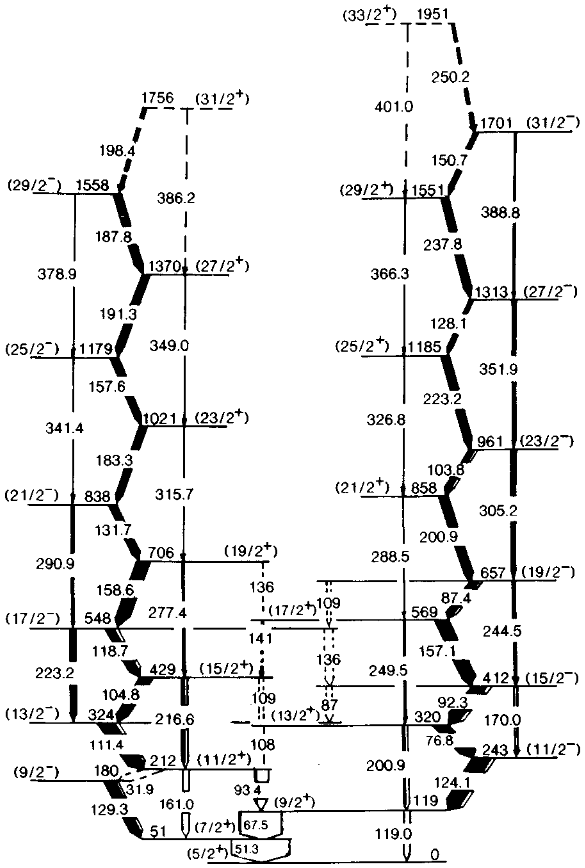

FIG. 31. Level scheme of ^{223}Th. The spin assignment was made under the assumption of a ground state spin $I^{\pi}=5/2^{+}$. The width of the arrows represents the transition intensity. Dotted transitions are unconfirmed (Dahlinger *et al.*, 1988). The level and transition energies are in keV.

particle-rotor calculations which did not include octupole deformation. For the ground-state spins of odd-odd Francium isotopes with $A=220$–228, and for ^{224,226}Ac, Sheline, Chen, and Leander (1988) were able to explain the values only in terms of parity-mixed orbits.

3. Coriolis matrix elements

In the strong-coupling limit, the diagonal Coriolis matrix element for K=1/2 bands is written in terms of the decoupling parameter a (Zaikin, 1966; Bohr and Mottelson, 1975):

$$a=-p\langle \mathscr{P}_{\rm s.p.}\chi^{\nu}_{1/2}|j_{+}|R_1\chi^{\nu}_{1/2}\rangle, \tag{79}$$

so that opposite-parity states of a doublet having a common intrinsic structure have values of the decoupling parameter a of equal magnitude but opposite sign. That is,

$$ap=\text{const} \tag{80}$$

within a doublet.

Ragnarsson (1983), and Leander and collaborators (Leander and Sheline, 1984; Leander and Chen, 1988), have made a systematic comparison of the experimental values of a with theoretical calculations using a model which is either reflection asymmetric or symmetric. Particularly for ^{227}Ra, reflection asymmetry appears necessary to account for the observed signs of a for the lowest $K^{p}=1/2^{\pm}$ band. Figure 35 shows the comparison between experimental values and values calculated by Leander and Chen (1988) from a reflection-asymmetric particle-plus-rotor model. The theory predicts some degree of divergence from the strong-coupling limit (80), but not as much as observed, although overall the agreement between theory and experiment is quite good. For $K>1/2$ bands, Leander and Chen (1988) calculated moment-of-inertia and signature splitting for both parity bands, and obtained parity decoupling of the same order as that observed experimentally, although the quality of the fit is rather poor. They speculated that the observed smaller size of the Coriolis matrix elements in their calculations for deformed nuclei is brought about by the presence of octupole deformation. For ^{219}Fr, Liang *et al.* (1991) were able to reproduce the experimental values of the decoupling parameter for the K=1/2 doublet using the intermediate-coupling scheme based on the quasiparticle-phonon nuclear model (Sec. III.F), which assigns quite different quasiparticle character to the bands of different parity.

4. Spectroscopic factors

An early attempt to reproduce the measured nuclear structure factors for states populated by one-neutron transfer reactions using an octupole model was made by Løvhøiden *et al.* (1986), who studied the ^{226}Ra(t,α)^{225}Ra reaction. They were able to reproduce the measured quantities for states associated with the $j_{15/2}$ intruder orbital using matrix elements calculated assuming nonzero β_3. More extensive calculations have been carried out for ^{227}Ac, ^{225}Ra, and ^{227}Ra by Leander and Chen (1988), giving reasonable agreement with experimental data for *relative* magnitudes of the nuclear structure factors, using the reflection-asymmetric particle-plus-rotor model. In contrast, Martz *et al.* (1988) reported that the spectroscopic strengths in ^{227}Ac populated by the ^{226}Ra(α,t) and ^{226}Ra$(^3$He$,d)$ reactions are in better agreement with models which assume reflection symmetry. Tables of spherical amplitudes C_J, useful for interpretation of one-particle transfer reactions, have been computed by Chasman (1984) for reflection-asymmetric valence-proton and -neutron single-particle states in the $A\sim225$ mass region.

5. Radii

The introduction of laser-spectroscopic techniques has enabled many new isotope-shift measurements to be made in the actinide and lanthanide region (Aufmuth *et al.*, 1987). The isotope shift is used to derive the change $\delta\langle r^2\rangle^{N,N'}$ in the mean-square nuclear-charge radii between nuclei having neutron numbers N and N', which is related to changes in the charge distribution between these nuclei by

$$\delta\langle r^2\rangle=\delta\langle r^2\rangle_{\rm sph}+\tfrac{5}{4}\,\pi\langle r^2\rangle_{\rm sph}(\delta\langle\beta_2^2\rangle+\delta\langle\beta_3^2\rangle+\cdots). \tag{81}$$

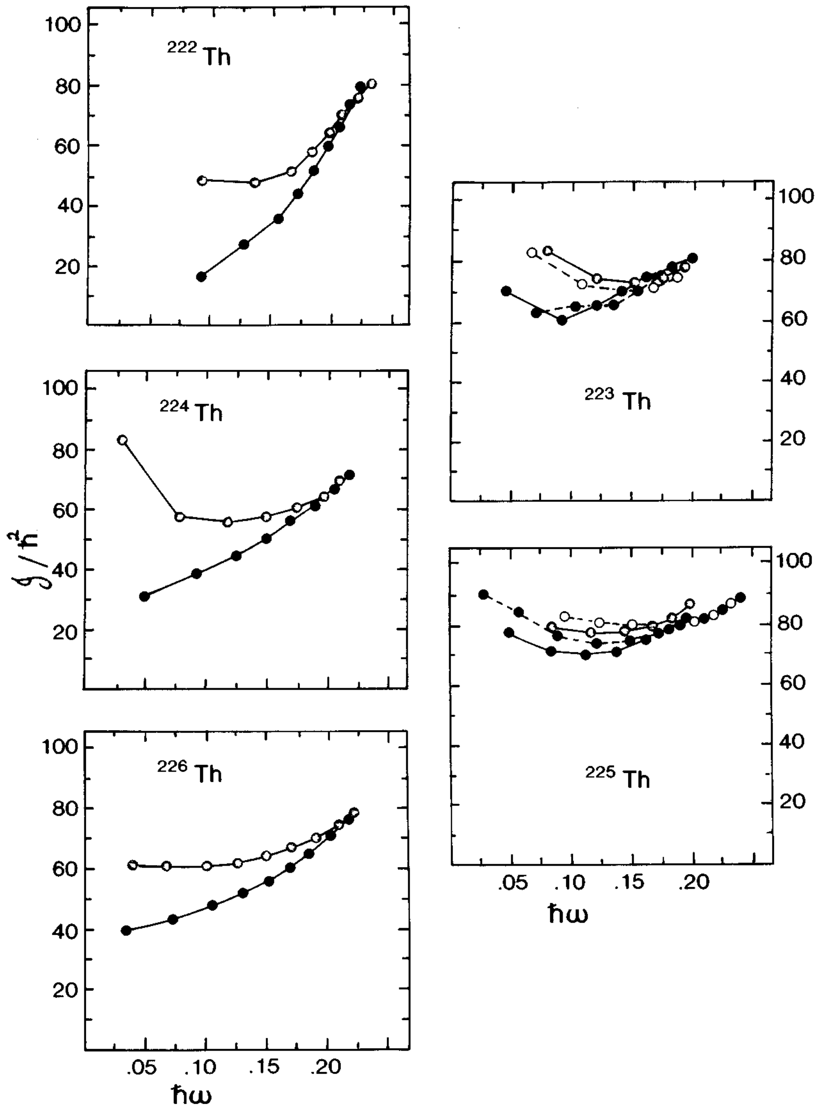

FIG. 32. Kinematic moment of inertia $\mathcal{J}/\hbar^2$ (in MeV^{-1}) as a function of rotational frequency $\hbar\omega$ (in MeV) for ground-state rotational bands in ^{223}Th and ^{225}Th, compared with their even-even neighbors. The ground-state spins of ^{223,225}Th are assumed to be 5/2 and 3/2 respectively. The positive (negative) parity bands are indicated by filled (open) symbols.

Figure 36, taken from Otten (1989), shows how the experimental value of $\delta\langle r^2\rangle^{A-1,A}$ between neighboring isotopes A–1 and A varies for isotopes of Rn (Borchers *et al.*, 1987), Fr (Coc *et al.*, 1985, 1987), and Ra (Ahmad *et al.*, 1983, 1985, 1988), as a function of N. This quantity shows a pronounced odd-even effect between N=132 and N=138, in that $\delta\langle r^2\rangle^{A-1,A}$ for odd A is larger than $\delta\langle r^2\rangle^{A-1,A}$ for even A, which is opposite to what is observed all over the chart of the nuclides with very few exceptions. The Th isotopes with $N\geqslant137$ do not exhibit this effect (Kälber *et al.*, 1989). The inversion of the normal odd-even staggering in the light actinides has been associated with the occurrence of strong octupole correlations (Ahmad *et al.*, 1984), with the suggestion that it arises from the stabilizing effect on the octupole deformation of the odd particle outside the even-even core (see also Sheline, Jain *et al.*, 1988, 1989). It should be pointed out, however, that the experimental values for the Rn, Fr, and Ra isotopes can be well reproduced using an extended Thomas-Fermi method, even though the octupole degree of freedom is not included in the calculation (Buchinger *et al.*, 1994).

For Ba and Cs isotopes around N=88–90, the effect is masked by the large overall increase observed with the onset of quadrupole deformation, although Sheline, Jain *et al.* (1988) have suggested that the odd-even effect is attenuated for these nuclei. For the Europium isotopes there is some evidence of an inversion of $\delta\langle r^2\rangle^{N,N-1}$ at $N=89$ (Dörschel *et al.*, 1984; Ahmad *et al.*, 1985; Alkhazov *et al.*, 1990), which may be associated with octupole deformation (Afanasjev, 1993).

6. *E*1 transitions

Experimentally, the first evidence that the presence of octupole correlations would give rise to relatively strong $E1$ transitions, of order 10^{-3} to 10^{-2} s.p.u. (see Sec. II.B), came from studies of low-lying transitions in odd nuclei (for example, Ahmad *et al.*, 1984). In the strong-coupling limit, the values of the electric dipole moment D_0 for odd-mass nuclei are expected to be the same as those for the even-even core. Butler and Nazarewicz (1991) compared the experimental values for even-even and odd-A nuclei with theoretical predictions of the SC

TABLE VI. Similar to Table V, but for odd-mass and odd-odd nuclei in the Pm-Eu region.

Nucleus	K^π	Energy (keV)	a	D_0 (e fm)	Other
^{151}Pm (Sood and Sheline, 1989; Urban *et al.*, 1990; Vermeer *et al.*, 1990)					
	$\frac{5}{2}^+$	0		0.16 ± 0.04	$\mu=1.29\pm0.03$
	$\frac{5}{2}^-$	116.8			$\mu=2.20\pm0.14$
	$\frac{3}{2}^+$	255.6			
	$\frac{3}{2}^-$	540.2			
^{152}Eu (Sheline and Sood, 1989)					
	4^+	89.9		0.076	
	4^-	141.8			
	5^+	108.1		0.034	
	5^-	180.6			
^{153}Eu (Sheline and Sood, 1990; Pearson *et al.*, 1994)					
	$\frac{5}{2}^+$	0		0.08 ± 0.02	$\mu=1.5330\pm0.0008$
	$\frac{5}{2}^-$	97.4			$\mu=3.22\pm0.23$ or -0.52 ± 0.23
^{154}Eu (Sheline, 1989a)					
	1^+	71.91		0.052 ± 0.008	
	1^-	82.82			
	3^+	281.68		0.081 ± 0.015	
	3^-	239.29			
^{155}Eu (Sheline and Sood, 1990)					
	$\frac{5}{2}^+$	0		0.22 ± 0.01	$\mu=1.56\pm0.10$
	$\frac{5}{2}^-$	104.3			$\mu=2.49\pm0.27$
	$\frac{1}{2}^+$	922.8	2.14		
	$\frac{1}{2}^-$	1106.7	-1.11		

method. In these calculations, the macroscopic contribution to D_0 should be similar to the even-even neighbors, although fluctuations can arise from the single-particle contribution. Leander and Chen (1988) have also carried out calculations for the $B(E1)$ values, including effects of Coriolis mixing and odd-quasiparticle contributions.

For $K_i=K_f=1/2$ transitions, Eq. (66) is modified by the presence of the signature-dependent term [Eq. (67)] proportional to D_1. Reich *et al.* (1986) have determined the amplitudes D_0 and D_1 for the $1/2^\pm$ doublet in ^{225}Ra.

VI. ROTATIONAL PROPERTIES OF REFLECTION-ASYMMETRIC NUCLEI

Rotational properties of octupole vibrational states were discussed in a rotor-plus-RPA model by Neergård and Vogel (1970a, 1970b) and Vogel (1976), and in the cranked RPA theory by Robledo *et al.* (1986), Mizutori *et al.* (1990, 1991a, 1991b), and Nakatsukasa *et al.* (1992, 1993, 1995) (see Sec. III.F). In this section we mainly concentrate on rotational motion of nuclei with stable reflection-asymmetric deformations.

Quasimolecular rotational bands in a reflection-asymmetric nucleus can be characterized by the "simplex" s, which is the eigenvalue of the S_1 operator [reflection through the (y,z) plane; see Sec. III.B.1]. Simplex has properties similar to those of the signature quantum number in the absence of reflection symmetry (Nazarewicz *et al.*, 1984a; Frauendorf and Pashkevich, 1984; Nazarewicz and Olanders, 1985a, 1985b).

The square of the S_1 operator is related to the total number of fermions:

$$S_1^2=(-1)^A. \tag{82}$$

The rotational band with simplex s is characterized by spin states I of alternating parity, (Bohr and Mottelson, 1975)

$$p=se^{-i\pi I}. \tag{83}$$

Thus for reflection-asymmetric systems with an even number of nucleons, one obtains

$$s=+1,\ I^p=0^+,1^-,2^+,3^-,\ldots, \tag{84}$$

$$s=-1,\ I^p=0^-,1^+,2^-,3^+,\ldots, \tag{85}$$

while for systems with odd particle number one has

$$s=+i,\ I^p=1/2^+,3/2^-,5/2^+,7/2^-,\ldots, \tag{86}$$

$$s=-i,\ I^p=1/2^-,3/2^+,5/2^-,7/2^+,\ldots. \tag{87}$$

In the mirror-symmetric case the simplex becomes $s=-pr$ (r is the signature quantum number).

The general structure of the cranked HFB equations and their solutions remains the same in the simplex formulation as in the usual signature-parity formulation. The simplex of the rotating vacuum is $s=+1$, and the simplex of an excited n-quasiparticle configuration becomes

$$s_{nqp}=s_1s_2\cdots s_n, \tag{88}$$

where s_i is the simplex of the ith particle.

High-spin properties of reflection-asymmetric nuclei

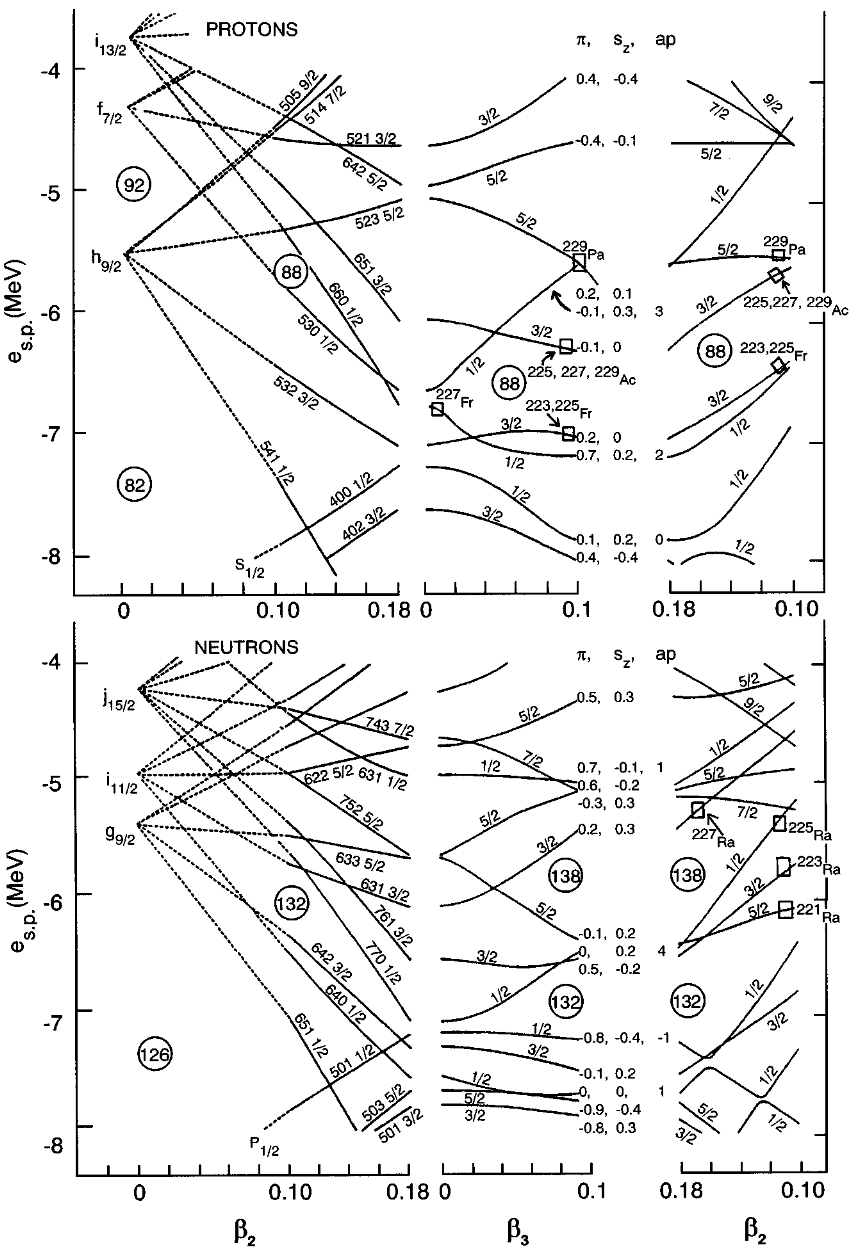

FIG. 33. Proton single-particle levels (top) and neutron levels (bottom) in a WS potential for β_2=0–0.18 with β_3=0, for β_3=0–0.1 with β_2=0.18, and for β_2=0.18–0.10 with β_3=0.1. Taken from Leander and Chen (1988).

were discussed by Nazarewicz and Olanders (1985a) in the cranking WS model. Octupole coupling between high-j unique-parity orbitals and normal-parity states leads to fragmentation of the aligned angular momentum over many quasiparticle states. The angular momentum content of the lowest Routhians, containing a significant component of high-j unique-parity states, decreases with octupole deformation. On the other hand, the average alignment of Routhians with a dominant component of normal parity increases. As a consequence, the quasiparticle-Routhian pattern becomes more uniform, and many quasiparticle Routhians have similar alignment.

The fragmentation effect is illustrated in Fig. 37, which displays the calculated quasiparticle Routhians for Z=56 and N=88 as functions of rotational frequency, without (left) and with (right) octupole deformation. As can be seen in Fig. 37, the frequency of the first band crossing increases at the reflection-asymmetric shape as a consequence of the reduced angular momentum alignment of the lowest Routhians. In addition, the interaction between the crossing bands increases. Other diagrams of Routhians as functions of octupole deformation and rotational frequency can be found in Faber and Płoszajczak (1981), Frauendorf and Pashkevich (1984), and Åberg (1990).

At high frequencies a shape transition towards β_3=0 is expected after the alignment of the high-j quasiparticles. Figure 38 illustrates the influence of rotational frequency on the octupole-shell structure. The single-particle Routhians for $N\sim$88 are shown as functions of β_3 for $\hbar\omega$=0, 0.3, and 0.6 MeV. At $\hbar\omega$=0.3 MeV the octupole-shell effects are quenched, although the proton numbers Z=56 and Z=62 and neutron numbers N=88

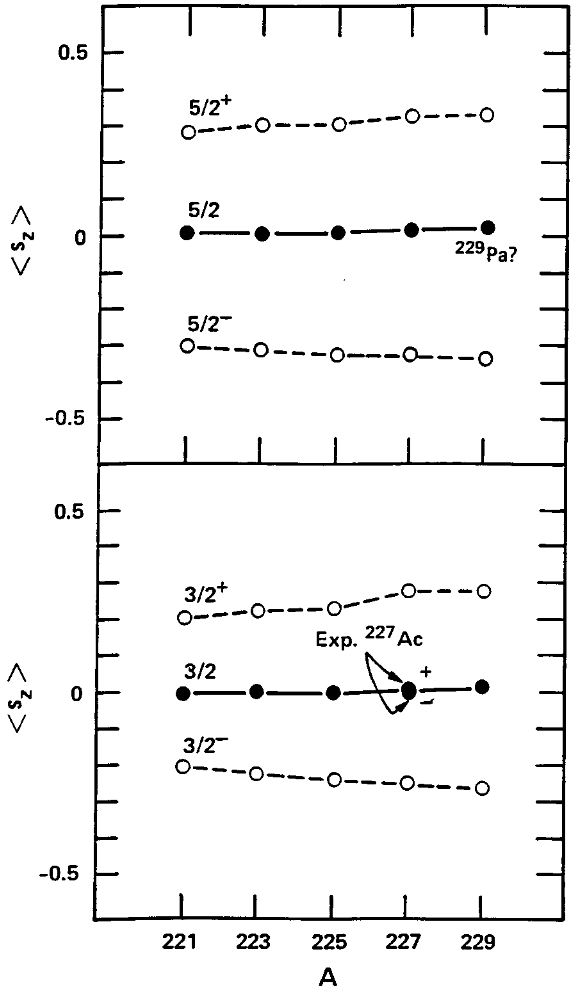

FIG. 34. Values of $\langle s_z \rangle$ for the $3/2^{\pm}$ and $5/2^{\pm}$ parity doublets in odd-A isotopes of Ac and Pa. Predictions of reflection-symmetric (ε_3=0) and reflection-asymmetric ($\varepsilon_3 \neq 0$) mean-field theory are indicated by dashed and solid lines, respectively (Leander and Sheline, 1984).

and N=94 are still octupole driving. However, at the higher rotational frequency $\hbar\omega$=0.6 MeV, the octupole-shell structure is almost completely washed out.

The octupole deformation explains the gradual angular momentum alignment in the light actinides. Calculations based on the cranked reflection-asymmetric WS model reproduce the absence of sharp band crossing in nuclei around ^{222}Th (Nazarewicz *et al.*, 1984a; 1987). Figure 39 displays the alignment plot $I_x(\omega)$ for ^{222}Th. Nazarewicz *et al.* (1987) have shown, using the particle-number projected cranking WS model with pairing, that the octupole-deformed ground-state band (β_2=0.116, β_3=0.104) crosses a neutron-aligned band at $\hbar\omega\approx$0.20 MeV, with a large interaction between the two bands. At the reflection-symmetric shape (β_2=0.12, β_3=0) the quasiparticle alignments are large and band interactions are small. The four-quasiparticle configurations $\nu(j_{15/2})^2\pi(i_{13/2})^2$ become yrast at $I\approx$26; that is, the shape transition from reflection asymmetric to reflection symmetric is expected. Experimentally, there is now evidence that the shape transition occurs at $I\approx$24 (Smith

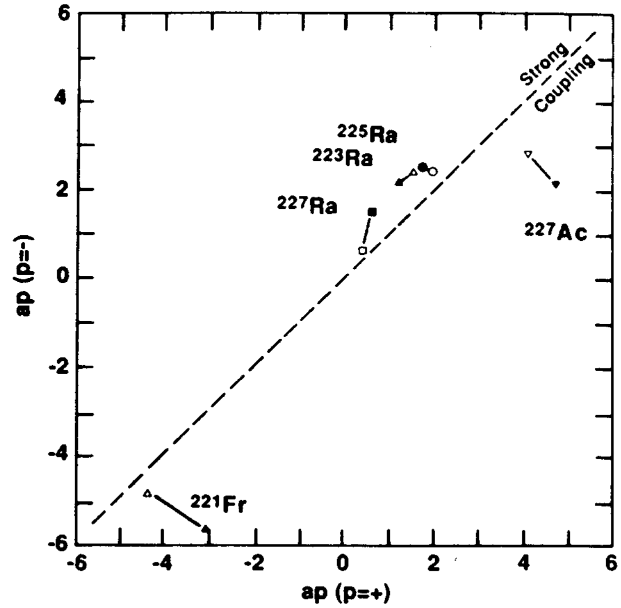

FIG. 35. The decoupling factor a times the total parity p for K=1/2 parity-doublet bands. Filled symbols represent measured data for the nuclei indicated on the plot; open symbols with connecting lines to the filled ones show the corresponding results of core-particle coupling calculations. The x axis gives the ap of the positive-parity band, and the y axis that of the negative-parity band. For strong coupling, the points would lie on the diagonal (dashed) (Leander and Chen, 1988).

et al., 1995; see also Schwartz *et al.*, 1987, 1988) while ^{220}Ra remains reflection asymmetric up to $I\approx$30.

A detailed discussion of rotation-induced shape changes in reflection-asymmetric nuclei from the Ra-Th and Ba-Ce regions has been given by Nazarewicz (1987), Nazarewicz *et al.* (1987), and Nazarewicz and Tabor (1992). They employed the so-called total Routhian surface method, in which the nuclear mean field is param-

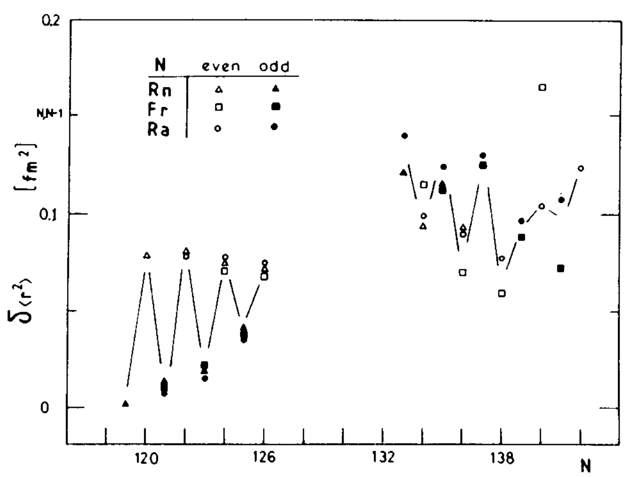

FIG. 36. Differential isotope shift $\delta\langle r^2\rangle^{N-1,N}$ for Rn, Fr, and Ra isotopes, showing regular odd-even staggering below N=126, and inverted sense for neutron numbers N=133, 135, and 137 (Otten, 1989).

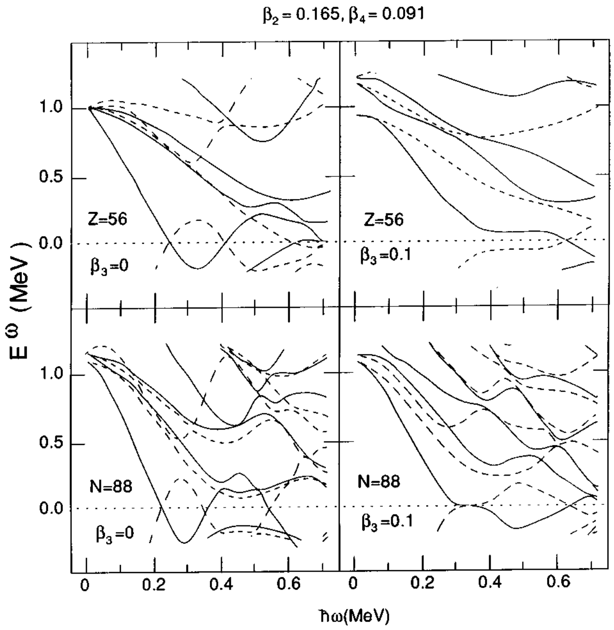

FIG. 37. Proton quasiparticle Routhians for Z=56 (top) and neutron quasiparticle Routhians for N=88 (bottom) as a function of rotational freqency. The deformation parameters used correspond to the yrast configurations of ^{144}Ba. The left panel, β_3=0, is representative of the reflection-symmetric configurations involving aligned neutron ($i_{13/2}$) and proton ($h_{11/2}$) pairs. The right panel, β_3=0.1, represents the structure of quasiparticle excitations associated with the reflection-asymmetric ground band. Levels are labeled by simplex, $s=i$ (solid line) and $s=-i$ (dashed line) (Nazarewicz and Tabor, 1992).

etrized by a WS single-particle potential and a BCS pair field. The energy E_{SC} of the nonrotating state, as a function of deformation $\hat{\beta}\equiv(\beta_2,\beta_3,\beta_4,\ldots)$, was obtained by the SC method. The total Routhian at frequency ω and deformation $\hat{\beta}$ was thus calculated as

$$E^{\omega}(\hat{\beta})=E_{\mathrm{SC}}(\hat{\beta})+[\langle H^{\omega}_{\hat{\beta}}\rangle-\langle H^{\omega=0}_{\hat{\beta}}\rangle]. \tag{89}$$

The absolute minimum of the Routhian at fixed ω corresponds to the solution for a yrast state. Secondary minima correspond to other solutions, which may be yrast if they have higher angular momentum. Figure 40 shows the equilibrium deformations as a function of rotational frequency, calculated with this method for the yrast configuration in doubly even $^{220-228}$Th.

Total Routhian surface calculations for nuclei predicted to have reflection-asymmetric ground states (such as ^{144}Xe, ^{144,146}Ba, ^{144,146}Ce, ^{222,224}Ra, and ^{222,224,226}Th) indicate that at medium spins the magnitude of octupole deformation increases, and the octupole minima are much better separated than in the ground state. Egido and Robledo (1990) added the rotational-energy term $I(I+1)/2\mathcal{J}(q_3)$ to the microscopic collective Hamiltonian (valid at I=0) to investigate the behavior of ^{146}Ba at high spins. They obtained stabilization of octupole deformation at high spins.

In general, the enhancement of octupole strength with rotation (see, for example, the behavior of ^{220}Th in Fig. 40) is caused by (a) weaker pairing correlations for the octupole shape, which increase the moments of inertia, and (b) increased octupole mixing between single-particle states of opposite parity which approach each other with increasing frequency (Nazarewicz, 1987; Egido and Robledo, 1990).

As discussed above, in the Ra and Th nuclei shape changes have been predicted to occur above I=24. In the Xe-Sm isotopes, the transition to reflection-symmetric shapes is expected to take place around I=12, which is much easier to reach experimentally; in ^{144,146}Ba, band crossings have been observed above I=12 (Zhu *et al.*, 1995).

The nuclei ^{218,220}Ra, ^{138,140}Xe, ^{140,142}Ba, ^{142}Ce, ^{144}Nd, and ^{146,148}Sm provide examples of strong quadrupole-octupole coupling. Their ground-state minima are predicted to be very β_2 and β_3 soft, but they become reflection asymmetric at medium spins. This shape transition is also associated with an increase in quadrupole deformation. Experimentally, the N=86 isotones are transitional systems showing an interplay between collective and noncollective modes. In ^{142}Ba, ^{146}Nd, and ^{148}Sm, the structures on top of the 8^+ and 11^- yrast states have been interpreted (Urban *et al.*, 1991; Zhu *et al.*, 1995) in terms of noncollective multiparticle excitations. The N=84 isotones of Nd, Sm, and Gd do not exhibit rotational behavior, and their excitation spectrum can be interpreted in terms of the spherical shell model, including octupole phonons (Bargioni *et al.*, 1995). In the Ra-Th region, spectacular examples of high-spin competition between noncollective excitations and octupole modes are the N=130 isotones ^{218}Ra (Schulz *et al.*, 1989) and ^{219}Ac (Cristancho *et al.*, 1994). Both nuclei exhibit enhanced $E1$ transitions and alternating-parity sequences. But the quadrupole collectivity is weak, as shown by their irregular quasivibrational spectra. The alignment process along the yrast line of ^{218}Ra can be reproduced by the cranked WS calculations with pairing, assuming very small quadrupole deformation, β_2=0.1, and a large value of $\beta_3\sim 0.09$ (Schulz *et al.*, 1989; see also Leandri and Piepenbring, 1993).

The nuclei ^{226}Ra, ^{228}Th, ^{146}Xe, ^{148}Ba, ^{146,148}Nd, ^{150}Sm, and ^{152}Gd are calculated to have well-developed quadrupole ground-state deformations, but they are β_3 soft. At low frequencies, the negative-parity states in these nuclei can be described in terms of very collective octupole vibrations. At medium spins, however, the static theory predicts a shape transition towards $\beta_3 \neq 0$, or at least the presence of near-yrast reflection-asymmetric configurations. The experimental data on ^{146}Nd (Urban *et al.*, 1988), and ^{150}Sm (Urban *et al.*, 1987), suggest that the above scenario indeed takes place in these nuclei.

Rotational properties of nuclei around ^{112}Ba were discussed by Heenen *et al.* (1994) in their total-Routhian-surface/WS calculations. They obtained a shape transition to β_3=0 at medium spins resulting from the alignment of $h_{11/2}$ neutrons and protons. For reflection-asymmetric cranked SC calculations for superdeformed nuclei, see Sec. IX.B.2.

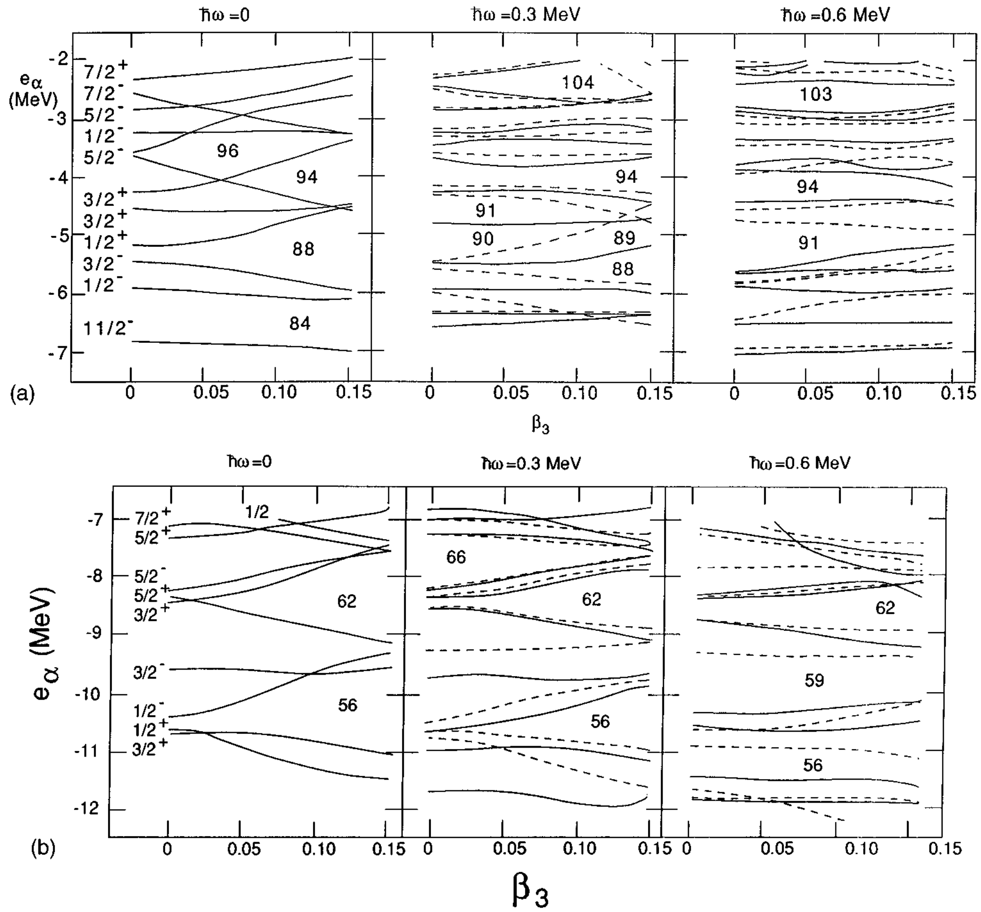

FIG. 38. Single-particle WS levels for neutrons (top) and protons (bottom) plotted versus octupole deformation β_3 at fixed values of β_2=0.2 and β_4=0.08. At zero rotational frequency, $\hbar\omega$=0, the single-particle levels are labeled by Ω. Intrinsic parity is indicated only at β_3=0 (for $\beta_3 \neq 0$ intrinsic parity is violated). At $\hbar\omega>0$, the levels are labeled by means of simplex, $s=i$ (solid line) and $s=-i$ (dashed line).

Kvasil and Nazmitdinov (1985) considered the RPA using the cranking reflection-asymmetric Hamiltonian with a pairing interaction plus quadrupole-quadrupole and octupole-octupole interactions. They gave expressions for energies and $E1$, $E2$, and $E3$ transition moments of reflection-asymmetric nuclei. Another application of the reflection-asymmetric cranked SC method can be found in work by Faber (1981), who investigated the influence of angular momentum on the mass distribution of heavy-ion induced fission.

The angular momentum dependence of the parity splitting in the actinides was discussed by Jolos *et al.* (1993, 1994, 1995), who employed the collective Hamiltonian of Eq. (48) with the spin-dependent collective potential $V(\beta_3,I)=U(\beta_3)+A(\beta_3)I(I+1)$. The parity splitting was estimated using the WKB approximation, and the resulting phenomenological expression accurately describes the alternating-parity rotational bands in even-even actinide nuclei. Zamfir *et al.* (1994) demonstrated that there is a simple correlation between the critical angular momentum I_{oct} at which the parity splitting disappears and the energy ratio $E(3_1^-)/E(2_1^+)$.

Alonso *et al.* (1995) used the *spdf* SU_3 Hamiltonian with quadrupole and octupole interaction to describe the positive- and negative-parity yrast bands in ^{226}Ra. They obtained a transition to reflection-asymmetric shapes at $I\sim 9$.

VII. INTRINSIC DIPOLE MOMENTS

In the presence of reflection-asymmetric deformations, a static electric dipole moment may arise in the intrinsic frame due to a shift between the center of charge and center of mass. Various theoretical treatments of this effect are discussed below.

A. Macroscopic models for the *E*1 moment

In the purely geometric picture, isoscalar dipole deformations are not independent degrees of freedom, but are determined from the c.m. condition, Eq. (3).

The collective electric dipole moment $\mathscr{D}_\mu$ appears in the second order as a product of quadrupole (λ=2) and octupole (λ=3) moments, namely,

$$\mathscr{D}_\mu=[\mathscr{Q}_2\times\mathscr{O}_3]_{1\mu}. \tag{90}$$

Thus one may expect that low-energy $E1$ collectivity should be pronounced in nuclei with strong quadrupole *and* octupole correlations. If higher moments ($\lambda=4,5,\ldots$) are present, they also contribute to D_μ through the $\lambda\leftrightarrow\lambda+1$ coupling (see below).

In the macroscopic liquid-drop model, dipole polarization results from asymmetry of the internal electric field caused by reflection-asymmetric shape deformations. Assuming an axially symmetric system, the induced dipole moment is proportional to $\beta_2\beta_3$ [see Eq.

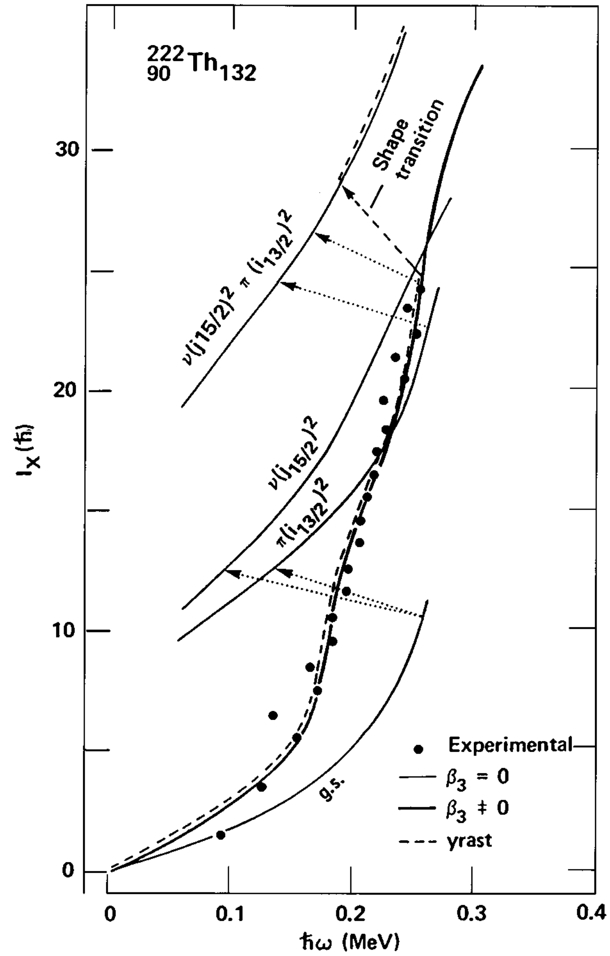

FIG. 39. Aligned angular momentum I_x for ^{222}Th, plotted as a function of rotational frequency. The calculated yrast line is plotted as a dashed line. The octupole-deformed band (thick solid line) remains yrast up to $I \sim 24$. Calculations predict, however, a backbending at higher spins, caused by crossing with a four-quasiparticle reflection-symmetric band (β_3=0, thin solid line). The experimental values are also plotted (Nazarewicz *et al.*, 1987).

(90)]. Bohr and Mottelson (1957, 1958) and Strutinsky (1956) calculated the $E1$ moment in the liquid-drop model (Strutinsky's derivation is the technically correct one). Expressing the liquid-drop energy in terms of nucleonic densities ρ_p and ρ_n, the local volume polarization of the electric charge becomes

$$\frac{\rho_p-\rho_n}{\rho_p+\rho_n}=-\frac{1}{4C_{\rm sym}}V_C(\boldsymbol{r}), \tag{91}$$

where $C_{\rm sym}$ is the volume-symmetry coefficient of the liquid-drop model and V_C is the Coulomb potential. This leads to

$$D_0=C_{LD}AZe\beta_2\beta_3, \tag{92}$$

where $C_{LD}\sim 0.0007$ fm (Strutinsky, 1957). (The $\beta_2\beta_3$ dependence of D_0 is often described as the "lightning rod" or charge-redistribution effect, referring to the tendency of electric charge to move toward regions of the surface with large curvature.)

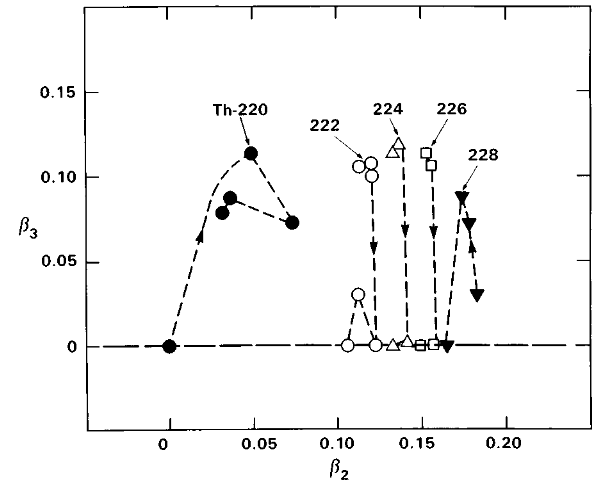

FIG. 40. Total Routhian surface predictions of equilibrium deformations in doubly even $^{220-228}$Th nuclei, at rotational frequencies ranging between 0 and 0.3 MeV/ħ (Nazarewicz *et al.*, 1987).

Lipas (1963) generalized Eq. (92) to triaxial shapes, and attempted to calculate values of D_0 using octupole mass parameters from experimental $B(E3)$ values, but found poor agreement with experiment. Further improvements to the liquid-drop contribution to the electric dipole moment hinged on the development of the two-fluid liquid-drop (or droplet) model (Myers and Swiatecki, 1974), which considers not only nuclear density nonuniformities (denoted in the following by $\delta\rho\equiv\rho-\tilde{\rho}$, where $\tilde{\rho}$ is the average value of density) but also the effect of the neutron skin. In the droplet model, the macroscopic intrinsic dipole moment can be expressed as (Dorso *et al.*, 1986)

$$\boldsymbol{D}=\boldsymbol{D}_{\text{v-red}}+\boldsymbol{D}_{\text{skin}}, \tag{93}$$

where

$$\boldsymbol{D}_{\text{v-red}}=e\int\left(\frac{N}{A}\delta\rho_p-\frac{Z}{A}\delta\rho_n\right)\boldsymbol{r}d^3\mathbf{r} \tag{94}$$

is the volume redistribution term, and

$$\boldsymbol{D}_{\text{skin}}=e\frac{NZ}{A}\frac{\Delta}{V}(\boldsymbol{R}_{\text{c.m.}}-\boldsymbol{R}_t) \tag{95}$$

is the neutron-skin contribution to the dipole moment. In Eq. (95), Δ is the neutron-skin layer volume, V is the nuclear volume, and $\boldsymbol{R}_t$ is the location of the center of mass of the neutron skin. By further splitting the neutron-skin contribution into $\boldsymbol{D}_{\text{skin}}=\boldsymbol{D}_{\text{s}}+\boldsymbol{D}_{\text{s-red}}$, and combining the volume and surface redistribution terms into the total redistribution term, $\boldsymbol{D}_{\text{r}}=\boldsymbol{D}_{\text{v-red}}+\boldsymbol{D}_{\text{s-red}}$, one finally obtains

$$\boldsymbol{D}=\boldsymbol{D}_{\text{r}}+\boldsymbol{D}_{\text{s}}. \tag{96}$$

It turns out that the two contributions in Eq. (96) are comparable in magnitude but opposite in sign. Thus, the presence of the neutron skin leads to a reduction of the intrinsic dipole moment in the droplet model.

In the limit of small deformations, the macroscopic dipole moment can be evaluated using a second-order expansion (Dorso *et al.*, 1986). Considering axial shapes only, one obtains

$$D_0=C_{\rm r}AZe\sum_{\lambda=2}^{\lambda_{\max}-1}\frac{49}{3\sqrt{35}}\frac{(\lambda^2-1)(8\lambda+9)}{[(2\lambda+1)(2\lambda+3)]^{3/2}}\beta_\lambda\beta_{\lambda+1}$$
$$-C_{\rm s}\sum_{\lambda=2}^{\lambda_{\max}-1}\frac{\sqrt{35}}{15}\frac{(\lambda^2-1)(\lambda+3)}{\sqrt{(2\lambda+1)(2\lambda+3)}}\beta_\lambda\beta_{\lambda+1}. \tag{97}$$

It is seen that the neutron-skin term is very sensitive to higher multipoles. Indeed, for large λ values it behaves like λ^2, while the expansion coefficients in the redistribution term are practically λ independent. [The validity of the estimate (97) was questioned by Denisov (1989, 1992), but this criticism has been shown to be without basis (Myers and Swiatecki, 1991).]

The magnitudes of $C_{\rm r},C_{\rm s}$ depend on the parameter values of the droplet-model mass formula. They are (Dorso *et al.*, 1986)

$$C_{\rm r}=\frac{9}{56\sqrt{35}}\frac{e^2}{\pi}\left[\frac{1}{J}+\frac{6L}{JK}I+\frac{15}{8Q}A^{-1/3}\right],$$
$$C_{\rm s}=\frac{15}{2\pi\sqrt{35}}\frac{NZ}{A}(I-\tilde{\delta})R_0, \tag{98}$$

where

$$I=\frac{N-Z}{A},\quad \tilde{\delta}=\frac{I+(9e^2/80r_0Q)ZA^{-2/3}}{1+(9J/4Q)A^{-1/3}}. \tag{99}$$

In the above, J is the volume symmetry-energy coefficient, Q is the effective neutron-skin stiffness, K is the compressibility coefficient, and L is the density symmetry coefficient. The values of J, Q, K, and L are not known very accurately. They are usually assumed to be in the range $25<J<44$ MeV, $17<Q<70$ MeV, $K\approx240$ MeV, and $0<L<100$ MeV.

The relation between the exact droplet-model expressions, Eqs. (93)–(95), and the second-order formula (97) was investigated by Skalski (1994). In the absence of high-multipole deformations (e.g., if only β_2 and β_3 are present), the second-order expansion is rather accurate. If higher-multipole deformations are taken into account, the approximate expression quickly diverges from the exact result with increasing β_2 and β_3. However, the difference can be compensated by changing the droplet-model parameters Q and L within the range of their uncertainty.

Since the macroscopic dipole moment is proportional to β_2, one expects D_0 to be very large for superdeformed, reflection-asymmetric systems. Indeed, for a large range of β_2 values, D_0 increases monotonically with elongation. Interestingly, for fixed values of odd-multipole deformations, the value of D_0 saturates at large elongations, $\beta_2\sim0.7$, and then falls with β_2 (Skalski, 1994). This effect arises from the reduction of the charge-redistribution term for very elongated shapes.

Donner and Greiner (1966), in their collective quadrupole-octupole model, suggested that the coupling between the collective amplitudes $\mathscr{D}_{\rm GDR}$ of the giant dipole resonance and the collective dipole moment of Eq. (90) gives rise to dipole transitions from collective octupole states.

Karpeshin (1992) has shown that reflection-asymmetric shapes during prompt fission give rise to anomalous $E1$ internal conversion.

By construction, macroscopic models for the intrinsic dipole moment do not contain shell effects. Those are discussed in the following section.

B. Shell-correction approach to $E1$ moments

The microscopic contribution to the $E1$ moment was introduced by Leander (1985b) In this approach, the $E1$ moment is written as the sum of a macroscopic (liquid-drop or droplet-model) term and a (renormalized) shell-correction term obtained using a single-particle potential,

$$\boldsymbol{D}=\boldsymbol{D}_{\rm macr}+\boldsymbol{D}_{\rm shell}. \tag{100}$$

The shell-correction contribution $\boldsymbol{D}_{\rm shell}$ can be expressed as

$$\boldsymbol{D}_{\rm shell}=e_p^{\rm eff}\frac{N}{A}\langle\boldsymbol{r}_p\rangle_{\rm shell}-e_n^{\rm eff}\frac{Z}{A}\langle\boldsymbol{r}_n\rangle_{\rm shell}, \tag{101}$$

where $\langle\boldsymbol{r}\rangle_{\rm shell}$ is the shell correction to $\langle\boldsymbol{r}\rangle$. In the presence of pairing correlations and rotation, it is equal to

$$\langle\boldsymbol{r}\rangle_{\rm shell}=\sum_{i,j}\rho_{i,j}\langle i|\boldsymbol{r}|j\rangle-\sum_i n_i\langle i|\boldsymbol{r}|i\rangle, \tag{102}$$

where $\hat{\rho}$ is the single-particle density matrix and n_i are the smoothed single-particle occupation numbers (Strutinsky, 1967; Brack *et al.*, 1972). In the absence of rotation, $\rho_{i,j}=v_i^2\delta_{i,j}$, where v_i^2 is the BCS occupation coefficient for the single-particle state i. As demonstrated by Leander *et al.* (1986) and Butler and Nazarewicz (1991), the values of $\langle z\rangle_{\rm shell}$ behave very regularly as a function of shell filling. They increase gradually until the middle of the shell, and decrease smoothly in the upper half of the shell (Fig. 41). These oscillations reflect the strength of unique-parity orbitals fragmented by the octupole interaction (Butler and Nazarewicz, 1991).

In contrast to wave functions obtained in the self-consistent approach based on the microscopic effective interaction, the single-particle wave functions appearing in Eq. (102) do not contain correlations of the dipole-dipole character. The screening effect caused by the particle-vibration coupling with the $E1$ giant resonance (Bohr and Mottelson, 1975) leads to renormalization of the single-particle matrix elements

$$\langle i|\boldsymbol{r}|j\rangle^{\rm eff}=(1+\chi_{ij})\langle i|\boldsymbol{r}|j\rangle, \tag{103}$$

where χ_{ij} is the state-dependent $E1$ polarizability coefficient [hence $e^{\rm eff}=e(1+\chi_{ij})$]. The average value of χ_{ij}, denoted χ, can be estimated in the harmonic-oscillator model with a separable dipole-dipole interaction. Assuming that the particle-hole energies are all equal to e_{ph}, one obtains

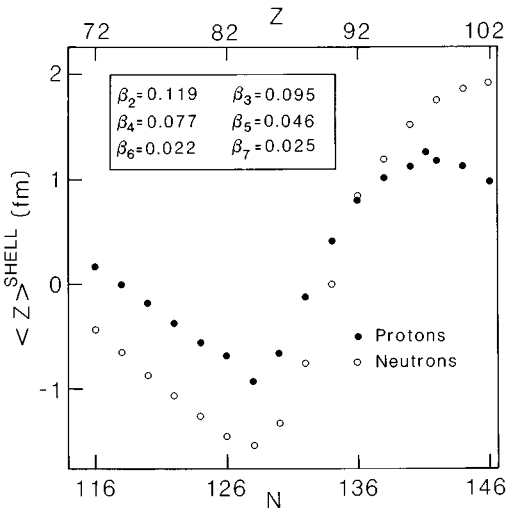

FIG. 41. Shell correction to $\langle z \rangle$ given by Eq. (102), calculated in a WS model as a function of the numbers of particles filling the lowest orbits, for protons (filled circles, upper axis) and neutrons (open circles, lower axis). The deformation used corresponds to the calculated ground-state shape of ^{222}Ra (Butler and Nazarewicz, 1991).

$$\chi(E)=\frac{e_{ph}^2-E_{\mathrm{GDR}}^2}{E_{\mathrm{GDR}}^2-E^2}, \tag{104}$$

where E_{GDR} is the energy of the giant dipole resonance and E is the transition energy. The ground-state (E=0) value of χ is given by (Bohr and Mottelson, 1975; Leander *et al.*, 1986)

$$\chi_{\mathrm{g.s.}}=\frac{e_{ph}^2}{E_{\mathrm{GDR}}^2}-1. \tag{105}$$

In the axial harmonic oscillator with deformation ε and frequency ω_0, assuming the doubly stretched dipole-dipole interaction (Sakamoto and Kishimoto, 1989), one obtains $e_{ph}=\hbar\omega_z=\hbar\omega_0(1-2\varepsilon/3)$, $E_{\mathrm{GDR}}\approx 1.9\hbar\omega_0(1-2\varepsilon/3)$ (K=0), and $e_{ph}=\hbar\omega_\perp=\hbar\omega_0(1+\varepsilon/3)$, $E_{\mathrm{GDR}}\approx 1.9\hbar\omega_0(1+\varepsilon/3)$ (K=1). An interesting consequence of Eq. (105) is that the deformation dependence in $\chi_{\mathrm{g.s.}}$ cancels out. The *deformation-independent* ground-state $E1$ polarizability coefficient becomes $\chi_{\mathrm{g.s.}}\approx -0.72$.

Leander *et al.* (1986) performed the analysis of $E1$ moments in nuclei that were predicted to have ground-state static deformations. In their calculations, the macroscopic part of the dipole moment was similar to that obtained by Strutinsky (1957). The shell correction was obtained using a deformed WS potential. In the calculations, the cranked SC method was also used to determine equilibrium shapes for different nuclei at various values of angular momentum, so that $E1$ moments could be evaluated as a function of Z, N, and I. The overall trend of the experimental results was reproduced in these calculations for Ra and Th nuclei. One feature observed is a cancellation of the liquid-drop and shell correction for ^{226}Ra, which gives a local minimum in Z, N for the $E1$ moment. Improvements to these calculations were made by Butler and Nazarewicz (1991), who used the droplet model of Dorso *et al.* (1986) to take into account effects of the neutron skin. These calculations were able to reproduce the systematic trends seen in experimental data in both medium-mass and heavy nuclei (see Fig. 22). The cancellation of liquid-drop and shell corrections was found to occur also for ^{224}Ra, in agreement with the experimental data (Poynter *et al.*, 1989a). The particular parametrization employed in the droplet model gave a very small macroscopic contribution to D_0 in the lanthanide region. Since the neutron and proton shell contributions can have opposite sign, zero or negative values of D_0 can arise. In particular, cancellation between proton and neutron contributions to $(D_0)_{\mathrm{shell}}$ explains the reduced $E1$ moment found in ^{146}Ba (Mach, Nazareweicz, *et al.*, 1990).

For several nuclei, such as ^{148}Ba and ^{226}Ra, the calculations yield a negative value of D_0. This interesting theoretical prediction can be tested experimentally by, for example, the measurement of an interference effect between the $E1$ and $E3$ ΔI=1 γ rays. Such a measurement would provide an excellent test for theoretical approaches aiming at reproducing enhanced $E1$ rates.

The macroscopic-microscopic approach to the intrinsic dipole moment was employed by Skalski (1994) to estimate the low-energy $E1$ collectivity in superdeformed and hyperdeformed configurations (see Sec. IX.B.2).

C. Self-consistent models

The most extensive and successful microscopic calculations of $E1$ moments for ground-state configurations in medium-mass and heavy even-even nuclei are those carried out by Egido, Robledo, and coworkers using the constrained HF+BCS model with the Gogny interaction. In the first study, based on a pure mean-field approach, Robledo *et al.* (1987) calculated intrinsic dipole moments in ^{222,224}Ra and ^{222}Rn. In the following papers (Egido and Robledo, 1989, 1990, 1991a, 1991b, 1992; Robledo *et al.*, 1988; Martín and Robledo, 1994) they solved the collective Schrödinger equation, with and without parity projection (Sec. III.C.3). They obtained excellent agreement with experimental B(E1) transition rates for nuclei from both octupole-deformed and octupole vibrational regions (see Fig. 22) and, in particular, they reproduced the very low values of D_0 in ^{224}Ra and ^{146}Ba.

Skalski *et al.* (1993b) employed the generator-coordinate HF+BCS model with the SkM* interaction to calculate low-energy $E1$ transitions in superdeformed Hg and Pb nuclei. For the lowest octupole μ=0 states, they predicted very large D_0 moments, ranging between 0.5 e fm and 0.8 e fm. For the μ=1 octupole modes, the calculated D_1 values were smaller and negative ($\sim -0.25\,e$ fm). In the two-mode calculations (involving coupling between the μ=0 and μ=2 octupole modes), these values were reduced by about 20%.

D. Algebraic models, boson models, and cluster models

In the $spdf$ version of the interacting-boson model (see Sec. III.D), the $E1$ operator is a one-boson operator obtained by a direct coupling of df, pd, and sp bosons to J=1:

$$D_{\mu}=e_1^{(df)}\{[d^+\times f^*]_{1\mu}+[f^+\times d^*]_{1\mu}\}+e_1^{(pd)}\{[p^+\times d^*]_{1\mu}+[d^+\times p^*]_{1\mu}\}+e_1^{(sp)}(p_{\mu}^+\times s+s^+\times p_{\mu}^*), \quad (106)$$

see Han *et al.* (1985), Engel and Iachello (1987), and Otsuka and Sugita (1988). By adjustment of the effective charges $e_1^{(bb')}$ in Eq. (106), the experimental data can be fitted, although fine-tuning is required in the cases of ^{218,220}Ra (see Fig. 11; Engel and Iachello, 1987) and ^{146}Ba (Kusnezov and Iachello, 1988, Mach, Nazarewicz *et al.*, 1990; Zamfir and von Brentano, 1992; Liu *et al.*, 1994).

For vibrational states, Barfield *et al.* (1989) concluded that the $E1$ operator must include a two-body term in the sdf interacting-boson model in order to reproduce the transition rates measured in ^{144}Sm. A similar conclusion was reached by Zamfir *et al.* (1990), von Brentano *et al.* (1992), and Zamfir and von Brentano (1992), who specified that the two-body operator must arise from mixing with the giant dipole resonance.

The SU_3 limit of expression (106) was applied by Alonso *et al.* (1995) to $E1$ transition rates in ^{226}Ra (Wollersheim *et al.*, 1993). The main features of the angular momentum pattern of observed D_0 values have been reproduced in the $spdf$-boson model.

In odd-A nuclei, the effective $E1$ operator can be constructed phenomenologically by coupling the odd quasiparticle to the interacting-boson model core. Dojnikov and Mikhailov (1994) assumed an sd-boson core, and performed interacting-boson-fermion model calculations for $B(E1)$ rates in ^{77}Se. In their description, however, the f-boson contribution has been neglected.

Electric dipole rates in ^{150}Sm were estimated by Badea *et al.* (1978) in the coherent-state model based on the boson expansion method. For the $E1$ transition operator, they took

$$D_{\mu}=e_1\{[B_2^+\times B_3^+]_{1\mu}+[B_3^+\times B_2]_{1\mu}+\text{H.c.}\}, \quad (107)$$

where B_2 (B_3) are quadrupole (octupole) phonon operators. Kammuri and Kishimoto (1978) studied $B(E1)/B(E2)$ ratios in ^{100}Ru, ^{112}Cd, ^{150}Sm, and ^{152}Gd using the microscopic boson expansion technique. Here the $E1$ operator arises from the quadrupole-octupole coupling and is given by an expression similar to Eq. (107), but with boson operators closely related to the RPA phonons. Kammuri and Kishimoto (1978) pointed out that the low-energy $E1$ strength in ^{100}Ru is reduced due to proton-neutron cancellation, and is enhanced in ^{150}Sm and ^{152}Gd. They concluded that the calculated $E1$ rates depend dramatically on shell structure and on the assumed shell-model space.

For nonconjugate nuclei such as ^{18}O, the interesting prediction of the cluster model and the vibron model discussed in Sec. III.D is that of large $B(E1)$ transition strengths (Nemoto and Bandō, 1972; Buck and Pilt, 1977; Iachello, 1981), which arise if the two clusters have different charge-mass ratios. Alhassid *et al.* (1982) have developed molecular sum rules for radiative deexcitation widths in nuclei comprised of two arbitrary clusters. For the nucleus (A,Z) decomposed into two clusters (A_1,Z_1) and (A_2,Z_2), the energy-weighted molecular sum rule is given by

$$S_{1m}(E1)=\frac{9\hbar^2e^2}{8\pi m}\frac{(Z_1A_2-Z_2A_1)^2}{A_1A_2A}. \quad (108)$$

For very asymmetric cluster configurations (such as those involving α-particle clustering), the molecular sum rule (108) is considerably smaller than the nuclear sum rule

$$S_1(E1;A)=\frac{9\hbar^2e^2}{8\pi m}\frac{NZ}{A}. \quad (109)$$

Consequently, the molecular sum rule provides a new scale ($\sim10^{-2}$ s.p.u.) for the $B(E1)$ enhancement [see also the discussion in Suzuki *et al.* (1985), and Eq. (112)]. For experimental systematics see Cottle and Kemper (1991). Sum rules for soft dipole modes in halo nuclei were discussed by Sagawa *et al.* (1992) (see Sec. X.D).

E. Influence of octupole vibrations on $E1$ moments

Enhanced $B(E1)$ rates can also be present in well-deformed reflection-symmetric nuclei, due to the coupling to low-lying octupole one-phonon states. This means that enhanced $B(E1)$'s do not always indicate octupole instability.

Kocbach and Vogel (1970) investigated the $E1$ transition rates between octupole and ground-state bands. Due to the Coriolis mixing between the K=0 and K=1 octupole phonons, Eq. (61), the $E1$ matrix elements are modified by the presence of a spin-dependent correction proportional to the ratio $\mathscr{Z}=D_1/D_0$. [For experimental values of $\mathscr{Z}$ see, for example, McGowan and Milner (1981) (^{156,158,160}Gd, ^{160}Dy); McGowan and Milner (1993) (^{232}Th); McGowan and Milner (1994) (^{238}U); Ackermann *et al.* (1993) (^{230,232}Th).]

In the particle-vibration coupling formulation, the $E1$ transition operator can be written as

$$D_{\mu}=D_{\mu}^{\text{s.p.}}+eb_{\mu}r^3Y_{3\mu}. \quad (110)$$

The second term in (110) represents the contribution coming from octupole vibrations, which is usually much larger than the single-particle term. It has been shown that after proper adjustment of b_{μ}, it is possible to reproduce the angular momentum dependence of the measured $B(E1)$ rates.

Early calculations of $E1$ transition moments between single-particle states in the Nilsson model with BCS pairing grossly underestimated the experimental values, particularly for ΔK=0 transitions in rare-earth nuclei (Monsonego and Piepenbring, 1964; Vergnes and Rasmussen, 1965) Improvement was achieved by the addition of octupole vibrations and particle-vibration interaction terms (Monsonego and Piepenbring, 1966; Faessler *et al.*, 1966) and, additionally, Coriolis coupling (Bernthal and Rasmussen, 1967). Systematic calculations of this type have been carried out recently by Hagemann *et al.* (1993) using the method described by Hamamoto *et al.* (1989); they find that the amplitude of the octupole term depends not only on Z and N, but also on the pair of bands selected (see also Hamamoto, 1993). The importance of mixing into low-lying states by the giant dipole resonance has been stressed by Donner and Greiner (1966) and Iachello (1985), and the application of a model which includes octupole-octupole and dipole-dipole interaction by Alikov *et al.* (1988) found that the contribution from the latter interaction derived from giant-dipole-resonance parameters plays a dominant role in low-lying transitions in odd Eu and Tb nuclei, and in the core 0^+-1^- transitions. Similar conclusions have been reached by Guhr *et al.* (1989), who used an octupole vibration model which included a small isovector dipole component to describe e^- scattering form factors, and by Dojnikov *et al.* (1991), Soloviev and Sushkov (1991, 1994), Zilges *et al.* (1992), and Govaert *et al.* (1994), who paid particular attention to the large $E1$ strengths found in low-lying states in many nuclei by nuclear resonance fluorescence studies [see Kneissl *et al.* (1993), Cottle (1994), and references therein]. For light nuclei, Castel *et al.* (1990) concluded that isospin mixing from the giant monopole resonance can be more important than from the giant dipole resonance.

VIII. MOLECULAR STATES IN LIGHT NUCLEI

The study of light nuclei from the sd region provided the first evidence for reflection asymmetry in rotating nuclei. Negative-parity bands with approximately rotational energy spacings have been observed in several nuclei. Figure 42 compares the behavior of the $K^\pi=0^-$ and 0^+ bands in ^{16}O and ^{20}Ne; in ^{16}O the negative-parity states become interleaved with the positive-parity states at the highest observed spins. Large α-decay widths are usually associated with the quasimolecular states (Horiuchi and Suzuki, 1973). Although large $E3$ strengths have been observed in these nuclei [typically 10–20 s.p.u. for the strongest transitions; see Häusser *et al.* (1971) and Krick *et al.* (1973)], measurements have been confined to transitions from lower-lying bands, such as the $K^\pi=2^-$ band in ^{20}Ne, or the well-known transition between the $1/2^+$ ground state and the $5/2^-$ state at 1.35 MeV in ^{19}F.

The $E1$ strengths are small in the self-conjugate nuclei ($<10^{-4}$ s.p.u.), but in nuclei with $Z \neq N$ large $B(E1)$'s have been observed (Cottle and Kemper, 1991).

The various theoretical descriptions of the negative-parity states in the light nuclei have invariably invoked a reflection-asymmetric basis to reproduce the observed experimental features. The natural model for describing

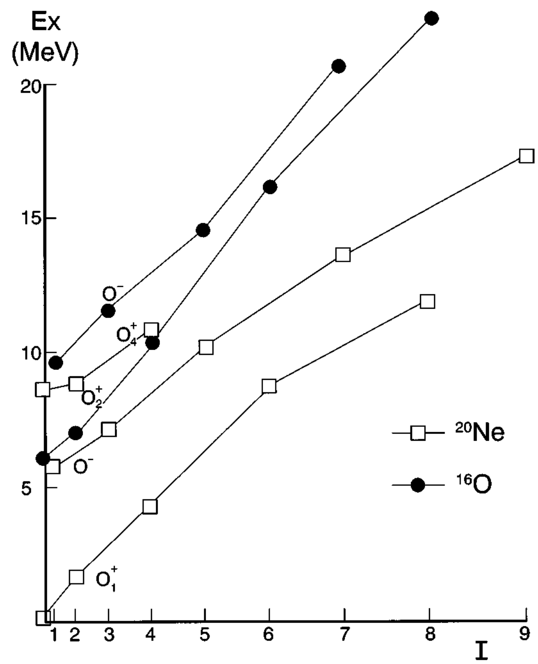

FIG. 42. The K^π=0^+ and 0^- rotational bands in ^{16}O and ^{20}Ne. The bands shown have large α-decay widths or spectroscopic factors, except for the ground-state band in ^{20}Ne. The assignment of states in ^{16}O is taken from Ajzenberg-Selove (1986), and in ^{20}Ne from Richards (1984) and Ajzenberg-Selove (1987).

the large α widths is the alpha-cluster model (Sec. III.E). Ikeda *et al.* (1968) suggested that cluster configurations would appear near the threshold energy for decay into the fragments. Figure 43 illustrates this idea, using the so-called Ikeda diagram (Horiuchi *et al.*, 1972). The alternative approach is that of the octupole-deformed mean field (Sec. III.B). For a review of the relationship between clusterlike configurations and deformed states see Rae (1988).

A. ^{16}O

The two bands in ^{16}O built on the 0_2^+ state at 6.05 MeV and the 1^- state at 9.58 MeV can be described adequately in terms of an α+^{12}C bimolecular system (Roth and Wildermuth, 1960; Arima *et al.*, 1967; Horiuchi and Ikeda, 1968; Nemoto and Bandō, 1972; Suzuki, 1976; Suzuki, 1980; Fujiwara *et al.*, 1980; Baldock and Stratton, 1985; Descouvemont, 1987, 1991).

In the early HF parity-mixing calculations, Kelson (1965) discussed the spectrum of ^{16}O in the $1p_{1/2}$, $2s$, $1d$ shell-model space. In these calculations, the first excited 0^+ state of O^{16} was described in terms of four particles in the sd shell with a small component in the $p_{1/2}$ state; however, Giraud and Sauer (1970) demonstrated that this parity-mixed state contained a large spurious component of center-of-mass motion. Do Dang *et al.* (1976) performed the HF calculations with parity projection before variation, and obtained the reflection-asymmetric ground state and the reflection-symmetric first excited 0^+ state.

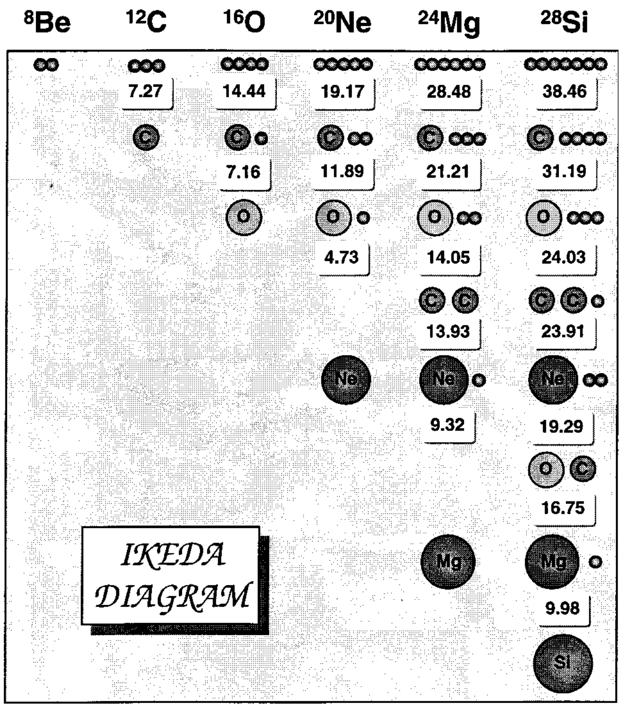

FIG. 43. Ikeda diagram for light nuclei. The threshold energy for each decay mode (in MeV) is indicated (Horiuchi *et al.*, 1972).

Many states in ^{16}O can be described in terms of four-alpha-particle configurations that break intrinsic parity (tetrahedron, bent rhomb, kite); see Dennison (1940, 1954), Kameny (1956), Bertsch and Bertozzi (1971), Robson (1979), Bauhoff *et al.* (1984), and references therein. Bauhoff *et al.* (1984) investigated the structure of ^{16}O in the alpha-cluster model with parity and angular momentum projection. They obtained tetrahedral symmetry for the ground state and several excited states, such as the 3^- state at 6.13 MeV. Elliott *et al.* (1985) performed an analysis based on the shell model perturbed by the tetrahedral potential, and concluded that the 0_1^+, 3^- (6.13 MeV), and 4^+ (11.09 MeV) states form a tetrahedral rotational band. They were able to explain the α-transfer cross sections, and also the measured lifetime for the $E3$ decay of the 3^- state.

The energy spectrum and alpha-particle spectroscopic factors of the $\alpha+^{12}$C system have been discussed within the vibron model (Cseh, 1989; Cseh *et al.*, 1991).

B. ^{18}O

The rotational band in ^{18}O built upon the 0_2^+ (3.63 MeV) state was identified by Buck *et al.* (1977), Sakuda (1977), and Sakuda *et al.* (1978, 1979) as being an $\alpha+^{14}$C dinuclear configuration.

Unlike in $n\alpha$ nuclei, where $E1$ transitions are isospin forbidden, the $E1$'s within an alternating-parity band built on the 0_2^+ state in ^{18}O are large, $\approx 10^{-2}$ s.p.u. (Gai *et al.*, 1983, 1987, 1989, 1991). The large electric transition strengths within the band, and the large α-decay widths of the 3^- and 4^+ members of this band, give strong support (Gai *et al.*, 1983) to the bimolecular interpretation.

Alhassid *et al.* (1982) found that for ^{18}O having the configuration $\alpha+^{14}$C, the measured $B(E1)$ transition rates within the molecular dipole band in ^{18}O exhaust a significant fraction of the molecular sum rule, Eq. (108). Iachello (1985) has estimated that the octupole model would give much smaller values than are observed experimentally, although microscopic cluster models (Baye and Descouvemont, 1984; Assenbaum *et al.*, 1984; Suzuki *et al.*, 1985) overestimate the $B(E1)$ strength. The detailed calculations (Descouvemont and Baye, 1985; Funck *et al.*, 1989) also suggest that the positive- and negative-parity cluster states in ^{18}O have different intrinsic structure, and therefore cannot be regarded as being members of the same dipole-molecular band: the band proposed by Gai *et al.* (1983) consists of states belonging to different molecular bands [see also the discussion in Gai *et al.* (1989, 1991)]. The foundation of the molecular dipole states is not supported by recent α-cluster calculations of Reidemeister and Michel (1993), in which the parameters of the optical potential are taken from $\alpha+^{14}$C elastic-scattering data. Instead they predict a negative-parity inversion-doublet band, an analogue to the cluster band in ^{16}O. A semimicroscopic algebraic cluster model has been applied by Lévai *et al.* (1992). They are able to interpret most experimental states below 10 MeV, and find smaller $B(E1)$ values than the earlier microscopic cluster calculations, while still overestimating the experimental values. The TDHF method has also been applied to the quasimolecular states in this nucleus, and predicts the existence of giant resonances in the $\alpha+^{14}$C system having large quadrupole and octupole deformation (Strayer *et al.*, 1984; Umar *et al.*, 1985).

C. ^{20}Ne

A classic example of a reflection-asymmetric light system is the nucleus ^{20}Ne. Horiuchi and Ikeda (1968), Nemoto and Bandō (1972), and Nemoto *et al.* (1975) have shown that the $K^\pi=0^-$ (5.78 MeV) and $K^\pi=0_4^+$ (8.3 MeV) bands of ^{20}Ne have a well-developed structure corresponding to a ^{16}O+α dinucleus configuration, while the $K^\pi=0^+$ band has an intermediate character, between clusterlike and shell-like. This is consistent with the experimental behavior of the α widths (Table VII): the widths from the negative-parity states remain large, while the α width of states in the $K^\pi=0_1^+$ band decrease at high spin. Tomoda and Arima (1978) have extended this description by combining a $(2s1d)^4$ shell-model space and a ^{16}O+α cluster-model space. A more recent development has been the use of the GC method to calculate $E1$ strengths in ^{20}Ne using $\alpha+^{16}$O T=0 and T=1 configurations (Descouvemont and Baye, 1986). For other calculations related to the $\alpha+^{16}$O clustering in ^{20}Ne, see Hiura *et al.* (1969), Tanabe and Nemoto (1974), Yamamoto (1974), Matsuse *et al.* (1975), Fujiwara *et al.* (1980), Kazama *et al.* (1984), Kazama (1987), and Buck *et al.* (1995). Zhang *et al.* (1994) applied the

TABLE VII. Experimental behavior of the α widths in ^{20}Ne (Cseh *et al.*, 1991).

K^{π}	I^{π}	E_x (MeV)	θ_{α}^2
0_1^+	0^+	0	0.15
	2^+	1.63	0.11
	4^+	4.25	0.12
	6^+	8.78	0.085
	8^+	11.95	0.01
0^-	1^-	5.79	1.03
	3^-	7.16	0.87
	5^-	10.26	0.90
	7^-	13.69	0.84
	9^-	17.43	0.48
0_4^+	0^+	$\approx$8.7	0.70
	2^+	$\approx$8.8	0.95
	4^+	10.80	0.33

Bloch-Brink model to ^{20}Ne, and found a low-lying mass-asymmetric configuration. Dufour *et al.* (1994) investigated the $\alpha+{}^{16}$O system using a multicluster GC method. Kanada-En'yo and Horiuchi (1995a) studied the structure of the yrast line of ^{20}Ne with antisymmetrized molecular dynamics (see Sec. III.E). They found that for both positive- and negative-parity low-spin states ($I<9$) the two-cluster structure of $\alpha+{}^{16}$O is dominant (see Fig. 44).

Leander and Larsson (1975) obtained octupole instability for the prolate ground state of ^{20}Ne, caused by the strong octupole interaction between the [110]1/2 and [200]1/2 levels. Noto *et al.* (1976) applied the variational method with a parity- and angular-momentum-projected wave function of the quadrupole-plus-octupole deformed-shell model (Noto *et al.*, 1974) and the Hamiltonian with the Volkov effective two-nucleon interaction. They obtained a static Y_{30} field in ^{20}Ne, and were able to reproduce the transition energies, the electromagnetic transition probabilities, and the charge form factors in the $0^+\rightarrow1^-$ (e,e') scattering. Marcos *et al.* (1983) performed parity-projected constrained HF calculations supplemented by GC calculations. They also found softness to octupole deformation in ^{20}Ne, and were able to reproduce the excitation energy of the 1^- state. A microscopic description of the clustering structure of ^{20}Ne was given by Provoost *et al.* (1984), using the quantized adiabatic TDHF theory with parity projection. They obtained a reflection-asymmetric ground state, and were able to reproduce the parity splitting.

The energy spectrum and the alpha-particle spectroscopic factors of the $\alpha+{}^{16}$O system have also been discussed within the vibron model (Cseh, 1989; Cseh *et al.*, 1991). Cseh (1993) also investigated a three-dimensional algebraic description of the $\alpha+{}^{16}$O cluster.

D. ^{24}Mg

Microscopic calculations using two alpha clusters plus a ^{16}O core (Katō and Bandō, 1975, 1979) have explained the ground-state $K^{\pi}=0^+$ band and the $K^{\pi}=0^-$ (7.55 MeV) band in terms of the parity doublet. Marsh and Rae (1986) applied the unconstrained alpha-cluster model with the Brink-Boeker $B1$ force. Several calculated energy minima have been associated with reflection-asymmetric intrinsic shapes corresponding to separation channels of ^{20}Ne+α, ^{16}O+2α, ^{12}C+^{12}C, and ^{12}C+3α (Fig. 45). For other cluster-model calculations for ^{24}Mg, see Pilt and Wheatley (1978), Fujiwara *et al.* (1980), Katō *et al.* (1986), Descouvemont and Baye (1987, 1989), and Buck *et al.* (1990).

Noto (1980, 1981) has applied the deformed-shell model of Noto *et al.* (1974) to the rotational bands of ^{24}Mg. The calculations predict nonzero static quadrupole and octupole moments in the lowest $K^{\pi}=0^+$, 0^-, 2^+, and 3^- bands. In particular, they reproduce the observed (Branford *et al.*, 1971) strong $E3$ transitions in the low-lying states of ^{24}Mg. The cranked SC calculations of Leander and Larsson (1975) predict a low-lying reflection-asymmetric hyperdeformed minimum in ^{24}Mg. This minimum, originating from the mixing between the [101] and [211] Nilsson states, can be associated with asymmetric ^{16}O+α+α or ^{16}O+^{8}Be structures seen in the ^{16}O + ^{8}Be and ^{20}Ne+α resonances [see discussion in Rae (1988)].

E. ^{28}Si

According to the Ikeda diagram of Fig. 43, the excited states of ^{28}Si can be described in terms of various cluster configurations. Bauhoff (1982) extended the microscopic alpha-cluster model to describe the experimental band structure of the negative-parity bands in ^{28}Si. Katō *et al.* (1985) studied molecular ^{12}C+^{16}O structures (Erb and Bromley, 1981) using a semimicroscopic cluster model. Cseh (1992) applied the vibron model coupled to the SU$_3$ shell model to describe ^{28}Si in terms of a ^{24}Mg+α configuration. Leander and Larsson (1975) found a hyperdeformed octupole shape in ^{28}Si having a similar configuration to that in ^{24}Mg. The same elongated structure has also been predicted to occur within the Bloch-Brink α-cluster model (Zhang *et al.*, 1993; Zhang *et al.*, 1994).

F. ^{32}S

Leander and Larssen (1975) found an excited minimum corresponding to $\varepsilon_3=0.3$, which has a configuration analogous to the hyperdeformed asymmetric minima in ^{24}Mg and ^{28}Si. The application of the alpha-cluster model by Zhang *et al.* (1994) has also yielded an extremely elongated minimum in this nucleus, having octupole deformation. Bauhoff *et al.* (1980), also in the alpha-cluster model, obtained intrinsic states with C_{2v} point symmetry. Experimental candidates for molecular bands having large alpha widths have been reported by Morita *et al.* (1985), using the ^{16}O(^{20}Ne, α) reaction and (at higher energy) by Brenner (1994) using α-particle elastic scattering (see Fig. 46).

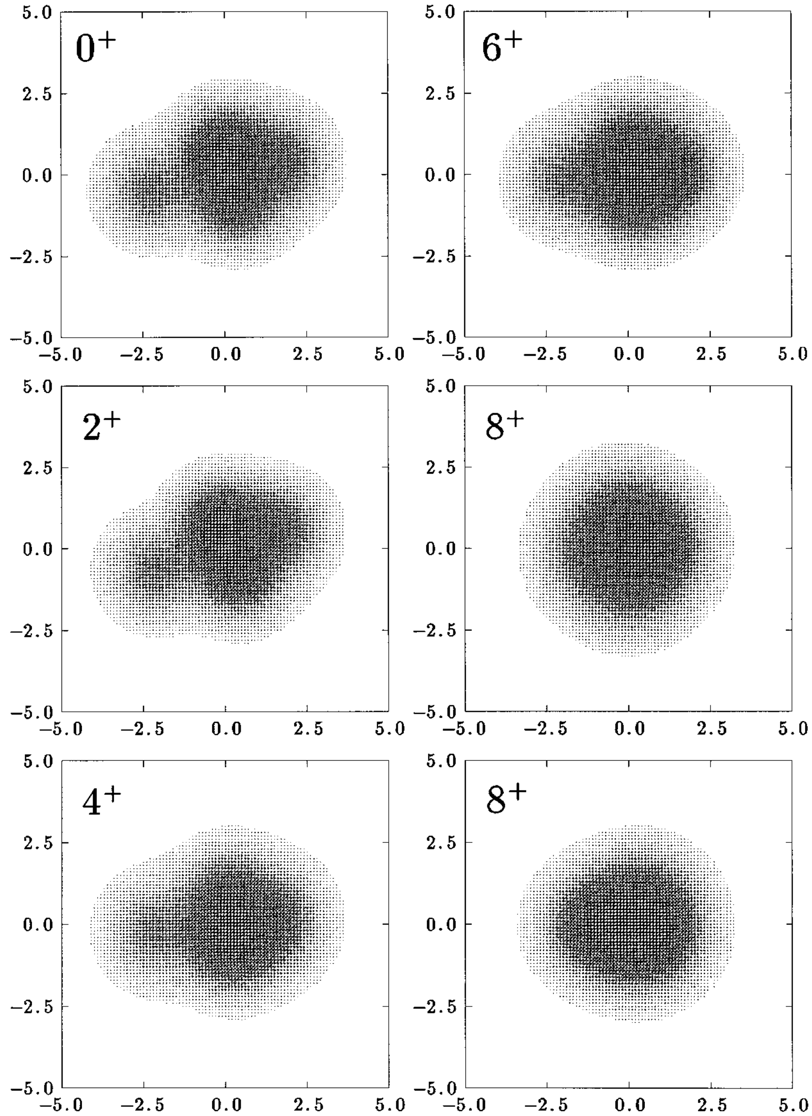

FIG. 44. Density distributions for ^{20}Ne, calculated in the parity-projected antisymmetrized molecular dynamics by Kanada-En'yo and Horiuchi (1995a). The scale of the axes is in fm.

G. ^{40}Ca

Alpha-cluster calculations have been carried out by Ogawa *et al.* (1977), who used the same model as Suzuki (1976); by Ohkubo and Umehara (1988), who used a method similar to that of Michel *et al.* (1986a, 1986b, 1988) (see next section); and by Reidemeister *et al.* (1990), who used an extension of the Buck-Dover-Vary model to describe cluster states. Although the negative-parity band is predicted to lie lower than in ^{44}Ti, and the α reduced widths are predicted to be larger (see next section), it is only recently that the parity-doublet band has been experimentally observed by Yamaya *et al.* (1993), using the ^{36}Ar(^{6}Li,d) reaction.

H. ^{44}Ti

The fp-shell analogue of ^{20}Ne has received considerable attention within various types of alpha-cluster models. Michel *et al.* (1986a, 1986b, 1988), using parameters for a squared WS potential from α-particle scattering off ^{40}Ca, predicted the existence of a mixed-parity band at an excitation just above the α threshold energy. This prediction has been repeated by Ohkubo (1987, 1988) using a folding model with an effective two-body force; by Wada and Horiuchi (1987, 1988) (see also Horiuchi, 1985), using the GC method with a realistic two-body force, and squared WS potential for the imaginary component; and by Merchant *et al.* (1989), using the Buck-Dover-Vary model (for review, see Merchant *et al.*, 1989). Earlier hybrid shell-cluster calculations had also predicted a negative-parity band lying at a lower excitation energy (Itonaga, 1981). The α-cluster band has been confirmed experimentally by Yamaya *et al.* (1990), who observed a negative-parity band at just above the α threshold energy using the (^{6}Li,d) reaction (see also Artemov *et al.*, 1995). There is also experimental evidence for a series of resonances with alternating natural parity in α-^{40}Ca elastic scattering at much higher excitation energy (Löhner *et al.*, 1978; Frekers *et al.*, 1983; Sellschop *et al.*, 1987); these have been interpreted as a molecular band on the basis of microscopic GC calculations (Friedrich and Langanke, 1975), and by using the Brink-Boeker force within the GC method (Langanke,

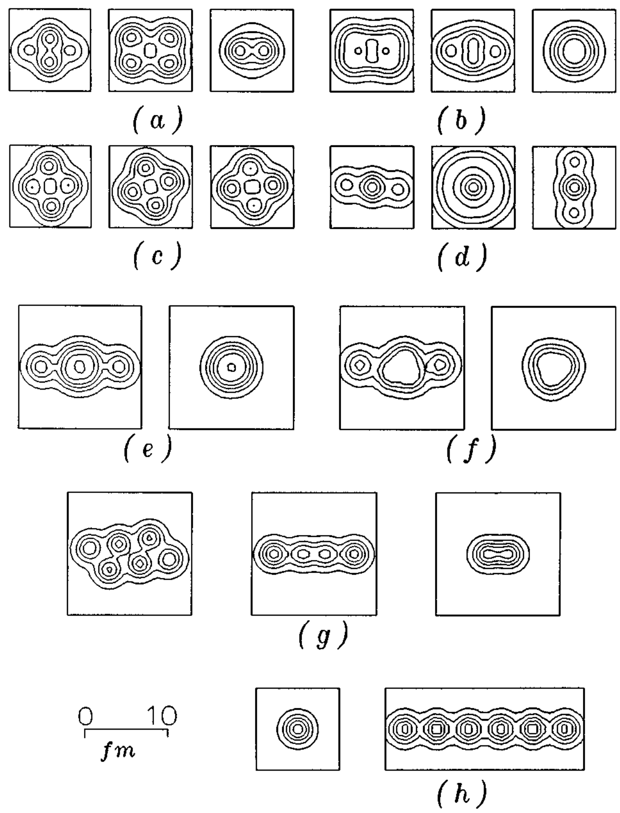

FIG. 45. Energy minima in ^{24}Mg, calculated (Marsh and Rae, 1986) with the unconstrained alpha-cluster model using the Brink-Boeker B1 force.

1982). The cluster calculations of Merchant *et al.* (1989) have also reproduced these states.

IX. LARGE DEFORMATIONS

The microscopic mechanism behind reflection asymmetry at very elongated shapes (for example, at the fission barrier, and for superdeformed and hyperdeformed configurations) is twofold (Johansson, 1961; Gustafson *et al.*, 1971; Larsson *et al.*, 1974; Ragnarsson *et al.*, 1978; Bengtsson *et al.*, 1981; Nazarewicz, 1991). First, the octupole interaction Y_{30} couples the single-particle orbitals with asymptotic quantum numbers $[Nn_z\Lambda]\Omega$ and $[N+1\,n_z\pm1\,\Lambda]\Omega$. The largest number of such matrix elements corresponds to states with the highest possible value of $n_\perp$, i.e., with n_z=0. The second mechanism is the octupole interaction between the high-N intruder orbitals and specific lower-N levels (e.g., levels belonging to the same superdeformed or hyperdeformed shell). For instance, the same pairs of orbitals, such as ([660]1/2-[530]1/2) or ([770]1/2-[640]1/2), which are responsible for octupole deformations in the light actinides, appear close to the Fermi level in superdeformed configurations around ^{148}Gd and ^{192}Hg. Another example is the pair of nearly degenerate Nilsson orbitals [624]9/2 and [512]5/2, which appear at the Fermi level of superdeformed ^{194}Hg. According to the calculations of Skalski (1992), these orbitals, strongly coupled by the Y_{32} field, are responsible for the μ=2 octupole instability in this nucleus.

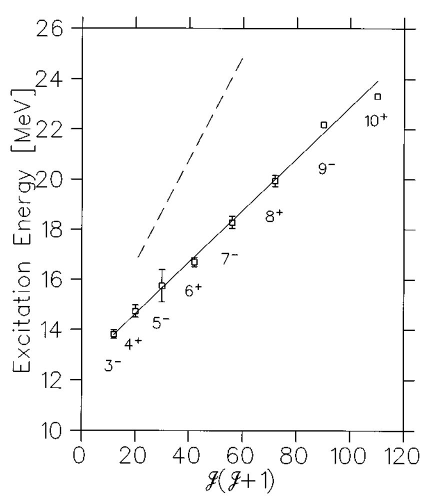

FIG. 46. Mean values of excitation energies of resonance states in ^{32}S with the same spin I, plotted versus $I(I+1)$. A *straight line* is fitted to the experimental points. The *broken line* is for an alpha particle orbiting the Si nucleus with a center-to-center radius r=(1.25$A^{1/3}$+1.6) fm (Brenner, 1994).

A. Fission

It has long been recognized that reflection asymmetry is an important degree of freedom in the description of the fission process. Below, a short overview of this topic is given; for more detailed discussion the reader is referred to the extensive review by Bjørnholm and Lynn (1980).

1. Reflection asymmetry of the fission barrier

Early calculations which included Y_{30} deformation of the modified harmonic-oscillator potential (Johansson, 1961) were able to relate the degree of observed mass asymmetry of fission fragments as a function of Z^2/A to the degree of octupole deformation at the saddle point. Application of the SC method (Möller and Nilsson, 1970; Pashkevich, 1971; Möller, 1972) allowed improved calculations of the fission path to be made; these demonstrated that instability with respect to asymmetric distortion can occur at the second barrier peak. [According to SC calculations by Gavron *et al.* (1977) and Åberg *et al.* (1980), the reflection-asymmetric third saddle point also appears unstable with respect to triaxial deformations.] Self-consistent HF calculations including the mass-asymmetry degree of freedom in fission have also been carried out (e.g., Kolb *et al.*, 1974); the accuracy of these calculations has been improved with better knowledge of the form of the nuclear interaction (see Berger *et al.*, 1989, and references therein).

2. Bimodal fission

A good example illustrating the importance of the fragment shell structure in fission is the existence of the symmetric maximum in the mass distribution of fragments following the fission of nuclei approaching

$^{264}_{100}\mathrm{Fm}_{164}$, and, in particular, the simultaneous appearance of two fission modes in ^{258}Fm, with low and high total kinetic energy of the fragment (Hulet *et al.*, 1986). The asymmetric two-center model of Mustafa *et al.* (1973) showed that the system can revert to symmetry in the path from the second saddle point to scission, for certain values of Z and N [see also Maruhn and Greiner (1974) and Lustig *et al.* (1980)]. Wilkins *et al.* (1976) associated this effect with the presence of the very strong ^{132}Sn+^{132}Sn channel. The shell-correction calculations (Möller *et al.*, 1987; Pashkevich, 1988; Ćwiok *et al.*, 1989), involving a rather rich space of nuclear shapes, predict the existence of several valleys on the potential-energy surface in the vicinity of the scission point. One family of fission valleys corresponds to reflection-symmetric configurations. However, there also exists a valley in which the asymmetric nuclear shape is close to the combination of spherical and elongated fragments.

The experimental observation of asymmetry in the fission mass distribution provides substantial clues to the nature of the mass distribution of the fissioning nucleus, but more direct evidence comes from the observation of nuclear levels at the elongated shapes. In particular, Blons and his collaborators (for a review, see Blons, 1989, and references therein) have measured fission resonances in Th and U nuclei. As discussed in Sec. IX.B.3, these have been interpreted as arising from reflection-asymmetric hyperdeformed shapes which exist in the third minimum of the fission barrier.

B. Strongly elongated configurations

1. Shell structure at strongly elongated configurations

The observation of superdeformed (SD) and hyperdeformed (HD) states constitutes an important confirmation of the shell structure of the nucleus; their unusual stability can be attributed to strong shell effects that are present in the average nuclear potential.

The SD and HD shell structures are often explained in terms of the deformed harmonic-oscillator model. At large deformations, corresponding to rational oscillator-frequency ratios (which characterize a *rational harmonic oscillator*), strong degeneracy of the harmonic-oscillator eigenstates occurs, leading to the appearance of SD and HD magic gaps and magic numbers (Bohr and Mottelson, 1975). In the case of an axial rational harmonic oscillator with frequencies ω_z and $\omega_\perp$, it is convenient to write the single-particle energies in terms of the shell frequency $\omega_{\rm shell}$ and the shell principal quantum number $N_{\rm shell}$, defined by (Bohr and Mottelson, 1975; Bengtsson *et al.*, 1981)

$$\omega_\perp n_\perp + \omega_z n_z = \omega_{\rm shell} N_{\rm shell}, \quad N_{\rm shell} = n_\perp k_z + n_z k_\perp,$$
$$\omega_{\rm shell} = \frac{\tilde{\omega}}{k_\perp k_z}, \tag{111}$$

where $\omega_z k_z = \omega_\perp k_\perp = \tilde{\omega}$, and $\tilde{\omega}$ can be calculated from the volume-conservation condition. The fact that degenerate single-particle orbitals forming SD ($k_\perp$=1, k_z=2) and HD ($k_\perp$=1, k_z=3) shells have different parities has profound consequences for the octupole mode, since the optimum condition for level hybridization is met.

Table VIII displays the energies e_{ph} of particle-hole excitations associated with various components of the octupole tensor $Q''_{3\mu}$ [Eq. (64)] (Nakatsukasa *et al.*, 1992; Nazarewicz *et al.*, 1992, 1995; Nazmitdinov and Åberg, 1992). For the SD shape, $2\omega_3 - \omega_\perp = 0$, and the particle-hole energy corresponding to the μ=1 mode is zero for states belonging to the same SD shell, $N_{\rm shell} = 2n_\perp + n_z$ [Eq. (111)]. This suggests that the triaxial modes with μ=1 can play a significant role in open-shell SD nuclei (see Sec. IX.B.2). Similarly, at the SD oblate shape ($k_\perp$=2, k_z=1) the rational-harmonic-oscillator model suggests an instability with respect to μ=0 and μ=2 octupole modes.

In quantum-mechanical systems, strong shell effects (i.e., degeneracies) usually reflect the presence of dynamical (self-consistent) symmetries of the Hamiltonian. This offers additional quantum numbers associated with the underlying dynamical symmetry, which are the eigenvalues of the Casimir operators of the corresponding symmetry group. The connection between the SU_3 dynamical symmetry of the rational harmonic oscillator, nuclear superdeformation, and octupole modes was discussed by Nazarewicz *et al.* (1992) and Nazarewicz and Dobaczewski (1992). The quantum numbers of the rational harmonic oscillator allow for a transparent classification of magic numbers at large deformations. In particular, they justify the scheme of touching harmonic oscillators suggested by Bengtsson *et al.* (1981) and Faber and Płoszajczak (1981).

The idea of the classification scheme is illustrated in Fig. 47. At SD shapes, two kinds of closed-shell systems are expected. In the "asymmetric" case (labeled A), the magic numbers are equal to sums of two consecutive spherical magic numbers, i.e., N=1, 5, 14, 30, 55, etc. In the "symmetric" variant (B), the magic numbers are equal to doubled spherical-oscillator magic numbers, N=2, 8, 20, 40, 70, etc. The situation becomes slightly more complex at HD shapes, where the magic numbers correspond to the superposition of three spherical-oscillator magic numbers. In the "strongly asymmetric" variant (A) magic numbers N=1, 6, 18, 40, 75, etc., are obtained by combining two spherical shells $\mathcal{N}$ and one higher shell $\mathcal{N}$+1. In the intermediate situation (B), two spherical shells $\mathcal{N}$+1 and one lower shell $\mathcal{N}$ are combined, i.e., N=2, 9, 24, 50, 90, etc. Finally, in the "symmetric" case (C), the magic numbers are equal to tripled spherical-oscillator magic numbers, i.e, N=3, 12, 30, 60, 105, etc.

The classification scheme shown in Fig. 47 suggests the description of deformed systems in terms of "multiclusters" of spherical magic subsystems, dictated by the decomposition of the rational-harmonic-oscillator representations into the isotropic ones (Nazarewicz *et al.*, 1992; Nazarewicz and Dobaczewski, 1992). The relation between multicluster classification and the mean-field picture was discussed by Nazarewicz and Dobaczewski (1992), who analyzed the octupole couplings in the

TABLE VIII. Energies of the particle-hole excitation, Δe_{ph}, associated with the octupole doubly stretched interaction $Q''_{3\mu}$.

μ	$\Delta e_{ph}/\hbar$	Optimal conditions for instability
0	ω_3, $2\omega_\perp-\omega_3$, $2\omega_\perp+\omega_3$, $3\omega_3$	superdeformed oblate shapes
1	$\omega_\perp$, $2\omega_3-\omega_\perp$, $2\omega_3+\omega_\perp$, $3\omega_\perp$	superdeformed prolate shapes
2	ω_3, $2\omega_\perp-\omega_3$, $2\omega_\perp+\omega_3$	superdeformed oblate shapes
3	$\omega_\perp$, $3\omega_\perp$	no instability

rational-harmonic-oscillator model using the doubly stretched octupole interaction, Eq. (64).

The results of rational-harmonic-oscillator calculations for the shell-energy octupole-stiffness coefficient C_{30} [Eq. (38)] (Nazarewicz and Dobaczewski, 1992) are displayed in Fig. 48. For the spherical shape [Fig. 48(a)] the octupole-driving shell force is positive, i.e., there is no tendency to develop stable octupole deformations. The situation at the SD prolate shape is shown in Fig. 48(b). For particle numbers representing the asymmetric cases (A), C_{30} is negative. For the symmetric cases (B), there is no shell octupole-driving force toward reflection-asymmetric shapes. Finally, the HD case is illustrated in Fig. 48(c). As expected, for the systems representing the asymmetric case of Fig. 47, the shell correction decreases with octupole deformations, while no octupole-driving tendency is predicted for the symmetric case. A similar pattern has also been predicted for the $\mu \neq 0$ octupole modes (Nazarewicz, 1992; Arita and Matsuyanagi, 1993). A similar result was obtained by Nazmitdinov and Åberg (1992) and Arita and Matsuyanagi (1993) for giant octupole vibrations built on SD states, namely, a lower vibrational energy arises for the asymmetric combination of spherical magic numbers than for the symmetric combination.

Calculations based on realistic mean-field potentials confirm the prediction of the rational harmonic oscillator that the particle-number regions favoring reflection-symmetric or reflection-asymmetric SD and HD shapes should alternate (Bengtsson *et al.*, 1981; Åberg, 1990; Höller and Åberg, 1990; Dudek *et al.*, 1990; Li *et al.*, 1991). As seen in Fig. 49, based on the Nilsson-Strutinsky model, for SD shapes (ε=0.6) the tendency towards mass asymmetry is strongly favored at particle numbers around 32, 64, and 116, while for particle numbers around 44, 86, and 144, the shell correction favors reflection-symmetric shapes. For HD shapes (ε=0.9), the mass asymmetry is strongly favored at particle numbers around 34, 82, and 150, while for particle numbers around 22, 48, 58, 116, and 130, the minimum shell-correction energy is found at ε_3=0. Shell-correction maps as a function of particle number and triaxial octupole deformations were calculated by Li *et al.* (1991) for SD nuclei.

2. Superdeformations

The first experimental evidence for octupole correlations in SD configurations at high spins was found by Cullen *et al.* (1990) in ^{193}Hg. They explained a low-frequency pseudocrossing in one of the observed SD bands in terms of an admixture of an octupole phonon. Further evidence for octupole vibrations in SD Hg nuclei was found by Crowell *et al.* (1994, 1995), who reported an excited SD band in ^{190}Hg, having a rather constant moment of inertia, and decaying directly into the yrast SD band. The extracted $B(E1)$ values, of the order of 10^{-3} s.p.u., agree well with the results of RPA calculations (see below). The strongest indication of octupole correlations in the SD $A\sim150$ mass region was found in excited bands of ^{152}Dy (Dagnall *et al.*, 1994), where the large-interaction band crossing in one band, and a decay branch of another band into the yrast SD band, can be understood in terms of octupole vibrations.

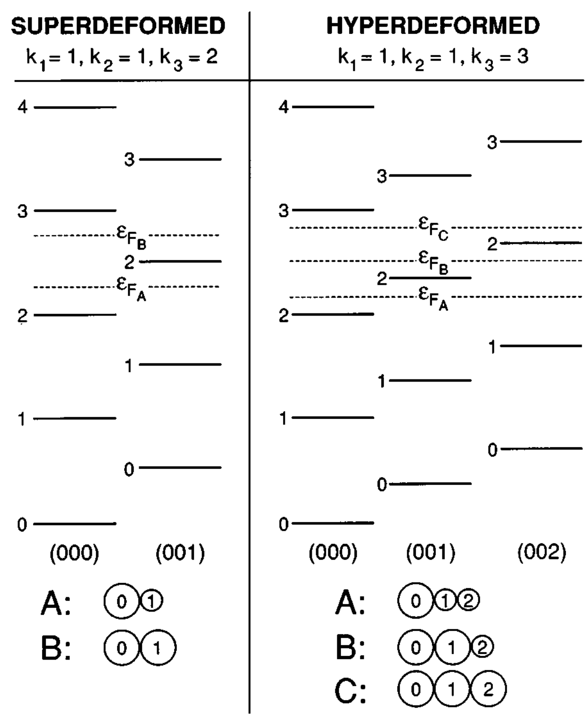

FIG. 47. Spectrum, in units of $\tilde{\omega}$, of the rational harmonic oscillator with $k_\perp$=1 and k_z=2 (SD prolate, left) or k_z=3 (HD prolate, right). Each level is labeled by the principal quantum number M and quantum numbers $(\lambda_1\lambda_2\lambda_3)$ of the rational harmonic oscillator. Except for the usual SU_3 degeneracy, $\frac{1}{2}(M+1)(M+2)$, there are no additional degeneracies present. Different positions of the Fermi level for closed-shell systems A, B, or C are indicated. The schematic diagrams in the bottom portion illustrate the number of occupied particles within each $\{\lambda\}$ family in cases A, B, and C (Nazarewicz and Dobaczewski, 1992).

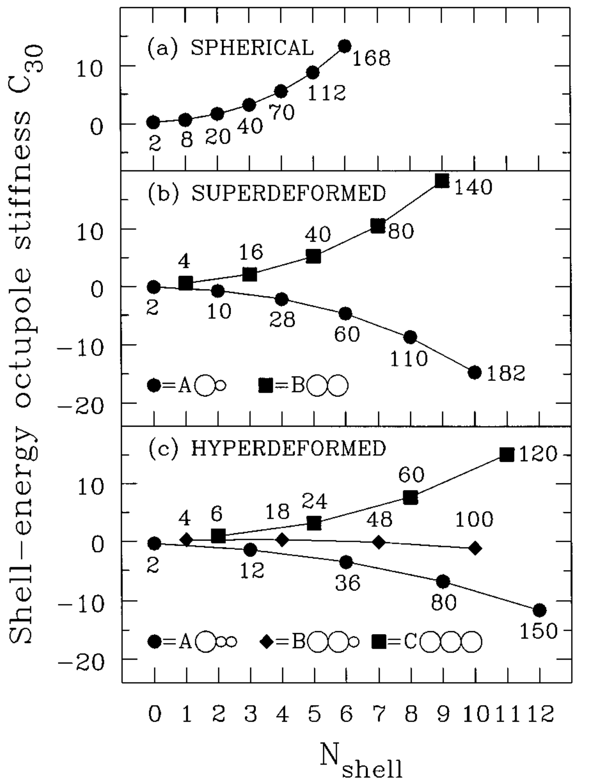

FIG. 48. Shell-correction octupole-stiffness coefficient C_{30} [in units of $7/(4\pi\omega_0^4)$] as a function of the shell quantum number, defined as $N_{\rm shell}\equiv n_\perp k_z+n_z$. Magic particle numbers A (with spin degeneracy included) are indicated for all closed-shell configurations of the rational harmonic oscillator at (a) spherical, (b) superdeformed, and (c) hyperdeformed shapes. If C_{30} is negative (positive), then there is (is not) a shell force favoring stable octupole deformations (Nazarewicz and Dobaczewski, 1992).

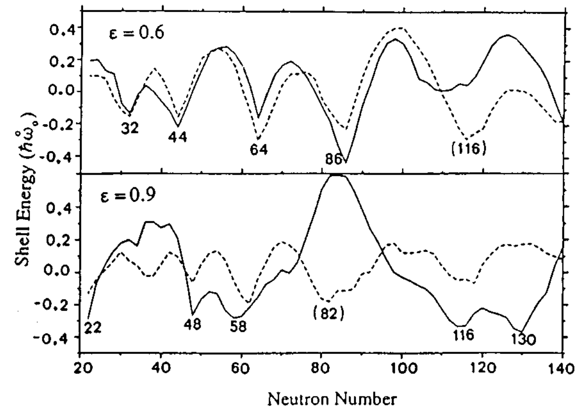

FIG. 49. Shell energy obtained in the modified oscillator model (Höller and Åberg, 1990) versus N for SD (top) and HD (bottom) shapes at ε_3=0 (solid lines) and ε_3=0.15 (dashed lines).

Dudek *et al.* (1987, 1990) studied the mirror-asymmetric deformations in high-spin states of SD nuclei using the cranked SC method with a WS potential. They found static octupole minima in a number of nuclei in the $Z\sim66$ and $Z\sim80$ mass regions (cf. Höller and Åberg, 1990).

According to RPA calculations based on the cranked shell model (Mizutori *et al.*, 1990; Mizutori *et al.*, 1991a, 1991b; Nakatsukasa *et al.*, 1992), low-lying octupole vibrations built on the SD shape are rather collective and, in some cases, can give rise to increased band interaction, shifts in the crossing frequency, reduced angular momentum alignment, and enhanced $E1$ transitions (see Sec. VI). In particular, the RPA calculations of Nakatsukasa *et al.* (1993), based on the doubly stretched octupole interaction of Eq. (64), demonstrate that inclusion of the coupling between quasiparticle and octupole vibrational modes is important for understanding the experimental data for SD ^{193}Hg. This treatment was successfully applied to SD octupole bands in ^{152}Dy (Nakatsukasa *et al.*, 1995) and ^{190}Hg (Crowell *et al.*, 1995).

Satuła *et al.* (1991) concluded, in the SC-WS model, that nuclei around ^{192}Hg are soft to octupole deformation β_3. Bonche *et al.* (1991) and Meyer *et al.* (1995), starting from the axial HF+BCS theory with the SkM* effective interaction, used parity projection and the GC method to investigate the octupole softness in the SD minimum of ^{194}Pb. They found octupole states in the energy range of 2 MeV above the SD ground state. Delaroche *et al.* (1992) investigated the octupole softness of SD ^{192}Hg in the HFB+GOA model with the D1 interaction. They obtained very excited $K^\pi=0^-$ states at $E\approx8$ MeV.

According to the rational-harmonic-oscillator model discussed in Sec. IX.B.1. triaxial octupole deformations, and especially the μ=1 component, are expected to be important at SD shapes (Mottelson, 1988). Li *et al.* (1991) searched for triaxial octupole shapes in SD nuclei, and found stable minima in ^{158}Hf (μ=1) and ^{156}Yb (μ=2). The effects of μ=1 octupole deformations on the total-energy surface of nuclei from the A=190 mass region were studied by Chasman (1991) using the cranked shell-correction method with a WS potential. In many nuclides, minima with rather small quadrupole and hexadecapole deformations and very large μ=1 octupole deformations have been found to become approximately yrast at moderate spins. This result was questioned by Skalski (1992) who concluded, using a similar model, that the μ=1 octupole modes are suppressed by shell effects and by rotation, and that the softest octupole modes in the SD Hg region are those with μ=0 and 2. In subsequent work, Skalski *et al.* (1993b) presented GC calculations for the octupole modes having μ=0, 1, and 2, using the Skyrme SkM* and SIII effective interactions. They predicted the presence of collective octupole K=0, 1, and 2 bands at energies 1.9–2.5 MeV above the SD minimum in Hg and Pb nuclei. They also calculated large $B(E3)$ transition rates ($\approx$30 s.p.u.), depopulating the octupole modes.

To estimate $E1$ moments in SD nuclei, Skalski (1994) employed the SC method of Sec. VII.B, with the macroscopic part described by the droplet model and the microscopic part computed using a WS model. In the SD Gd–Dy region, the shell-correction contributions

$(D_0)_{\rm shell}$ are negative, and tend to cancel the macroscopic part. In the SD Hg-Pb region, in contrast, both contributions have equal signs, resulting in sizable dipole moments.

The GC+HF+BCS calculations by Skalski *et al.* (1993b) predicted the presence of very large $E1$ matrix elements $[B(E1)\sim 0.02$ s.p.u.$]$ connecting octupole vibrational states with the yrast band in SD Hg and Pb nuclei.

3. Hyperdeformations

Hyperdeformed nuclei, i.e., nuclei with quadrupole deformations significantly larger than β_2=0.6, are known or predicted in several mass regions. As discussed in Sec. IX.B.1, HD configurations can be stabilized in some cases by developing reflection-asymmetric deformations. Good cases of HD configurations can be found in light nuclei. For instance, the calculated (Leander and Larsson, 1975) low-lying reflection-asymmetric HD minimum in ^{24}Mg can be associated with the asymmetric ^{16}O+α+α (or ^{16}O+^{8}Be) structure (see Sec. VIII.D). Other examples are the HD states in ^{36}Ar (^{16}O+^{16}O+α) and ^{48}Cr (^{16}O+^{16}O+^{16}O) (Rae and Merchant, 1992). HD reflection-asymmetric structures are also discussed by Faber and Płoszajczak (1981), who performed cranked SC-WS calculations for nuclei around ^{28}Si.

According to the cranked SC method calculations by Höller and Åberg (1990), the best candidates for HD reflection-asymmetric configurations at high spins are nuclei around ^{146}Gd, ^{194}Hg, and ^{200}Rn. Figure 50 (Åberg, 1993) displays the potential-energy surface for ^{146}Gd at I=60. The reflection-asymmetric HD band ($\varepsilon_2\approx 0.93$, $\varepsilon_3\approx 0.13$) in ^{146}Gd is expected to cross the SD (reflection-symmetric) band at $I\sim 80$. The single-particle properties of HD configurations around ^{146}Gd are discussed by Åberg (1993). He concluded that, because of octupole mixing, the high-$\mathcal{N}$ classification scheme is expected to break down in HD configurations; i.e., the calculations suggest rather small differences in the moments of inertia between different HD bands.

Hyperdeformed reflection-asymmetric states in the neutron-deficient Hg and Pb isotopes with $98<N<110$ have been calculated (Nazarewicz, 1993) to occur at excitation energies >6–7.5 MeV at I=0. These minima are rather shallow, although due to their large moments of inertia they become deeper at high angular momenta (Höller and Åberg, 1990). Energy surfaces in the $A\sim 180$ region have been investigated by Chasman and Robledo (1995), who found octupole softness in the very extended nuclear shapes in a number of nuclei.

In the actinide nuclei, the HD states are the so-called third minima around ^{232}Th (Pashkevich, 1971; Möller, 1972). In these nuclei the second saddle point is split, leading to an excited reflection-asymmetric configuration with large quadrupole and octupole deformations ($\beta_2\sim 0.90$, $\beta_3\sim 0.35$), as predicted in a number of calculations based on the mean-field approach (Pashkevich, 1971; Möller, 1972; Möller and Nix, 1973; Howard and Möller, 1980; Bengtsson *et al.*, 1987; Berger *et al.*, 1989; Pal, 1993; Ćwiok *et al.*, 1994; Rutz *et al.*, 1994). Experimentally, the third minimum is indicated from a microstructure in the resonances found in the light actinides using the (n,f), (t,pf), and (d,pf) reactions (Back *et al.*, 1972; Blons *et al.*, 1975, 1978, 1984; Bjørnholm and Lynn, 1980; Fabbro *et al.*, 1984; Blons, 1989; Nakagome *et al.*, 1991). The position and intensities of the resonances observed in the best-studied case, ^{231}Th (Fig. 51), are best explained as the superposition of two rotational bands of opposite parity, with K=1/2, and having very large moments of inertia ($\approx$250 MeV^{-1}). Evidence for intrinsic parity mixing comes from the measured asymmetry in the fission angular distributions (Baumann *et al.*, 1989). Other evidence supporting the third-minimum hypothesis comes from analysis of the slopes of the near-barrier photofission cross sections of actinides (Bhandari and Al-Kharam, 1989).

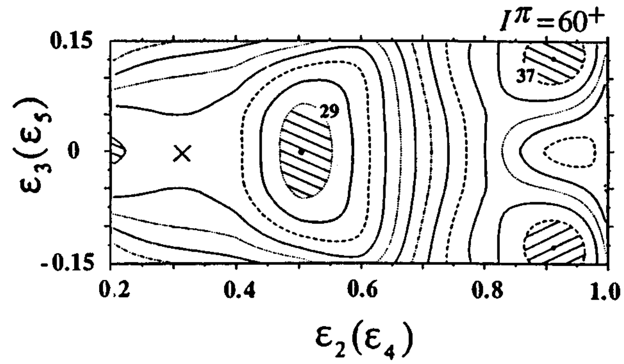

FIG. 50. Potential-energy surface in the $(\varepsilon_2,\varepsilon_3)$ plane for the I^π=60$^+$ configuration in ^{146}Gd, calculated by Åberg (1993) in the cranked modified harmonic-oscillator model. The solid contours are separated by 2 MeV, the intermediate ones by 1 MeV.

A systematic study of HD states in actinides using the SC method (Bengtsson *et al.*, 1987) yielded very shallow reflection-asymmetric third minima. The HD states around ^{232}Th also appear in self-consistent calculations based on the HFB model with the D1S interaction (Berger *et al.*, 1989), adiabatic TDHF-Skyrme-Yukawa calculations (Pal, 1993), and in relativistic mean field calculations (Rutz *et al.*, 1994).

In their systematic calculations for the even-even Rn, Ra, Th, and U isotopes, based on the SC method with a WS potential, Ćwiok *et al.* (1994) employed a many-dimensional deformation space (β_2–β_7), allowing for a rather general description of axially deformed reflection-asymmetric shapes. The potential-energy surfaces in the (β_2,β_3) plane for several even-even Rn, Ra, Th, and U nuclei, covering the region between the second minimum and the outer barrier, are displayed in Fig. 52. For all the nuclei shown in Fig. 52, there exist well-developed reflection-asymmetric HD minima ($\beta_2\sim 0.9$, $0.35<\beta_3<0.65$). It is interesting to note that in the nuclei around ^{234}U, the HD minimum splits into two distinct minima with very different values of β_λ (λ=3–7).

Ćwiok *et al.* (1994) pointed out that the structure of the third minimum corresponds to a binuclear configuration involving a spherical (or nearly spherical) heavy fragment around ^{132}Sn and a well-deformed lighter fragment around ^{100}Zr. This is illustrated in Fig. 53, which shows the predicted equilibrium shapes of ^{232}Th. The shape corresponding to the HD minimum looks like a superposition of the ^{132}Sn and ^{100}Zr ground-state shapes. Recently, this result has been confirmed by the self-consistent calculations of Rutz *et al.* (1994).

The clustering effect predicted in the third minima is a striking manifestation of nuclear shell structure; in the rational harmonic oscillator model (Sec. IX.B.1), the particle numbers 80 and 150 correspond to a situation which formally resembles one spherical doubly magic fragment and one well-deformed (or SD) lighter fragment. The very special role played by the ^{132}Sn structure in the fission process has been noted before in connection with mass distributions of fission fragments (Wilkins *et al.*, 1976), the analysis of cold-fission data (Asghar *et al.*, 1993; Gönnenwein, 1994), measurements of mass and kinetic-energy distributions for the photofission of ^{232}Th (Piessens *et al.*, 1993), and the existence of two fission modes around ^{258}Fm (see the discussion in Sec. IX.A).

The spectroscopic properties of HD minima in actinides (single-particle levels, parity doublets, decoupling parameters, g factors, moments of inertia, etc.) were discussed by Bengtsson *et al.* (1987). Skalski (1994) calculated a very large intrinsic dipole moment in the HD minimum of ^{232}Th, $D_0 \approx 2.2$ e fm.

X. PERSPECTIVES

In this last section, a different landscape of reflection asymmetry is viewed and suggestions made as to how this topic could be further explored experimentally and theoretically.

A. Unexplored mass regions

For nuclei, manifestations of reflection asymmetry in the intrinsic system, such as interleaved positive- and negative-parity states, parity doubling in odd-mass systems, and large odd electric moments, are most pronounced in the Ra-Th region with $N \approx 134$, and, to a lesser extent, in the Ba-Sm region with $N \approx 88$. Other regions in N,Z and deformation space are expected to exhibit similar characteristics whenever there are orbitals near the Fermi surface differing by three units in ℓ and j. For normal deformed nuclei, two examples in the transitional region above ^{100}Sn have been studied, ^{114}Xe (Rugari *et al.*, 1993) and ^{110}Te (Paul *et al.*, 1994). Experimental evidence for octupole correlations has also been cited for other mass regions: ^{64}Ge (Görres *et al.*, 1987, Ennis *et al.*, 1991); ^{74}Se, ^{78}Kr (Cottle, 1990b; Cottle *et al.*, 1990); ^{128}Ba (Cottle *et al.* 1989, Cottle, 1990b, 1991), and ^{128}Gd (Cottle, 1990a) (but see Cottle *et al.*, 1992, 1993). So far, both SC calculations (Skalski, 1990) and self-consistent calculations (Heenen *et al.*,

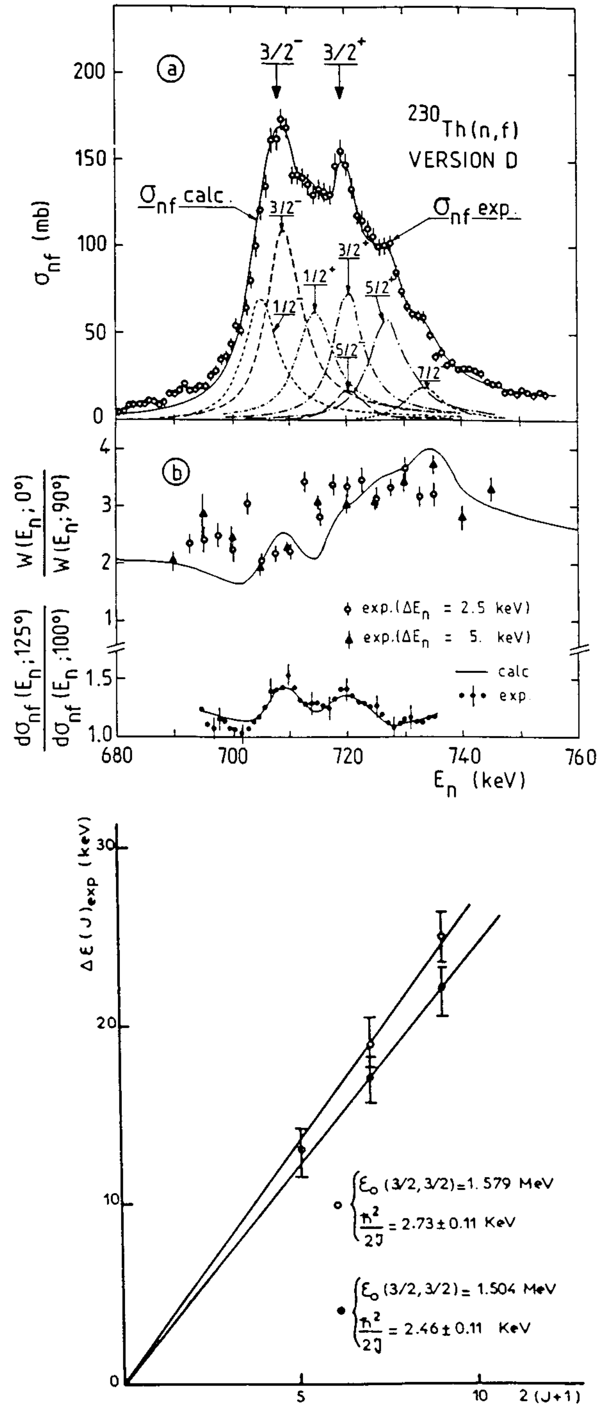

FIG. 51. Top: (n,f) resonances in ^{231}Th. Bottom: resulting rotational band of alternating parity (Blons *et al.*, 1984).

1994) have been applied to the region near ^{112}Ba, and lend support to a description of these transitional nuclei having strong octupole collectivity with very shallow octupole minima. The light Ba nuclei have been investigated using a microscopic treatment which requires a μ=1 octupole component (Piepenbring and Leandri, 1991).

Shell-correction calculations have also been applied to ^{64}Ge, predicting octupole softness at nonzero values of γ (Skalski, 1991; Ennis *et al.*, 1991). Nakatsukasa *et al.*

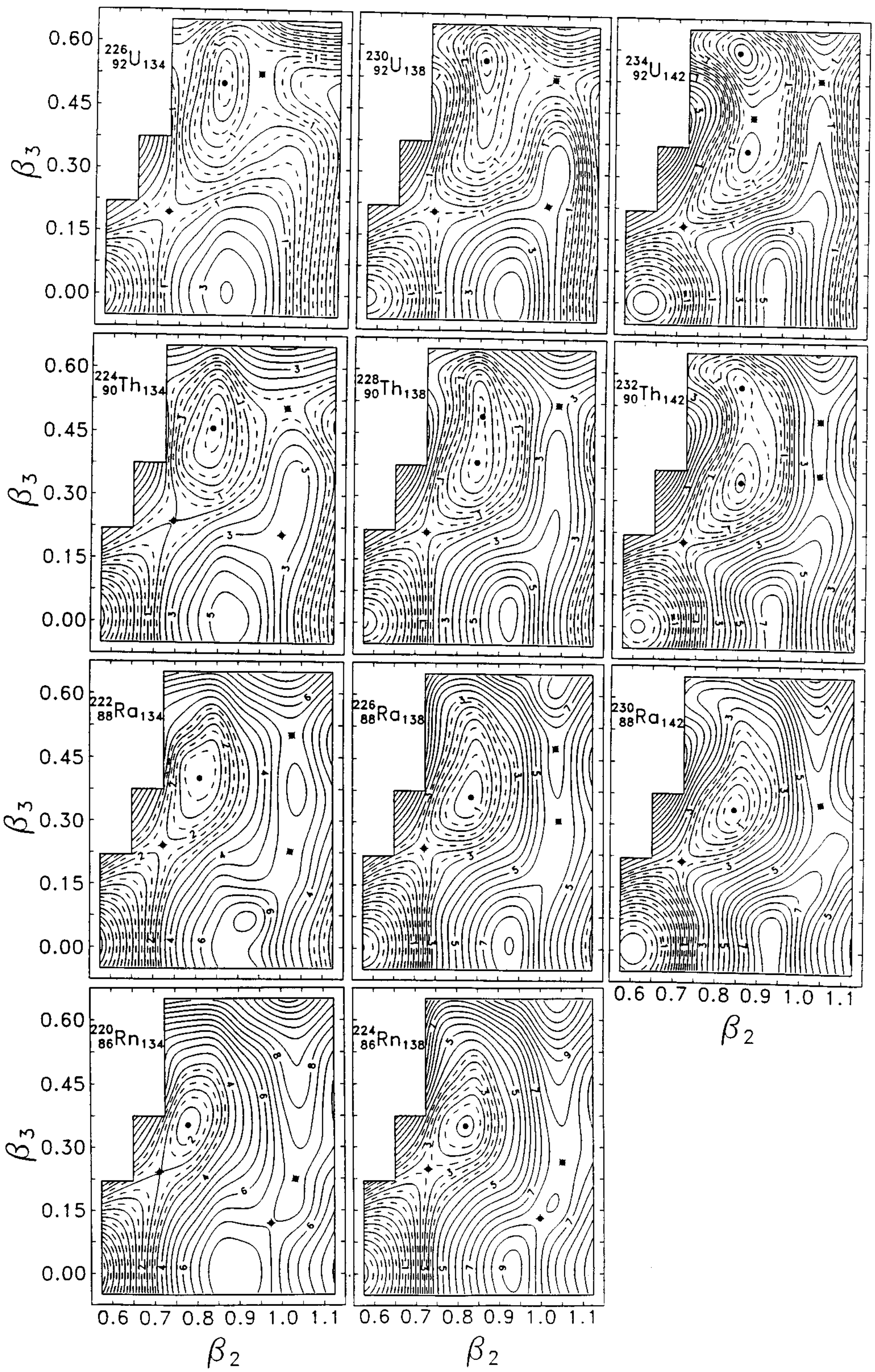

FIG. 52. The SC-WS total potential energy for ^{220,224}Rn, ^{222,226,230}Ra, ^{224,228,232}Th, and ^{226,230,234}U, as a function of β_2 and β_3. At each (β_2,β_3) point the energy was minimized with respect to β_4–β_7. The distance between the solid contour lines is 0.5 MeV. The additional dashed contour lines are 0.25 MeV apart. The minima (saddle points) are marked by dots (crossed dots) (Ćwiok *et al.*, 1994).

(1994) investigated low-energy octupole states in the even-even proton-rich Kr, Sr, and Zr nuclei using the quasiparticle RPA. They demonstrated that, unlike in the heavier nuclei, the octupole collectivity in the light Kr-Zr region is weak, and not directly correlated with the excitation energy systematics of the lowest negative-parity states.

More experimental evidence is needed, particularly for the transitional nuclei near closed shells or subshells. These systems are rather difficult to study experimentally, being either very neutron deficient or very neutron rich. Experimental limitations also restrict at present the study of ^{224}U, predicted to be the most octupole-deformed nucleus in its ground state (Nazarewicz *et al.*, 1984b).

In ^{96}Zr, the strength of the octupole coupling arises from $2p_{3/2}\rightarrow 1g_{9/2}$ proton and $2d_{5/2}\rightarrow 1h_{11/2}$ neutron particle-hole excitations. Ohm *et al.* (1990) have at-

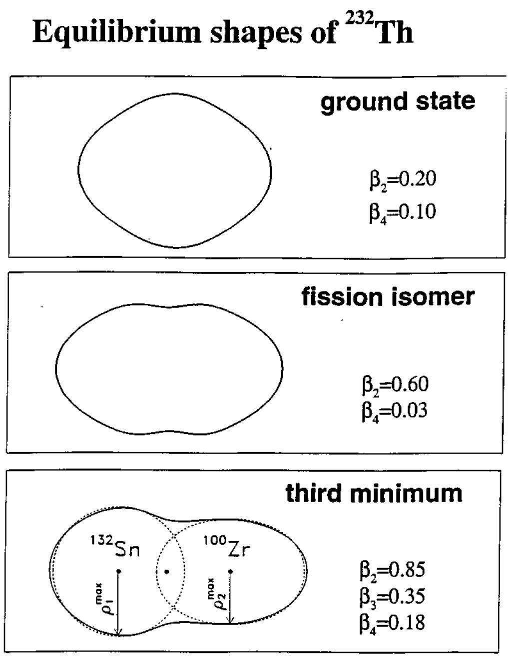

FIG. 53. Calculated equilibrium shapes of ^{232}Th at the ground-state (top), fission-isomeric (middle), and third-minimum (bottom) configuration. The values of $\rho_1^{\max}$ and $\rho_2^{\max}$ are 6.42 and 5.22 fm, respectively.

tempted to calculate both the excitation energy of the 3^- state at 1.897 MeV and the $B(E3)$ strength using the quasiparticle RPA. The difficulties encountered using the quasiparticle RPA (Abbas *et al.*, 1981) suggest that there is a large degree of anharmonicity in the octupole degree of freedom in this mass region. Octupole correlations in ^{96}Zr were investigated by Fayans *et al.* (1994) in the continuum quasiparticle RPA based on a density-functional approach. They obtained $E(3_1^-)$=1.74 MeV and $B(E3)$=39.5 s.p.u., in reasonable agreement with the recent lifetime data (Horen *et al.*, 1993). See also Rosso *et al.* (1993). Mach, Ćwiok *et al.* (1990) have performed SC calculations which suggest that, while ^{96}Zr contains rather complex anharmonic motion, the neighboring isotope ^{98}Zr should have strong octupole instability with $\beta_3=0.13$ in its ground-state configuration. Skalski *et al.* (1993a) have made GC+HF calculations for $^{94-100}$Zr. Although they were able to reproduce the energy of the lowest 3^- state, the calculated value of the $B(E3;0^+\rightarrow 3^-)$ in the case of ^{96}Zr was gravely underestimated, irrespective of the effective force used.

B. Reflection-asymmetric shapes at large deformations

That strong octupole correlations should exist for certain SD states is supported by several theoretical calculations, and is suggested by recent experimental evidence (Sec. IX.B.2). The development of more sophisticated γ-ray arrays will enable the properties of low-lying octupole bands to be measured systematically in the SD region. Perhaps more exciting is the possible occurrence of reflection asymmetry in HD structures (Blons, 1989, Ćwiok *et al.*, 1994). It remains an experimental challenge to identify bound nuclear states in HD heavy nuclei.

C. Angular momentum dependence of electromagnetic moments and reaction aspects

The determination of $E3$ moments between members of rotational bands has been performed for a few nuclei using Coulomb excitation techniques (see Sec. IV.D). These techniques, which demonstrate directly how octupole collectivity varies with spin, cannot be applied at present to short-lived nuclei, precluding studies for nuclei having the deepest octupole minimum.

More detailed measurements might allow the nature of the octupole minimum to be determined. Indeed, static reflection-asymmetric deformations are expected to show up in the low-energy heavy-ion induced reactions, such as Coulomb excitation or sub-barrier fusion. Catara *et al.* (1989) calculated fusion cross sections for ^{16}O induced reactions on ^{144}Ba and different Ra isotopes. They concluded that the presence of static octupole deformation gives rise to a significant enhancement of the total fusion cross section. Consequently, systematic measurements of the sub-barrier fusion cross sections for the chain of isotopes (in which octupole deformation varies quickly with neutron number) could provide a signature for the presence of octupole deformation. Dasso *et al.* (1993) studied Coulomb-excitation patterns for systems with stable octupole deformations. According to their calculations, the probabilities for Coulomb excitation of the different members of the rotational band can discriminate between the deformed and vibrational limits of octupole deformation. In the static case, the predicted spin population does not depend on the parity of the state, whereas in the vibrational case the population of negative-parity states is strongly reduced.

D. Halos

Interesting modifications of the $E1$ strength distributions have already been observed in nuclei such as ^{11}Li and ^{11}Be that have very weak binding of their outermost neutrons (halo nuclei). As pointed out by Uchiyama and Morinaga (1985), in systems with loosely bound states the hindrance of low-energy $E1$ transitions may be removed, since the transition takes place outside the nucleus where the core polarizability vanishes (see Sec. VII.B). They introduced a cutoff model in which the effective charge vanishes inside a certain radius (the core radius plus the nuclear-force range). Hoshino *et al.* (1991) confirmed this assumption in large-scale shell-model calculations for ^{11}Li and ^{11}Be (see also Hansen and Jonson, 1987; Bertsch and Foxwell, 1990; Suzuki and Tosaka, 1990; Hayes and Strottman, 1990; Hayes, 1991; Esbensen and Bertsch, 1992; Danilin *et al.*, 1994).

Sagawa *et al.* (1992) studied sum rules for soft modes in halo nuclei. The corresponding $E1$ sum rule is

$$S_{\text{halo}}(E1)=S(E1;A1)+S(E1;A2)+S_{1m}(E1), \qquad (112)$$

where the sum rules $S_{1m}(E1)$ and $S(E1;A)$ are given by Eqs. (108) and (109), respectively.

In one-body halo nuclei such as ^{11}Be, or in nuclei such as ^{6}He or ^{11}Li that can be considered as three-body halos, reflection-asymmetric intrinsic configurations appear in calculations (see, for example, Horiuchi *et al.*, 1994; Fedorov *et al.*, 1994; Kanada-En'yo and Horiuchi, 1995b, 1995c).

E. Parity violation

Parity violation (in the laboratory frame) is caused by the parity-nonconserving component, V^{PNC}, of the weak interaction. The magnitude of this effect is of the order of $\alpha_p = G_F m_\pi^2 / G_S \sim 10^{-7}$, where G_F is the Fermi constant and G_S is the strong coupling constant.

The relationship between intrinsic reflection asymmetry and real parity mixing is as follows. First, in nuclei with reflection-asymmetric shapes there is a large probability of finding parity doublets very close in energy, especially in the odd-A and odd-odd systems (Leander and Sheline, 1984). This is the necessary condition for experimental studies of parity mixing (Ahmad *et al.*, 1982; Haxton and Henley, 1983; Adelberger and Haxton, 1985). Second, it can indeed be demonstrated (Sushkov and Flambaum, 1980; Flambaum and Sushkov, 1980) that the parity-mixing amplitude can be expressed through the matrix elements of V^{PNC} between the *intrinsic states* characterizing the parity doublet. In particular, Sushkov and Flambaum (1980) and Flambaum and Sushkov (1980) pointed out that the spatial parity violation induced by polarized thermal neutrons observed in the fission of some actinide nuclei could be related to the presence of intermediate pear-shaped states during the fission process.

The latest focus of parity-violation measurements in nuclei is on symmetry breaking in compound nuclear states (Bowman *et al.*, 1990; Zhu *et al.*, 1992; Frankle *et al.*, 1992), motivated by the extremely large enhancement observed for parity violation in neutron resonances. In the statistical approach, the parity-nonconserving matrix elements are treated as random variables and, in most cases, this method gives qualitative agreement with experimental data (Zhu *et al.*, 1992). However, for one nucleus (^{232}Th), strong sign correlations have been observed (Frankle *et al.*, 1992). This phenomenon has been the subject of much study, and cannot be explained as a general property of the nucleon-nucleus weak interaction (Auerbach, 1992; Bowman *et al.*, 1992). Recently, the nonstatistical effects in ^{232}Th have been discussed (Auerbach *et al.*, 1995; Flambaum and Zelevinsky, 1995) in terms of parity doublets resulting from reflection-asymmetric deformations, which are expected to exist in the third HD minimum of ^{232}Th (see Sec. IX.B.3). In particular, Flambaum and Zelevinsky (1995) related the parity-mixing amplitude to the ratio of matrix elements involving the parity-nonconserving interaction, and to the part of the interaction giving rise to nonadiabatic mixing, leading to parity splitting.

F. Reflection-asymmetric deformations in mesoscopic systems

The presence of reflection-asymmetric deformations can be attributed to strong shell effects that are present in the average potential of finite Fermi systems such as atomic nuclei or metallic clusters (Hamamoto, Mottelson, *et al.*, 1991; Frauendorf and Pashkevich, 1993; Frisk *et al.*, 1994; Koskinen *et al.*, 1995). The shapes of light nuclei and jellium clusters were studied by Koskinen *et al.* (1995) in the symmetry-unrestricted local density approximation, assuming a simplified energy functional. The shapes obtained for light $N=Z$ nuclei show a striking similarity to those of atomic clusters. In particular, they obtained reflection-asymmetric shapes in jellium clusters of N=10, 12, 16, and 18 electrons. (For corresponding nuclear examples, see Sec. VIII.)

Figure 38 shows an example of a situation where the *combined* reflection-symmetric and reflection-asymmetric deformations give rise to the new nuclear shell structure. The single-particle WS levels (ω=0 portions), characteristic of nuclei from the Ba-Nd region, are plotted as a function of octupole deformation β_3. Due to octupole mixing between the $h_{11/2}$ and $d_{5/2}$ subshells, two large energy gaps open up at Z=56 and $Z=62$ in the proton spectrum. In the neutron system a large gap at N=88 can be seen; this is a consequence of the $i_{13/2}$–$f_{7/2}$ octupole interaction. A close inspection of Fig. 38 (ω=0) leads to the conclusion that, at large octupole deformations, the single-particle levels become nearly degenerate, forming quasi-j subshells. For example, at β_3=0.15, the two orbitals with Ω=1/2 and 3/2 are close to each other, and just below the Z=56 gap, forming a "j"=3/2 multiplet. Similar "j"=5/2 and "j"=7/2 multiplets can be seen above the Z=56 and Z=62 gaps, respectively. An analogous structure can also be observed in the neutron system.

Theoretically, the variation in the single-particle level density with shell filling (the level bunching), the existence of spherical and deformed magic numbers, and the unusual shell stability of certain shapes in mesoscopic systems, have an interpretation in terms of semiclassical periodic orbits (Balian and Bloch, 1972; Bohr and Mottelson, 1975; Strutinsky and Magner, 1976). The single-particle level density and the shell energy can be expressed (Gutzwiller, 1967, 1971) as a sum over semiclassical periodic orbits. Consequently, the shell structure of a many-body system (and hence the presence or absence of large deformations) has its deep roots in the nonlinear dynamics of the corresponding classical Hamiltonian and the geometry of classical orbits.

Several authors (Frisk, 1990; Arita and Matsuyanagi, 1993, 1994, 1995; Arita, 1994; Heiss *et al.*, 1994, 1995a, 1995b) have analyzed the classical single-particle motion in axially symmetric potentials with quadrupole and octupole deformations. They demonstrated that strong shell effects present at large quadrupole and octupole deformations are associated with bifurcations of short periodic orbits. Examples of classical periodic orbits for the harmonic-oscillator Hamiltonian with the doubly stretched octupole field,

$$H = h_{\mathrm{ho}} - \lambda_{30} M \omega_0^2 [r^2 Y_{30}(\Omega)]'', \tag{113}$$

are shown in Fig. 54. Such a semiclassical analysis can shed new light on shell structures stabilizing reflection-asymmetric shapes, and on associated constants of motion.

The character of the collective dynamics (and in particular, the nature of energy dissipation) of independent classical particles moving in a deformed, axially symmetric container, oscillating with a frequency much smaller than a typical single-particle frequency, was discussed by Błocki *et al.* (1992, 1993, 1995). They demonstrated that largely ordered motion characteristic of quadrupole shapes becomes chaotic if octupole and higher-order deformations are included. Bauer *et al.* (1994) considered a harmonic-oscillator potential with a time-dependent multipole-multipole force, treated self-consistently.

The problems of strong quantum numbers, strong shell effects, and so on, appear naturally in the context of large-amplitude collective motion, which embraces such phenomena as anharmonic vibrations, shape coexistence, exotic decays, fission, fusion, and heavy-ion collisions. All those phenomena involve dynamical interaction between various stable mean fields characterized by different symmetries. The transition from one stable mean field to another goes through one of several level crossings, around which the original symmetry of the system is broken and the intrinsic quantum numbers disappear. In the context of this Review, two examples of large-amplitude collective motion can be mentioned, both related to the physics of quantum-mechanical tunneling.

The first example is the description of parity splitting in a nuclear rotational band. As discussed in Sec. IV.B and Sec. VI, very small parity splitting between the high-spin members of the parity doublet has been observed in, for example, ^{220}Ra. Since most calculations predict rather modest octupole barriers (1–2 MeV), the unusual octupole rigidity at high spins, and the variation of the parity splitting with angular momentum, are challenges for theoretical models of large-amplitude collective motion.

The second example deals with the microscopic descriptions of fission and exotic decay. There exist many descriptions of fission based on the adiabatic assumption, most employing the adiabatic TDHF theory and variations of it (such as the collective Schrödinger equation with microscopic mass tensor). By construction, adiabatic approaches cannot take into account properly the dynamics of level crossing and the associated symmetry breaking (see Sec. III.A). An interesting development is the imaginary-time mean-field theory (Levit *et al.*, 1980; Negele, 1989), which allows for a TDHF treatment of quantum tunneling. An example of this method is the description of the fission of ^{32}S in three dimensions (Wolff *et al.*, 1992). In particular, the crossings between positive- and negative-parity levels give rise to a dramatic difference between the results of the static constrained HF (or adiabatic TDHF) and TDHF; the corresponding collective-motion paths are strongly influenced by the breaking of reflection symmetry, and are very different in both cases.

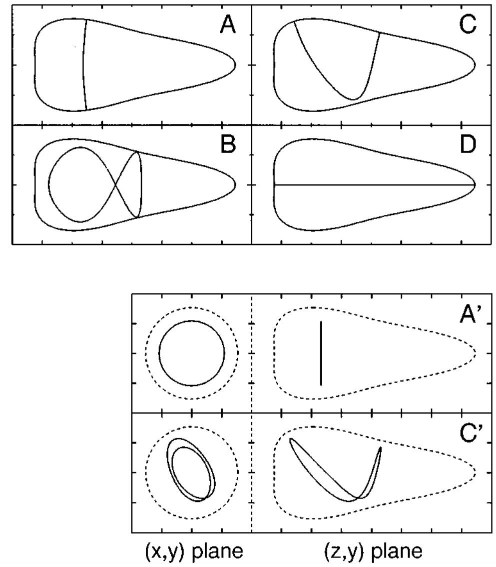

FIG. 54. Some classical periodic orbits for the Hamiltonian (113), with the frequency ratio $\omega_\perp/\omega_z = \sqrt{3}$ (Arita and Matsuyanagi, 1994).

A better understanding of the basic aspects of nuclear dynamics that govern large-amplitude collective motion will certainly be provided by the vigorous interdisciplinary interaction between nuclear physics and nonlinear dynamics.

ACKNOWLEDGMENTS

Valuable comments and suggestions from Sven Åberg and George Bertsch are gratefully acknowledged. Theoretical nuclear physics research at the University of Tennessee is supported by the U.S. Department of Energy through Contract No. DE-FG05-93ER40770. Oak Ridge National Laboratory is managed for the U.S. Department of Energy by Lockheed Martin Energy Systems under Contract No. DE-AC05-84OR21400. Nuclear physics research at the University of Liverpool is supported by grants from the U.K. Engineering and Physical Sciences Research Council (previously the Science and Engineering Research Council). P. A. Butler is grateful for support from the Joint Institute for Nuclear Research (Oak Ridge) for various visits there in which some of this work was completed; similarly W. Nazarewicz acknowledges support from the EPSRC for visits to the University of Liverpool. W. Nazarewicz thanks the Department of Energy's Institute for Nuclear Theory at the University of Washington for its hospitality and partial support during the completion of this work.

APPENDIX: COMPILATION OF SHAPE PARAMETRIZATIONS

The standard α and β parametrization of the nuclear shape is introduced in Sec. II.A. This Appendix contains a brief compilation of other shape parametrizations of reflection-asymmetric shapes.

For the modified oscillator potential (Nilsson, 1955), the shape is defined through the equipotential surfaces of the average field:

$$\rho_t^2=\frac{\rho_0^2}{c(\bar{\varepsilon})}\left\{1+2\varepsilon_1 P_{10}(\theta_t)-\frac{2}{3}\varepsilon_2 P_{20}(\theta_t)\right.$$
$$\left.+2\sum_\lambda \varepsilon_\lambda P_\lambda(\theta_t)\right\}^{-1/2}. \tag{A1}$$

Here, the nuclear radius is denoted by ρ_t because it, together with the angles entering P_λ in Eq. (A1), is defined in the stretched coordinate system (Nilsson, 1955; Larsson, 1973). The dipole deformation ε_1 is determined from Eq. (3). Expressed in terms of Nilsson's deformation ε_3, the octupole moment $\mathcal{Q}_{30,c}$ is given by (Leander and Chen, 1988)

$$\mathcal{Q}_{30,c}=-\frac{6}{7}ZR_0^3\varepsilon_3. \tag{A2}$$

Another way of parametrizing axial shapes has been suggested by Chasman *et al.* (1977). Here the deformations ν_λ are introduced via the transformation

$$r^2\rightarrow r^2\left[\exp\left(\frac{2\nu_2}{3}\right)\sin^2\theta+\exp\left(-\frac{4\nu_2}{3}\right)\cos^2\theta\right.$$
$$\left.+\sum_{\lambda=3}^{\lambda_{\max}}\nu_\lambda\sqrt{\lambda+\frac{1}{2}}P_\lambda(\cos\theta)\right]. \tag{A3}$$

When discussing asymmetric fission, straightforward expansions in spherical harmonics are not very appropriate. Parametrizations have to be introduced that are capable of describing the bifurcation of the surface into two parts. The three-quadratic surface parametrization of Nix (1969) is sometimes used at large elongations. For axial systems, the (c,h,α) cylindrical parametrization of nuclear shape is particularly useful (Nix, 1972; Brack *et al.*, 1972):

$$(x^2+y^2)/C^2$$
$$=\begin{cases}(1-z^2/C^2)(A+Bz^2/C^2+\alpha z/C) & \text{for } B\geqslant 0,\\ (1-z^2/C^2)[(A+\alpha z/C)\exp(Bc^3z^2/C^2)] & \text{for } B<0,\end{cases} \tag{A4}$$

where C is determined by the volume-conservation condition, $B=2h+(c-1)/2$, and $A=1/c^3-B/5$. The parameter c describes the elongation of the system, h is the neck coordinate, and α is an asymmetry parameter.

A different parametrization has been used by Pashkevich (1971). It is based on the observation that the nuclear shapes at the saddle point are well approximated by Cassinian ovals. For axial shapes, the Cassinian coordinates (R,t) are related to the Cartesian coordinates (x,y,z) by the expressions

$$R=[(x^2+y^2+z^2)^2-2s(z^2-x^2-y^2)+s^2]^{1/4},$$
$$t=\frac{\mathrm{sgn}(z)}{\sqrt{2}}\left\{1+\frac{z^2-x^2-y^2-s}{R^2}\right\}^{1/2}, \tag{A5}$$

where s is the squared distance from the focus of the Cassinian ovals to the origin of coordinates. The surface $R(t)$=const defines the Cassinian oval. In order to describe deviations from such shapes, R is written as a series in Legendre polynomials:

$$R(t)=R_0\left[1+\sum_m \alpha_m P_m(\cos t)\right]. \tag{A6}$$

The reflection-asymmetric shapes correspond to odd-m deformations α, i.e., α_1,α_3, and so on.

There is no unique way to relate one set of deformation parameters to another. A standard method of comparing shapes is to require equality between the collective multipole moments $\mathcal{Q}_{\lambda\mu}$ (Dudek *et al.*, 1984; Nazarewicz and Ragnarsson, 1995). For instance, in first order, the relations for λ=3 deformations are (Rohoziński, 1988)

$$\beta_3=-2\sqrt{\frac{\pi}{7}}\varepsilon_3,\quad \nu_3=2\sqrt{\frac{2}{7}}\varepsilon_3 \tag{A7}$$

[see Eqs. (6) and (A2)].

REFERENCES

Abbas, A., N. Auerbach, N. Van Giai, and L. Zamick, 1981, Nucl. Phys. A **367**, 189.

Abbas, A., and L. Zamick, 1980, Phys. Rev. C **80**, 1755.

Abdul-Hadi, A., V. Barci, B. Weiss, H. Maria, G. Ardisson, M. Hussonnois, and O. Constantinescu, 1993, Phys. Rev. C **47**, 94.

Åberg, S., 1990, Nucl. Phys. A **520**, 35c.

Åberg, S., 1993, Nucl. Phys. A **557**, 17c.

Åberg, S., H. Flocard, and W. Nazarewicz, 1990, Annu. Rev. Nucl. Part. Sci. **40**, 439.

Åberg, S., S.E. Larsson, P. Möller, S.G. Nilsson, G. Leander, and I. Ragnarsson, 1980, in *Physics and Chemistry of Fission 1979* (IAEA, Vienna), Vol. I, p. 303.

Ackermann, B., H. Baltzer, C. Ensel, K. Freitag, V. Grafen, C. Günther, P. Herzog, J. Manns, M. Marten-Tölle, U. Müller, J. Prinz, I. Romanski, R. Tölle, J. deBoer, N. Gollwitzer, and H.J. Maier, 1993, Nucl. Phys. A **559**, 61.

Ackermann, B., T. Bihn, P.A. Butler, V. Grafen, C. Günther, J.R. Hughes, G.D. Jones, Ch. Lauterbach, H.J. Maier, M. Marten-Tölle, R. Tölle, R. Wadsworth, D.L. Watson, and C.A. White, 1989, Z. Phys. A **332**, 375.

Adelberger, E.G., and W.C. Haxton, 1985, Annu. Rev. Nucl. Part. Sci. **35**, 501.

Afanasjev, A.V., 1993, J. Phys. G **19**, L143; **20**, 511(E).

Afanasjev, A.V., T.V. Guseva, and J.J. Tambergs, 1991, Izv. Akad. Nauk. **55**, 2223.

Afanasjev, A.V., and S. Mizutori, 1995, Z. Phys. A **353**, 267.

Afanasjev, A.V., and I. Ragnarsson, 1995, Phys. Rev. C **51**, 1259.

Agassi, D., H.J. Lipkin, and N. Meshkov, 1966, Nucl. Phys. **86**, 321.

Ahmad, I., and P.A. Butler, 1993, Annu. Rev. Nucl. Part. Sci. **43**, 71.

Ahmad, I., R.R. Chasman, J.E. Gindler, and A.M. Friedman, 1984, Phys. Rev. Lett. **52**, 503.

Ahmad, S.A., C. Ekström, W. Klempt, R. Neugart, E.W. Otten, and K. Wendt, 1984, in *Proceedings of the 7th International Conference on Atomic Masses and Fundamental Constants, AMCO-7*, edited by O. Klepper (Seeheim, Darmstadt), p. 361.

Ahmad, I., J.E. Gindler, R.R. Betts, R.R. Chasman, and A.M. Friedman, 1982, Phys. Rev. Lett. **49**, 1758.

Ahmad, I., J.E. Gindler, M.P. Carpenter, D.J. Henderson, E.F. Moore, R.V.F. Janssens, I.G. Bearden, and C.C. Foster, 1994, Nucl. Phys. A **576**, 246.

Ahmad, I., J.E. Gindler, A.M. Friedman, R.R. Chasman, and T. Ishii, 1987, Nucl. Phys. A **472**, 285.

Ahmad, I., R. Holzmann, R.V.F. Janssens, P. Dendooven, M. Huyse, G. Reusen, J. Wauters, and P. Van Duppen, 1989, Nucl. Phys. A **505**, 257.

Ahmad, S.A., W. Klempt, C. Ekström, R. Neugart, and K. Wendt, 1985, Z. Phys. A **321**, 35.

Ahmad, S.A., W. Klempt, R. Neugart, E.W. Otten, P.-G. Reinhard, G. Ulm, and K. Wendt, 1988, Nucl. Phys. A **483**, 244.

Ahmad, S.A., W. Klempt, R. Neugart, E.W. Otten, K. Wendt, C. Ekström, and the ISOLDE Collaboration, 1983, Phys. Lett. B **133**, 47.

Aïche, M., M. Bentaleb, Ch. Briançon, A. Chevallier, J. Chevallier, J.S. Dionisio, J. Fernández-Niello, R. Kulessa, E. Lubkiewicz, C. Mittag, F. Riess, E. Ruchowska, N. Schulz, A. Seghour, J.C. Sens, Ch. Vieu, and M. Wieland, 1994, Nucl. Phys. A **567**, 685.

Aïche, M., A. Chevallier, J. Chevallier, S. Hulne, S. Khazrouni, N. Schulz, and J.C. Sens, 1988, J. Phys. G **14**, 1191.

Ajzenberg-Selove, F., 1986, Nucl. Phys. A **460**, 1.

Ajzenberg-Selove, F., 1987, Nucl. Phys. A **475**, 1.

Alder, K., A. Bohr, T. Huus, B.R. Mottelson, and A. Winther, 1956, Rev. Mod. Phys. **28**, 432.

Alhassid, Y., M. Gai, and G.F. Bertsch, 1982, Phys. Rev. Lett. **49**, 1482.

Alikov, B.A., Kh.N. Badalov, V.O. Nesterenko, A.V. Sushkov, and J. Wawryszczuk, 1988, Z. Phys. A **331**, 265.

Alkhazov, G.D., A.E. Barzakh, V.A. Bolshakov, V.P. Denisov, V.S. Ivanov, Yu.Ya. Sergeyev, I.Ya. Chubukov, V.I. Tikhonov, V.S. Letokhov, V.I. Mishin, S.K. Sekatsky, and V.N. Fedoseyev, 1990, Z. Phys. A **337**, 257.

Alonso, C.E., J.M. Arias, A. Frank, H.M. Sofia, S.M. Lenzi, and A. Vitturi, 1995, Nucl. Phys. A **586**, 100.

Amiet, J.-P., and P. Huguenin, 1963, Nucl. Phys. **63**, 171.

Amiet, J.-P., and P. Huguenin, 1966, Nucl. Phys. **80**, 353.

Andersen, E., M.J.G. Borge, D.G. Burke, H. Gietz, P. Hill, N. Kaffrell, W. Kurcewicz, G. Løvhøiden, S. Mattsson, R.A. Naumann, K. Nybø, G. Nyman, and T.F. Thorsteinsen, 1989, Nucl. Phys. A **491**, 290.

Arima, A., H. Horiuchi, and T. Sebe, 1967, Phys. Lett. B **24**, 129.

Arima, A., and F. Iachello, 1975, Phys. Lett. B **57**, 39.

Arima, A., and F. Iachello, 1976, Ann. Phys. (N.Y.) **99**, 253.

Arita, K., 1994, Phys. Lett. B **336**, 279.

Arita, K., and K. Matsuyanagi, 1993, Prog. Theor. Phys. **89**, 389.

Arita, K., and K. Matsuyanagi, 1994, Prog. Theor. Phys. **91**, 723.

Arita, K., and K. Matsuyanagi, 1995, Nucl. Phys. A **592**, 9.

Artemov, K.P., M.S. Sokolov, V.V. Pankratov, and V.P. Rudakov, 1995, Yad. Fiz. **58**, 219.

Asaro, F., F. Stephens, Jr., and I. Perlman, 1953, Phys. Rev. **92**, 1495.

Asghar, M., N. Boucheneb, G. Medkour, P. Geltenbort, and B. Leroux, 1993, Nucl. Phys. A **560**, 677.

Assenbaum, H.J., K. Langanke, and A. Weiguny, 1984, Z. Phys. A **318**, 35.

Auerbach, N., 1992, Phys. Rev. C **45**, R514.

Auerbach, N., J.D. Bowman, and V. Spevak, 1995, Phys. Rev. Lett. **74**, 2638.

Aufmuth, P., K. Heilig, and A. Steudel, 1987, At. Data Nucl. Data Tables **37**, 455.

Back, B.B, H.C. Britt, J.D. Garrett, and O. Hansen, 1972, Phys. Rev. Lett. **28**, 1707.

Badea, M., A.A. Raduta, and H. Stock, 1978, Phys. Scr. **18**, 167.

Bal'butsev, E.B., I.V. Molodtsova, and I. Piperova, 1991, Sov. J. Nucl. Phys. **53**, 419.

Baldock, R.A., and R.A. Stratton, 1985, J. Phys. G **11**, 515.

Balian, R., and C. Bloch, 1972, Ann. Phys. (N.Y.) **69**, 76.

Balodis, M.K., N.D. Kramer, P.T. Prokofjev, A.V. Afanasjev, T.V. Guseva, J.J. Tambergs, K. Schreckenbach, W.F. Davidson, D.D. Warner, J.A. Pinston, P.H.M. Van Assche, and A.M.J. Spits, 1991, Nucl. Phys. A **523**, 261.

Barfield, A.F., B.R. Barrett, J.L. Wood, and O. Scholten, 1988, Ann. Phys. (N.Y.) **182**, 344.

Barfield, A.F., P. von Brentano, A. Dewald, K.O. Zell, N.V. Zamfir, D. Bucurescu, M. Ivaşcu, and O. Scholten, 1989, Z. Phys. A **332**, 29.

Barfield, A.F., J.L. Wood, and B.R. Barrett, 1986, Phys. Rev. C **34**, 2001.

Bargioni, L., P.G. Bizzeti, A.M. Bizzeti-Sona, D. Bazzacco, S. Lunardi, P. Pavan, C. Rossi-Alvarez, G. de Angelis, G. Maron, and J. Rico, 1995, Phys. Rev. C **51**, R1057.

Barranco, F., E. Vigezzi, R.A. Broglia, and G.F. Bertsch, 1988, Phys. Rev. C **38**, 1523.

Barts, B.I., E.V. Inopin, and N.A. Shlyakhov, 1984, Sov. J. Nucl. Phys. **40**, 423.

Barwick, S.W., P.B. Price, H.L. Ravn, E. Hourani, and M. Hussonnois, 1986, Phys. Rev. C **34**, 362.

Bassichis, W.H., and J.P. Svenne, 1967, Phys. Rev. Lett. **18**, 80.

Basu, S., J.M. Chatterjee, D. Banik, R.K. Chattopadhyay, R.P. Sharma, and S.K. Pardha Saradhi, 1994, Phys. Rev. C **49**, 650.

Bauer, W., D. McGrew, V. Zelevinsky, and P. Schuck, 1994, Phys. Rev. Lett. **72**, 3771.

Bauhoff, W., 1982, Z. Phys. A **305**, 187.

Bauhoff, W., H. Schultheis, and R. Schultheis, 1980, Phys. Rev. C **22**, 861.

Bauhoff, W., H. Schultheis, and R. Schultheis, 1984, Phys. Rev. C **29**, 1046.

Baumann, F.-M., K.Th. Brinkmann, H. Freiesleben, J. Kiesewetter, and H. Sohlbach, 1989, Nucl. Phys. A **502**, 271c.

Baye, D., and P. Descouvemont, 1983, Nucl. Phys. A **407**, 77.

Baye, D., and P. Descouvemont, 1984, Phys. Lett. B **146**, 285.

Bemis, C.E., Jr., F.K. McGowan, J.L.C. Ford, Jr., W.T. Milner, R.L. Robinson, and P.H. Stelson, 1988, Phys. Scr. **38**, 657.

Bengtsson, T., M.E. Faber, G. Leander, P. Möller, M. Płoszajczak, I. Ragnarsson, and S. Åberg, 1981, Phys. Scr. **24**, 200.

Bengtsson, R., I. Ragnarsson, S. Åberg, A. Gyurkovich, A. Sobiczewski, and K. Pomorski, 1987, Nucl. Phys. A **473**, 77.

Berger, J.F., M. Girod, and D. Gogny, 1989, Nucl. Phys. A **502**, 85c.

Bernthal, F.M., and J.O. Rasmussen, 1967, Nucl. Phys. A **101**, 513.

Bertsch, G.F., and W. Bertozzi, 1971, Nucl. Phys. A **165**, 199.

Bertsch, G.F., and J. Foxwell, 1990, Phys. Rev. C **41**, 1300.

Bès, D.R., 1963, Nucl. Phys. **49**, 544.

Bhandari, B.S., and A.S. Al-Kharam, 1989, Phys. Rev. C **39**, 917.

Bjørnholm, S., and J.E. Lynn, 1980, Rev. Mod. Phys. **52**, 725.

Bleuler, K., and Ch. Terreaux, 1957, Helv. Phys. Acta **30**, 183.

Błocki, J., F. Brut, T. Srokowski, and W. Swiatecki, 1992, Nucl. Phys. A **545**, 511c.

Błocki, J., and W. Kurcewicz, 1969, Phys. Lett. B **30**, 458.

Błocki, J., J.-J. Shi, and W. Swiatecki, 1993, Nucl. Phys. A **554**, 387.

Błocki, J., J. Skalski, and W. Swiatecki, 1995, Preprint No. LBL-37241.

Blomquist, J., and A. Molinari, 1968, Nucl. Phys. A **106**, 545.

Blons, J., 1989, Nucl. Phys. A **502**, 121c.

Blons, J., C. Mazur, and D. Paya, 1975, Phys. Rev. Lett. **35**, 1749.

Blons, J., C. Mazur, D. Paya, M. Ribrag, and H. Weigmann, 1978, Phys. Rev. Lett. **41**, 1282.

Blons, J., C. Mazur, D. Paya, M. Ribrag, and H. Weigmann, 1984, Nucl. Phys. **414**, 1.

Bohr, A., 1952, K. Dan. Vidensk. Selsk. Mat.-Fys. Medd. **26**, No. 14.

Bohr, A., 1976, Rev. Mod. Phys. **48**, 365.

Bohr, A., and B.R. Mottelson, 1957, Nucl. Phys. **4**, 529.

Bohr, A., and B.R. Mottelson, 1958, Nucl. Phys. **9**, 687.

Bohr, A., and B.R. Mottelson, 1975, *Nuclear Structure Vol. II* (Benjamin, New York).

Bonche, P., 1988, in *The Variety of Nuclear Shapes*, edited by J.D. Garrett *et al.* (World Scientific, Singapore), p. 302.

Bonche, P., E. Chabanat, B.Q. Chen, J. Dobaczewski, H. Flocard, B. Gall, P.-H. Heenen, J. Meyer, N. Tajima, and M.S. Weiss, 1994, Nucl. Phys. A **574**, 185c.

Bonche, P., P.-H. Heenen, H. Flocard, and D. Vautherin, 1986, Phys. Lett. B **175**, 387.

Bonche, P., S.J. Krieger, M.S. Weiss, J. Dobaczewski, H. Flocard, and P.-H. Heenen, 1991, Phys. Rev. Lett. **66**, 876.

Bonin, W., H. Backe, M. Dahlinger, S. Glienke, D. Habs, E. Hanelt, E. Kankeleit, and B. Schwartz, 1985, Z. Phys. A **322**, 59.

Bonin, W., M. Dahlinger, S. Glienke, E. Kankeleit, M. Krämer, D. Habs, B. Schwartz, and H. Backe, 1983, Z. Phys. **310**, 249.

Böning, K., A. Sobiczewski, B. Nerlo-Pomorska, and K. Pomorski, 1985, Phys. Lett. B **161**, 231.

Borchers, W., R. Neugart, E.W. Otten, H.T. Duong, G. Ulm, and K. Wendt, 1987, Hyperfine Interact. **34**, 25.

Borge, M.J.G., D.G. Burke, H. Gietz, P. Hill, N. Kaffrell, W. Kurcewicz, G. Løvhøiden, S. Mattsson, R.A. Naumann, K. Nybø, G. Nyman, and T.F. Thorsteinsen, 1987, Nucl. Phys. A **464**, 189.

Bowman, J.D., C.D. Bowman, J.E. Bush, P.P.J. Delheij, C.M. Frankle, C.R. Gould, D.G. Haase, J. Knudson, G.E. Mitchell, S. Penttila, H. Postma, N.R. Roberson, S.J. Seestrom, J.J. Szymanski, V.W. Yuan, and X. Zhu, 1990, Phys. Rev. Lett. **65**, 1192.

Bowman, J.D., G.T. Garvey, C.R. Gould, A.C. Hayes, and M.B. Johnson, 1992, Phys. Rev. Lett. **68**, 780.

Brack M., J. Damgård, A.S. Jensen, H.C. Pauli, V.M. Strutinsky, and C.Y. Wong, 1972, Rev. Mod. Phys. **44**, 320.

Brack, M., and P. Quentin, 1981, Nucl. Phys. A **361**, 35.

Branford, D., N. Gardner, and I.F. Wright, 1971, Phys. Lett. B **36**, 456.

Brenner, M., 1994, Z. Phys. A **349**, 233.

Briançon, Ch., S. Ćwiok, S.A. Eid, V. Green, W.D. Hamilton, C.F. Liang, and R.J. Walen, 1990, J. Phys. G **16**, 1735.

Brillard, L., A.G. Elayi, E. Hourani, M. Hussonnois, J.F. Le Du, L.H. Rosier, and L. Stab, 1989, C. R. Acad. Sci. II, Mec. Phys. Chim. Sci. Terre Univers **309**, 1105.

Brink, D.M., 1957, Nucl. Phys. **4**, 215.

Brink, D.M., 1966, in *Many-body description of nuclear structure and reactions*, Proceedings of the International School of Physics "Enrico Fermi;" course 36 (Academic, New York), p. 247.

Brink, D.M., B. Buck, R. Huby, M.A. Nagarajan, and N. Rowley, 1987, J. Phys. G **13**, 629.

Brockstedt, A., J. Lyttkens-Lindén, M. Bergström, L.P. Ekström, H. Ryde, J.C. Bacelar, J.D. Garrett, G.B. Hagemann, B. Herskind, F.R. May, P.O. Tjøm, and S. Frauendorf, 1994, Nucl. Phys. A **571**, 337.

Buchinger, F., J.E. Crawford, A.K. Dutta, J.M. Pearson, and F. Tondeur, 1994, Phys. Rev. C **49**, 1402.

Buck, B., C.B. Dover, and J.P. Vary, 1975, Phys. Rev. C **11**, 1803.

Buck, B., H. Friederich, and A.A. Pilt, 1977, Nucl. Phys. A **290**, 205.

Buck, B., P.D.B. Hopkins, and A.C. Merchant, 1990, Nucl. Phys. A **513**, 75.

Buck, B., A.C. Merchant, and S.M. Perez, 1995, Phys. Rev. C **51**, 559.

Buck, B., and A.A. Pilt, 1977, Nucl. Phys. A **280**, 133.

Burr, W., D. Schütte, and K. Bleuler, 1969, Nucl. Phys. A **133**, 581.

Burrows, J.D., P.A. Butler, K.A. Connell, A.N. James, G.D. Jones, A.M.Y. El-Lawindy, T.P. Morrison, J. Simpson, and R. Wadsworth, 1984, J. Phys. G **10**, 1449.

Butler, P.A., 1988, in *Heavy Ions in Nuclear and Atomic Physics*, edited by Z. Wilhelmi and G. Szeflińska (Hilger, Bristol), p. 295.

Butler, P.A., 1990, in *Proceedings of the International Conference on High Spin Physics and Gamma-Soft Nuclei*, edited by J.X. Saladin, R.A. Sorensen, and C.M. Vincent (World Scientific, Singapore), p. 552.

Butler, P.A., and W. Nazarewicz, 1991, Nucl. Phys. A **533**, 249.

Castel, B., Y. Okuhara, and H. Sagawa, 1990, Phys. Rev. C **42**, R1203.

Castel, B., and J.P. Svenne, 1969, Can. J. Phys. **47**, 1393.

Casten, R.F., W.-T. Chou, and N.V. Zamfir, 1993, Nucl. Phys. A **555**, 563.

Catara, F., C.H. Dasso, and A. Vitturi, 1989, J. Phys. G **15**, L191.

Catara, F., M. Sambataro, A. Insolia, and A. Vitturi, 1986, Phys. Lett. B **180**, 1.

Ceauşescu, V., and A.A. Raduta, 1976, Ann. Phys. (N.Y.) **100**, 94.
Celler, A., Ch. Briançon, J.S. Dionisio, A. Lefebvre, Ch. Vieu, J. Żylicz, R. Kulessa, C. Mittag, J. Fernández-Niello, Ch. Lauterbach, H. Puchta, and F. Riess, 1985, Nucl. Phys. A **423**, 421.
Chasman, R.R., 1979, Phys. Rev. Lett. **42**, 630.
Chasman, R.R., 1980, Phys. Lett. B **96**, 7.
Chasman, R.R., 1984, Phys. Rev. C **30**, 1753.
Chasman, R.R., 1986, Phys. Lett. B **175**, 254.
Chasman, R.R., 1989, Phys. Lett. B **219**, 232.
Chasman, R.R., 1991, Phys. Lett. B **266**, 243.
Chasman, R.R., and I. Ahmad, 1986, Phys. Lett. B **182**, 261.
Chasman, R.R., I. Ahmad, A.M. Friedman, and J.R. Erskine, 1977, Rev. Mod. Phys. **49**, 833.
Chasman, R.R., and L.M. Robledo, 1995, Phys. Lett. B **351**, 18.
Chou, W.-T., R.F. Casten, and N.V. Zamfir, 1992, Phys. Rev. C **45**, R2545.
Chuu, D.-S., S.T. Hsieh, and H.C. Chiang, 1993, Phys. Rev. C **47**, 183.
Coc, A., C. Thibault, F. Touchard, H.T. Duong, P. Juncar, S. Liberman, J. Pinard, M. Carre, J. Lermé, J.L. Vialle, S. Büttgenbach, A.C. Mueller, A. Pesnelle, and the ISOLDE Collaboration, 1987, Nucl. Phys. A **468**, 1.
Coc, A., C. Thibault, F. Touchard, H.T. Duong, P. Juncar, S. Liberman, J. Pinard, J. Lermé, J.L. Vialle, S. Büttgenbach, A.C. Mueller, A. Pesnelle, and the ISOLDE Collaboration, 1985, Phys. Lett. B **163**, 66.
Cottle, P.D., 1990a, Phys. Rev. C **42**, 1264.
Cottle, P.D., 1990b, Phys. Rev. C **41**, 517.
Cottle, P.D., 1991, Z. Phys. A **338**, 281.
Cottle, P.D., 1994, Z. Phys. A **349**, 115.
Cottle, P.D., and D.A. Bromley, 1986, Phys. Lett. B **182**, 129.
Cottle, P.D., M. Gai, J.F. Ennis, J.F. Shriner, Jr., D.A. Bromley, C.W. Beausang, L. Hildingsson, W.F. Piel, Jr., D.B. Fossan, J.W. Olness, and E.K. Warburton, 1986, Phys. Rev. C **33**, 1855.
Cottle, P.D., T. Glasmacher, J.L. Johnson, and K.W. Kemper, 1993, Phys. Rev. C **48**, 136.
Cottle, P.D., T. Glasmacher, and K.W. Kemper, 1992, Phys. Rev. C **45**, 2733.
Cottle, P.D., J.W. Holcomb, T.D. Johnson, K.A. Stuckey, S.L. Tabor, P.C. Womble, S.G. Buccino, and F.E. Durham, 1990, Phys. Rev. C **42**, 1254.
Cottle, P.D., and K.W. Kemper, 1991, Phys. Rev. C **44**, 1901.
Cottle, P.D., J.F. Shriner, Jr., F. Dellagiacoma, J.F. Ennis, M. Gai, D.A. Bromley, J.W. Olness, E.K. Warburton, L. Hildingsson, M.A. Quader, and D.B. Fossan, 1984, Phys. Rev. C **30**, 1768.
Cottle, P.D., K.A. Stuckey, and K.W. Kemper, 1988, Phys. Rev. C **38**, 365.
Cottle, P.D., K.A. Stuckey, and K.W. Kemper, 1989, Phys. Lett. B **219**, 27.
Cristancho, F., J.X. Saladin, M.P. Metlay, W. Nazarewicz, C. Baktash, M. Halbert, I-Y. Lee, D.F. Winchell, S.M. Fischer, and M.K. Kabadiyski, 1994, Phys. Rev. C **49**, 663.
Crowell, B., M.P. Carpenter, R.V.F. Janssens, D.J. Blumenthal, J. Timar, A.N. Wilson, J.F. Sharpey-Schafer, T. Nakatsukasa, I. Ahmad, A. Astier, F. Azaiez, L. du Croux, B.J.P. Gall, F. Hannachi, T.L. Khoo, A. Korichi, T. Lauritsen, A. Lopez-Martens, M. Meyer, D. Nisius, E.S. Paul, M.G. Porquet, and N. Redon, 1995, Phys. Rev. C **51**, R1599.
Crowell, B., R.V.F. Janssens, M.P. Carpenter, I. Ahmad, S. Harfenist, R.G. Henry, T.L. Khoo, T. Lauritsen, D. Nisius, A.N. Wilson, J.F. Sharpey-Schafer, and J. Skalski, 1994, Phys. Lett. B **333**, 320.
Cseh, J., 1989, J. Phys. Soc. Jpn. Suppl. **58**, 604.
Cseh, J., 1992, Phys. Lett. B **281**, 173.
Cseh, J., 1993, J. Phys. G **19**, L63.
Cseh, J., G. Lévai, and K. Katō, 1991, Phys. Rev. C **43**, 165.
Cseh, J., G. Lévai, and W. Scheid, 1993, Phys. Rev. C **48**, 1724.
Cseh, J., and W. Scheid, 1992, J. Phys. G **18**, 1419.
Cullen, D.M., M.A. Riley, A. Alderson, I. Ali, C.W. Beausang, T. Bengtsson, M.A. Bentley, P. Fallon, P.D. Forsyth, F. Hanna, S.M. Mullins, W. Nazarewicz, R.J. Poynter, P.H. Regan, J.W. Roberts, W. Satuła, J.F. Sharpey-Schafer, J. Simpson, G. Sletten, P.J. Twin, R. Wadsworth, and R. Wyss, 1990, Phys. Rev. Lett. **65**, 1547.
Ćwiok, S., J. Kvasil, and B. Choriev, 1984, J. Phys. G **10**, 903.
Ćwiok, S., and W. Nazarewicz, 1989a, Phys. Lett. B **224**, 5.
Ćwiok, S., and W. Nazarewicz, 1989b, Nucl. Phys. A **496**, 367.
Ćwiok, S., and W. Nazarewicz, 1991, Nucl. Phys. A **529**, 95.
Ćwiok, S., W. Nazarewicz, J.X. Saladin, W. Płóciennik, and A. Johnson, 1994, Phys. Lett. B **322**, 304.
Ćwiok, S., P. Rozmej, A. Sobiczewski, and Z. Patyk, 1989, Nucl. Phys. A **491**, 281.
Dagnall, P.J., C.W. Beausang, P.J. Twin, M.A. Bentley, F.A. Beck, Th. Byrski, S. Clarke, D. Curien, G. Duchene, G. de France, P.D. Forsyth, B. Haas, J.C. Lisle, E.S. Paul, J. Simpson, J. Styczen, J.P. Vivien, J.N. Wilson, and K. Zuber, 1994, Phys. Lett. B **335**, 313.
Dahlinger, M., E. Hanelt, E. Kankeleit, B. Schwartz, D. Schwalm, D. Habs, R.S. Simon, and H. Backe, 1985, Z. Phys. A **321**, 535.
Dahlinger, M., E. Kankeleit, D. Habs, D. Schwalm, B. Schwartz, R.S. Simon, J.D. Burrows, and P.A. Butler, 1988, Nucl. Phys. A **484**, 337.
Daley, H.J., and B.R. Barrett, 1986, Nucl. Phys. A **449**, 256.
Daley, H.J., and M. Gai, 1984, Phys. Lett. B **149**, 13.
Daley, H.J., and F. Iachello, 1983, Phys. Lett. B **131**, 281.
Daley, H.J., and F. Iachello, 1986, Ann. Phys. (N.Y.) **167**, 73.
Daley, H.J., and M.A. Nagarajan, 1986, Phys. Lett. B **166**, 379.
Danilin, B.V., I.J. Thompson, M.V. Zhukov, J.S. Vaagen, and J.M. Bang, 1994, Phys. Lett. B **333**, 299.
Dasso, C.H., S.M. Lenzi, A. Vitturi, and F. Zardi, 1993, Nucl. Phys. A **563**, 162.
Davidson, J.P., 1962, Nucl. Phys. **33**, 664.
Davidson, M.G., 1965, Nucl. Phys. **69**, 455.
De Voigt, M.J.A., Z. Sujkowski, D. Chmielewska, J.F.W. Jansen, J. Van Klinken, and S.J. Feenstra, 1975, Phys. Lett. B **59**, 137.
Debray, M.E., J. Davidson, M. Davidson, A.J. Kreiner, D. Hojman, D. Santos, K. Ahn, D.B. Fossan, Y. Liang, R. Ma, E.S. Paul, W.F. Piel, Jr., and N. Xu, 1990, Phys. Rev. C **41**, R1895.
Debray, M.E., A.J. Kreiner, M. Davidson, J. Davidson, D. Hojman, D. Santos, V.R. Vanin, N. Schulz, M. Aiche, A. Chevallier, J. Chevallier, and J.C. Sens, 1994, Nucl. Phys. A **568**, 141.
Delaroche, J.P., J.F. Berger, M. Girod, J. Libert, I. Deloncle, and L.M. Robledo, 1992, in *Nuclear Shapes and Nuclear Structure at Low Excitation Energies*, edited by M. Vergnes *et al.* (Plenum, New York), p. 323.

Delion, D.S., A. Insolia, and R.J. Liotta, 1992, Phys. Rev. C **46**, 1346.
Delion, D.S., A. Insolia, and R.J. Liotta, 1994, J. Phys. G **20**, 1483.
Denisov, V. Yu., 1989, Sov. J. Nucl. Phys. **49**, 399.
Denisov, V. Yu., 1992, Sov. J. Nucl. Phys. **55**, 1478.
Denisov, V. Yu., and A.Ya. Dzyublik, 1993, Phys. At. Nucl. **56**, 303.
Denisov, V. Yu., and A.Ya. Dzyublik, 1995, Nucl. Phys. **589**, 17.
Dennison, D.M., 1940, Phys. Rev. **57**, 454.
Dennison, D.M., 1954, Phys. Rev. **96**, 378.
Depta, K., J.A. Maruhn, W. Greiner, W. Scheid, and A. Sandulescu, 1986, Mod. Phys. Lett. A **1**, 377.
Descouvemont, P., 1987, Nucl. Phys. A **470**, 309.
Descouvemont, P., 1991, Phys. Rev. C **44**, 306.
Descouvemont, P., and D. Baye, 1985, Phys. Rev. **31**, 2274.
Descouvemont, P., and D. Baye, 1986, Nucl. Phys. A **459**, 374.
Descouvemont, P., and D. Baye, 1987, Nucl. Phys. A **475**, 219.
Descouvemont, P., and D. Baye, 1989, Phys. Lett. B **228**, 6.
Do Dang, G., K.W. Schmid, R.M. Dreizler, and H.G. Miller, 1976, Phys. Lett. B **62**, 1.
Dobaczewski, J., and J. Skalski, 1989, Phys. Rev. C **40**, 1025.
Dojnikov, D.N., A.D. Efimov, K.I. Erokhina, and V.M. Mikhajlov, 1991, Nucl. Phys. A **531**, 326.
Dojnikov, D.N., and V.M. Mikhajlov, 1994, Phys. Lett. B **334**, 259.
Donner, W., and W. Greiner, 1966, Z. Phys. **197**, 440.
Dörschel, K., W. Heddrich, H. Hühnermann, E.W. Peau, H. Wagner, G.D. Alkhazov, E.Ye. Berlovich, V.P. Denison, V.N. Panteleev, and A.G. Polyakov, 1984, Z. Phys. A **317**, 233.
Dorso, C.O., W.D. Myers, and W.J. Swiatecki, 1986, Nucl. Phys. A **451**, 189.
Drigert, M.W. and J.A. Cizewski, 1985, Phys. Rev. C **31**, 1977.
Drigert, M.W., and J.A. Cizewski, 1986, Phys. Rev. C **33**, 1344.
Dudek, J., 1987, in *The Variety of Nuclear Shapes*, edited by J. Garrett *et al.* (World Scientific, Singapore), p. 195.
Dudek J., W. Nazarewicz, and P. Olanders, 1984, Nucl. Phys. A **420**, 285.
Dudek, J., T.R. Werner, and Z. Szymański, 1990, Phys. Lett. **248**, 235.
Dufour, M., P. Descouvemont, and D. Baye, 1994, Phys. Rev. **50**, 795.
Dukelsky, J., J. Fernández-Niello, H.M. Sofia, and R.P.J. Perazzo, 1983, Phys. Rev. C **28**, 2183.
Dukelsky, J., R.P.J. Perazzo, S.L. Reich, and H.M. Sofia, 1985, Phys. Lett. B **158**, 361.
Dumitrescu, O., 1994, Phys. Rev. C **49**, 1466.
Durell, J.L., Y. Abdelrahman, W.R. Phillips, M.A.C. Hotchkis, J. McNeil, B.J. Varley, and W. Gelletly, 1988, in *Daresbury Laboratory Annual Report 1987/88*, p. 28.
Dzyublik, A.Ya., and V.Yu. Denisov, 1993, Phys. At. Nucl. **56**, 477.
Ebenhöh, W., 1966, Z. Phys. **195**, 171.
Egido, J.L., and L.M. Robledo, 1989, Nucl. Phys. A **494**, 85.
Egido, J.L., and L.M. Robledo, 1990, Nucl. Phys. A **518**, 475.
Egido, J.L., and L.M. Robledo, 1991a, Nucl. Phys. A **524**, 65.
Egido, J.L., and L.M. Robledo, 1991b, in *Future Directions in Nuclear Physics with 4π Gamma Detection Systems of the New Generation*, AIP Conf. Proc. No. 259, edited by J. Dudek and B. Haas (American Institute of Physics, New York), 259.
Egido, J.L., and L.M. Robledo, 1992, Nucl. Phys. A **545**, 589.
Eichler, J., and A. Faessler, 1970, Nucl. Phys. A **157**, 166.
Ekström, C., L. Robertsson, and A. Rosén, 1986, Phys. Scr. **34**, 624.
Elliott, J.P., J.A. Evans, and E.E. Maqueda, 1985, Nucl. Phys. A **437**, 208.
Engel, J., A. Frank, and S. Pittel, 1987, Phys. Rev. C **35**, 1973.
Engel, J., and F. Iachello, 1985, Phys. Rev. Lett. **54**, 1126.
Engel, J., and F. Iachello, 1987, Nucl. Phys. A **472**, 61.
Ennis, P.J., C.J. Lister, W. Gelletly, H.G. Price, B.J. Varley, P.A. Butler, T. Hoare, S. Ćwiok, and W. Nazarewicz, 1991, Nucl. Phys. A **535**, 392; A **560**, 1079(E).
Erb, K.A., and D.A. Bromley, 1981, Phys. Rev. C **23**, 2781.
Esbensen, H. and G.F. Bertsch, 1992, Nucl. Phys. A **542**, 310.
Fabbro, B., J. Blons, A. Greiner, J.M. Hisleur, C. Mazur, Y. Patin, D. Paya, and M. Ribrag, 1984, J. Phys. Lett. **45**, L-843.
Faber, M., 1981, Phys. Rev. C **24**, 1047.
Faber, M., and M. Płoszajczak, 1981, Phys. Scr. **24**, 189.
Faessler, A., T. Udagawa, and R. K. Sheline, 1966, Nucl. Phys. **85**, 670.
Faessler, A., and A. Plastino, 1967, Z. Phys. **203**, 333.
Faessler, A., A. Plastino, and S.A. Moszkowski, 1967, Phys. Rev. **156**, 1064.
Fayans, S.A., A.P. Platonov, G. Graw, and D. Hofer, 1994, Nucl. Phys. A **577**, 557.
Fedorov, D.V., A.S. Jensen, and K. Riisager, 1994, Phys. Rev. C **49**, 201.
Fernández-Niello, J., C. Mittag, F. Riess, E. Ruchowska, and M. Stallknecht, 1991, Nucl. Phys. A **531**, 164.
Fernández-Niello, J., H. Puchta, F. Riess, and W. Trautmann, 1982, Nucl. Phys. A **391**, 221.
Flambaum, V.V., and O.P. Sushkov, 1980, Phys. Lett. B **94**, 277.
Flambaum, V.V., and V.G. Zelevinsky, 1995, Phys. Lett. B **350**, 8.
Fogelberg, B., M. Hellström, D. Jerrestam, H. Mach, J. Blomqvist, A. Kerek, L.O. Norlin, and J.P. Omtvedt, 1994, Phys. Rev. Lett. **73**, 2413.
Frankle, C.M., J.D. Bowman, J.E. Bush, P.P.J. Delheij, C.R. Gould, D.G. Haase, J.N. Knudson, G.E. Mitchell, S. Penttilä, H. Postma, N.R. Roberson, S.J. Seestrom, J.J. Szymanski, S.H. Yoo, V.W. Yuan, and X. Zhu, 1992, Phys. Rev. C **46**, 778.
Frauendorf, S., and V.V. Pashkevich, 1984, Phys. Lett. B **141**, 23.
Frauendorf, S., and V.V. Pashkevich, 1993, Z. Phys. D **26**, S98.
Frekers, D., R. Santo, and K. Langanke, 1983, Nucl. Phys. A **394**, 189.
Friedrich, H., and K. Langanke, 1975, Nucl. Phys. A **252**, 47.
Friedrichs, H., B. Schlitt, J. Margraf, S. Lindenstruth, C. Wesselborg, R.D. Heil, H.H. Pitz, U. Kneissl, P. von Brentano, R.D. Herzberg, A. Zilges, D. Häger, G. Müller, and M. Schumacher, 1992, Phys. Rev. C **45**, R892.
Frisk, H., 1990, Nucl. Phys. A **511**, 309.
Frisk, F., I. Hamamoto, and F.R. May, 1994, Phys. Scr. **50**, 628.
Fujiwara, Y., H. Horiuchi, K. Ikeda, M. Kamimura, K. Sato, Y. Suzuki, and E. Uegaki, 1980, Prog. Theor. Phys. Suppl. **68**, 29.
Funck, C., B. Grund, and K. Langanke, 1989, Z. Phys. A **334**, 1.
Gai, M., 1988, Phys. Rev. Lett. **61**, 2424.
Gai, M., J.F. Ennis, D.A. Bromley, H. Emling, F. Azgui, E. Grosse, H.J. Wollersheim, C. Mittag, and F. Riess, 1988, Phys. Lett. B **215**, 242.

Gai, M., R. Keddy, D.A. Bromley, J.W. Olness, and E.K. Warburton, 1987, Phys. Rev. C **36**, 1256.

Gai, M., S.L. Rugari, R.H. France, III, B.J. Lund, Z. Zhao, D.A. Bromley, B.A. Lincoln, W.W. Smith, M.J. Zarcone, and Q.C. Kessel, 1989, Phys. Rev. Lett. **62**, 874.

Gai, M., M. Ruscev, D.A. Bromley, and J.W. Olness, 1991, Phys. Rev. C **43**, 2127.

Gai, M., M. Ruscev, A.C. Hayes, J.F. Ennis, R. Keddy, E.C. Schloemer, S.M. Sterbenz, and D.A. Bromley, 1983, Phys. Rev. Lett. **50**, 239.

Garrett, J.D., 1984, Nucl. Phys. **421**, 313c.

Gavron, A., H.C. Britt, P.D. Goldstone, J.B. Wilhelmy, and S.E. Larsson, 1977, Phys. Rev. Lett. **38**, 1457.

Giraud, B., and P.U. Sauer, 1970, Nucl. Phys. A **154**, 587.

Gönnenwein, F., 1994, Z. Phys. A **349**, 259.

Gono, Y., T. Kohno, M. Sugawara, Y. Ishikawa, and M. Fukuda, 1986, Nucl. Phys. A **459**, 427.

Goodman, A.L., 1974, Nucl. Phys. A **230**, 466.

Görres, J., T. Chapuran, D.P. Balamuth, and J.W. Arrison, 1987, Phys. Rev. Lett. **58**, 662.

Govaert, K., L. Govor, E. Jacobs, D. De Frenne, W. Mondelaers, K. Persyn, M.L. Yoneama, U. Kneissl, J. Margraf, H.H. Pitz, K. Huber, S. Lindenstruth, R. Stock, K. Heyde, A. Vdovin, and V. Yu Ponomarev, 1994, Phys. Lett. B **335**, 113.

Grafen, V., B. Ackermann, H. Baltzer, T. Bihn, C. Günther, J. deBoer, N. Gollwitzer, G. Graw, R. Hertenberger, H. Kader, A. Levon, and A. Lösch, 1991, Phys. Rev. C **44**, R1728.

Guglielmetti, A., R. Bonetti, G. Poli, P.B. Price, A.J. Westphal, Z. Janas, H. Keller, R. Kirchner, O. Klepper, A. Piechaczek, E. Roeckl, K. Schmidt, A. Płochocki, J. Szerypo, and B. Blank, 1995, Phys. Rev. **52**, 740.

Guhr, T., K.-D. Hummel, G. Kilgus, D. Bohle, A. Richter, C.W. de Jager, H. de Vries, and P.K.A. de Witt Huberts, 1989, Nucl. Phys. A **501**, 95.

Gustafsson, C., P. Möller, and S.G. Nilsson, 1971, Phys. Lett. B **34**, 349.

Gutzwiller, M.C., 1967, J. Math. Phys. **8**, 1979.

Gutzwiller, M.C., 1971, J. Math. Phys. **12**, 343.

Haenni, D.R., and T.T. Sugihara, 1977, Phys. Rev. C **16**, 120.

Hagemann, G.B., I. Hamamoto, and W. Satuła, 1993, Phys. Rev. C **47**, 2008.

Hamamoto, I., 1993, Nucl. Phys. A **557**, 515c.

Hamamoto, I., J. Höller, and X.-z. Zhang, 1989, Phys. Lett. B **226**, 17.

Hamamoto, I., B. Mottelson, H.-x. Xie, and X.-z. Zhang, 1991, Z. Phys. D **21**, 163.

Hamamoto, I., X.-z. Zhang, and H.-x. Xie, 1991, Phys. Lett. B **257**, 1; B **278**, 511(E).

Han, C.S., D.S. Chuu, S.T. Hsieh, and H.C. Chiang, 1985, Phys. Lett. B **163**, 295.

Hansen, P.G., and B. Jonson, 1987, Europhys. Lett. **4**, 409.

Häusser, O., T.K. Alexander, A.B. McDonald, G.T. Ewan, and A.E. Litherland, 1971, Nucl. Phys. A **168**, 17.

Haxton, W.C., and E.M. Henley, 1983, Phys. Rev. Lett. **51**, 1937.

Hayes, A.C., 1991, Phys. Lett. B **254**, 15.

Hayes, A.C., and D. Strottman, 1990, Phys. Rev. C **42**, 2248.

Heenen, P.-H., J. Skalski, P. Bonche, and H. Flocard, 1994, Phys. Rev. C **50**, 802.

Heiss, W.D., R.G. Nazmitdinov, and S. Radu, 1994, Phys. Rev. Lett. **72**, 2351.

Heiss, W.D., R.G. Nazmitdinov, and S. Radu, 1995a, Phys. Rev. B **51**, 1874.

Heiss, W.D., R. G. Nazmitdinov, and S. Radu, 1995b, Phys. Scr. Vol. T **56**, 182.

Hellström, G., M.S. thesis, Lund University, 1977 (unpublished).

Helmer, R.G., M.A. Lee, C.W. Reich, and I. Ahmad, 1987, Nucl. Phys. A **474**, 77.

Herrmann, R., J.A. Maruhn, and W. Greiner, 1986, J. Phys. G **12**, L285.

Herrmann, G.D., B. Prillwitz, U. Dämmrich, K. Freitag, P. Herzog, D. Mayer, K. Schlösser, and I. Ragnarsson, 1989, Nucl. Phys. A **493**, 83.

Hill, D.L., and J.A. Wheeler, 1953, Phys. Rev. **89**, 1102.

Hiura, J., Y. Abe, S. Saitō, and O. Endō, 1969, Prog. Theor. Phys. **42**, 555.

Hofer, D., M. Bisenberger, R. Hertenberger, H. Kader, H.J. Maier, E. Müller-Zanotti, P. Schiemenz, G. Graw, P. Maier-Komor, G. Molnár, W. Unkelbach, J. Hebenstreit, H. Ohm, D. Paul, P. von Rossen, and M. Fujiwara, 1993, Nucl. Phys. A **551**, 173.

Höller, J., and S. Åberg, 1990, Z. Phys. A **336**, 363.

Horen, D.J., R.L. Auble, G.R. Satchler, J.R. Beene, I.Y. Lee, C.Y. Wu, D. Cline, M. Devlin, R. Ibbotson, and M. W. Simon, 1993, Phys. Rev. C **48**, R2131.

Horiuchi, H., 1985, Prog. Theor. Phys. **73**, 1172.

Horiuchi, H., 1991, Nucl. Phys. A **522**, 257c.

Horiuchi, H., and K. Ikeda, 1968, Prog. Theor. Phys. **40**, 277.

Horiuchi, H., K. Ikeda, and Y. Suzuki, 1972, Prog. Theor. Phys. Suppl. **52**, 89.

Horiuchi, H., Y. Kanada-En'yo, and A. Ono, 1994, Z. Phys. A **349**, 279.

Horiuchi, H., and Y. Suzuki, 1973, Prog. Theor. Phys. **49**, 1974.

Hoshino, T., H. Sagawa, and A. Arima, 1991, Nucl. Phys. A **523**, 228.

Hourani, E., G. Berrier-Ronsin, A. Elayi, P. Hoffmann-Rothe, A.C. Mueller, L. Rosier, G. Rotbard, G. Renou, A. Lièbe, D.N. Poenaru, and H.L. Ravn, 1995, Phys. Rev. C **52**, 267.

Hourani, E., L. Rosier, G. Berrier-Ronsin, A. Elayi, A.C. Mueller, G. Rappenecker, G. Rotbard, G. Renou, A. Lièbe, L. Stab, and H.L. Ravn, 1991, Phys. Rev. C **44**, 1424.

Howard, W.M., and P. Möller, 1980, At. Data Nucl. Data Tables, **25**, 219.

Hughes, J.R., R. Tölle, J. de Boer, P.A. Butler, C. Günther, V. Grafen, N. Gollwitzer, V.E. Holliday, G.D. Jones, C. Lauterbach, M. Marten-Tölle, S.M. Mullins, R.J. Poynter, R.S. Simon, N. Singh, R.J. Tanner, R. Wadsworth, D.L. Watson, and C.A. White, 1990, Nucl. Phys. A **512**, 275.

Hulet, E.K., J.F. Wild, R.J. Dougan, R.W. Lougheed, J.H. Landrum, A.D. Dougan, M. Schädel, R.L. Hahn, P.A. Baisden, C.M. Henderson, R.J. Dupzyk, K. Sümmerer, and G.R. Bethune, 1986, Phys. Rev. Lett. **56**, 313.

Hussonnois, M., and G. Ardisson, 1994, Z. Phys. A **349**, 311.

Hussonnois, M., J.F. Le Du, L. Brillard, and G. Ardisson, 1990a, Phys. Rev. C **42**, R495; **43**, 916(E) (1991).

Hussonnois, M., J. F. Le Du, L. Brillard, and G. Ardisson, 1990b, J. Phys. G **16**, L77.

Hussonnois, M., J.F. Le Du, L. Brillard, and G. Ardisson, 1991, Phys. Rev. C **44**, 2884.

Iachello, F., 1981, Phys. Rev. C **23**, 2778.

Iachello, F., 1984, Nucl. Phys. A **421**, 97c.

Iachello, F., 1985, Phys. Lett. B **160**, 1.

Iachello, F., 1989, Phys. Rev. Lett. **62**, 2440.

Iachello, F., and A. Arima, 1974, Phys. Lett. B **53**, 309.

Iachello, F., and A.D. Jackson, 1982, Phys. Lett. B **108**, 151.

Ibbotson, R., B. Kotliński, D. Cline, K.G. Helmer, A.E. Kavka, A. Renalds, E.G. Vogt, P.A. Butler, C.A. White, R. Wadsworth, and D.L. Watson, 1991, Nucl. Phys. A **530**, 199.

Ibbotson, R., C.A. White, T. Czosnyka, P.A. Butler, N. Clarkson, D. Cline, R.A. Cunningham, M. Devlin, K.G. Helmer, T.H. Hoare, J.R. Hughes, G.D. Jones, A.E. Kavka, B. Kotlinski, R.J. Poynter, P. Regan, E.G. Vogt, R. Wadsworth, D.L. Watson, and C.Y. Wu, 1993, Phys. Rev. Lett **71**, 1990.

Ikeda, K., N. Takigawa, and H. Horiuchi, 1968, Prog. Theor. Phys. Suppl. (Extra Number), 464.

Insolia, A., P. Curutchet, R.J. Liotta, and D.S. Delion, 1991, Phys. Rev. C **44**, 545.

Ishii, T., I. Ahmad, J.E. Gindler, A.M. Friedman, R.R. Chasman, and S.B. Kaufman, 1985, Nucl. Phys. A **444**, 237.

Itonaga, K., 1981, Prog. Theor. Phys. **66**, 2103.

Ivanova, S.P., A.L. Komov, L.A. Malov, and V.G. Solov'ev, 1976, Sov. J. Part. Nuclei **7**, 175.

Jahn, H.A., and E. Teller, 1937, Proc. Roy. Soc. A **161**, 220.

Jain, A.K., R.K. Sheline, P.C. Sood, and K. Jain, 1990, Rev. Mod. Phys. **62**, 393.

Jammari, K., R. Piepenbring, and B. Silvestre-Brac, 1983, Phys. Rev. C **28**, 2136.

Johansson, S.A.E., 1961, Nucl. Phys. **22**, 529.

Jolos, R.V., and P. von Brentano, 1994, Phys. Rev. C **49**, R2301.

Jolos, R.V., and P. von Brentano, 1995, Nucl. Phys. A **587**, 377.

Jolos, R.V., P. von Brentano, and F. Dönau, 1993, J. Phys. G **19**, L151.

Jongman, J.R., J.C.S. Bacelar, W. Urban, R.F. Noorman, J. van Pol, Th. Steenbergen, M.J.A. De Voigt, J. Nyberg, G. Sletten, J. Dionisio, and Ch. Vieu, 1994, Phys. Rev. C **50**, 3159.

Jungclaus, A., T. Belgya, D.P. DiPrete, M. Villani, E.L. Johnson, E.M. Baum, C.A. McGrath, S.W. Yates, and N.V. Zamfir, 1993, Phys. Rev. C **48**, 1005.

Jungclaus, A., H.G. Börner, J. Jolie, S. Ulbig, R.F. Casten, N.V. Zamfir, P. von Brentano, and K.P. Lieb, 1993, Phys. Rev. C **47**, 1020.

Kälber, W., J. Rink, K. Bekk, W. Faubel, S. Göring, G. Meisel, H. Rebel, and R.C. Thompson, 1989, Z. Phys. A **334**, 103.

Kameny, S.L., 1956, Phys. Rev. **103**, 358.

Kammuri, T., and T. Kishimoto, 1978, Z. Phys. A **288**, 203.

Kanada-En'yo, Y., and H. Horiuchi, 1995a, Prog. Theor. Phys. **93**, 115.

Kanada-En'yo, Y., and H. Horiuchi, 1995b, Phys. Rev. C **52**, 628.

Kanada-En'yo, Y., and H. Horiuchi, 1995c, Phys. Rev. C **52**, 647.

Karpeshin, F.F., 1992, Z. Phys. **344**, 55.

Katō, K., and H. Bandō, 1975, Prog. Theor. Phys. **54**, 1887.

Katō, K., and H. Bandō, 1979, Prog. Theor. Phys. **62**, 644.

Katō, K., H. Kazama, and H. Tanaka, 1986, Prog. Theor. Phys. **76**, 75.

Katō, K., S. Okabe, and Y. Abe, 1985, Prog. Theor. Phys. **74**, 1053.

Kazama, H., 1987, Prog. Theor. Phys. **77**, 1178.

Kazama, H., K. Katō, and H. Tanaka, 1984, Prog. Theor. Phys. **71**, 215.

Kelson, I., 1965, Phys. Lett. **16**, 143.

Khan, M.K., W. J. Vermeer, W. Urban, J.B. Fitzgerald, A.S. Mowbray, B.J. Varley, J.L. Durell, and W.R. Phillips, 1994, Nucl. Phys. A **567**, 495.

Khazrouni, S., A. Chevallier, J. Chevallier, O. Helene, G. Ramanantsizehena, and N. Schulz, 1985, Z. Phys. A **320**, 535.

Kirson, M.W., 1982, Phys. Lett. B **108**, 237.

Kneissl, U., A. Zilges, J. Margraf, I. Bauske, P. von Brentano, H. Friedrichs, R.D. Heil, R.-D. Herzberg, H.H. Pitz, B. Schlitt, and C. Wesselborg, 1993, Phys. Rev. Lett. **71**, 2180.

Kocbach, L., and P. Vogel, 1970, Phys. Lett. B **32**, 434.

Kolb, D., R.Y. Cusson, and H.W. Schmitt, 1974, Phys. Rev. C **10**, 1529.

Koskinen, M., P.O. Lipas, and M. Manninen, 1995, Nucl. Phys. A **591**, 421.

Krappe, H.J., and H.G. Wahsweiler, 1967, Nucl. Phys. A **104**, 633.

Krappe, H.J., and U. Wille, 1969, Nucl. Phys. A **124**, 641.

Krick, T.P., N.M. Hinz, and D. Dehnhard, 1973, Nucl. Phys. A **216**, 549.

Kurcewicz, W., N. Kaffrell, N. Trautmann, A. Płochocki, J. Żylicz, K. Stryczniewicz, and I. Yutlandov, 1976, Nucl. Phys. A **270**, 175.

Kurcewicz, W., N. Kaffrell, N. Trautmann, A. Płochocki, J. Żylicz, M. Matul, and K. Stryczniewicz, 1977, Nucl. Phys. A **289**, 1.

Kurcewicz, W., G. Lövhöiden, T.F. Thorsteinsen, M.J.G. Borge, D.G. Burke, M. Cronqvist, H. Gabelmann, H. Gietz, P. Hill, N. Kaffrell, R.A. Naumann, K. Nybö, G. Nyman, and J. Rogowski, 1992, Nucl. Phys. A **539**, 451.

Kusnezov, D., and F. Iachello, 1988, Phys. Lett. B **209**, 420.

Kvasil, J., S. Ćwiok, and B. Choriev, 1981, Z. Phys. A **303**, 313.

Kvasil, J., and R.G. Nazmitdinov, 1985, Nucl. Phys. A **439**, 86.

Lac, V.-S., and I. Morrison, 1995, Nucl. Phys. A **581**, 73.

Landolt-Börnstein, 1974, in *Numerical Data and Functional Relationships in Science and Technology*, edited by K.-H. Hellwege and A.M. Hellwege (Springer, Berlin), Vol. VI.

Lane, A.M., 1964, *Nuclear Theory* (Benjamin, New York).

Lane, A.M., and E.D. Pendlebury, 1960, Nucl. Phys. **15**, 39.

Langanke, K., 1982, Nucl. Phys. A **377**, 53.

Langanke, K., R. Stademann, and D. Frekers, 1984, Phys. Rev. C **29**, 40.

Larsson, S.E., 1973, Phys. Scr. **8**, 17.

Larsson, S.E., P. Möller, and S.G. Nilsson, 1974, Phys. Scr. **10** A, 53.

Lauterbach, Ch., J. de Boer, Ch. Mittag, F. Reiss, Ch. Schandera, Ch. Briançon, A. Levebvre, S. Hlavač, and R.S. Simon, 1984, Phys. Lett. B **140**, 187.

Leander, G.A., 1985a, in *Nuclear Structure 1985*, edited by R.A. Broglia, G.B. Hagemann, and B. Herskind (North-Holland, Amsterdam), p. 249.

Leander, G.A., 1985b, in *Capture Gamma-Ray Spectroscopy and Related Topics*, AIP Conf. Proc. No. 125 (American Institute of Physics, New York), p. 125.

Leander, G.A., and Y.S. Chen, 1987, Phys. Rev. C **35**, 1145.

Leander, G.A., and Y.S. Chen, 1988, Phys. Rev. C **37**, 2744.

Leander, G., and S.E. Larsson, 1975, Nucl. Phys. A **239**, 93.

Leander, G.A., W. Nazarewicz, G.F. Bertsch, and J. Dudek, 1986, Nucl. Phys. A **453**, 58.

Leander, G.A., W. Nazarewicz, P. Olanders, I. Ragnarsson, and J. Dudek, 1985, Phys. Lett. B **152**, 284.

Leander, G.A., and R.K. Sheline, 1984, Nucl. Phys. A **413**, 375.

Leander, G.A., R.K. Sheline, P. Möller, P. Olanders, I. Ragnarsson, and A.J. Sierk, 1982, Nucl. Phys. A **388**, 452.

Leandri, J., and R. Piepenbring, 1989, Phys. Lett. B **232**, 437.

Leandri, J., and R. Piepenbring, 1993, Z. Phys. A **347**, 21.

Lee, K., and D.R. Inglis, 1957, Phys. Rev. **108**, 774.

Leper, D.P., 1964, Nucl. Phys. **50**, 234.

Lévai, G., J. Cseh, and W. Scheid, 1992, Phys. Rev. C **46**, 548.

Levit, S., J.W. Negele, and Z. Paltiel, 1980, Phys. Rev. C **21**, 1603.

Levon, A.I., J. de Boer, G. Graw, R. Hertenberger, D. Hofer, J. Kvasil, A. Lösch, E. Müller-Zanotti, M. Würkner, H. Baltzer, V. Grafen, and C. Günther, 1994, Nucl. Phys. A **576**, 267.

Li, X., and J. Dudek, 1994, Phys. Rev. C **94**, R1250.

Li, X., J. Dudek, and P. Roman, 1991, Phys. Lett. B **271**, 281.

Liang, C.F., P. Paris, Ch. Briançon, and R.K. Sheline, 1990, Int. J. Mod. Phys. A **5**, 1551.

Liang, C.F., P. Paris, J. Kvasil, and R.K. Sheline, 1991, Phys. Rev. C **44**, 676.

Liang, C.F., P. Paris, R.K. Sheline, D. Nosek, and J. Kvasil, 1995, Phys. Rev. C **51**, 1199.

Liang, C.F., A. Péghaire, and R.K. Sheline, 1990, Mod. Phys. Lett. A **5**, 1243.

Liang, C.F., R.K. Sheline, P. Paris, M. Hussonois, J.F. Ledu, and D.B. Isabelle, 1994, Phys. Rev. C **49**, 2230.

Lipas, P.O., 1963, Nucl. Phys. **40**, 629.

Lipas, P.O., and J.P. Davidson, 1961, Nucl. Phys. **26**, 80.

Lipkin, H.J., N. Meshkov, and A.J. Glick, 1965, Nucl. Phys. **62**, 188.

Liu, Y.-x., H.-z. Sun, and E.-g. Zhao, 1994, J. Phys. G **20**, 1771.

Löhner, H., H. Eickhoff, D. Frekers, G. Gaul, K. Poppensieker, R. Santo, A.G. Drentje, and L.W. Put, 1978, Z. Phys. A **286**, 99.

Lösch, A., J. de Boer, J. Kvasil, A.I. Levon, M. Würkner, H. Baltzer, V. Grafen, and C. Günther, 1994, Z. Phys. A **348**, 235.

Løvhøiden, G., T.F. Thorsteinsen, K. Nybø, and D.G. Burke, 1986, Nucl. Phys. A **452**, 30.

Lustig, H.J., J.A. Maruhn, and W. Greiner, 1980, J. Phys. G **6**, L25.

Mach, H., J. Billowes, M.J.G. Borge, D.G. Burke, P.A. Butler, J.F.C. Cocks, B. Fogelberg, S.J. Freeman, I.S. Grant, K. Gulda, G.D. Jones, E. Hagebø, P. Hoff, J. Hønsi, W. Kurcewicz, G. Løvhøiden, R.A. Naumann, K. Nybø, G. Nyman, H. Ravn, B. Rubio, J. Simpson, A.G. Smith, J.F. Smith, K. Steffensen, J.L. Tain, O. Tengblad, and T.F. Thorsteinsen, 1994, in *Nuclear Shapes and Nuclear Structures at Low Excitation Energies*, edited by Michel Vergnes, D. Goutte, P. H. Heenen, and J. Sauvage (Editions Frontières, Gif-sur-Yvette, France), p. 391.

Mach, H., S. Ćwiok, W. Nazarewicz, B. Fogelberg, M. Moszyński, J. Winger, and R.L. Gill, 1990, Phys. Rev. C **42**, R811.

Mach, H., W. Nazarewicz, D. Kusnezov, M. Moszyǹski, B. Fogelberg, M. Hellström, L. Spanier, R.L. Gill, R.F. Casten, and A. Wolf, 1990, Phys. Rev. C **41**, R2469.

Marcos, S., H. Flocard, and P.-H. Heenen, 1983, Nucl. Phys. A **410**, 125.

Marsh, S., and W.D.M. Rae, 1986, Phys. Lett. B **180**, 185.

Marten-Tölle, M., B. Ackermann, H. Baltzer, T. Bihn, V. Grafen, C. Günther, H. Hausmann, N. Singh, R. Tölle, J. de Boer, and N. Gollwitzer, 1990, Z. Phys. A **336**, 27.

Martín, V., and L.M. Robledo, 1994, Phys. Rev. C **49**, 188; C **50**, 520(E).

Martz, H.E., R.K. Sheline, R.G. Lanier, R.W. Hoff, G.L. Struble, D.J. Decman, D.G. Burke, R.R. Chasman, and R.A. Neumann, 1988, Phys. Rev. C **37**, 1407.

Maruhn, J., and W. Greiner, 1974, Phys. Rev. Lett. **32**, 548.

Matsuse, T., M. Kamimura, and Y. Fukushima, 1975, Prog. Theor. Phys. **53**, 706.

McGowan, F.K., and W.T. Milner, 1981, Phys. Rev. C **23**, 1926.

McGowan, F.K., and W.T. Milner, 1993, Nucl. Phys. A **562**, 241.

McGowan, F.K., and W.T. Milner, 1994, Nucl. Phys. A **571**, 569.

Merchant, A.C., K.F. Pál, and P.E. Hodgson, 1989, J. Phys. G **15**, 601.

Metzger, F.R., 1965, Phys. Rev. **137**, B1415.

Metzger, F.R., 1976, Phys. Rev. C **14**, 543.

Meyer, J., P. Bonche, M.S. Weiss, J. Dobaczewski, H. Flocard, and P.-H. Heenen, 1995, Nucl. Phys. A **588**, 597.

Michel, F., G. Reidemeister, and S. Ohkubo, 1986a, Phys. Rev. Lett. **57**, 1215.

Michel, F., G. Reidemeister, and S. Ohkubo, 1986b, Phys. Rev. C **34**, 1248.

Michel, F., G. Reidemeister, and S. Ohkubo, 1988, Phys. Rev. C **37**, 292.

Mikhailov, I.N., E.G. Nadjakov, M. Aïche, Ch. Briançon, N. Schulz, and V. Vanin, 1989, J. Phys. G **15**, L19.

Millener, D.J., J.W. Olness, E.K. Warburton, and S.S. Hanna, 1983, Phys. Rev. C **28**, 497.

Mizutori, S., Y.R. Shimizu, and K. Matsuyanagi, 1990, Prog. Theor. Phys. **83**, 666.

Mizutori, S., Y.R. Shimizu, and K. Matsuyanagi, 1991a, Prog. Theor. Phys. **85**, 559.

Mizutori, S., Y.R. Shimizu, and K. Matsuyanagi, 1991b, Prog. Theor. Phys. **86**, 131.

Möller, P., 1972, Nucl. Phys. A **192**, 529.

Möller, P., and S.G. Nilsson, 1970, Phys. Lett. B **31**, 283.

Möller, P., S.G. Nilsson, and R.K. Sheline, 1972, Phys. Lett. B **40**, 329.

Möller, P., and J.R. Nix, 1973, in *Physics and Chemistry of Fission 1973* (IAEA, Vienna), Vol. I, p. 103.

Möller, P., and J.R. Nix, 1981, Nucl. Phys. A **361**, 117.

Möller, P., J.R. Nix, W.D. Myers, and W.J. Swiatecki, 1995, At. Data Nucl. Data Tables **59**, 185.

Möller, P., J.R. Nix, and W.J. Swiatecki, 1987, Nucl. Phys. A **469**, 1.

Monsonego, G., and R. Piepenbring, 1964, Nucl. Phys. **58**, 593.

Monsonego, G., and R. Piepenbring, 1966, Nucl. Phys. **78**, 265.

Morinaga, H., 1956, Phys. Rev. **101**, 254.

Morita, K., S. Kubono, M.H. Tanaka, H. Utsunomiya, M. Sugitani, S. Kato, J. Schimizu, T. Tachikawa, and N. Takahashi, 1985, Phys. Rev. Lett. **55**, 185.

Moszkowski, S.A., 1955, Phys. Rev. **99**, 803.

Mottelson, B.R., 1988, in *Proceedings of the Conference on High-Spin Nuclear Structure and Novel Nuclear Shapes*, Argonne National Laboratory, Report No. ANL-PHY-88-2, p. 1.

Mowbray, A.S., J.B. Fitzgerald, J.L. Durell, M.A.C. Hotchkis, W.R. Phillips, and B.J. Varley, 1989, in *Daresbury Laboratory Annual Report 1988/89*, p. 22.

Mueller, A.C., F. Buchinger, W. Klempt, E.W. Otten, R. Neugart, C. Ekström, and J. Heinemeier, 1983, Nucl. Phys. A **403**, 234.

Müller-Schwartz, J., 1967, Z. Phys. **203**, 389.

Müller-Schwartz, J., 1968, Nucl. Phys. A **119**, 337.

Mustafa, M.G., U. Mosel, and H.W. Schmitt, 1973, Phys. Rev. C **7**, 1519.

Myers, W.D., and W.J. Swiatecki, 1969, Ann. Phys. (N.Y.) **55**, 395.

Myers, W.D., and W.J. Swiatecki, 1974, Ann. Phys. (N.Y.) **84**, 186.
Myers, W.D., and W.J. Swiatecki, 1991, Nucl. Phys. A **531**, 93.
Nakagome, Y., R.C. Block, R.E. Slovacek, and E.B. Bean, 1991, Phys. Rev. C **43**, 1824.
Nakatsukasa, T., 1996, Acta Phys. Pol. B **27**, 59.
Nakatsukasa, T., K. Matsuyanagi, I. Hamamoto, and W. Nazarewicz, 1994, Nucl. Phys. A **573**, 333.
Nakatsukasa, T., K. Matsuyanagi, S. Mizutori, and W. Nazarewicz, 1995, Phys. Lett. B **343**, 19.
Nakatsukasa, T., S. Mizutori, and K. Matsuyanagi, 1992, Prog. Theor. Phys. **87**, 607.
Nakatsukasa, T., S. Mizutori, and K. Matsuyanagi, 1993, Prog. Theor. Phys. **89**, 847.
Nazarewicz W., 1985, in *Nuclear Structure 1985*, edited by R.A. Broglia, G.B. Hagemann, and B. Herskind (North-Holland, Amsterdam), p. 263.
Nazarewicz, W., 1987, in *Nuclear Structure Through Static and Dynamic Moments*, edited by H.H. Bolotin (Conference Proceedings Press, Melbourne), p. 180.
Nazarewicz, W., 1991, in *Recent Advances in Nuclear Structure*, edited by D. Bucurescu, G. Cata-Danil, and N.V. Zamfir (World Scientific, Singapore), p. 175.
Nazarewicz, W., 1992, in *Nuclear Shapes and Nuclear Structure at Low Excitation Energies*, edited by M. Vergnes *et al.* (Plenum, New York), p. 247.
Nazarewicz, W., 1993, Phys. Lett. B **305**, 195.
Nazarewicz, W., S. Ćwiok, J. Dobaczewski, and J.X. Saladin, 1995, Acta. Phys. Pol. **26**, 189.
Nazarewicz, W., and J. Dobaczewski, 1992, Phys. Rev. Lett. **68**, 154.
Nazarewicz, W., J. Dobaczewski, and P. Van Isacker, 1992, in *Future Directions in Nuclear Physics with 4π Gamma Detection Systems*, edited by J. Dudek and B. Haas, AIP Conf. Proc. No. 259 (American Institute of Physics, New York), p. 30.
Nazarewicz, W., G.A. Leander, and J. Dudek, 1987, Nucl. Phys. A **467**, 437.
Nazarewicz, W., and P. Olanders, 1985a, Nucl. Phys. A **441**, 420.
Nazarewicz, W., and P. Olanders, 1985b, Phys. Rev. C **32**, 602.
Nazarewicz, W., P. Olanders, I. Ragnarsson, J. Dudek, and G.A. Leander, 1984a, Phys. Rev. Lett. **52**, 1272; **53**, 2060(E).
Nazarewicz, W., P. Olanders, I. Ragnarsson, J. Dudek, G.A. Leander, P. Möller, and E. Ruchowska, 1984b, Nucl. Phys. A **429**, 269.
Nazarewicz, W., and I. Ragnarsson, 1995, in *Handbook of Nuclear Decay Modes* (Oxford University, New York), in press.
Nazarewicz, W., and S.L. Tabor, 1992, Phys. Rev. C **45**, 2226.
Nazmitdinov, R., and S. Åberg, 1992, Phys. Lett. B **289**, 238.
Neergård, K., and P. Vogel, 1970a, Nucl. Phys. A **145**, 33.
Neergård, K., and P. Vogel, 1970b, Nucl. Phys. A **149**, 209 (I); **149**, 217 (II).
Negele, J.W., 1989, Nucl. Phys. A **502**, 371c.
Nemoto, F., and H. Bandō, 1972, Prog. Theor. Phys. **47**, 1210.
Nemoto, F., Y. Yamamoto, H. Horiuchi, Y. Suzuki, and K. Ikeda, 1975, Prog. Theor. Phys. **54**, 104.
Nilsson, S.G., 1955, K. Dan. Vidensk. Selsk. Mat.-Fys. Medd. **29**, No. 16.
Nix, J.R., 1969, Nucl. Phys. A **130**, 241.
Nix, J.R., 1972, Annu. Rev. Nucl. Sci. **22**, 65.
Nosek, D., R.K. Sheline, P.C. Sood, and J. Kvasil, 1993a, Z. Phys. A **344**, 277.
Nosek, D., R.K. Sheline, P.C. Sood, and J. Kvasil, 1993b, Int. J. Mod. Phys. E **2**, 187.
Noto, H., 1980, Prog. Theor. Phys. **63**, 1567.
Noto, H., 1981, Prog. Theor. Phys. **66**, 195.
Noto, H., Y. Abe, J. Hiura, and H. Tanaka, 1974, Prog. Theor. Phys. **52**, 339.
Noto, H., Y. Abe, J. Hiura, and H. Tanaka, 1976, Prog. Theor. Phys. **55**, 1432.
Ogawa, T., Y. Suzuki, and K. Ikeda, 1977, Prog. Theor. Phys. **57**, 1072.
Ogaza, S., J. Kownacki, M.P. Carpenter, J. Gascon, G.B. Hagemann, Y. Iwata, H.J. Jensen, T. Komatsubara, J. Nyberg, G. Sletten, P.O. Tjøm, and W. Waluś, 1993, Nucl. Phys. A **559**, 100.
Ohkubo, S., 1987, Phys. Rev. C **36**, 551.
Ohkubo, S., 1988, Phys. Rev. C **38**, 2377.
Ohkubo, S., and K. Umehara, 1988, Prog. Theor. Phys. **80**, 598.
Ohm, H., M. Liang, G. Molnár, S. Raman, K. Sistemich, and W. Unkelbach, 1990, Phys. Lett. B **241**, 472.
Otsuka, T., 1986, Phys. Lett. B **182**, 256.
Otsuka, T., and M. Sugita, 1988, Phys. Lett. B **209**, 140.
Otten, E.W., 1989, in *Treatise on Heavy-Ion Science, Vol. 8: Nuclei Far From Stability*, edited by D.A. Bromley (Plenum, New York), p. 517.
Pal, M.K., 1993, Nucl. Phys. A **556**, 201.
Parikh, J.C., and N. Ullah, 1967, Nucl. Phys. A **99**, 529.
Pashkevich, V.V., 1971, Nucl. Phys. A **169**, 275.
Pashkevich, V.V., 1988, Nucl. Phys. A **477**, 1.
Paul, E.S., H.R. Andrews, T.E. Drake, J. DeGraaf, V.P. Janzen, S. Pilotte, D.C. Radford, and D. Ward, 1994, Phys. Rev. C **50**, R534.
Pearson, C.J., W.R. Phillips, J.L. Durell, B.J. Varley, W.J. Vermeer, W. Urban, and M.K. Khan, 1994, Phys. Rev. C **49**, R1239.
Peker, L.K., J.H. Hamilton, and J.O. Rasmussen, 1981, Phys. Rev. C **24**, 1336.
Petrovici, A., K.W. Schmid, and A. Faessler, 1994, Nucl. Phys. A **571**, 77.
Phillips, W.R., I. Ahmad, H. Emling, R. Holzmann, R.V.F. Janssens, T.-L. Khoo, and M.W. Drigert, 1986, Phys. Rev. Lett. **57**, 3257.
Phillips, W.R., R.V.F. Janssens, I. Ahmad, H. Emling, R. Holzmann, T.-L. Khoo, and M.W. Drigert, 1988, Phys. Lett. B **212**, 402.
Piepenbring, R., 1983, Phys. Rev. C **27**, 2968.
Piepenbring, R., 1984, J. Phys. Lett. **45**, L-1023.
Piepenbring, R., 1985, Z. Phys. A **322**, 495.
Piepenbring, R., and J. Leandri, 1991, Phys. Lett. B **267**, 17.
Piessens, M., E. Jacobs, S. Pommé, and D. De Frenne, 1993, Nucl. Phys. A **556**, 88.
Pignanelli, M., N. Blasi, S. Micheletti, R. de Leo, M.A. Hofstee, J.M. Schippers, S.Y. van der Werf, and M.N. Harakeh, 1990, Nucl. Phys. A **519**, 567.
Piiparinen, M., P. Kleinheinz, J. Blomqvist, A. Virtanen, A. Ataç, D. Müller, J. Nyberg, T. Ramsøy, and G. Sletten, 1993, Phys. Rev. Lett. **70**, 150.
Pilt, A.A., and C. Wheatley, 1978, Phys. Lett. B **76**, 11.
Pitz, H.H., R.D. Heil, U. Kneissl, S. Lindenstruth, U. Seemann, R. Stock, C. Wesselborg, A. Zilges, P. von Brentano, S.D. Hoblit, and A.M. Nathan, 1990, Nucl. Phys. A **509**, 587.

Poenaru, D.N., W. Greiner, E. Hourani, and M. Hussonnois, 1994, Z. Phys. A **349**, 307.
Poenaru, D.N., M. Ivaşcu, A. Săndulescu, and W. Greiner, 1984, J. Phys. G. **10**, L183.
Poenaru, D.N., M. Ivaşcu, A. Săndulescu, and W. Greiner, 1985, Phys. Rev. C **32**, 572.
Poynter, R.J., P.A. Butler, N. Clarkson, D. Cline, K.A. Connell, R.A. Cunningham, L. Goettig, T.H. Hoare, J.R. Hughes, N.S. Jarvis, G.D. Jones, S. Juutinen, S.M. Mullins, C.N. Pass, J. Simpson, R. Wadsworth, D.L. Watson, and C.A. White, 1989a, Phys. Lett. B **232**, 447.
Poynter, R.J., P.A. Butler, G.D. Jones, R.J. Tanner, C.A. White, J.R. Hughes, S.M. Mullins, R. Wadsworth, D.L. Watson, and J. Simpson, 1989b, J. Phys. G **15**, 449.
Praharaj, C.R., 1986, J. Phys. G **12**, L139.
Price, P.B., 1989, Annu. Rev. Nucl. Part. Sci. **39**, 19.
Provoost, D., F. Grümmer, K. Goeke, and P.-G. Reinhardt, 1984, Nucl. Phys. A **431**, 139.
Pyatov, N.I., and D.I. Salamov, 1977, Nukleonika **22**, 127.
Raduta, A., A. Sandulescu, and P.O. Lipas, 1970, Nucl. Phys. A **149**, 11.
Rae, W.D.M., 1988, Int. J. Mod. Phys. A **3**, 1343.
Rae, W.D.M., and A.C. Merchant, 1992, Phys. Lett. B **279**, 207.
Ragnarsson, I., 1983, Phys. Lett. B **130**, 353.
Ragnarsson, I., S.G. Nilsson, and R.K. Sheline, 1978, Phys. Rep. **45**, 1.
Rainwater, J., 1950, Phys. Rev. **79**, 432.
Raman, S., C.W. Nestor, Jr., S. Kahane, and K.H. Bhatt, 1991, Phys. Rev. C **43**, 556.
Rasmussen, J. O., 1959, Phys. Rev. **113**, 1593.
Reich, C.W., I. Ahmad, and G.A. Leander, 1986, Phys. Lett. B **169**, 148.
Reidemeister, G., and F. Michel, 1993, Phys. Rev. **47**, R1846.
Reidemeister, G., S. Ohkubo, and F. Michel, 1990, Phys. Rev. C **41**, 63.
Reinhard, P.-G., and E.W. Otten, 1984, Nucl. Phys. A **420**, 173.
Richards, H.T., 1984, Phys. Rev. C **29**, 276.
Ring, P., and P. Schuck, 1980, *The Nuclear Many-Body Problem* (Springer, New York).
Robledo, L.M., 1992, Phys. Rev. C **46**, 238.
Robledo, L.M., J.L. Egido, J.F. Berger, and M. Girod, 1987, Phys. Lett. B **187**, 223.
Robledo, L.M., J.L. Egido, B. Nerlo-Pomorska, and K. Pomorski, 1988, Phys. Lett. B **201**, 409.
Robledo, L.M., J.L. Egido, and P. Ring, 1986, Nucl. Phys. A **449**, 201.
Robson, D., 1979, Phys. Rev. Lett. **42**, 876.
Röhl, W.H., 1966, Z. Phys. **195**, 389.
Rohoziński, S.G., 1978, J. Phys. G **4**, 1075.
Rohoziński, S.G., 1988, Rep. Prog. Phys. **51**, 541.
Rohoziński, S.G., 1990, J. Phys. G. **16**, L173.
Rohoziński, S.G., M. Gajda, and W. Greiner, 1982, J. Phys. G **8**, 787.
Rohoziński, S.G., and W. Greiner, 1980, J. Phys. G **6**, 969.
Rohoziński, S.G., and W. Greiner, 1983, Phys. Lett. B **128**, 1.
Rose, H.J., and G.A. Jones, 1984, Nature **307**, 245.
Rosso, O.A., W. Unkelbach, and G. Molnár, 1993, Nucl. Phys. A **563**, 74.
Roth, B., and K. Wildermuth, 1960, Nucl. Phys. **20**, 10.
Roy, N., D.J. Decman, H. Kluge, K.H. Maier, A. Maj, C. Mittag, J. Fernández-Niello, H. Puchta, and F. Riess, 1984, Nucl. Phys. A **426**, 379.
Rozmej, P., S. Ćwiok, and A. Sobiczewski, 1988, Phys. Lett. B **203**, 197.
Ruchowska, E., W. Kurcewicz, N. Kaffrell, T. Björnstad, and G. Nyman, 1982, Nucl. Phys. A **383**, 1.
Ruchowska, E., J. Żylicz, C.F. Liang, P. Paris, and Ch. Briancon, 1992, J. Phys. G **18**, 131.
Rugari, S.L., R.H. France III, B.J. Lund, Z. Zhao, M. Gai, P.A. Butler, V.A. Holliday, A.N. James, G.D. Jones, R.J. Poynter, R.J. Tanner, K.L. Ying, and J. Simpson, 1993, Phys. Rev. C **48**, 2078.
Rutz, K., J.A. Maruhn, P.-G. Reinhard, and W. Greiner, 1994, Nucl. Phys. A **590**, 680.
Sagawa, H., N. Takigawa, and N. van Giai, 1992, Nucl. Phys. A **543**, 575.
Sakamoto, H., and T. Kishimoto, 1989, Nucl. Phys. A **501**, 205.
Sakuda, T., 1977, Prog. Theor. Phys. **57**, 855.
Sakuda, T., S. Nagata, and F. Nemoto, 1978, Prog. Theor. Phys. **59**, 1543.
Sakuda, T., S. Nagata, and F. Nemoto, 1979, Prog. Theor. Phys. Suppl. **65**, 111.
Sandor, R.K.J., H.P. Blok, M. Girod, M.N. Harakeh, C.W. de Jager, and H. de Vries, 1993a, Nucl. Phys. A **551**, 349.
Sandor, R.K.J., H.P. Blok, M. Girod, M.N. Harakeh, C.W. de Jager, V. Yu. Ponomarev, and H. de Vries, 1993b, Nucl. Phys. A **551**, 378.
Sandulescu, A., and W. Greiner, 1992, Rep. Prog. Phys. **55**, 1423.
Satuła, W., S. Ćwiok, W. Nazarewicz, R. Wyss, and A. Johnson, 1991, Nucl. Phys. A **529**, 289.
Scholten, O., F. Iachello, and A. Arima, 1978, Ann. Phys. (N.Y.) **115**, 325.
Schüler, P., Ch. Lauterbach, Y.K. Agarwal, J. de Boer, K.P. Blume, P.A. Butler, K. Euler, Ch. Fleischmann, C. Günther, E. Hauber, H.J. Maier, M. Marten-Tölle, Ch. Schandera, R.S. Simon, R. Tölle, and P. Zeyen, 1986, Phys. Lett. B **174**, 241.
Schulz, N., V.R. Vanin, M. Aïche, Ch. Briançon, A. Chevallier, J. Chevallier, M.E. Debray, A.J. Kreiner, E. Ruchowska, and J.C. Sens, 1990, Z. Phys. A **335**, 107.
Schulz, N., V.R. Vanin, M. Aïche, A. Chevallier, J. Chevallier, J.C. Sens, Ch. Briançon, S. Ćwiok, E. Ruchowska, J. Fernandez-Niello, Ch. Mittag, and J. Dudek, 1989, Phys. Rev. Lett. **63**, 2645.
Schulz, N., V.R. Vanin, A.J. Kreiner, E. Ruchowska, M. Aïche, Ch. Briançon, A. Chevallier, J. Chevallier, M.E. Debray, and J.C. Sens, 1991, Z. Phys. A **339**, 325.
Schwartz, B., Ch. Ender, D. Habs, D. Schwalm, M. Dahlinger, E. Kankeleit, H. Folger, R.S. Simon, and H. Backe, 1986, Z. Phys. A **323**, 489.
Schwartz, B., D. Habs, D. Schwalm, M. Dahlinger, E. Kankeleit, H. Folger, and R.S. Simon, 1987, GSI Scientific Report 87-1, p. 31.
Schwartz, B., D. Habs, D. Schwalm, M. Dahlinger, E. Kankeleit, H. Folger, and R.S. Simon, 1988, GSI Scientific Report 88-1, p. 33.
Sellschop, J.P.F., A. Zucchiatti, L. Mirman, M.Z.I. Gering, and E. Di Salvo, 1987, J. Phys. G **13**, 1129.
Sheline, R.K., 1980, Phys. Rev. C **21**, 1660.
Sheline, R.K., 1986, Phys. Lett. B **166**, 269.
Sheline, R.K., 1988a, Phys. Rev. C **37**, 423.
Sheline, R.K., 1988b, Phys. Lett. B **205**, 11.
Sheline, R.K., 1989a, Phys. Lett. B **219**, 222.
Sheline, R.K., 1989b, Phys. Lett. B **222**, 179.
Sheline, R.K., 1993a, Int. J. Mod. Phys. E **2**, 657.

Sheline, R.K., 1993b, Phys. Rev. C **48**, 1003.

Sheline, R.K., and B.B. Bossinga, 1991, Phys. Rev. C **44**, 218.

Sheline, R.K., Y.S. Chen, and G.A. Leander, 1988, Nucl. Phys. A **486**, 306.

Sheline, R.K., D. Decman, K. Nybø, T.F. Thorsteinsen, G. Løvhøiden, E.R. Flynn, J.A. Cizewski, D.K. Burke, G. Sletten, P. Hill, N. Kaffrell, W. Kurcewicz, G. Nyman, and G. Leander, 1983, Phys. Lett. B **133**, 13.

Sheline, R.K., A.K. Jain, and K. Jain, 1988, Phys. Rev. C **38**, 2952.

Sheline, R.K., A.K. Jain, K. Jain, and I. Ragnarsson, 1989, Phys. Lett. B **219**, 47.

Sheline, R.K., J. Kvasil, C.F. Liang, and P. Paris, 1991, Phys. Rev. C **44**, R1732.

Sheline, R.K., J. Kvasil, C.F. Liang, and P. Paris, 1993, J. Phys. G **19**, 617.

Sheline, R.K., and G.A. Leander, 1983, Phys. Rev. Lett. **51**, 359.

Sheline, R.K., C.F. Liang, and P. Paris, 1990, Int. J. Mod. Phys. A **5**, 2821.

Sheline, R.K., C.F. Liang, P. Paris, J. Kvasil, and D. Nosek, 1995, Phys. Rev. C **51**, 1708.

Sheline, R.K., and I. Ragnarsson, 1991a, Phys. Rev. C **43**, 1476.

Sheline, R.K., and I. Ragnarsson, 1991b, Phys. Rev. C **44**, 2886.

Sheline, R.K., and P.C. Sood, 1986, Phys. Rev. C **34**, 2362.

Sheline, R.K., and P.C. Sood, 1989, Prog. Theor. Phys. **81**, 1057.

Sheline, R.K., and P.C. Sood, 1990, Int. J. Mod. Phys. A **5**, 2677.

Sheline, R.K., and P.C. Sood, 1991, Fizika (Zagreb) **23**, 1.

Sheline, R.K., and K. Wildermuth, 1960, Nucl. Phys. **21**, 196.

Shi, Y.-J., and W.J. Swiatecki, 1987, Nucl. Phys. A **464**, 205.

Shriner, J.F., Jr., P.D. Cottle, J.F. Ennis, M. Gai, D.A. Bromley, J.W. Olness, E.K. Warburton, L. Hildingsson, M.A. Quader, and D.B. Fossan, 1985, Phys. Rev. **32**, 1888.

Skalski, J., 1990, Phys. Lett. B **238**, 6.

Skalski, J., 1991, Phys. Rev. C **43**, 140.

Skalski, J., 1992, Phys. Lett. B **274**, 1.

Skalski, J., 1994, Phys. Rev. C **49**, 2011.

Skalski, J., P.-H. Heenen, and P. Bonche, 1993a, Nucl. Phys. A **559**, 221.

Skalski, J., P.-H. Heenen, P. Bonche, H. Flocard, and J. Meyer, 1993b, Nucl. Phys. A **551**, 109.

Smith, J.F., J.F.C. Cocks, N. Schulz, M. Aïche, M. Bentaleb, P.A. Butler, F. Hannachi, G.D. Jones, P.M. Jones, R. Julin, S. Juutinen, R. Kulessa, E. Lubkiewicz, A. Płochocki, F. Riess, E. Ruchowska, A. Savelius, J.C. Sens, J. Simpson, and E. Wolf, 1995, Phys. Rev. Lett. **75**, 1050.

Sobiczewski, A., and K. Böning, 1987, Acta Phys. Pol. B **18**, 393.

Sobiczewski, A., Z. Patyk, S. Ćwiok, and P. Rozmej, 1988, Nucl. Phys. A **485**, 16.

Soloviev, V.G., 1965, Nucl. Phys. **69**, 1.

Soloviev, V.G., 1976, *Theory of Complex Nuclei* (Pergamon, New York).

Soloviev, V.G., and A.V. Sushkov, 1991, Phys. Lett. B **262**, 189.

Soloviev, V.G., and A.V. Sushkov, 1994, Phys. At. Nuclei **57**, 1304.

Soloviev, V.G., and P. Vogel, 1963, Phys. Lett. **6**, 126.

Sood, P.C., and R.K. Sheline, 1989, Phys. Rev. C **40**, 1530.

Spear, R.H., 1989, At. Data Nucl. Data Tables **42**, 55.

Spear, R.H., and W.N. Catford, 1990, Phys. Rev. **41**, R1351.

Spear, R.H., W.J. Vermeer, S.M. Burnett, G.J. Gyapong, and C.S. Lim, 1989, Aust. J. Phys. **42**, 345.

Stephens, F.S., Jr., F. Asaro, and I. Perlman, 1954, Phys. Rev. **96**, 1568.

Stephens, F.S., Jr., F. Asaro, and I. Perlman, 1955, Phys. Rev **100**, 1543.

Strayer, M.R., R.Y. Cusson, A.S. Umar, P.-G. Reinhard, D.A. Bromley, and W. Greiner, 1984, Phys. Lett. B **135**, 261.

Strutinsky, V.M., 1956, At. Energ. **4**, 150.

Strutinsky, V.M., 1957, J. Nucl. Energy **4**, 523.

Strutinsky, V.M., 1967, Nucl. Phys. A **95**, 420.

Strutinsky, V.M., 1974, Nucl. Phys. A **218**, 169.

Strutinsky, V.M., and A.G. Magner, 1976, Sov. J. Part. Nucl. **7**, 138.

Sujkowski, Z., D. Chmielewska, M.J.A. De Voigt, J.F.W. Jansen, and O. Scholten, 1977, Nucl. Phys. A **291**, 365.

Sushkov, O.P., and V.V. Flambaum, 1980, Sov. J. Nucl. Phys. **31**, 28.

Suzuki, Y., 1976, Prog. Theor. Phys. **55**, 1751.

Suzuki, Y., 1980, Prog. Theor. Phys. **64**, 2041.

Suzuki, Y., and Y. Tosaka, 1990, Nucl. Phys. A **517**, 599.

Suzuki, Y., A. Yamamoto, and K. Ikeda, 1985, Nucl. Phys. A **444**, 365.

Tamura, T., and T. Udagawa, 1962, Nucl. Phys. **35**, 382.

Tanabe, F., and F. Nemoto, 1974, Prog. Theor. Phys. **51**, 2009.

Thouless, D.J., 1961, Nucl. Phys. **22**, 78.

Tomoda, T., and A. Arima, 1978, Nucl. Phys. A **303**, 217.

Toth, K.S., H.J. Kim, M.N. Rao, and R.L. Mlekodaj, 1986, Phys. Rev. Lett. **56**, 2360.

Uchiyama, T., and H. Morinaga, 1985, Z. Phys. A **320**, 273.

Umar, A.S., M.R. Strayer, R.Y. Cusson, P.-G. Reinhard, and D.A. Bromley, 1985, Phys. Rev. C **32**, 172.

Urban, W., J.C. Bacelar, W. Gast, G. Hebbinghaus, A. Krämer-Flecken, R.M. Lieder, T. Morek, and T. Rząca-Urban, 1990, Phys. Lett. B **247**, 238.

Urban, W., J.L. Durell, W.R. Phillips, B.J. Varley, Ch.P. Hess, M.A. Jones, C.J. Pearson, W.J. Vermeer, Ch. Vieu, J.S. Dionisio, M. Pautrat, and J.C. Bacelar, 1995, Nucl. Phys. A **587**, 541.

Urban, W., R.M. Lieder, J.C. Bacelar, P.P. Singh, D. Alber, D. Balabanski, W. Gast, H. Grawe, G. Hebbinghaus, J.R. Jongman, T. Morek, R.F. Noorman, T. Rząca-Urban, H. Schnare, M. Thoms, O. Zell, and W. Nazarewicz, 1991, Phys. Lett. B **258**, 293.

Urban, W., R.M. Lieder, W. Gast, G. Hebbinghaus, A. Krämer-Flecken, K.P. Blume, and H. Hübel, 1987, Phys. Lett. B **185**, 331.

Urban, W., R.M. Lieder, W. Gast, G. Hebbinghaus, A. Krämer-Flecken, T. Morek, T. Rząca-Urban, W. Nazarewicz, and S.L. Tabor, 1988, Phys. Lett. B **200**, 424.

Vdovin, A.I., and V.G. Soloviev, 1983, Fiz. Elem. Chastits At. Yadra **14**, 237 [Sov. J. Part. Nucl. **14**, 99].

Veje, C.J., 1966, K. Dan. Vidensk. Selsk. Mat.-Fys. Medd. **35**.

Vergnes, M.N., and J.O. Rasmussen, 1965, Nucl. Phys. **62**, 233.

Vermeer, W.J., M.K. Khan, A.S. Mowbray, J.B. Fitzgerald, J.A. Cizewski, B.J. Varley, J.L. Durell, and W.R. Phillips, 1990, Phys. Rev. C **42**, R1183.

Vermeer, W.J., W. Urban, M.K. Khan, C.J. Pearson, A.B. Wiseman, B.J. Varley, J.L. Durell, and W.R. Phillips, 1993, Nucl. Phys. A **559**, 422.

Vogel, P., 1968, Nucl. Phys. A **112**, 583.

Vogel, P., 1976, Phys. Lett. B **60**, 431.

von Brentano, P., N.V. Zamfir, and A. Zilges, 1992, Phys. Lett. B **278**, 221.

Wada, T., and H. Horiuchi, 1987, Phys. Rev. Lett. **58**, 2190.

Wada, T., and H. Horiuchi, 1988, Phys. Rev. C **38**, 2063.

Ward, D., H.R. Andrews, G.C. Ball, A. Galindo-Uribarri, V.P. Janzen, T. Nakatsukasa, D.C. Radford, T.E. Drake, J. DeGraaf, S. Pilotte, and Y.R. Shimizu, 1995, Preprint No. TASCC-P-95-29.

Ward, D., G.D. Dracoulis, J.R. Leigh, R.J. Charity, D.J. Hinde, and J.O. Newton, 1983, Nucl. Phys. A **406**, 591.

Wieland, M., J. Fernández-Niello, F. Riess, M. Aïche, A. Chevallier, J. Chevallier, N. Schulz, J.C. Sens, Ch. Briançon, R. Kulessa, and E. Ruchowska, 1992a, Phys. Rev. C **45**, 1035.

Wieland, M., J. Fernández-Niello, B. von Fromberg, F. Riess, M. Aïche, A. Chevallier, J. Chevallier, N. Schulz, J.C. Sens, Ch. Briançon, and E. Ruchowska, 1992b, Phys. Rev. C **46**, 2628.

Wildermuth, K., and Th. Kanellopoulos, 1958a, Nucl. Phys. **7**, 150.

Wildermuth, K., and Th. Kanellopoulos, 1958b, Nucl. Phys. **9**, 449.

Wilkins, B.D., E.P. Steinberg, and R.R. Chasman, 1976, Phys. Rev. C **14**, 1832.

Wolff, R., G. Puddu, and J.W. Negele, 1992 (unpublished).

Wollersheim, H.J., H. Emling, H. Grein, R. Kulessa, R.S. Simon, C. Fleischmann, J. de Boer, E. Hauber, C. Lauterbach, C. Schandera, P.A. Butler, and T. Czosnyka, 1993, Nucl. Phys. A **556**, 261.

Yamamoto, Y., 1974, Prog. Theor. Phys. **52**, 471.

Yamaya, T., S. Oh-ami, M. Fujiwara, T. Itahashi, K. Katori, M. Tosaki, S. Kato, S. Hatori, and S. Ohkubo, 1990, Phys. Rev. C **42**, 1935.

Yamaya, T., M. Saito, M. Fujiwara, T. Itahashi, K. Katori, T. Suehiro, S. Kato, S. Hatori, and S. Ohkubo, 1993, Phys. Lett. B **306**, 1.

Yang, B., and Z. Hwang, 1987, Phys. Rev. C **35**, 851.

Yi, G.Y., F. Catara, M. Sambataro, and A. Vitturi, 1991, Europhys. Lett. **16**, 711.

Yoshida, S., 1962, Nucl. Phys. **38**, 380.

Yoshinaga, N., T. Mizusaki, and T. Otsuka, 1993, Nucl. Phys. A **559**, 193.

Zaikin, D.A., 1966, Nucl. Phys. A **86**, 638.

Zamfir, N.V., R.F. Casten, and P. von Brentano, 1989, Phys. Lett. B **226**, 11.

Zamfir, N.V., O. Scholten, and P. von Brentano, 1990, Z. Phys. A **337**, 293.

Zamfir, N.V., and P. von Brentano, 1992, Phys. Lett. B **289**, 245.

Zamfir, N.V., P. von Brentano, and R.F. Casten, 1994, Phys. Rev. C **49**, R605.

Zhang, J., A.C. Merchant, and W.D.M. Rae, 1993, Phys. Rev. C **48**, 2117.

Zhang, J., W.D.M. Rae, and A.C. Merchant, 1994, Nucl. Phys. A **575**, 61.

Zhu, X., J.D. Bowman, C.D. Bowman, J.E. Bush, P.P.J. Delheij, C.M. Frankle, C.R. Gould, D.G. Haase, J.N. Knudson, G.E. Mitchell, S. Penttilä, H. Postma, N.R. Roberson, S.J. Seestrom, J.J. Szymanski, and V.W. Yuan, 1992, Phys. Rev. C **46**, 768.

Zhu, S.J., Q.H. Lu, J.H. Hamilton, A.V. Ramayya, L.K. Peker, M.G. Wang, W.C. Ma, B.R.S. Babu, T.N. Ginter, J. Kormicki, D. Shi, J.K. Deng, W. Nazarewicz, J.O. Rasmussen, M.A. Stoyer, S.Y. Chu, K.E. Gregorich, M.F. Mohar, S. Asztalos, S.G. Prussin, J.D. Cole, R. Aryaeinejad, Y.K. Dardenne, M. Drigert, K.J. Moody, R.W. Lougheed, J.F. Wild, N.R. Johnson, I.Y. Lee, F.K. McGowan, G.M. Ter-Akopian, and Yu.Ts. Oganessian, 1995, Phys. Lett. B **357**, 273.

Zilges, A., P. von Brentano, H. Friedrichs, R.D. Heil, U. Kneissl, S. Lindenstruth, H.H. Pitz, and C. Wesselborg, 1991, Z. Phys. A **340**, 155.

Zilges, A., P. von Brentano, and A. Richter, 1992, Z. Phys. A **341**, 489.

Zolnowski, D.R., T. Kishimoto, Y. Gono, and T.T. Sugihara, 1975, Phys. Lett. B **55**, 453.

Żylicz, J., 1986, in *Nuclear Structure, Reactions and Symmetries*, edited by R.A. Meyer and V. Paar (World Scientific, Singapore), p. 79.